REVIEW

A Minimal Toolset for Positional Diamond Mechanosynthesis

Robert A. Freitas Jr.* and Ralph C. Merkle

Institute for Molecular Manufacturing, Palo Alto, CA 94301, USA

This paper presents the first theoretical quantitative systems level study of a complete suite of reaction pathways for scanning-probe based ultrahigh-vacuum diamond mechanosynthesis (DMS). A minimal toolset is proposed for positionally controlled DMS consisting of three primary tools— the (1) Hydrogen Abstraction (HAbst), (2) Hydrogen Donation (HDon), and (3) Dimer Placement (DimerP) tools—and six auxiliary tools—the (4) Adamantane radical (AdamRad) and (5) Germyladamantane radical (GeRad) handles, the (6) Methylene (Meth), (7) Germylmethylene (GM), and (8) Germylene (Germ) tools, and (9) the Hydrogen Transfer (HTrans) tool which is a simple compound of two existing tools (HAbst + GeRad). Our description of this toolset, the first to exhibit 100% process closure, explicitly specifies all reaction steps and reaction pathologies, also for the first time. The toolset employs three element types (C, Ge, and H) and requires inputs of four feedstock molecules—CH_4 and C_2H_2 as carbon sources, Ge_2H_6 as the germanium source, and H_2 as a hydrogen source. The present work shows that the 9-tooltype toolset can, using only these simple bulk-produced chemical inputs: (1) fabricate all nine tooltypes, including their adamantane handle structures and reactive tool intermediates, starting from a flat passivated diamond surface or an adamantane seed structure; (2) recharge all nine tooltypes after use; and (3) build both clean and hydrogenated molecularly-precise unstrained cubic diamond C(111)/C(110)/C(100) and hexagonal diamond surfaces of process-unlimited size, including some Ge-substituted variants; methylated and ethylated surface structures; handled polyyne, polyacetylene and polyethylene chains of process-unlimited length; and both flat graphene sheet and curved graphene nanotubes. Reaction pathways and transition geometries involving 1620 tooltip/workpiece structures were analyzed using Density Functional Theory (DFT) in Gaussian 98 at the B3LYP/6-311+G(2*d*, *p*) // B3LYP/3-21G* level of theory to compile 65 Reaction Sequences comprised of 328 reaction steps, 354 unique pathological side reactions and 1321 reported DFT energies. The reactions should exhibit high reliability at 80 K and moderate reliability at 300 K. This toolset provides clear developmental targets for a comprehensive near-term DMS implementation program.

Keywords: Adamantane, Carbon, Diamond, Diamondoid, Dimer Placement, DMS, Germanium, Mechanosynthesis, Nanotechnology, Positional Control, Reaction Sequence, Toolset, Tooltips.

CONTENTS

*Author to whom correspondence should be addressed.

1. INTRODUCTION

Arranging atoms in most of the ways permitted by physical law is a fundamental objective of molecular manufacturing. A more modest and specific objective is the ability to synthesize molecularly precise diamondoid structures using positionally controlled molecular tools. Such positional control might be achieved using an instrument like a Scanning Probe Microscope (SPM). The landmark experimental demonstration of positional atomic assembly occurred in 1989 when Eigler and Schweizer[1] employed an SPM to spell out the IBM logo using 35 xenon atoms arranged on nickel surface, though no covalent bonds were formed. The use of precisely applied mechanical forces to induce site-specific chemical transformations is called positional mechanosynthesis. In 2003, Oyabu et al.[2] achieved the first experimental demonstration of purely mechanical positional chemical synthesis (mechanosynthesis) on a heavy atom using only mechanical forces to make and break covalent bonds, first abstracting and then rebonding a single silicon atom to a silicon surface with SPM positional control in vacuum at low temperature.

The assumption of positionally controlled highly reactive tools operating in vacuum permits the use of novel and relatively simple reaction pathways. Following early general proposals in 1992 by Drexler[3] for possible diamond mechanosynthetic tools and sketches of a few possible approaches to specific reaction pathways, in 1997 Merkle[4] outlined a possible set of tools and reaction pathways for diamond mechanosynthesis (DMS). Merkle's "hydrocarbon metabolism" scheme used 9 primary tooltypes plus several intermediates (some incompletely defined), employed at least 6 different element types (C, Si, Sn, H, Ne, and one unspecified transition metal), also required another unspecified "vitamin molecule" possibly including additional element types, did not show 100% process closure, in most cases did not specify complete reaction sequences, was an almost purely qualitative analysis (only one rotation-constrained cluster model B3LYP/6-31G* energy calculation was provided for part of one proposed reaction), included no analysis of pathological side reactions (e.g., only two *ab initio* transition structures or barrier estimates were presented in the paper), and neglected both the fabrication of handle structures and the fabrication of the initial toolset itself. In this paper, we propose that 100% process closure can be achieved using a minimal toolset for diamond mechanosynthesis (Fig. 1) consisting of only three primary tooltypes—a Hydrogen Abstraction (HAbst) tool, a Hydrogen Donation (HDon) tool, and a Dimer Placement (DimerP) tool—assisted by six auxiliary structures including the discharged handle structures for HAbst (the 1-adamantyl radical or Adam-Rad; Fig. 1(E)) and for HDon (the 1,1-germano-adamantyl radical or GeRad; Fig. 1(F)), three intermediate transfer tools (the Methylene (Meth), Germylmethylene (GM), and Germylene (Germ) tools), and finally a Hydrogen Transfer

Robert A. Freitas Jr. is Senior Research Fellow at the Institute for Molecular Manufacturing (IMM) in Palo Alto, California, and was a Research Scientist at Zyvex Corp. (Richardson, Texas), the first molecular nanotechnology company, during 2000–2004. He received B.S. degrees in Physics and Psychology from Harvey Mudd College in 1974 and a J.D. from University of Santa Clara in 1979. Freitas co-edited the 1980 NASA feasibility analysis of self-replicating space factories and in 1996 authored the first detailed technical design study of a medical nanorobot ever published in a peer-reviewed mainstream biomedical journal. Freitas is the author of Nanomedicine, the first book-length technical discussion of the potential medical applications of molecular nanotechnology and medical nanorobotics; the first two volumes of this 4-volume series were published in 1999 and 2003 by Landes Bioscience. His research interests include: nanomedicine, medical nanorobotics design, molecular machine systems, diamondoid mechanosynthesis (theory and experimental pathways), molecular assemblers and nanofactories, and self-replication in machine and factory systems. He has published 32 refereed journal publications and contributed book chapters, co-authored Kinematic Self-Replicating Machines (Landes Bioscience, 2004), and in 2006 co-founded the Nanofactory Collaboration. His home page is at www.rfreitas.com.

Dr. Merkle received his Ph.D. from Stanford University in 1979 where he co-invented public key cryptography. He joined Xerox PARC in 1988, where he pursued research in security and computational nanotechnology until 1999. He was a Nanotechnology Theorist at Zyvex until 2003, when he joined the Georgia Institute of Technology as a Professor of Computing until 2006. He is now a Senior Research Fellow at the Institute for Molecular Manufacturing. He chaired the Fourth and Fifth Foresight Conferences on Nanotechnology. He was co-recipient of the 1998 Feynman Prize for Nanotechnology for theory, co-recipient of the ACM's Kanellakis Award for Theory and Practice and the 2000 RSA Award in Mathematics. Dr. Merkle has fourteen patents and has published extensively. His home page is at www.merkle.com.
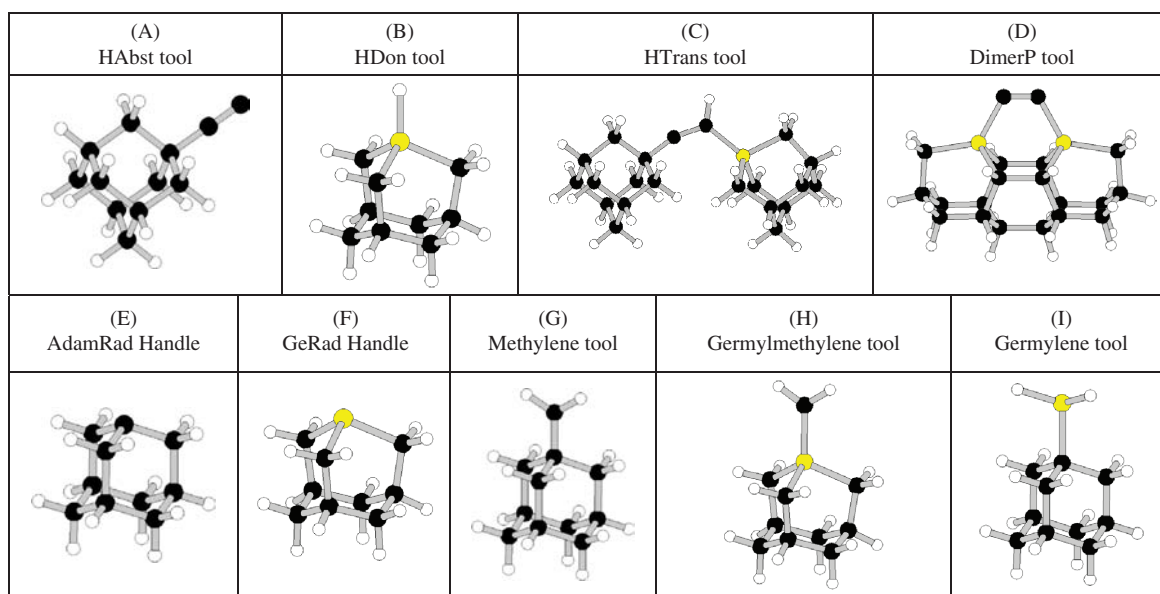
Fig. 1. A minimal toolset for diamond mechanosynthesis, including primary, auxiliary, and compound tools.

(HTrans) tool that is a simple compound of two existing tools (HAbst + GeRad).

The simplest possible self-contained DMS system might employ one heavy element type (C) and one passivating element type (H). Analyses of purely hydrocarbon tools for hydrogen abstraction[3–8] and C_2 dimer placement[4, 9–11] have been published, and a purely hydrocarbon hydrogen donation tool is conceivable. However, allowing only 1 or 2 tool attachments per atom on either side of two atoms joined by a single bond, then a C/H-only toolset can apply just 1 unique nonzero bilateral bond scission force differential, rendering most covalent bonding events irreversible in the absence of double (C=C) or triple (C≡C) bonds. Our proposed minimal toolset employs three element types (C, Ge, and H) because the addition of a second heavy element from the same chemical group as carbon dramatically increases the number of distinct mechanical force differentials that can be applied to achieve targeted bond scission, while retaining analogous chemical reactions for both heavy elements thus not adding significantly to reaction sequence complexity. Allowing only 1 or 2 tool attachments per atom on either side of two atoms joined by a single bond, a C/Ge/H toolset can apply 10 unique nonzero bilateral bond scission force differentials. This permits reversible bond formation and greatly increases toolset functional flexibility either during simple deposition operations or during bond-breaking using multiple handle attachment points and opposing force vectors (Section 3.5). Additional opportunities for bond strength modulation via side bonding into aromatic or other high-bond-order systems are likewise more numerous when two heavy element types are employed instead of one. Using more element types also extends the range of useful properties that can be possessed by products the system can fabricate.[12, 13]

Our proposed C/Ge/H DMS system requires only four simple feedstock molecules—CH_4 (methane) and C_2H_2 (acetylene) as the carbon sources, Ge_2H_6 (digermane) as the germanium source, and H_2 as a hydrogen source, all available commercially at 6N–9N purity. A flat depassivated diamond surface[14] is also required to serve as a hydrogen dump (transient H atom source and sink), and a flat depassivated germanium surface[15] is required for positionally precise methane, acetylene and digermane presentation (though a future more sophisticated DMS system might employ engineered high-specificity binding sites[16] to achieve more efficient and reliable feedstock molecule presentation). Both diamond[17] and germanium[18] flat surfaces can be produced using currently available bulk chemical vapor deposition (CVD) techniques.

The present work shows that, using only these simple bulk-produced inputs, the proposed 9-tooltype minimal toolset can: (1) fabricate all nine tooltypes, including their adamantane handle structures and reactive tool intermediates, starting from flat passivated diamond surface or a handle-bound adamantane seed structure ("Adam"); (2) recharge all nine tooltypes after use; and (3) build both clean and hydrogenated molecularly-precise unstrained cubic diamond C(111)/C(110)/C(100) and hexagonal diamond (lonsdaleite) surfaces of process-unlimited size including some Ge-substituted variants, methylated and ethylated surface structures, and also handled polyyne, polyacetylene and polyethylene chains of process-unlimited length, along with both flat graphene sheet and curved graphene nanotubes. The procedure for building an adamantane molecule on the end of an existing adamantane-terminated handle can be extended indefinitely to generate larger diamond handles[19, 20] of many desired sizes and shapes, including simple pyramidal

RS1. Hydrogen Abstraction ("HAbst") tool (at top, left) abstracts H from C111 surface or from Adam bridgehead.

Step	Description of Reaction	Mult.	Ener. (eV)	Barr. (eV)
1	**Abstract H from hydrogenated C111 bridgehead using HAbst tool**			
	R: Diam1 (ACC0B/50) + HAbst (ACC0A/27)	S + D		
	P: Diam2 (ACC0A/49) + HAbstH (ACC0A/28)	D + S	−1.59	
1^1	**Abstract H from hydrogenated Adam bridgehead using HAbst tool**			
	R: Adam (ACC0A/26) + HAbst (ACC0A/27)	S + D		
	P: AdamRad (ACC0A/25) + HAbstH (ACC0A/28)	D + S	−1.59	
1^2	**Abstract H from hydrogenated C110 ridge site using HAbst tool**			
	R: C110A (ACC0A/42) + HAbst (ACC0A/27)	S + D		
	P: C110B (AXCXA/41) + HAbstH (ACC0A/28)	D + S	−1.55	
1^3	**Abstract H from hydrogenated C100 dimer site using HAbst tool**			
	R: C100A (ACC0A/23) + HAbst (ACC0A/27)	S + D		
	P: C100B (ACC0A/22) + HAbstH (ACC0A/28)	D + S	−1.38	
1^4	**Abstract H from benzene (C_6H_6) ring using HAbst tool**			
	R: C6H6 (ACC0A/12) + HAbst (ACC0A/27)	S + D		
	P: C6H5 (ACC0A/11) + HAbstH (ACC0A/28)	D + S	−0.98	
1^5	**Abstract H from hydrogenated HDon tooltip using HAbst tool**			
	R: HDon (ACC0A/26) + HAbst (ACC0A/27)	S + D		
	P: GeRad (ACC0A/25) + HAbstH (ACC0A/28)	D + S	−2.19	

(Section 3.4). It is assumed that all constructions are initiated either on a bulk-fabricated atomically smooth diamond surface such as a well-characterized flat diamond lattice plane or diamond shard tip, or on a positionally constrained fully-passivated adamantane cage.

Minimum acceptable reaction energies were guided by reaction reliability requirements. If the absolute value of an energy barrier or reaction exoergicity is E_{react}, then the Boltzmann population of the examined product structure may be approximated as $P_{react} \sim \exp(-E_{react}/k_B T)$ with $k_B = 1.381 \times 10^{-23}$ J/K and T = temperature in K. At $T = 300$ K, a reaction exoergicity of $E_{react} = 0.40$ eV gives $P_{react} = 2 \times 10^{-7}$ for the failed reaction, reliable enough for products requiring $< \sim 10^7$ reaction steps for fabrication (e.g., products containing $\sim 10^6$ heavy atoms, assuming ~ 10 steps are required per heavy atom), at room temperature. At $T = 80$ K (LN$_2$ temperature), $E_{react} = 0.20$ eV gives $P_{react} = 3 \times 10^{-13}$ ($P_{react} = 5 \times 10^{-26}$ at 0.40 eV), indicating extreme reliability for fabricating products with very high atom counts at low temperature. Likewise, a barrier of $E_{react} = 0.40$ eV that blocks formation of an

unwanted pathological structure along a second reaction pathway that competes with the desired more exoergic main reaction pathway gives $P_{react} = 2 \times 10^{-7}$ at $T = 300$ K for the unwanted structure, yielding similar reliability estimates as before. For these reasons, all proposed reactions have minimum energy barriers (blocking an undesired outcome) or relative exoergicities (favoring a desired outcome) of ~ 0.40 eV for operation at 300 K and ~ 0.20 eV for 80 K operation. Also, while radical coupling reactions are usually barrierless,[25] tooltip/workpiece proximation should be maintained for a long enough time during each mechanosynthetic reaction step to allow any required intersystem crossing (e.g., from triplet to singlet state) to spontaneously occur (typically in 10^{-10}–10^{-6} sec),[26–29] since two radicals with parallel spins must undergo an electronic transition to antiparallel spins to enable radical coupling, leading to bond formation. Triplet decay should occur spontaneously at 300 K if the transition is exoergic or only weakly endoergic;[30] triplet decay rates can often be enhanced several orders of magnitude via IR laser irradiation.[31]

RS2. Hydrogen Donation ("HDon") tool (at top, left) donates H to C111 surface or to Adam bridgehead and Recharge GeRad tool from HDon tool.

Step	Description of Reaction	Mult.	Ener. (eV)	Barr. (eV)
1	**Donate H to dehydrogenated C111 bridgehead using HDon tool**			
	R: Diam2 (ACC0A/49) + HDon (ACC0A/26)	D + S		
	P: Diam1 (ACC0B/50) + GeRad (ACC0A/25)	S + D	−0.61	
1D2	Sidewall H migrates to Ge● radical site			
	R: GeRad (ACC0A/25)	D		
	P: GeRadp1 (ACC0A/25)	D	+ 0.61	
	T: GeRadp1TS (ACC1A/25)	D		+2.99
1F6	H● dissociates from tool handle			
	R: HDon (ACC0A/26)	S		
	P: GeRad (ACC0A/25) + H (ACC0A/1)	D + D	+ 3.51	
1[1]	**Donate H to dehydrogenated AdamRad bridgehead w/HDon tool**			
	R: AdamRad (ACC0A/25) + HDon (ACC0A/26)	D + S		
	P: Adam (ACC0A/26) + GeRad (ACC0A/25)	S + D	−0.60	
1[2]	**Donate H to dehydrogenated C110 ridge site using HDon tool**			
	R: C110B (AXCXA/41) + HDon (ACC0A/26)	D + S		
	P: C110A (ACC0A/42) + GeRad (ACC0A/25)	S + D	−0.73	
1[3]	**Donate H to dehydrogenated C100 dimer site using HDon tool**			
	R: C100B (ACC0A/22) + HDon (ACC0A/26)	D + S		
	P: C100A (ACC0A/23) + GeRad (ACC0A/25)	S + D	−0.81	
1[4]	**Donate H to dehydrogenated benzyl (C_6H_5) radical w/HDon tool**			
	R: C6H5 (ACC0A/11) + HDon (ACC0A/26)	D + S		
	P: C6H6 (ACC0A/12) + GeRad (ACC0A/25)	S + D	−1.21	

During mechanosynthetic operations it may be necessary either to push two reactive moieties together to overcome a positive energy reaction barrier via mechanical compression, or alternatively to compel an endoergic bond scission by applying a mechanical tensile force. The application of compressive loads can be limited by mechanical instabilities, e.g., in the case of a single-atom tip pressed against a workpiece atom, the tip atom will tend to slip sideways unless resisted by an adequate transverse stiffness.[3] Using a conservative model of hard spheres of radius r_{tip} and r_{work}, then taking a typical transverse stiffness of $k_{instab} \sim 20$ N/m characteristic of angle bending for a C-C-C system and atomic radii $r_{tip} = r_{work} \sim 1$ Å for a nonbonded contact under substantial loads suggests that the maximum compressive force applicable without slip is of order $F_{compr} \sim (r_{tip} + r_{work})\, k_{instab} \sim 4$ nN, allowing reaction barriers of order $E_{compr} \sim F_{compr}\, r_{tip} \sim 2.5$ eV to be overcome by the application of compressive force,

RS3. Hydrogen Transfer ("HTrans") tool (at top, left) donates H to C111 surface or to Adam bridgehead.

Step	Description of Reaction	Mult.	Ener. (eV)	Barr. (eV)
1	**Donate H to dehydrogenated C111 bridgehead using HTrans tool**			
	R: Diam2 (ACC0A/49) + S15cis (ACC0A/11)	D + D		
	P: Diam1 (ACC0B/50) + S16Run0 (ACCCA/10)	S + S	−1.43	
1¹	**Donate H to dehydrogenated Adam bridgehead using HTrans tool**			
	R: AdamRad (ACC0A/25) + S15cis (ACC0A/11)	D + D		
	P: Adam (ACC0A/26) + S16Run0 (ACCCA/10)	S + S	−1.43	

or ∼2.0 eV for a C-C-Ge system. Tensile loads leading to bond scission must not exceed the combined bond strength of the weakest bonds comprising the diamondoid mechanosynthetic tooltip that is applying the force (Section 3.5).

Additional constraints imposed on reaction sequence design include:

(1) a maximum allowance of 2 tool attachments per atom, 2 tool attachments to any surface-bound workpiece, or 3 tool attachments to any workpiece held in free space, to minimize steric congestion (Section 2.4);

(2) availability of repeatable positional control with six degrees of freedom (assuming dead reckoning of tooltip placement in the workpiece vicinity) that restricts tooltip misplacement error to 0.5 Å or less in all three Cartesian coordinates;

(3) no conditional operations requiring testing the results of a given reaction to ascertain which of two or more states the products are in, before the reaction sequence may be continued, except for mapping the initial feedstock presentation surface;

(4) a conservative preference for maximally valence-satisfied (i.e., no radicals), surface-passivated, or fully saturated intermediate workpiece parking structures whenever possible, and a conservative preference for monovalent over divalent radicals when the presence of radicals cannot be avoided, in order to minimize unplanned reactivity and maximize duration of nonpoisoned operability in imperfect vacuum environments, although monovalent and divalent radicals may appear frequently as intermediates; and

(5) a restriction to purely mechanical synthesis operations requiring no externally imposed electrical fields or tunnel current flow, as distinguished from, for example, the experimental STM-based work of Ho and Lee[32] (electrically-mediated CO abstraction/donation),

Hla et al.[33] (tunnel current-mediated synthesis of biphenyl from two iodobenzene molecules), or of Lyding et al.[34–36] and Basu et al.[37] (tunnel current-mediated H abstraction), because external electric fields can induce nonlocal diffusion processes and many organic molecules are susceptible to unwanted electron-stimulated desorption.[37]
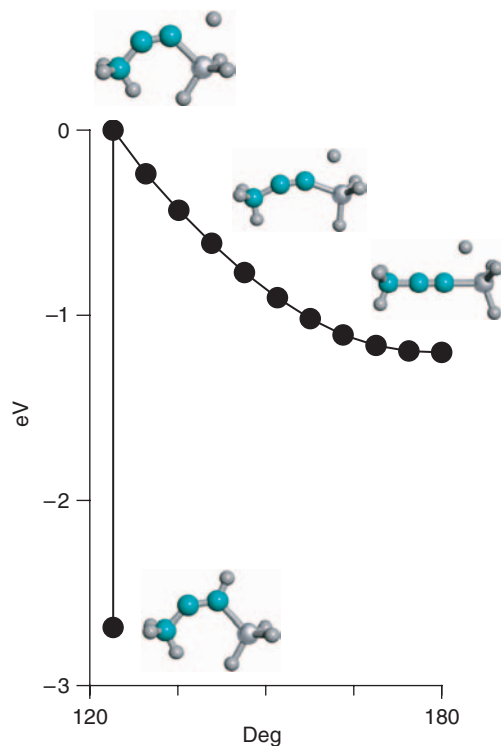
Fig. 2. Discharge of compound hydrogen donation tool modeled as a positionally constrained H_3C-C=CH-GeH_3 cluster and simulated at 6-311 + G($2d, p$)/B3LYP // 3-21G*/B3LYP level of theory as relaxed PES with C=C-Ge (shown in figure) and C-C=C angle constraints.

RS4.   Dimer Placement ("DimerP") tool (at top, left) donates C_2 dimer to DCB6C, a lonsdaleite C111 proxy.

	Step 1			

Step	Description of Reaction	Mult.	Ener. (eV)	Barr. (eV)
1	**Donate C_2 across** DCB6C **bridgehead radicals using DimerP tool**			
	R: Cluster88S (ACC0A/44) + DimerP (ACC0A/46)	S + S		
	P: Cluster92 (ACC0A/46) + DCB6GeOffS (ACC0A/44)	S + S	−0.78	
	R: Cluster88T (ACC0A/44) + DimerP (ACC0A/46)	T + S		
	P: Cluster92 (ACC0A/46) + DCB6GeOffT (ACC0A/44)	S + T	+0.69	
1F5	C_2 dissociates from tool handle			
	R: DimerP (ACC0A/46)	S		
	P: DCB6GeOffS (ACC0A/44) + C2S (ACC0A/2)	S + S	+7.81	
	P: DCB6GeOffT (ACC0A/44) + C2S (ACC0A/2)	T + S	+8.01	

(A)

(B)

(C)

(D)

Fig. 3.   (A) Adam tooltip mounted on pyramidal handle, (B) four DimerP tooltips forced into unstable cubane geometry in free space, and two handled DimerP tools in close (C) and more distant (D) apposition on a workpiece surface.

RS5.   Recharge HAbst tool and recharge HDon tool from GeRad tool (Step 2) [full cage models illustrated].

Step	Description of Reaction	Mult.	Ener. (eV)	Barr. (eV)
1	**Join GeRad tool to apical C atom of HAbstH tool**			
	R: HAbstH (ACC0A/28) + GeRad (ACC0A/25)	S + D		
	P: C15FCcis (ACC0A/53) **[≡HTrans tool]**	D	−0.43 [a]	
	T: Barrier map minimum from Tarasov et al. (2007)			+0.10 [b]
	P: C15FCtrans (ACC0A/53)	D	−0.55	
	R: CH33Ge (ACC0A/13) + ClusterHAbH (ACC0A/16)	D + S		
	T: R1415Trans-QST3 (ACC1A/29)	D		+0.27 [b]
1B1	H steal from HAbstH workpiece to GeRad tool			
	R: HAbstH (ACC0A/28) + GeRad (ACC0A/25)	S + D		
	P: HAbst (ACC0A/27) + HDon (ACC0A/26)	D + S	+2.19	
1D1	H migrates to radical site from adjacent CH in chain on HTrans			
	R: C15FCcis (ACC0A/53)	D		
	P: C15FCp2 (ACC0A/53)	D	−0.13	
	T: C15FCp2TS (ACC1A/53)	D		+1.66
1F6	H dissociates from -C●=CH- group on HTrans tool			
	R: S15cis (ACC0A/11)	D		
	P: S16Run0 (ACCCA/10) + H (ACC0A/1)	S + D	+2.68	
2	**Abstract apical H from HAbstH using GeRad tool**			
	R: S15cis (ACC0A/11) + GeRad (ACC0A/25)	D + D		
	P: S16Run0 (ACCCA/10) + HDon (ACC0A/26)	S	−0.83 [cd]	
	R: S15trans (ACC0A/11) + GeRad (ACC0A/25)	D + D		
	P: S16Run0 (ACCCA/10) + HDon (ACC0A/26)	S	−0.84 [c]	
2F6	H dissociates from GeRad handle of HDon tool			
	R: HDon (ACC0A/26)	S		
	P: GeRad (ACC0A/25) + H (ACC0A/1)	D + D	+3.51	
2H	Ge● radical bonds to C● adjacent to target CH group			
	R: Cluster15cis (ACC1A/29) + CH33Ge (ACC0A/13)	D + D		
	P: Cluster28cis (ACC0A/42)	S	−2.66 [e]	
2¹	**Abstract apical H from HAbstH using AdamRad tool**			
	R: S15cis (ACC0A/11) + AdamRad (ACC0A/25)	D + D		
	P: S16Run0 (ACCCA/10) + Adam (ACC0A/26)	S	−1.43 [c]	
2¹F6	H dissociates from Adam bridgehead site			
	R: HDon (ACC0A/26)	S		
	P: GeRad (ACC0A/25) + H (ACC0A/1)	D + D	+4.12	
3	**Detach GeRad handle from workpiece**			
	R: C16FC-2 (ACC0A/52)	S		
	P: HAbst (ACC0A/27) + GeRad (ACC0A/25)	D + D	+4.81	
	Rotationally constrained:			
	R: S16Run10 (ACCCA/10) (CC-GeRad angle = 180º)	S		
	P: CH3CC (ACC0A/6) + GeH3 (ACC0A/4)	D + D	+4.83	
	R: S16Run0 (ACCCA/10) (CC-GeRad angle = 124º)	S		
	P: CH3CC (ACC0A/6) + GeH3 (ACC0A/4)	D + D	+3.62	
3C4	C≡C steal from workpiece by departing GeRad handle			
	R: C16FC-2 (ACC0A/52)	S		
	P: AdamRad (ACC0A/25) + GeRadCC (ACC0B/27)	D + D	+5.06 [f]	

[a] This energy improves to −0.50 eV using an optimal tool approach trajectory as reported by Tarasov et al. (2007).

[b] The minimum barrier height improves to +0.10 eV using an optimal tool approach trajectory with full-cage

REVIEW

positionally-constrained models producing only a ~0.3 Å deflection at the HAbstH tip prior to bonding, as reported by Tarasov et al. (2007).

c Deletion of apical H from S15cis (doublet) structure, followed by single point evaluation of the resulting structure either as singlet S16initS (ACC0S/10) or triplet S16initT (ACC1S/10), indicates singlet (C≡C) is significantly preferred (by −2.21 eV) to triplet (•C=C•).

d This energy may improve to −1.62 eV using constrained optimally-positioned full-cage models as reported by Tarasov et al. (2007), but our more conservative figure is used in the present paper pending a more detailed analysis of the HTrans tool in future work.

e This highly exoergic pathology is easily avoided by positional control because the H and C• are 2.07 Å apart, well in excess of the assumed 0.50 Å positional uncertainty.

f Even though the reaction energy for pathology 3C4 is only +0.25 eV above the main reaction, this dimer transfer pathology will not occur because C-C bonds (dimer to Adam handle) can withstand greater tensile loads (~5.53 nN) than C-Ge bonds (dimer to GeRad handle) can tolerate (~3.64 nN); see Section 3.5 of text.

Relaxing this restriction might greatly expand the available parameter space for mechanosynthetic reaction design but an analysis of this possibility is beyond the scope of the present paper.

The current work focuses on the energetics of specific mechanosynthetic tools, reaction steps and sequences, rather than on the details of mechanical actuation of handles, the characterization of the atomic structure and orientation of tooltips and handles, or the positional registration of handle-bound mechanosynthetic tools relative to a workpiece, all of which may be the subject of future studies. Tool placement in DMS may occur by dead reckoning without sensory feedback during a mechanosynthetic operation, assuming positional registration of tooltips relative to the workpiece before and after use can be established and maintained. Positional placement tolerances required for successful molecularly-precise site-specific positionally controlled diamond mechanosynthesis are discussed elsewhere at length.[3, 19–24]

2. COMPUTATIONAL METHODS

After a preliminary assessment of possible reaction sequences involving >2600 tooltip/workpiece structures initially screened using semi-empirical AM1 electronic structure optimizations,[38] a more detailed analysis was begun on promising tools, reaction pathways and transition structures using Density Functional Theory (DFT) in Gaussian 98.[39] For the survey work reported in this paper, reaction pathways and transition geometries involving 1630 tooltip/workpiece structures were analyzed to compile 65 Reaction Sequences comprised of 328 reaction steps, 354 unique pathological side reactions and 1321 reported DFT energies, consuming 102,188 CPU-hours (using 1-GHz CPUs). Unless otherwise noted, DFT runs in this study employed singlet or doublet geometries optimized with no constrained degrees of freedom using spin-unrestricted Hartree-Fock (UHF) analysis at the B3LYP/3-21G* level of theory,[40] single point energy calculations performed at the B3LYP/6-311 + G(2d, p) level of theory, and zero-point corrections taken from frequency calculations at the B3LYP/3-21G* level of theory assuming a ZPE scale factor of unity (which introduces negligible error when comparing relative reaction energies between similar structures). The nature of the stationary point was verified using the frequency calculations, with transition structures for barrier height estimation located and optimized using traditional transition state optimizations via the Berny algorithm (TS keyword) and the Synchronous Transit-Guided Quasi-Newton method (QST2, QST3 keywords), along with intrinsic reaction coordinate reaction path following (IRC Forward/Reverse keywords) when needed, as available in Gaussian 98. B3LYP is a hybrid Hartree-Fock/DFT method using Becke's three-parameter gradient-corrected exchange functional (B3)[40] with the Lee-Yang-Parr correlation functional (LYP).[40A]
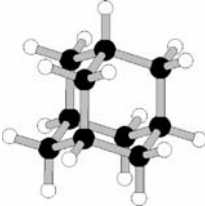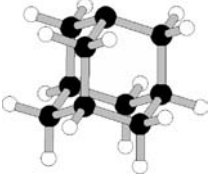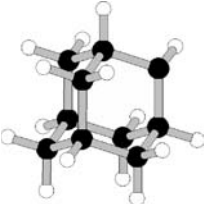
The mean absolute deviation from experiment (MAD) for B3LYP/6-311 + G(2d, p) // B3LYP/3-21G* energies is estimated[41] as 0.14 eV for carbon-rich molecules, which should be adequate for the purposes of this survey-type analysis while conserving computational resources, and which appears slightly superior to the MAD of 0.34 eV estimated[41] for the more commonly reported B3LYP/6-31G* // B3LYP/6-31G* basis set. In conventional positionally uncontrolled chemistry, errors on the order of 0.14 eV might well influence reaction rates and also the dominant reaction pathway taken when multiple alternative reaction pathways are present. However, in the context of the present analysis this should not be an issue because alternative reaction pathways are limited by using positional control and all relevant reaction energy barriers or reaction exoergicities have been chosen to equal or exceed ~0.40 eV for 300 K operation, ~0.20 eV for 80 K operation. Thermal noise is ~0.026 eV at 300 K (~0.007 eV at 80 K). The DFT results for energy barriers should be regarded as conservative because of the well-known underestimation of barrier heights by DFT related to the errors in the self-interaction energy.[42–44]

In this paper, each proposed Reaction Sequence (RS) is reported in a table that lists the positionally-controlled reactant, product, and transition structures, their spin multiplicities and the reaction or barrier energy for each

RS6. Recharge DimerP tool.

Step	Description of Reaction	Mult.	Ener. (eV)	Barr. (eV)
1	**Join GeRad tool to proximal C• radical site of HTrans tool**			
	R: Cluster15cis (ACC1A/29) + CH33Ge (ACC0A/13)	D + D		
	P: Cluster28cis (ACC0A/42)	S	−2.66	
1B2	H steal from adjacent CCH site on HTrans tool by GeRad tool			
	R: S15cis (ACC0A/11) + GeRad (ACC0A/25)	D + D		
	P: S16Run0 (ACCCA/10) + HDon (ACC0A/26)	S	−0.83 [a,b]	
2	**Detach Adam handle from workpiece (handle exchange)**			
	R: Cluster28cis (ACC0A/42)	S		
	P: Cluster29cis (ACC0A/29) + CH33C (ACC0A/13)	D + D	+2.52	
2D1	H migrates to radical site from adjacent CH site			
	R: Cluster29cis (ACC0A/29)	D		
	T: C29p1TS (ACC1A/29)	D		+1.67
3	**Abstract H from Adam bridgehead using HAbst tool**			
	R: Cluster29cis (ACC0A/29) + HAbst (ACC0A/27)	D + D		
	P: Cluster30 (ACC0A/28) + HAbstH (ACC0A/28)	S + S	−4.35	
4	**Attach 2-handled dimer across open radicals on spent DimerP tool**			
	R: Cluster30 (ACC0A/28) + DCB6GeOffS (ACC0A/44)	S + S		
	P: Cluster31 (CXCXA/72)	S	−2.54 [c]	
5	**Detach first GeRad handle from workpiece**			
	R: Cluster31 (CXCXA/72)	S		
	P: Cluster32 (ACC0A/59) + CH33Ge (ACC0A/13)	D + D	+3.32	
6	**Detach second GeRad handle from workpiece**			
	R: Cluster32 (ACC0A/59)	D		
	P: DimerP (ACC0A/46) + CH33Ge (ACC0A/13)	S + D	+1.50	
6C4	C≡C steal from workpiece by departing GeRad handle			
	R: Cluster32 (ACC0A/59)	D		
	P: DCB6GeOffS (ACC0A/44) + CH33GeCC (ACC0A/15)	S + D	+4.05	
	P: DCB6GeOffT (ACC0A/44) + CH33GeCC (ACC0A/15)	T + D	+5.14	

[a] Deletion of apical H from S15cis (doublet) structure, followed by single point evaluation of the resulting structure either as singlet S16 initS (ACC0S/10) or triplet S16initT (ACC1S/10), suggests singlet (C≡C) is very energetically preferred to triplet (•C=C•) by −2.21 eV.

[b] Pathology 1B2 (singlet) can occur but requires a large mispositioning of the tooltip by ~2.09 Å, hence can be avoided by proper positional control.

[c] Bending Cluster30 from linear to trapezoidal geometry prior to joining with the discharged DimerP tool elevates Cluster30 energy, further increasing the exoergicity of this reaction.

REVIEW

Table I. Structural stability of monoradical adamantane. migration, insertion, and *cis-trans* rearrangements of H atoms and CH_3 groups on an isolated adamantane molecule having one monovalent radical site, using DFT at the B3LYP/6-311+G($2d, p$) // B3LYP/3-21G* level of theory with zero-point corrections at B3LYP/3-21G*.

Adamantane ("Adam")	Bridgehead radical site	Sidewall radical site

Migration/insertion rearrangement	Reaction energy $E_{R\rightarrow P}$ (eV)	Forward reaction barrier $\Delta E_{R\rightarrow TS}$ (eV)	Reverse reaction barrier $\Delta E_{P\rightarrow TS}$ (eV)
H migration to cage radical site from cage:			
Sidewall H → sidewall C•	0.00	+1.93	+1.93
Bridgehead H → sidewall C•	0.00	+2.62	+2.62
Bridgehead H → bridgehead C•	0.00	+4.96	+4.96
H migration to cage radical site from methyl:			
Sidewall methyl H → sidewall C•	+0.06	+1.14	+1.08
Bridgehead methyl H → sidewall C•	+0.11	+2.18	+2.07
Bridgehead methyl H → bridgehead C•	+0.11	**>+4.00**[a]	**>+4.00**[a]
H migration to methyl radical site from cage:			
Sidewall H → sidewall CH_2•, cis/cis	−0.06	+1.08	+1.14
Sidewall H → adjacent CH_2•	−0.24	+1.52	+1.76
Bridgehead H → sidewall CH_2•	−0.01	+2.08	+2.09
Methyl migration from cage to cage radical site:			
Bridgehead methyl → sidewall C•	+0.15	+3.43	+3.28
Sidewall methyl → sidewall C•	+0.00	+3.00	+3.00
Bridgehead methyl → bridgehead C•	+0.00	**>+3.40**[b]	**>+3.40**[b]
H migration between two methyls:			
Bridgehead methyl H → sidewall CH_2•	+0.05	+1.05	+1.00
Sidewall methyl H → sidewall CH_2•, cis/cis	+0.00	+1.60	+1.60
Sidewall methyl H → sidewall CH_2•, trans/trans	+0.00	+3.46	+3.47
Methyl migration to second methyl:			
Bridgehead methyl → sidewall CH_2•	+0.04	+3.04	+3.00
Sidewall methyl → sidewall CH_2•, cis/cis	−0.23	+2.57	+2.80
Sidewall methyl → sidewall CH_2•, trans/trans	−0.03	+3.33	+3.36
Methylene insertions:			
Insert bridgehead CH_2• → nearest sidewall C-C	+0.11	+2.45	+2.34
Insert sidewall CH_2• → nearest bridgehead C-C	+0.06	+2.77	+2.71
Insert sidewall CH_2• → neighboring sidewall C-C	+0.35	+3.02	+2.67
Sidewall carbon H-C-CH_3 *cis-trans flips*:			
H-C-H | H-C-(CH_3) → H-C-H | (CH_3)-C-H	0.00	**>+3.40**[c]	**+3.40**[c]
H-C-(CH_3) | H-C-(CH_3) → H-C-(CH_3) | (CH_3)-C-H	+0.09	**>+3.40**[c]	**+3.40**[c]

[a]large distance (4.17 Å) between methyl H and destination C• requires C-H bond dissociation.
[b]large distance (3.85 Å) between methyl C and destination C• requires C-CH_3 bond dissociation.
[c]QST3 runs indicate that C-CH_3 bond dissociation must occur.

reaction step. Every structure has a 6-item computational key. The first three items in each key identify the basis set used to compute the single-point energy, the zero-point correction, and the molecular geometry, respectively, coded as follows: A = B3LYP/6-311+ G($2d, p$), B = B3LYP/6-31G*, C = B3LYP/3-21G*, D = AM1, E = MM2/MM+, X = not used. The fourth item gives results of the normal mode analysis: 0 = energy minimum, 1 = transition state (first-order saddle), 2/3 = transition state (second/third-order saddle), C = geometry-constrained energy minimum, X = not used. (Most instances of imaginary frequencies in non-transition structures represent low-energy (<0.01 eV) handle rotations that do not significantly affect the estimated reaction energies.) The fifth item reports quality of convergence (since full convergence could not be obtained

RS7. Add 1st CH$_3$ to Adam sidewall using GM tool.

Step	Description of Reaction	Mult.	Ener. (eV)	Barr. (eV)
1	**Abstract H from Adam sidewall using HAbst tool**			
	R: Adam (ACC0A/26) + HAbst (ACC0A/27)	S + D		
	P: AdamDot (ACC0A/25) + HAbstH (ACC0A/28)	D + S	−1.58	
2	**Join GM tool to Adam sidewall radical site**			
	R: AdamDot (ACC0A/25) + CH33GeCH2 (ACC0A/16)	D + D		
	P: Cluster51 (ACC0B/41)	S	−3.09	
2A	H steal from GM tool to workpiece CH● radical site			
	R: AdamDot (ACC0A/25) + GM tool (ACC0A/28)	D + D		
	P: Adam (ACC0A/26) + GMA5HS (ABB0A/27)	S + S	+1.02	
	P: Adam (ACC0A/26) + GMA5HT (ACC0A/27)	S + T	+0.31	
	R: AdamDot (ACC0A/25) + CH33GeCH2 (ACC0A/16)	D + D		
	T: AdamHCHGM–QST3 (ABB1B/41)	T		+0.54
2B1	H steal from workpiece to GM tool			
	R: AdamDot (ACC0A/25) + CH33GeCH2 (ACC0A/16)	D + D		
	P: Adam2DotS (ACC1A/24) + CH33GeCH3 (ACC0A/17)	S + S	+0.18	
	T: ADotGM5S–QST3 (ACC2B/41)	S		+0.43
	P: Adam2DotT (ACC0A/24) + CH33GeCH3 (ACC0A/17)	T + S	+0.32	
	T: ADotGM5T–QST3run2 (ACC1A/41)	T		+0.62
2B2	H steal from adjacent bridgehead CH to GM tool (creates			
	C=C on workpiece; "ethenylation" pathology)			
	R: AdamDot (ACC0A/25) + GM tool (ACC0A/28)	D + D		
	P: Side3p3S (ACC0A/24) + GMACH3 (ACC0A/29)	S + S	−0.55 [a]	
	P: Side3p3T (ACC0A/24) + GMACH3 (ACC0A/29)	T + S	−0.05	
	R: AdamDot (ACC0A/25) + GM tool cluster (ACC0A/7)	D + D		
	T: Side3p3TTS (ACC2A/32)	T		+0.48
3	**Detach GeRad handle from workpiece**			
	R: Cluster51 (ACC0B/41)	S		
	P: Cluster52 (ACC0A/28) + CH33Ge (ACC0A/13)	D + D	+2.80	
3B1	H steal from workpiece by departing GeRad handle			
	R: Cluster51 (ACC0B/41)	S		
	P: C52pathS (ACC0A/27) + CH33GeH (ACC0A/14)	S + S	+4.05	
	P: C52pathT (ACC0A/27) + CH33GeH (ACC0A/14)	T + S	+3.80	
4	**Hydrogenate CH$_2$● radical site using HDon tool**			
	R: Cluster52 (ACC0A/28) + HDon (ACC0A/26)	D + S		
	P: Cluster53run2 (ABB0A/29) + GeRad (ACC0A/25)	S + D	−0.67	

[a] The singlet pathology is exoergic with C=C formation and no singlet barrier could be found, but the distance between the target workpiece sidewall CH● radical site and the H atom on the adjacent bridgehead CH is 2.16 Å so this ethenylation pathology can be avoided by positional control.

RS8.   Add 1st CH_3 to Adam sidewall using Meth tool.

| Step 1 | Step 2 | Step 3 | Step 4 | Step 5 ... |

| ... Step 5 | Step 6 | Step 7 | Step 8 |

Step	Description of Reaction	Mult.	Ener. (eV)	Barr. (eV)
1	**Abstract H from Adam sidewall using HAbst tool**			
	R: Adam (ACC0A/26) + HAbst (ACC0A/27)	S + D		
	P: AdamDot (ACC0A/25) + HAbstH (ACC0A/28)	D + S	−1.58	
2	**Join Meth tool to Adam sidewall radical site**			
	R: AdamDot (ACC0A/25) + Meth tool (ACC0A/28)	D + D		
	P: Structure47 (ACC0A/53)	S	−3.03	
2A	H steal from Meth tool to workpiece radical site			
	R: AdamDot (ACC0A/25) + Meth tool (ACC0A/28)	D + D		
	P: Adam (ACC0A/26) + AdamCHS (ACC0A/27)	S + S	+0.61	
	P: Adam (ACC0A/26) + AdamCHT (ACC0A/27)	S + T	+0.47	
2B1	H steal from workpiece to Meth tool			
	R: AdamDot (ACC0A/25) + Meth tool (ACC0A/28)	D + D		
	P: Adam2DotS (ACC1A/24) + AdamCH3 (ACC0A/29)	S + S	+0.22	
	T: TS2sing (ACC1A/53)	S		+1.24
	P: Adam2DotT (ACC0A/24) + AdamCH3 (ACC0A/29)	T + S	+0.36	
	T: TS2trip (ACC1A/53)	T		+2.06
2B2	H steal from adjacent bridgehead CH to Meth tool (creates C=C on workpiece; "ethenylation" pathology)			
	R: AdamDot (ACC0A/25) + Meth tool (ACC0A/28)	D + D		
	P: Side3p3S (ACC0A/24) + AdamCH3 (ACC0A/29)	S + S	**−0.52**[a]	
	P: Side3p3T (ACC0A/24) + AdamCH3 (ACC0A/29)	T + S	−0.03	
	R: AdamDot (ACC0A/25) + CH3CH3 (ACC0A/8)	D + S		
	T: Side3p3MTTS (ACC1A/32)	T		+0.58
3	**Abstract H from Meth tool CH_2 group using HAbst tool**			
	R: Cluster47 (ACC0A/41) + HAbst (ACC0A/27)	S + D		
	P: Cluster48 (ACC0A/40) + HAbstH (ACC0A/28)	D + S	−1.74	
3D7	H migrates to CH• radical from same Adam sidewall worksite			
	R: Cluster48 (ACC0A/40)	D		
	P: Cluster48H (ACC0A/40)	D	−0.13	
	T: Cluster48H-QST2 (ACC1A/40)	D		+1.75
4	**Join GeRad handle to Meth tool CH• radical site**			
	R: Cluster48 (ACC0A/40) + CH33Ge (ACC0A/13)	D + D		
	P: Cluster49 (ACC0A/53)	S	−1.81	
4B1	H steal from CH• radical to GeRad tool			
	R: Cluster48 (ACC0A/40) + GeRad tool (ACC0A/25)	D + D		
	P: C48pathS (ACC0A/39) + HDon tool (ACC0A/26)	S + S	+0.99	
	P: C48pathT (ACC0A/39) + HDon tool (ACC0A/26)	T + S	+0.87	
4B5	H steal from Adam sidewall to which CH• radical is attached			
	R: Cluster48 (ACC0A/40) + CH33Ge (ACC0A/13)	D + D		
	P: C48HStealS (ACC0A/39) + CH33GeH (ACC0A/14)	S + S	−2.14	
	T: ADotC48HGS-QST3 (ACC1A/53)	S		+1.31

Continued

		T: ADotC48HGS-QST3 (ACC1A/53)	S		
		P: C48HStealT (ACC0A/39) + CH33GeH (ACC0A/14)	T + S	+0.32	
		T: ADotC48HGT-QST3 (ACC1A/53)	T		+0.93
5		**Detach Adam handle from workpiece (handle exchange)**			
		R: Cluster49 (ACC0A/53)	S		
		P: Cluster50 (ACC0A/40) + CH33C (ACC0A/13)	D + D	+1.84	
5B1		H steal from workpiece by departing Adam handle			
		R: Cluster49 (ACC0A/53)	S		
		P: Cluster50HS (ACC0A/39) + CH33CH (ACC0A/14)	S + S	+2.72	
		P: Cluster50HT (ACC0B/39) + CH33CH (ACC0A/14)	T + S	+2.14	
		R: C49 (ACC0A/35)	S		
		T: C50p1T-QST2 (ACC2A/35)	T		+3.63
5B5		H steal from Adam sidewall to which CH• radical is attached			
		R: Cluster49 (ACC0A/53)	S		
		P: C49HStealS (ACC0A/39) + CH33CH (ACC0A/14)	S + S	−0.70	
		T: C49HStealS-QST3 (ACC1A/53)	S		+3.71
		P: C49HStealTTS (ACC0B/39) + CH33CH (ACC0A/14)	T + S	+1.80	
		T: C49Path2TTS (ACC1A/53)	T		+2.60
5D7		Hmigrates to CH• radical from same Adam sidewall worksite			
		R: Cluster50 (ACC0A/40)	D		
		P: C50HSteal (ACC0A/40)	D	−0.20	
		T: C50HStealTS (ACC1A/40)	D		+1.51
6		**Hydrogenate CH• radical site using HDon or HTrans tool**			
		R: Cluster50 (ACC0A/40) + HDon (ACC0A/26)	D + S		
		P: Cluster51 (ACC0B/41) + GeRad (ACC0A/25)	S + D	−0.45	
		R: Cluster50 (ACC0A/40) + S15cis (ACCCA/11)	D + S		
		P: Cluster51 (ACC0B/41) + S16Run0 (ACCCA/10)	S + D	−1.28	
7		**Detach GeRad handle from workpiece**			
		R: Cluster51 (ACC0B/41)	S		
		P: Cluster52 (ACC0A/28) + CH33Ge (ACC0A/13)	D + D	+2.80	
8		**Hydrogenate CH₂• radical site using HDon tool**			
		R: Cluster52 (ACC0A/28) + HDon (ACC0A/26)	D + S		
		P: Cluster53run2 (ABB0A/29) + GeRad (ACC0A/25)	S + D	−0.67	

[a] The singlet pathology is exoergic with C=C formation and no singlet barrier could be found, but the distance between the target workpiece sidewall CH• radical site and the H atom on the adjacent bridgehead CH is 2.16 Å so this ethenylation pathology can be avoided by positional control.

in all cases using available resources): A = fully converged (standard Gaussian criteria), B = provisionally converged (on 2–3 standard Gaussian criteria, but with cycling/wandering), C = partly converged (on 1 standard Gaussian criteria, with cycling/wandering), D = beginning approach to convergence (on 1 or more Gaussian criteria; B, C, or D may require higher level of theory), F = unconverged, M = converged (standard default AM1 or MM2/MM+ criteria), S = single-point energy calculation only. The sixth item is atom count.

Reaction steps include possible pathological side reactions that may occur during or after step completion. Each pathology is placed in one of 10 possible classes: A = workpiece steals hydrogen atom from incoming/departing tool, B = incoming/departing tool steals hydrogen atom from workpiece (10 variants), C = incoming/departing tool steals non-hydrogen group from workpiece (4 variants), D = hydrogen atom migrates on workpiece product structure (19 variants), E = CH₃ group migrates on workpiece product structure, F = workpiece dissociates during/after reaction (6 variants), G = radical group inserts into adjacent bond on workpiece product structure (7 variants), H = structure having two or more radicals crossbonds during reaction, I = geometric isomer transition, and J = hydrogen atom migration does not occur. Pathologies that are endoergic by more than +0.40 eV at 300 K (+0.20 eV at 80 K), or pathologies that are more endoergic than endoergic class A or class B main reactions by these amounts, are assumed not to occur. In the Reaction Sequence tables, duplicative pathological reactions or rearrangements already reported in a prior RS are omitted for brevity. RS structure drawings are provided to indicate atomic identity and connectivity, not to precisely illustrate energy-minimized DFT geometries (which are provided in the supplemental structure files).

To conserve computational resources, smaller cluster models of HAbst, HDon, GeRad, adamantyl/adamantane and germantyl/germantane structurally analogous to isobutane or methane were sometimes employed in the DFT studies. This substitution usually introduces at most a small error less than or comparable to the presumed 0.14 eV MAD for the classes of molecules examined here.

RS9. Add 1st CH$_3$ to Adam bridgehead using GM tool.

	Step 1	Step 2	Step 3	Step 4	

Step	Description of Reaction	Mult.	Ener. (eV)	Barr. (eV)
1	**Abstract H from Adam bridgehead using HAbst tool**			
	R: Adam (ACC0A/26) + HAbst (ACC0A/27)	S + D		
	P: AdamRad (ACC0A/25) + HAbstH (ACC0A/28)	D + S	−1.59	
2	**Join GM tool to Adam bridgehead radical site**			
	R: AdamRad (ACC0A/25) + GM tool (ACC0A/28)	D + D		
	P: GMA7 (ACC0A/53)	S	−3.17	
2A	H steal from GM tool to workpiece radical site			
	R: AdamRad (ACC0A/25) + GM tool (ACC0A/28)	D + D		
	P: Adam (ACC0A/26) + GMA5HS (ABB0A/27)	S + S	+1.02	
	P: Adam (ACC0A/26) + GMA5HT (ACC0A/27)	S + T	+0.32	
	R: AdamRad (ACC0A/25) + GM5 (ACC0A/16)	D + D		
	T: AdamHCHGM5TTS (ABB3B/41)	T		+1.60
2B2	H steal from adjacent sidewall CH$_2$ to GM tool (creates C=C on workpiece; "ethenylation" pathology)			
	R: AdamRad (ACC0A/25) + GM tool (ACC0A/28)	D + D		
	P: Adam2RadS (ACC0A/24) + GMACH3 (ACC0A/29)	S + S	−0.54 [a]	
	P: Adam2RadT (ACC0A/24) + GMACH3 (ACC0A/29)	T + S	−0.04	
	R: AdamRad (ACC0A/25) + GM tool cluster (ACC0A/7)	D + D		
	T: Adam2RadTTS (ACC1A/32)	T		+0.63
3	**Detach GeRad handle from workpiece**			
	R: GMA7 (ACC0A/53)	S		
	P: Meth tool (ACC0A/28) + GeRad (ACC0A/25)	D + D	+2.76	
3B1	H steal from workpiece by departing GeRad handle			
	R: GMA7 (ACC0A/53)	S		
	P: AdamCHS (ACC0A/27) + HDon (ACC0A/26)	S + S	+3.98	
	P: AdamCHT (ACC0A/27) + HDon (ACC0A/26)	T + S	+3.84	
4	**Hydrogenate CH$_2$• radical site using HDon tool**			
	R: Meth tool (ACC0A/28) + HDon (ACC0A/26)	D + S		
	P: AdamCH3 (ACC0A/29) + GeRad (ACC0A/25)	S + D	−0.70	

[a] The singlet pathology is exoergic with C=C formation and no singlet barrier could be found, but the distance between the target workpiece bridgehead C• radical site and the H atom on the adjacent sidewall CH$_2$ is 2.17 Å so this ethenylation pathology can be avoided by positional control.
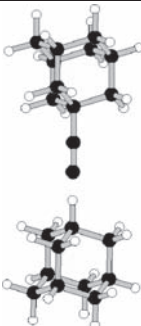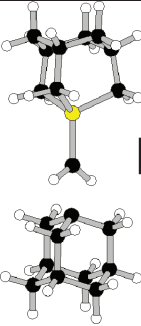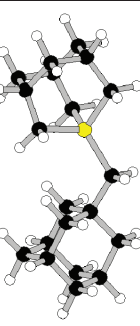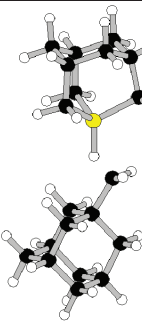
For example, in Step 3 of RS5 (HAbst recharge), the singlet reaction energy is +4.83 eV using the smallest possible H$_3$C-CC• and H$_3$Ge• cluster models, +4.95 eV using the larger $(CH_3)_3$C-CC• and $(CH_3)_3$Ge• cluster models, and +4.81 eV using still larger full-cage (C_9H_{15})C-CC• and (C_9H_{15})Ge• models ($\Delta_{range} = 0.14$ eV). For Step 2 of RS9 (AdamRad + GM Tool radical coupling), the reaction is exoergic by −3.33 eV using an H$_3$Ge• handle or by −3.17 eV using a full cage (C_9H_{15})Ge• handle ($\Delta_{range} = 0.16$ eV); pulling off the GeRad handle from the

resulting structure (Step 3 of RS9) is computed as endoergic by +2.91 eV for H$_3$Ge•, +2.81 eV for $(CH_3)_3$Ge•, or +2.76 eV for (C_9H_{15})Ge• ($\Delta_{range} = 0.15$ eV). In pathology 3B1 of RS41 (build Meth tool), the triplet reaction energy is +0.30 eV using a $(GeH_3)_3$Ge-CH$_2$• cluster to model the Ge surface and +0.12 eV using a full-cage germantane $(Ge_{10}H_{15}$-CH$_2$•) model ($\Delta_{range} = 0.18$ eV). Basis set effects for these molecules appear small: in line with the general basis set insensitivity of DFT, the B3LYP/6-311+G(2d, p) energy computed for the B3LYP/3-21G* geometry of, for

774

*J. Comput. Theor. Nanosci. 5, 760–861, **2008***

RS10. Add 1st CH$_3$ to Adam bridgehead using Meth tool.

	Step 1	Step 2	Step 3	Step 4	Step 5 …

… Step 5	Step 6	Step 7	Step 8	

Step	Description of Reaction	Mult.	Ener. (eV)	Barr. (eV)
1	**Abstract H from Adam bridgehead using HAbst tool**			
	R: Adam (ACC0A/26) + HAbst (ACC0A/27)	S + D		
	P: AdamRad (ACC0A/25) + HAbstH (ACC0A/28)	D + S	−1.59	
2	**Join Meth tool to Adam bridgehead radical site**			
	R: AdamRad (ACC0A/25) + CH33CCH2 (ACC0A/16)	D + D		
	P: Cluster10MA3 (ACC0A/41)	S	−2.96	
2A	H steal from Meth tool to workpiece radical site			
	R: AdamRad (ACC0A/25) + Meth tool (ACC0A/28)	D + D		
	P: Adam (ACC0A/26) + AdamCHS (ACC0A/27)	S + S	+0.62	
	P: Adam (ACC0A/26) + AdamCHT (ACC0A/27)	S + T	+0.47	
2B2	H steal from adjacent sidewall CH$_2$ to GM tool (creates C=C on workpiece; "ethenylation" pathology)			
	R: AdamRad (ACC0A/25) + Meth tool (ACC0A/28)	D + D		
	P: Adam2RadS (ACC0A/24) + AdamCH3 (ACC0A/29)	S + S	−0.52[a]	
	P: Adam2RadT (ACC0A/24) + AdamCH3 (ACC0A/29)	T + S	−0.02	
	R: AdamRad (ACC0A/25) + GM tool cluster (ACC0A/7)	D + D		
	T: Adam2RadMTTS (ACC1A/32)	T		+0.72
3	**Abstract H from Meth tool CH$_2$ group using HAbst tool**			
	R: Cluster10MA3 (ACC0A/41) + HAbst (ACC0A/27)	S + D		
	P: Cluster10MA4 (ACC0A/40) + HAbstH (ACC0A/28)	D + S	−1.74	
4	**Join GeRad handle to Meth tool CH• radical site**			
	R: Cluster10MA4 (ACC0A/40) + CH33Ge (ACC0A/13)	D + D		
	P: Cluster10M3 (ACC0B/53)	S	−1.88	
4B1	H steal from CH• radical to GeRad tool			
	R: Cluster10MA4 (ACC0A/40) + GeRad tool (ACC0A/25)	D + D		
	P: Cluster10MA4HS (ACC0A/39) + HDon tool (ACC0A/26)	S + S	+1.05	
	P: Cluster10MA4HT (ACC0A/39) + HDon tool (ACC0A/26)	T + S	+0.80	
5	**Detach Adam handle from workpiece (handle exchange)**			
	R: Cluster10M3 (ACC0B/53)	S		
	P: Cluster10M4 (ACC0A/40) + CH33C (ACC0A/13)	D + D	+1.77	
5B1	H steal from workpiece by departing Adam handle			
	R: Cluster10M3 (ACC0B/53)	S		

Continued

	P: C10M4HS (ACC0A/39) + CH33CH (ACC0A/14)	S + S	+2.64	
	P: C10M4HT (ACC0A/39) + CH33CH (ACC0A/14)	T + S	+2.07	
	R: C10M4H (ACC0A/35)	S		
	T: C10M4HT-QST2 (ACC1A/35)	T		+3.58
6	**Hydrogenate CH• radical site using HDon tool**			
	R: Cluster10M4 (ACC0A/40) + HDon (ACC0A/26)	D + S		
	P: Cluster10M5 (ACC0A/41) + GeRad (ACC0A/25)	S + D	−0.49	
7	**Detach GeRad handle from workpiece**			
	R: Cluster10M5 (ACC0A/41)	S		
	P: Meth tool (ACC0A/28) + CH33Ge (ACC0A/13)	D + D	+2.81	
7B1	H steal from workpiece by departing GeRad handle			
	R: Cluster10M5 (ACC0A/41)	S		
	P: AdamCHS (ACC0A/27) + CH33GeH (ACC0A/14)	S + S	+3.94	
	P: AdamCHT (ACC0A/27) + CH33GeH (ACC0A/14)	T + S	+3.80	
8	**Hydrogenate CH$_2$• radical site using HDon tool**			
	R: Meth tool (ACC0A/28) + HDon (ACC0A/26)	D + S		
	P: AdamCH3 (ACC0A/29) + GeRad (ACC0A/25)	S + D	−0.70	

[a] The singlet pathology is exoergic with C=C formation and no singlet barrier could be found, but the distance between the target workpiece bridgehead C• radical site and the H atom on the adjacent sidewall CH$_2$ is 2.17 Å so this ethenylation pathology can be avoided by positional control.

example, the Adambenzene (GRAP9D) structure produced by RS61 lies +0.011 eV above the B3LYP/6-31G* geometry, which in turn lies only +0.009 eV above the B3LYP/6-311+G(2d, p) geometry.

The present analysis is the first quantitative systems level study of a complete suite of positionally controlled reaction pathways for diamond mechanosynthesis. Additional theoretical examination of transition structures and reaction barriers using higher levels of theory is desirable to validate all reaction steps and to confirm the stability of all intermediate structures proposed here. The present results may also serve as a framework for more intensive computational analyses of alternative reaction pathways and more complex product structures.

3. STRUCTURE AND FUNCTION OF THE THREE PRIMARY TOOLS

3.1. Hydrogen Abstraction Tool (HAbst)

Undoped diamond normally consists of a rigid lattice of carbon atoms surface-passivated by hydrogen atoms, so a necessary aspect of diamond mechanosynthesis is the positionally-controlled abstraction (removal) of hydrogen atoms from stiff hydrocarbon structures—including hydrogens terminating the surface of the diamond crystal lattice, hydrogens present in feedstock molecules, and hydrogen atoms bonded to partly or fully completed mechanosynthetic tools or handle structures. The archetypal hydrogen abstraction tool makes use of an ethynyl (acetylene) radical[45] attached to a handle structure that first approaches a hydrogenated diamond surface as a site-specific active tool and then is retracted from a partially dehydrogenated diamond surface as a spent tool (RS1). The simplest practical HAbst tool is the ethynyl radical mounted on an

adamantane base (1-ethynyladamantane; Fig. 1(A)) which is readily covalently bonded to a larger handle structure by extension of a regular diamond lattice of which the adamantane base is a unit cage.

The hydrogen abstraction tool has received substantial theoretical study and computational validation.[3–8, 46–49] In early work, Valone et al.[46] found no activation energy was required to abstract an H atom from a C$_{20}$H$_{35}$ cluster model of the diamond C(111) surface, using AM1 semi-empirical self-consistent field calculations. Chang et al.[7] employed Brenner's empirical potential energy function[50] and found an abstraction barrier energy of ~0.4 eV, while Page and Brenner[5] used *ab initio* MCSCF to calculate a +0.33 eV reaction barrier for H abstraction from H-C(CH$_3$)$_3$ or isobutane, the simplest sp^3 cluster model of the C(111) surface. In later more accurate work, Musgrave et al.[6] used generalized valence-bond configuration-interaction self-consistent field *ab initio* quantum-chemistry techniques including electron correlation to calculate reaction barriers for H abstraction from sp^3 hybridized carbons of <0.18 eV for H-CH$_3$ (methane) and <0.02 eV for H-C(CH$_3$)$_3$ (isobutane) cluster models; the reaction was found to be exoergic by −1.16 eV in both cases.

The most recent and highest-accuracy computational analysis of the ethynyl radical operating on small cluster targets by Temelso et al.[8] reports H abstraction from sp^3 carbon (isobutane model) to be exoergic by $\Delta H(298) = −1.53$ eV (close to the −1.59 eV experimental value) with zero reaction barrier at the CCSD(T)/DZ** level of theory using UHF references with ΔZPVE, thermal, and Wigner tunneling corrections evaluated at the UMP2/cc-pVDZ level of theory at 298 K. The HAbst tool is extremely unlikely to auto-abstract its own hydrogens[8] or to rearrange its tip geometry, despite its highly reactive distal tip, because the energy barriers to such rearrangements

RS11. Add 1st CH_3 to Adam bridgehead using Meth tool.

Step 1–2	Step 3	Step 4	Step 5	Step 6 …

… Step 6	Step 7	Step 8	Step 9	Step 10	

Step	Description of Reaction	Mult.	Ener. (eV)	Barr. (eV)
1	**Abstract H from Adam bridgehead using HAbst tool**			
	R: Adam (ACC0A/26) + HAbst (ACC0A/27)	S + D		
	P: AdamRad (ACC0A/25) + HAbstH (ACC0A/28)	D + S	−1.59	
2	**Join Meth tool to Adam bridgehead radical site**			
	R: AdamRad (ACC0A/25) + CH33CCH2 (ACC0A/16)	D + D		
	P: Cluster10MA3 (ACC0A/41)	S	−2.96	
3	**Abstract H from Meth tool CH_2 group using HAbst tool**			
	R: Cluster10MA3 (ACC0A/41) + HAbst (ACC0A/27)	S + D		
	P: Cluster10MA4 (ACC0A/40) + HAbstH (ACC0A/28)	D + S	−1.74	
4	**Abstract H from Meth tool CH• group using HAbst tool**			
	R: Cluster10MA4 (ACC0A/40) + HAbst (ACC0A/27)	D + D		
	P: Cluster10MA4HS (ACC0A/39) + HAbstH (ACC0A/28)	S + S	−1.14	
	P: Cluster10MA4HT (ACC0A/39) + HAbstH (ACC0A/28)	T + S	−1.39	
4D2	H migrates to C: radical site from adjacent sidewall CH_2			
	R: Cluster10MA4HS (ACC0A/39)	S		
	P: Cluster10MA4HSH15 (ACC0A/39)	S	−1.44	
	T: C10MA4HSH15-QST2 (ACC1A/39)	S		+1.00
	R: Cluster10MA4HT (ACC0A/39)	T		
	P: Cluster10MA4HTH22 (ACC0A/39)	T	−0.22	
	T: C10MA4HTH22-QST3 (ACC1A/39)	T		+1.87
4G2	C: radical inserts into adjacent sidewall CH_2 in handle cage			
	R: Cluster10MA4HS (ACC0A/39)	S		
	P: C10MA4HTIns20 (ACC0B/39)	S	−1.30	
	T: C10MA4HTIns20-QST3S (ACC1A/39)	S		+0.56
	R: Cluster10MA4HT (ACC0A/39)	T		
	P: C10MA4HTIns20T (ACC0A/39)	T	−0.37	
	T: C10MA4HTIns20T-QST2 (ACC1A/39)	T		+2.35
5	**Join GeRad tool to Meth tool C: radical site**			
	R: Cluster10MA4HS (ACC0A/39) + CH33Ge (ACC0A/13)	S + D		
	P: Cluster10M3A (ACC0A/52)	D	−2.63	
	R: Cluster10MA4HT (ACC0A/39) + CH33Ge (ACC0A/13)	T + D		
	P: Cluster10M3A (ACC0A/52)	D	−2.38	
6	**Detach Adam handle from workpiece (handle exchange)**			
	R: Cluster10M3A (ACC0A/52)	D		
	P: C10M4HS (ACC0A/39) + CH33C (ACC0A/13)	S + D	+2.73	

Continued

	P: C10M4HT (ACC0A/39) + CH33C (ACC0A/13)	T + D	+2.16	
6D2	H migrates to C: radical site from adjacent sidewall CH$_2$			
	R: C10M4HS (ACC0A/39)	S		
	P: C10M4HTH16S (ACC0A/39)	S	−1.48	
	T: C10M4HTH16S-QST2 (ACC1A/39)	S		+0.84
	R: C10M4HT (ACC0A/39)	T		
	P: C10M4HTH16T (ACC0A/39)	T	−0.10	
	T: C10M4HTH16T-QST2 (ACC1A/39)	T		+1.95
6G2	C: radical inserts into adjacent sidewall CH$_2$ in handle cage			
	R: C10M4HS (ACC0A/39)	S		
	P: C10M4HTIns8run3 (ABB0A/39)	S	−1.81	
	T: C10M4HTIns8-QST2 (ACC1A/39)	S		**+0.31**[a]
	R: C10M4HT (ACC0A/39)	T		
	P: C10M4HTIns8T (ACC0A/39)	T	−0.21	
	T: C10M4HTIns8T-QST2 (ACC2D/39)			+0.65
7	**Hydrogenate C: radical site using HDon tool**			
	R: C10M4HS (ACC0A/39) + HDon (ACC0A/26)	S + S		
	P: Cluster10M4 (ACC0A/40) + GeRad (ACC0A/25)	D + D	−1.25	
	R: C10M4HT (ACC0A/39) + HDon (ACC0A/26)	T + S		
	P: Cluster10M4 (ACC0A/40) + GeRad (ACC0A/25)	D + D	−0.68	
8	**Hydrogenate CH● radical site using HDon tool**			
	R: Cluster10M4 (ACC0A/40) + HDon (ACC0A/26)	D + S		
	P: Cluster10M5 (ACC0A/41) + GeRad (ACC0A/25)	D + D	−0.49	
9	**Detach GeRad handle from workpiece**			
	R: Cluster10M5 (ACC0A/41)	S		
	P: Meth tool (ACC0A/28) + CH33Ge (ACC0A/13)	D + D	+2.81	
10	**Hydrogenate CH$_2$● radical site using HDon tool**			
	R: Meth tool (ACC0A/28) + HDon (ACC0A/26)	D + S		
	P: Adam CH$_3$ (ACC0A/29) + GeRad (ACC0A/25)	S + D	−0.70	

[a] Despite an apparently insufficient energy barrier to prevent pathology 6G (singlet), this pathology will not occur because (1) positional restraints imposed by fixed tool handles should add >0.10 eV of supplemental mechanical barrier energy, and (2) the singlet Reactant (C10M4HS) lies +0.57 eV above the triplet Reactant (C10M4HT), hence the Reactant should remain in the triplet state.

appear quite large. For example, the energy barrier preventing auto-abstraction of an H atom from a neighboring sidewall carbon atom on the handle exceeds +2.47 eV at the MP2/DZ level of theory.[8] An analysis of tooltip bending stiffness at 298 K by examining the classical turning points on the bending potential indicates that the four most populated vibrational levels (62% population of $n = 0$ level, 24% of $n = 1$, 9% of $n = 2$, 3% of $n = 3$; total 98%) imply positional uncertainties of 0.12, 0.15, 0.19 and 0.24 Å, respectively.[8] Given that adjacent H atoms on C(111)-H(1×1) surface lie 2.5 Å apart, even a vibrationally excited tooltip should have good positional selectivity at modest temperatures. Of greater concern, the short-lived (approx. transition time ~20–60 μsec) but non-reactive A^{2}Π excited electronic state of the ethynyl radical is kinetically accessible and may be thermally populated, relative to the long-lived reactive ground state, to 10^{-4} at 298 K and 10^{-14} at 77 K.[8] Regarding the contribution to reaction error rate caused by tooltip unreactivity in the excited state and the required transition time from excited to ground state, if a ~10^{-4} error rate at 298 K or a ~10^{-14} error rate at 77 K is acceptable then the speed of tool operation is unconstrained by the required transition

time; otherwise, the HAbst tool may be restricted to operation at ~10 KHz at 300 K, while being essentially speed-unrestricted at 80 K.

Apparently single-cage HAbstH (1-ethynyladamantane or adamantane-1-ethynyl)[51] and related species (e.g., 1-ethynyl-3,5-dimethyladamantane)[52] have been investigated experimentally. Site-specific hydrogen abstraction from crystal surfaces, though not purely mechanical abstraction, has also been achieved experimentally. For example, Lyding et al.[34–36] demonstrated the ability to abstract an individual hydrogen atom from a specific atomic position in a covalently-bound hydrogen monolayer on a flat Si(100) surface, using an electrically-pulsed STM tip in ultrahigh vacuum. Ho's group[53] has similarly demonstrated positionally controlled single-atom hydrogen abstraction experimentally, using an STM. Hydrogen abstraction from CH$_4$,[54–56] H$_2$,[56–61] C$_2$H$_2$,[60–63] H$_2$O,[64] NH$_3$,[65–68] C$_2$H$_4$,[54] C$_2$H$_6$,[54, 69] C$_6$H$_6$,[66] and other organics[70] by positionally unconstrained ethynyl radicals has been extensively investigated both experimentally and theoretically.

Interestingly, the HAbst (ethynyl) tool might also be used as a vertical dimer placement tool (RS48) (Section 8.2).

RS12. Add 1st CH_3 to C111 bridgehead using GM tool.

Step	Description of Reaction	Mult.	Ener. (eV)	Barr. (eV)
1	**Abstract H from C111 bridgehead using HAbst tool**			
	R: Diam1 (ACC0B/50) + HAbst (ACC0A/27)	S + D		
	P: Diam2 (ACC0A/49) + HAbstH (ACC0A/28)	D + S	−1.59	
1D3	H migrates to radical from adjacent C111 bridgehead CH			
	R: Diam2 (ACC0A/49)	D		
	T: Diam2HTS (ACC1A/49)	D		+2.22
2	**Join GM tool to C111 bridgehead radical site**			
	R: Diam2 (ACC0A/49) + GM tool cluster (ACC0A/7)	D + D		
	P: Diam3 (ACC0A/56)	S	−2.37	
2A	H steal from GM tool to C111 bridgehead radical site			
	R: Diam2 (ACC0A/49) + GM tool (ACC0A/28)	D + D		
	P: Diam1 (ACC0B/50) + GMA5HS (ABB0A/27)	S + S	+1.02	
	P: Diam1 (ACC0B/50) + GMA5HT (ACC0A/27)	S + T	+0.32	
	R: Diam2 (ACC0A/49) + GM tool cluster (ACC0A/7)	D + D		
	T: Diam3HT-QST3 (ACC2A/56)	T		+0.66
2B2	H steal from adjacent CH site on C111 surface by GM tool			
	R: Diam2 (ACC0A/49) + GM tool (ACC0A/28)	D + D		
	P: Diam2RadS (ACC0A/48) + GMACH3 (ACC0A/29)	S + S	+0.79	
	P: Diam2RadT (ACC0A/48) + GMACH3 (ACC0A/29)	T + S	−0.14	
	R: Diam2 (ACC0A/49) + GM tool cluster (ACC0A/7)	D + D		
	T: Diam2RadTTS (ACC1B/56)	T		+0.60
3	**Detach GeRad handle from workpiece**			
	R: Diam3 (ACC0A/56)	S		
	P: Diam4run2 (ABB1B/52) + GeH3 (ACC0A/4)	D + D	+2.33	
3B1	H steal from worksite on workpiece by departing GeRad handle			
	R: Diam3 (ACC0A/56)	S		
	T: Diam4HSTS (ACC1A/51) + GeH4 (ACC0A/5)	S + S		+3.47
	P: Diam4HT (ACC0B/51) + GeH4 (ACC0A/5)	T + S	+3.19	
3D5	H migrates to $CH_2\bullet$ radical site from adjacent surface site			
	R: Diam4run2 (ABB1B/52)	D		
	P: Diam4HH (ACC0A/52)	D	0.00	
	T: Diam4HH-QST2 (AXCXA/52)	D		+1.09
4	**Hydrogenate $CH_2\bullet$ radical site using HDon tool**			
	R: Diam4run2 (ABB1B/52) + HDon (ACC0A/26)	D + S		
	P: Diam5 (ACC0A/53) + GeRad (ACC0A/25)	S + D	−0.52	

3.2. Hydrogen Donation Tool (HDon)

Another necessary aspect of diamond mechanosynthesis is the positionally-controlled donation of hydrogen atoms to stiff hydrocarbon structures—including hydrogens terminating the surface of the diamond crystal lattice or to partly or fully completed mechanosynthetic tools or handle structures. The simplest hydrogen donation tool is the Group IV-substituted adamantane such as the germanium-substituted adamantane (1,1-germanoadamantane) (Fig. 1(B)) that is brought up to a partially

dehydrogenated diamond surface as a site-specific active tool and then is retracted from a now-rehydrogenated diamond surface as a spent tool (RS2). The HDon tool is readily covalently bonded to a larger handle structure by extension of a regular diamond lattice of which the adamantane base is a unit cage.

The radical chemistry of H donation has been studied[71–76] and hydrogen donation tools for DMS have been described qualitatively,[3, 4] but only recently have such tools been investigated theoretically using the tools of computational chemistry. The first high-quality analysis

RS13.   Add 1st CH$_3$ to C110 ridge site using GM tool.

Step	Description of Reaction	Mult.	Ener. (eV)	Barr. (eV)
1	**Abstract H from C110 ridge site using HAbst tool**			
	R: C110A (ACC0A/42) + HAbst (ACC0A/27)	S + D		
	P: C110B (AXCXA/41) + HAbstH (ACC0A/28)	D + S	−1.22	
1D5	H migrates to radical from adjacent ridge site			
	R: C110B (AXCXA/41)	D		
	T: C110BHTS (AXCXA/41)	D		+2.74
2	**Join GM tool to C110 ridge radical site**			
	R: C110B (AXCXA/41) + GM tool cluster (ACC0A/7)	D + D		
	P: C110Crun2 (ACC0A/48)	S	−3.17	
2A	H steal from GM tool to workpiece radical site			
	R: C110B (AXCXA/41) + GM tool (ACC0A/28)	D + D		
	P: C110A (ACC0A/42) + GMA5HS (ABB0A/27)	S + S	+0.98	
	P: C110A (ACC0A/42) + GMA5HT (ACC0A/27)	S + T	+0.29	
	R: C110B (AXCXA/41) + GM tool cluster (ACC0A/7)	D + D		
	T: C110Cp1TTS (ACC1A/48)	T		+0.64
2B2	H steal from adjacent CH site on same ridge by GM tool, leading to ethenylation pathology			
	R: C110B (AXCXA/41) + GM tool cluster (AXC0A/7)	D + D		
	T: C110Bp2S-QST3 (AXC2C/48)	S		+0.88
	R: C110B (AXCXA/41) + GM tool (AXC0A/28)	D + D		
	P: C110Bp2T (AXC0A/40) + GMACH3 (AXC0A/29)	T + S	−0.03	
	R: C110B (AXCXA/41) + GM tool cluster (AXC0A/7)	D + D		
	T: C110Bp2TTS (AXC1A/48)	T		+0.59
3	**Detach GeRad handle from workpiece**			
	R: C110Crun2 (ACC0A/48)	S		
	P: C110Drun2 (ACC0A/44) + GeH3 (ACC0A/4)	D + D	+2.69	
3B1	H steal from worksite on workpiece by departing GeRad handle			
	R: C110Crun2 (ACC0A/48)	S		
	P: C110DHS (ACC0A/43) + GeH4 (ACC0A/5)	S + S	+3.82	
	P: C110DHT (ACC0A/43) + GeH4 (ACC0A/5)	T + S	+3.63	
3D5	H migrates to CH$_2\bullet$ radical site from adjacent surface site			
	R: C110Drun2 (ACC0A/44)	D		
	P: C110DHH (ACC0A/44)	D	−0.04	
	T: C110DHHTS (ACC1A/44)	D		+1.01
3G5	CH$_2\bullet$ bonds to adjacent ridge carbon and inserts into ridge			
	R: C110Drun2 (ACC0A/44)	D		
	P: C110DIns3 (ACC0A/44)	D	+0.36	
	T: C110DIns3-QST3 (ACC1A/44)	D		+2.63
4	**Hydrogenate CH$_2\bullet$ radical site using HDon tool**			
	R: C110Drun2 (ACC0A/44) + HDon (ACC0A/26)	D + S		
	P: C110E (ACC0A/45) + GeRad (ACC0A/25)	S + D	−0.57	

REVIEW

RS14. Add 1st CH_3 to C100 dimer site using GM tool.

	Step 1	Step 2	Step 3	Step 4	

Step	Description of Reaction	Mult.	Ener. (eV)	Barr. (eV)
1	**Abstract H from C100 dimer site using HAbst tool**			
	R: C1002d (ACC0A/35) + HAbst (ACC0A/27)	S + D		
	P: C1002dBH (ACC0A/34) + HAbstH (ACC0A/28)	D + S	−1.38	
1D5	H migrates to radical from nearest adjacent dimer in same dimer row			
	R: C1002dBH (ACC0A/34)	D		
	T: C1002dBHTS (ACC1A/34)	D		+2.73
1D8	H migrates to radical from same dimer site			
	R: C100B (ACC0A/22)	D		
	T: C100MBp3TS (ACC1A/37)	D		+2.19
2	**Join GM tool to C100 dimer radical site**			
	R: C1002dBH (ACC0A/34) + GM tool cluster (ACC0A/7)	D + D		
	P: C1002dC (ACC0B/41)	S	−3.29	
2A	H steal from GM tool to workpiece radical site			
	R: C100B (ACC0A/22) + GM tool (ACC0A/28)	D + D		
	P: C100A (ACC0A/23) + GMA5HS (ABB0A/27)	S + S	+0.82	
	P: C100A (ACC0A/23) + GMA5HT (ACC0A/27)	S + T	+0.11	
	R: C100B (ACC0A/22) + GM tool cluster (ACC0A/7)	D + D		
	T: C100Bp1TTS (ACC1A/29)	T		+0.42
2B4	H steal from nearest CH site on adjacent dimer by GM tool			
	R: C1002dBH (ACC0A/34) + GM tool (ACC0A/28)	D + D		
	P: C1002dBp3S (ACC0A/33) + GMACH3 (ACC0A/29)	S + S	+0.71	
	P: C1002dBp3T (ACC0A/33) + GMACH3 (ACC0A/29)	T + S	+0.11	
	R: C1002dBH (ACC0A/34) + GM tool cluster (ACC0A/7)	D + D		
	T: C1002dBp3TTS (ACC1A/41)	T		+0.55
2B6	H steal from CH site on same dimer by incoming GM tool			
	R: C100B (ACC0A/22) + GM tool (ACC0A/28)	D + D		
	P: C100Bp2S (ACC0A/21) + GMACH3 (ACC0A/29)	S + S	−0.93[a]	
	P: C100Bp2T (ACC0A/21) + GMACH3 (ACC0A/29)	T + S	+0.30	
	R: C100B (ACC0A/22) + GM tool cluster (ACC0A/7)	D + D		
	T: C100Bp2TTS (ACC2A/29)	T		+0.63
3	**Detach GeRad handle from workpiece**			
	R: C1002dC (ACC0B/41)	S		
	P: C1002dD (ACC0A/37) + GeH3 (ACC0A/4)	D + D	+2.66	
3B1	H steal from CH_2 group on workpiece by departing GeRad handle			
	R: C100C (ACC0A/29)	S		
	P: C100DHS (ACC0A/24) + GeH4 (ACC0A/5)	S + S	+3.88	
	P: C100DHT (ACC0A/24) + GeH4 (ACC0A/5)	T + S	+3.79	
3B4	H steal from nearest CH on adjacent dimer by departing GeRad handle			
	R: C1002dC (ACC0B/41)	S		
	P: C1002dCp3S (ACC0A/36) + GeH4 (ACC0A/5)	S + S	+2.02	
	R: C1002dC (ACC0B/41)	S		
	T: C1002dCp3SasTS (ACC1A/36) + GeH4 (ACC0A/5)	S + S		+4.47
	P: C1002dCp3T (ACC0A/36) + GMACH3 (ACC0A/29)	T + S	+3.36	
3B6	H steal from CH site on same dimer by departing GeRad handle			
	R: C1002dC (ACC0B/41)	S		
	P: C1002dCp2S (ACC0A/36) + GeH4 (ACC0A/5)	S + S	+1.62	
	R: C100C (ACC0A/29)	S		
	T: C100Cp2SasTS (ACC1A/24) + GeH4 (ACC0A/5)	S + S		+5.03

Continued

3D5	P: C1002dCp2T (ACC0A/36) + + GeH4 (ACC0A/5)	T + S	+3.41	
	H migrates to $CH_2\bullet$ radical from nearest CH site on adjacent dimer			
	R: C1002dD (ACC0A/37)	D		
	P: C1002dDp5 (ACC0A/37)	D	+0.13	
	T: C1002dDp5TSrun2 (ACC0A/37)	D		+1.26
3D8	H migrates to $CH_2\bullet$ radical from CH site on same dimer			
	R: C100D (ACC0A/25)	D		
	P: C100DHH (ACC0A/25)	D	+0.18	
	T: C100DHHTS (ACC1A/25)	D		+1.91
3G6	$CH_2\bullet$ bonds to same-dimer carbon and inserts into same dimer			
	R: C100D (ACC0A/25)	D		
	P: C100DIns1 (ACC0A/25)	D	−0.44	
	T: C100DIns1-QST3 (ACC1A/25)	D		+2.16
4	**Hydrogenate $CH_2\bullet$ radical site using HDon tool**			
	R: C1002dD (ACC0A/37) + HDon (ACC0A/26)	D + S		
	P: C1002dE (ACC0A/38) + GeRad (ACC0A/25)	S + D	−0.64	

[a] Pathology 2B6 (singlet) can occur (no barrier found), resulting in ethenylation (C=C) of single-bonded surface atoms; however, this requires a very large mispositioning of the tooltip by ~2.19 Å, hence can be avoided by proper positional control. The nearest cross-row terminating H atom is ~2.5 Å away and is also avoided by proper positional control.

of the Ge-based HDon tool operating on small cluster targets by Temelso et al.[77] reports H donation from a Ge-substituted isobutane model tooltip to an sp^3 carbon monoradical recipient site (isobutane model) to be exoergic by $\Delta E = -0.62$ eV at the CCSD(T)/DZ-PP level of theory with a +0.21 eV reaction barrier (easily overcome by mechanical force; Section 1) calculated at the UMP2/DZ-PP level of theory. Based on bending potentials calculated at the MP2/cc-pVDZ[-PP] level of theory, positional uncertainty of the donor H atom is estimated to be <0.22 Å at 298 K or one-tenth the ~2.5 Å spacing between potential donation sites on an unreconstructed C(111) diamond surface, thus allowing adequate positional control during the donation operation.

Site-specific hydrogen donation to crystal surfaces, but not purely mechanical donation, has been achieved experimentally. For instance, McIntyre et al.[78] demonstrated nanocatalytic capabilities of a platinum-rhodium STM tip operating in a reactor cell with excess H_2 by rehydrogenating partially dehydrogenated hydrocarbon clusters adsorbed to the Pt(111) surface. Muller et al.[79] used a Pt-coated AFM tip to hydrogenate terminal azide groups on a self-assembled monolayer, producing highly localized amines. Yamamoto et al.[80] demonstrated the deposition of hydrogen atoms from an STM tungsten tip to a monohydride Si(100)-H(2 × 1) surface by applying a +3.5 V voltage bias to diffuse the hydrogens to the tungsten tip, followed by −8.5 V 300 ms pulses to induce electronic excitations to break the W-H bond. Thirstrup et al.[81] used clean and H-coated STM tips to perform atomic scale desorption and deposition of hydrogens from Si(001)-H(2 × 1) and Si(001)-H(3 × 1) surfaces for both positive and negative sample bias voltages with a resolution of one to two atomic rows, and Shimokawa et al.[82] studied the temperature dependence of

thermal desorption, abstraction and collision-induced desorption of H_2 and D_2 from Ge(100) and Si(100) surfaces.

After donating an H atom, the discharged HDon tool—now a Group IV-substituted adamantyl radical (GeRad)—should be regarded as a separate tool (Fig. 1(F)) that subsequently may be used either as a bond strength modulator (e.g., RS5) or as a reversible mechanical bonding tool or handle to permit kinematic manipulation of intermediate workpiece structures (e.g., RS6, RS8, RS10, RS11, RS34–RS36, RS61–RS64).

Hydrogen may also be donated using a hydrogen transfer or "HTrans" tool (Fig. 1(C)) that is a composite of the HAbst and GeRad tools (Step 1, RS5) and which enables more exoergic H donation reactions (RS3) than are possible with HDon. The energy of the HTrans system varies significantly after tooltip discharge if the tool is mechanically straightened to its minimized structure, allowing the third (pi) bond to fully form (Fig. 2).

3.3. Dimer Placement Tool (DimerP)

A principal challenge in diamond mechanosynthesis is the controlled addition of carbon atoms to the growth surface of a diamond crystal lattice. The analysis of carbon atom insertion and carbon dimer placement on diamond has received substantial theoretical study and computational validation.[3, 4, 9–11, 19–24] One efficient method is to add a pair of triple-bonded carbon atoms (a C_2 dimer) in one operation. The function of a dimer placement tool is to position the dimer, then to bond the dimer at a precisely chosen lattice location on a growing molecular structure, and finally to withdraw the tool—leaving behind two carbon atoms bonded to the growing structure. This tool allows fabrication of diamond structures having an even number of C atoms[20] that are geometrically accessible to the tool, given the limits imposed by tool aspect ratio.[24]

782

J. Comput. Theor. Nanosci. 5, 760–861, 2008

RS15. Add 1st CH_3 to DCB6C bridgehead using GM tool.

Step	Description of Reaction	Mult.	Ener. (eV)	Barr. (eV)
1	**Abstract H from DCB6C bridgehead using HAbst tool**			
	R: Cluster86 (ACC0B/46) + HAbst (ACC0A/27)	S + D		
	P: Cluster87 (ACC0A/45) + HAbstH (ACC0A/28)	D + S	−1.69	
1D2	H migrates to radical from adjacent shoulder sidewall CH_2			
	R: Cluster87 (ACC0A/45)	D		
	P: C87H17 (ACC0A/45)	D	+0.08	
	T: C87H17TS (ACC1A/45)	D		+2.60
1D3	H migrates to radical from adjacent bridgehead CH			
	R: Cluster87 (ACC0A/45)	D		
	P: C87H33 (ACC0A/45)	D	+0.03	
	T: C87H33TS (ACC1A/45)	D		+2.53
1D9	H migrates to radical from apposing DCB6C bridgehead CH			
	R: Cluster87 (ACC0A/45)	D		
	T: C46BTS (ACC1A/45)	D		+1.45
2	**Join GM tool to DCB6C bridgehead radical site**			
	R: Cluster87 (ACC0A/45) + GM tool cluster (ACC0A/7)	D + D		
	P: Lons3 (ACC0A/52)	S	−2.62	
2A	H steal from GM tool to DCB6C bridgehead radical site			
	R: Cluster87 (ACC0A/45) + GM tool (ACC0A/28)	D + D		
	P: Cluster86 (ACC0B/46) + GMA5HS (ABB0A/27)	S + S	+1.13	
	P: Cluster86 (ACC0B/46) + GMA5HT (ACC0A/27)	S + T	+0.42	
2B7	H steal from adjacent shoulder sidewall CH_2 by GM tool			
	R: Cluster87 (ACC0A/45) + GM tool (ACC0A/28)	D + D		
	P: Lons3p2S (ACC0A/44) + GMACH3 (ACC0A/29)	S + S	**−0.59** [a]	
	P: Lons3p2T (ACC0A/44) + GMACH3 (ACC0A/29)	T + S	−0.08	
	R: Cluster87 (ACC0A/45) + GM tool cluster (ACC0A/7)	D + D		
	T: Lons3p2TTS (ACC1A/52)	T		+0.61
2B8	H steal from adjacent bridgehead CH by GM tool			
	R: Cluster87 (ACC0A/45) + GM tool (ACC0A/28)	D + D		
	P: Lons3p3S (ACC0A/44) + GMACH3 (ACC0A/29)	S + S	**−0.79** [a]	
	P: Lons3p3T (ACC0A/44) + GMACH3 (ACC0A/29)	T + S	−0.03	
	R: Cluster87 (ACC0A/45) + GM tool cluster (ACC0A/7)	D + D		
	T: Lons3p3TTS (ACC1A/52)	T		+0.53
2B9	H steal from apposing DCB6C bridgehead CH by GM tool			
	R: Cluster87 (ACC0A/45) + GM tool (ACC0A/28)	D + D		
	P: Cluster88S (ACC0A/44) + GMACH3 (ACC0A/29)	S + S	+0.28	
	R: Cluster87 (ACC0A/45) + GM tool cluster (ACC0A/7)	D + D		
	T: Lons3p4STS (ACC1A/52)	S		+1.50
	P: Cluster88T (ACC0A/44) + GMACH3 (ACC0A/29)	T + S	−0.10	
	R: Cluster87 (ACC0A/45) + GM tool cluster (ACC0A/7)	D + D		
	T: Lons3p4TTS (ACC1A/52)	T		+0.49
3	**Detach GeRad handle from workpiece**			
	R: Lons3 (ACC0A/52)	S		
	P: Cluster52B (ACC0A/48) + GeH3 (ACC0A/4)	D + D	+2.47	
3B1	H steal from CH_2 by departing GeRad handle			
	R: Lons3 (ACC0A/52)	S		
	T: C52BpathS-TS (ACC1A/47) + GeH4 (ACC0A/5)	S + S		+3.88
	P: C52BpathT (ACC0A/47) + GeH4 (ACC0A/5)	T + S	+3.40	
3B7	H steal from adjacent shoulder sidewall CH_2 by GeRad handle			
	R: Lons3 (ACC0A/52)	S		

	P: Lons4p4SasTS (ACC1A/47) + GeH4 (ACC0A/5)	S + S	+4.28	
	P: Lons4p4T (ACC0A/47) + GeH4 (ACC0A/5)	T + S	+2.96	
3B8	H steal from adjacent bridgehead CH by GeRad handle			
	R: Lons3 (ACC0A/52)	S		
	P: Lons4p5SasTS (ACC1A/47) + GeH4 (ACC0A/5)	S + S	+3.79	
	P: Lons4p5T (ACC0A/47) + GeH4 (ACC0A/5)	T + S	+2.95	
3B9	H steal from apposing DCB6C bridgehead CH by GeRad handle			
	R: Lons3 (ACC0A/52)	S		
	T: C52BHSTS (ACC1D/47) + GeH4 (ACC0A/5)	S + S		+3.79
	T: C52BHT (ACC1A/47) + GeH4 (ACC0A/5)	T + S		+2.96
3D2	H migrates to $CH_2\bullet$ radical from adjacent shoulder sidewall CH_2			
	R: Cluster52B (ACC0A/48)	D		
	T: Lons4H17TS (ACC1A/48)	D		+1.92
3D3	H migrates to $CH_2\bullet$ radical from adjacent bridgehead CH			
	R: Cluster52B (ACC0A/48)	D		
	T: Lons4H33TS (ACC1A/48)	D		+2.22
3D9	H migrates to $CH_2\bullet$ radical from apposing DCB6C bridgehead CH			
	R: Cluster52B (ACC0A/48)	D		
	P: C52Bpath (ACC0A/48)	D	−0.17	
	T: C52Bpath-QST2 (ACC1A/48)	D		+0.41
4	**Hydrogenate $CH_2\bullet$ radical site using HDon or HTrans tool**			
	R: Cluster52B (ACC0A/48) + HDon (ACC0A/26)	D + S		
	P: Cluster53B (ACC0A/49) + GeRad (ACC0A/25)	S + D	−0.44	
	R: Cluster52B (ACC0A/48) + S15cis (ACCCA/11)	D + D		
	P: Cluster53B (ACC0A/49) + S16Run0 (ACCCA/10)	S + S	−1.27	

[a] Pathologies 2B7 (singlet) and 2B8 (singlet) can occur (no barriers found), resulting in ethenylation (C=C) of single-bonded carbon cage atoms; however, this requires a very large mispositioning of the tooltip by ~2.23 Å (2B7) or ~2.71 Å (2B8), hence can be avoided by proper positional control. Pathology 2B9 requires a mispositioning of ~2.34 Å but is blocked by a sufficient barrier.

Monomer C and Ge atoms can more conveniently be transferred to diamondoid workpieces by adding $\bullet CH_2$ groups using the Methylene (Section 7.2) or Germylmethylene (Section 7.3) tools, and $\bullet GeH_2$ groups using the Germylene (Section 7.4) tool, respectively.
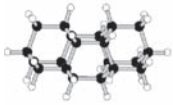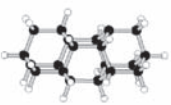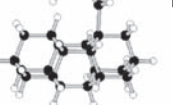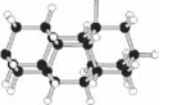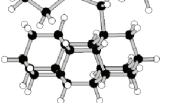
Except for HAbst, the most extensive theoretical analysis of any proposed mechanosynthetic tool to date has been done on DCB6Ge, one of a large family of possible variants[24] of the horizontal dimer placement tool first proposed in 2003 by Merkle and Freitas[21] in which a C_2 dimer is bonded to fused Group IV-substituted adamantane frameworks that position and orient them. DCB6X (X = Si, Ge, Sn) is at present the only class of carbon transfer tools that has been computationally validated on a specific diamond surface.[19, 20, 22] Ge is strongly preferred[20] as the dimer supporting atom in DCB6Ge ($H_{12}C_9Ge$-$C\equiv C$-GeC_9H_{12}), influencing the selection of Ge over Si/Sn/Pb alternatives for HDon[77] thus minimizing the number of different elements required in the proposed minimal toolset. The DCB6Ge dimer placement or "DimerP" tool (Fig. 1(D)) is brought up to a dehydrogenated C(110) diamond surface as an active tool and then is retracted as a spent tool after performing a site-specific placement of a C_2 dimer on the surface (RS4). The DimerP tool is readily covalently bonded to a larger handle structure by extension of a regular diamond lattice of which the adamantane base is a unit cage.[19, 20]

Interactions between DimerP and the C(110) diamond surface have been extensively investigated via DFT in stepwise *ab initio* molecular dynamics simulations, implemented using VASP.[20] There is no energy barrier to the transfer of a single carbon dimer from the Ge-based tooltip onto the clean C(110) surface,[19] and the Ge-based tool remains reliable up to at least 300 K with the energy barrier against dimer misreaction having a lower bound of at least +3 eV, as crudely estimated from a related series of VASP DFT/GGA simulation runs.[20] DFT predicts that dimer deposition onto two apposed C bridgehead monoradical sites on a clean (111) lonsdaleite surface is exoergic by −0.78 eV.[24] Interestingly, the net deposition reaction onto clean C(110) appears slightly endoergic by +0.66 eV,[19] but the tool nevertheless properly transfers its dimer payload because C-C bonds (dimer to surface) can withstand greater tensile loads than C-Ge bonds (dimer to tooltip) (Section 3.5), and because at low enough temperatures the dimer loses thermal access to the deeper potential well on the misreaction side due to the presence of a significant energy barrier separating the two wells as the surface-dimer-tool complex is slowly pulled apart.

The pick-and-place of individual carbon atoms or carbon dimers has yet to be accomplished experimentally using SPM tips. However, a possible experimental procedure for demonstrating SPM-based C_2 dimer deposition has been proposed,[23] and Ho and Lee[32] have demonstrated

RS16.   Add 1st CH_3 to DCB6C bridgehead using Meth tool.

Step 1	Step 2	Step 3	Step 4	Step 5 ...

... Step 5	Step 6	Step 7	Step 8

Step	Description of Reaction	Mult.	Ener. (eV)	Barr. (eV)
1	**Abstract H from DCB6C bridgehead using HAbst tool**			
	R: Cluster86 (ACC0B/46) + HAbst (ACC0A/27)	S + D		
	P: Cluster46B (ACC0A/45) + HAbstH (ACC0A/28)	D + S	−1.69	
2	**Join Meth tool to DCB6C bridgehead radical site**			
	R: Cluster46B (ACC0A/45) + CH33CCH2 (ACC0A/16)	D + D		
	P: Cluster47B (ACC0A/61)	S	−2.33	
2A	H steal from Meth tool to DCB6C bridgehead radical site			
	R: Cluster46B (ACC0A/45) + CH33CCH2 (ACC0A/16)	D + D		
	P: Cluster86 (ACC0B/46) + CH33CCHS (ACC0A/15)	S + S	+0.73	
	P: Cluster86 (ACC0B/46) + CH33CCHT (ACC0A/15)	S + T	+0.59	
2^1	**Join GeRad tool and Meth tool by radical coupling**			
	R: CH33Ge (ACC0A/13) + CH33CCH2 (ACC0A/16)	D + D		
	P: Cluster47C (ACC0B/29)	S	−2.80	
2^1A	H steal from Meth tool to GeRad radical site			
	R: CH33Ge (ACC0A/13) + CH33CCH2 (ACC0A/16)	D + D		
	P: CH33GeH (ACC0A/14) + CH33CCHS (ACC0A/15)	S + S	+1.15	
	P: CH33GeH (ACC0A/14) + CH33CCHT (ACC0A/15)	S + T	+1.01	
3	**Abstract H from Meth tool CH_2 group using HAbst tool**			
	R: Cluster47B (ACC0A/61) + HAbst (ACC0A/27)	S + D		
	P: Cluster48B (ACC0A/60) + HAbstH (ACC0A/28)	D + S	−1.97	
3D9	H migrates to CH• radical site from apposing bridgehead site			
	R: Cluster48B (ACC0A/60)	D		
	P: C48Bpath (ACC0A/60)	D	+0.04	
	T: C48Bpath-QST2 (ACC1A/60)	D		+0.43
3^1	**Abstract H from Cluster47C CH_2 group using HAbst tool**			
	R: Cluster47C (ACC0B/29) + HAbst (ACC0A/27)	S + D		
	P: Cluster48C (ACC0A/28) + HAbstH (ACC0A/28)	D + S	−1.70	
4	**Join GeRad handle to Meth tool CH• radical site**			
	R: Cluster48B (ACC0A/60) + CH33Ge (ACC0A/13)	D + D		
	P: Cluster49B (CXCXB/73)	S	−2.29	
4B1	H steal from CH• radical to GeRad tool			
	R: Cluster48B (ACC0A/60) + GeRad tool (ACC0A/25)	D + D		
	P: C48BpathS (ACC0A/59) + HDon tool (ACC0A/26)	S + S	+0.79	
	P: C48BpathT (ACC0A/59) + HDon tool (ACC0A/26)	T + S	+0.71	
4^1	**Join Cluster48C to DCB6C dehydrogenated radical site**			
	R: Cluster48C (ACC0A/28) + Cluster46B (ACC0A/45)	D + D		
	P: Cluster49B (CXCXB/73)	S	−2.13	
4^1A	H steal from Cluster48C to Cluster 46B radical site			
	R: Cluster48C (ACC0A/28) + Cluster46B (ACC0A/45)	D + D		
	P: Cluster49CHS (ACC0A/27) + Cluster86 (ACC0B/46)	S + S	+0.78	
	P: Cluster49CHT (ACC0A/27) + Cluster86 (ACC0B/46)	T + S	**+0.19** [a]	

Continued

REVIEW

	Proximity Continuation Reaction:			
	R: Cluster49CHT (ACC0A/27) + Cluster86 (ACC0B/46)	T + S		
	P: Cluster48C (ACC0A/28) + Cluster46B (ACC0A/45)	D + D	**−0.19**[a]	
5	**Detach Adam handle from workpiece (handle exchange)**			
	R: Cluster49B (CXCXB/73)	S		
	P: Cluster50B (ACC0A/60) + CH33C (ACC0A/13)	D + D	+2.21	
5B1	H steal from workpiece by departing Adam handle			
	R: Cluster49B (CXCXB/73)	S		
	P: C50BpathS (ACC0B/59) + CH33CH (ACC0A/14)	S + S	+2.52	
	R: C49BA (ACC0A/55)	S		
	T: C50BAp1STS (ACC2C/55)	S		+3.48
	P: C50BpathT (ACC0A/59) + CH33CH (ACC0A/14)	T + S	+2.18	
	R: C49BA (ACC0A/55)	T		
	T: C50BAp1TTS (ACC1A/55)	T		+3.20
5D9	H migrates to CH● radical site from apposing bridgehead site			
	R: Cluster50B (ACC0A/60)	D		
	P: Cluster50Bpath (ACC0A/60)	D	+0.03	
	T: C50BpathH-QST2 (ACC1A/60)	D		**+0.45**[b]
6	**Hydrogenate CH● radical site using HDon or HTrans tool**			
	R: Cluster50B (ACC0A/60) + HDon (ACC0A/26)	D + S		
	P: Cluster51B (ACC0A/61) + GeRad (ACC0A/25)	S + D	−0.22	
	R: Cluster50B (ACC0A/60) + S15cis (ACCCA/11)	D + D		
	P: Cluster51B (ACC0A/61) + S16Run0 (ACCCA/10)	S + S	−1.05	
7	**Detach GeRad handle from workpiece**			
	R: Cluster51B (ACC0A/61)	S		
	P: Cluster52B (ACC0A/48) + CH33Ge (ACC0A/13)	D + D	+2.50	
7B1	H steal from workpiece by departing GeRad handle			
	R: Cluster51B (ACC0A/61)	S		
	T: C52BpathSasTS (ACC0A/47) + CH33GeH (ACC0A/14)	S + S		+3.90
	P: C52BpathT (ACC0A/47) + CH33GeH (ACC0A/14)	T + S	+3.42	
7D9	H migrates to CH$_2$● radical site from apposing bridgehead site			
	R: Cluster52B (ACC0A/48)	D		
	P: C52Bpath (ACC0A/48)	D	−0.17	
	T: C52Bpath-QST2 (ACC1A/48)	D		**+0.41**[b]
8	**Hydrogenate CH$_2$● radical site using HDon or HTrans tool**			
	R: Cluster52B (ACC0A/48) + HDon (ACC0A/26)	D + S		
	P: Cluster53B (ACC0A/49) + GeRad (ACC0A/25)	S + D	−0.44	
	R: Cluster52B (ACC0A/48) + S15cis (ACCCA/11)	D + D		
	P: Cluster53B (ACC0A/49) + S16Run0 (ACCCA/10)	S + S	−1.27	

[a] As a slightly endoergic (+0.19 eV) reaction, pathology 4^1A (triplet) is unlikely to go forward at 80 K but may (rarely) proceed uphill at 300 K. However, by holding the pathology 4^1A Products in close proximity for a sufficient time, they will undergo an exoergic reverse reaction and proceed downhill by −0.19 eV, yielding the original Reactants for whom the desired subsequent main reaction 4^1 is extremely exoergic (−2.13 eV). No intersystem crossing is required for the reverse reaction because two radicals are present in both Reactants and Products of pathology 4^1A (triplet).

[b] Both barriers appear marginally sufficient. If further analysis reveals lower barriers, either pathology may be accommodated by presenting the H donation tool to both possible radical sites, possibly repeatedly. The radical site will accept the H, the nonradical site will not, yielding the desired hydrogenated structure of the following step. Any uncertainty in the condition of the donation tool is eliminated by positioning the donation tool one H-bond distance above a known radical site in the H dump, reliably yielding in any case a clean GeRad handle.

the first repeatable site-specific covalent bonding operation of a diatomic carbon-containing molecule (CO) on a crystal surface, albeit electrically-mediated. There has been some success with other Group-IV elements. For instance, Becker and Golovchencko[83] used voltage pulses on an STM tip to extract a single germanium atom from the Ge(111) surface of a sample. Others have used STMs to bind silicon atoms to the tip, first pulling the atoms off the surface of a Si(111) crystal face and then re-inserting them back into the crystal,[84, 85] and segments of individual dimer rows of silicon atoms have been extracted from the Si(100) face to create structures with atomically straight edges and lateral features that are only one dimer in width.[86] Other researchers have moved clusters and single atoms of silicon across a silicon surface at room temperature.[85–90]

Most notably, the first experimental demonstration of purely mechanical positional synthesis, or true mechanosynthesis, of any kind was achieved in 2003 by Oyabu and colleagues at Osaka University[2] for a single Si atom.

RS17. Add 1st CH_3 to HAbstH using GM tool [full cage models illustrated].

Step	Description of Reaction	Mult.	Ener. (eV)	Barr. (eV)
1	**Join GM tool to apical CH of HAbstH tool**			
	R: CH3CCH (ACC0A/7) + GM tool cluster (ACC0A/7)	S + D		
	P: ChainH2 (ACC0A/14)	D	−0.90	
1A	H steal from GM tool to apical CH of HAbstH tool			
	R: CH3CCH (ACC0A/7) + GM tool cluster (ACC0A/7)	S + D		
	P: ChainH2p2 (ACC0A/8) + GeH3CHS (ACC0A/6)	D + S	+3.52	
	P: ChainH2p2 (ACC0A/8) + GeH3CHT (ACC0A/6)	D + T	+2.82	
1B1	H steal from apical CH of HAbstH tool by GM tool			
	R: CH3CCH (ACC0A/7) + GM tool cluster (ACC0A/7)	S + D		
	P: CH3CC (ACC0A/6) + GeH3CH3 (ACC0A/8)	D + S	+1.47	
2	**Abstract H from apical CH of HAbstH using HAbst tool**			
	R: ChainH2 (ACC0A/14) + HAbst (ACC0A/27)	D + D		
	P: ChainH1 (ACC1A/13) + HAbstH (ACC0A/28)	S + S	−4.26	
3	**Detach GeRad handle from workpiece**			
	R: ChainH1 (ACC1A/13)	S		
	P: ChainH3 (ACC0A/9) + GeH3 (ACC0A/4)	D + D	+2.42	
3B1	H steal from CH2 by departing GeRad handle			
	R: ChainH1 (ACC1A/13)	S		
	P: ChainH3p1S (ACC0A/8) + GeH4 (ACC0A/5)	S + S	+3.40	
	P: ChainH3p1T (ACC1A/8) + GeH4 (ACC0A/5)	T + S	+2.89	
4	**Hydrogenate $CH_2\bullet$ radical site using HTrans tool**			
	R: ChainH3 (ACC0A/9) + S15cis (ACCCA/11)	D + D		
	P: ChainH4 (ACC0A/10) + S16Run0 (ACCCA/10)	S + S	−0.98	

A silicon AFM tip was lowered towards a cold silicon surface and pushed down onto a single atom, mechanically breaking its bonds to neighboring atoms, allowing it to bind to the AFM tip, with subsequent images showing a hole where the atom had been. Pressing the tip back into the vacancy replaced the selected atom, this time using mechanical pressure to break the bond with the tip.

3.4. Steric Constraints on Multitool Apposition

With two exceptions, all primary and auxiliary tools in our minimal toolset are mounted on simple pyramidal diamond handles consisting of stacked planes of adamantane cages. The simplest 1, 2, 3, ... adamantane stack (Fig. 3(A)) has an aspect angle of ∼60°, which may be considered typical for most tooltypes in our toolset. The two exceptions are the DimerP tool, essentially a fused double GeRad tool, which requires a handle with a ∼60° aspect angle in the common dimension and ∼140° in the transverse

dimension, and the two-handled HTrans tool, similarly at ∼60–90° × ∼140–160°, adjustable by manipulating the component HAbst and GeRad handles independently.

For tool operations in free space, the 360° of available planar angle can conservatively accommodate at most four proximated tools (4 × 60° = 240°), again occupying only 2/3 of available planar angle. However, tools arranged tetrahedrally rather than coplanarly use only half of the effectively available 120° tetrahedral angle between each pair, leaving extra room for positional and rotational adjustments during mechanosynthetic operations. A tetrahedral arrangement of 4 tooltips on a single workpiece may be regarded as 3 coplanar tools at 120° separation with any single tool positioned above the plane, with that single tool having much of an entire hemisphere of free space in which to maneuver. Purely for illustrative purposes, the most severe geometry (Fig. 3(B)) occurs when four proximated DimerP tools whose C_2 dimer payloads are shown bonded in an energetically unstable cubane

RS18. Add 1st CH$_3$ to two-handled polyyne chain using GM tool [full cage models illustrated].

Step	Description of Reaction	Mult.	Ener. (eV)	Barr. (eV)
1	**Join GM tool to chain C atom adjacent to GeRad attachment site**			
	R: BCR2 (ABB0B/18) **[from RS57]** + GM tool cluster (ACC0A/7)	D + D		
	P: ChainM2 (ABB0A/25)	S	−3.29	
1A	H steal from GM tool to workpiece			
	R: BCR2 (ABB0B/18) + GM tool cluster (ACC0A/7)	D + D		
	P: Chain3run2 (ABB2A/19) + GeH3CHS (ACC0A/6)	S + S	+1.22	
	P: Chain3run2 (ABB2A/19) + GeH3CHT (ACC0A/6)	S + T	+0.52	
2	**Detach GeRad handle from GM tool**			
	R: ChainM2 (ABB0A/25)	S		
	P: ChainM3 (ABB0A/21) + GeH3 (ACC0A/4)	D + D	+2.25	
2B1	H steal from CH$_2$ by departing GeRad handle			
	R: ChainM2 (ABB0A/25)	S		
	P: ChainM3p1S (ABB1A/20) + GeH4 (ACC0A/5)	S + S	+3.86	
	P: ChainM3p1T (ABB1A/20) + GeH4 (ACC0A/5)	T + S	+3.34	
3	**Hydrogenate CH$_2$• radical site using HTrans tool**			
	R: ChainM3 (ABB0A/21) + S15cis (ACCCA/11)	D + S		
	P: ChainM4 (ABB0A/22) + S16Run0 (ACCCA/10)	S + D	−0.82	

configuration (while the addition of the fourth DimerP tool is exoergic by −1.03 eV, subsequent retraction of this tool retrieves the donated C$_2$ dimer because such retrieval is strongly exoergic compared to C$_2$ deposition).

For tool operations in the proximity of a flat surface, the 180° of available planar angle can conservatively accommodate at most two proximated tools (60° + 60° = 120°), occupying only 2/3 of available planar angle, since three proximated tools would occupy the entire 180° planar angle, leaving no room for positional or rotational adjustments during mechanosynthetic operations. The most severe instance is again illustrated by two proximated DimerP tools on a flat C(110) surface. In Figure 3(C), the two tools are very close (∼5° relative angle), yielding an estimated van der Waals intertool attraction of ∼1.3 nN which is reduced to ∼0.4 nN when the tools are tipped to a ∼30° relative angle as in Figure 3(D). (Adhesive force is crudely estimated by integrating the Israelachvili relation[91] for opposed planar surfaces across the entire tool height for the two nearest tipped central planes taken as the width of 3 adamantane cages on each tool, and taking the Hamaker constant as ∼3.4 × 10^{-19} J for diamond surface.)

Experimentally, the first opposable STM tip pair was fabricated by MacDonald's group in 1991 using the Cornell Nanofabrication Facility,[92] and two-handed coordinated micromanipulation under the view of an SEM

was reported in 1993.[93] In 2005, Xidex reported opposable AFM dual-tip calipers for metrology, with each cantilever probe tiltable in up to three rotational degrees of freedom allowing tips to touch each other's apices and to access vertical and re-entrant feature sidewalls, using tips with 10 nm radius of curvature and a 10° cone angle but without closed-loop control.[94, 95] In 2005 a dual probe system available from Nanonics allowed two tips to approach within 10 nm of each other,[96] and other dual-tip SPM systems have been described in the experimental literature.[97–99] In 1998, Zyvex demonstrated the first simultaneous coordinated operation of three independently controlled AFM tips within the same workspace at different orientations;[100, 101] a successor 4-tip system was designed as early as 1999 and finally offered as a commercial product starting in 2003.

3.5. Force Constraints on Multitool Bond Scission

When building structures using positionally controlled DMS it is often convenient to make use of mechanically reversible covalent bonds. This allows the design of handles which can be temporarily strongly bonded to a structure, used to physically manipulate the structure while maintaining continuous positional control, then debonded from the structure once the manipulations are completed.

RS19. Add 2nd CH_3 in chain to Adam sidewall.

Step	Description of Reaction	Mult.	Ener. (eV)	Barr. (eV)
1	**Abstract H from Adam sidewall CH_3 using HAbst tool**			
	R: Cluster53run2 (ABB0A/29) + HAbst (ACC0A/27)	S + D		
	P: Cluster52 (ACC0A/28) + HAbstH (ACC0A/28)	D + S	−1.52	
2	**Join GM tool to apical radical site on chain**			
	R: Cluster52 (ACC0A/28) + GM tool cluster (ACC0A/7)	D + D		
	P: TTMeth3 (ACC0A/35)	S	−3.24	
2A	H steal from GM tool to workpiece $CH_2 \bullet$ radical site			
	R: Cluster52 (ACC0A/28) + GM tool (ACC0A/28)	D + D		
	P: Cluster53run2 (ABB0A/29) + GMA5HS (ABB0A/27)	S + S	+0.95	
	P: Cluster53run2 (ABB0A/29) + GMA5HT (ACC0A/27)	S + T	+0.25	
	T: TTMeth3p1TTS (ACC1A/35)	T		+0.68
2B1	H steal from workpiece to GM tool			
	R: Cluster52 (ACC0A/28) + GM tool (ACC0A/28)	D + D		
	P: C52pathS (ACC0A/27) + GMACH3 (ACC0A/29)	S + S	+0.62	
	P: C52pathT (ACC0A/27) + GMACH3 (ACC0A/29)	T + S	+0.36	
	T: TTMeth3p2TTS (ACC1A/35)	T		+0.66
3	**Detach GeRad handle from workpiece**			
	R: TTMeth3 (ACC0A/35)	S		
	P: TMethR2 (ACC0A/31) + GeH3 (ACC0A/4)	D + D	+2.89	
3B1	H steal from workpiece by departing GeRad handle			
	R: TTMeth3 (ACC0A/35)	S		
	T: TTMeth4p1STS (ACC1A/30) + GeH4 (ACC0A/5)	S + S		+4.16
	T: TTMeth4p1TTS (ACC1A/30) + GeH4 (ACC0A/5)	T + S		+3.95
3D1	H migrates to radical from adjacent CH_2 in chain			
	R: TMethR2 (ACC0A/31)	D		
	P: TTMeth4p2 (ACC0A/31)	D	−0.20	
	T: TTMeth4p2TS (ACC1A/31)	D		+1.57
3D2	H migrates to radical from adjacent Adam sidewall CH_2			
	R: TMethR2 (ACC0A/31)	D		
	P: TMethR2p2 (ACC0A/31)	D	+0.08	
	T: TMethR2p2TS (ACC1A/31)	D		+0.73
3D3	H migrates to radical from adjacent Adam bridgehead CH			
	R: TMethR2 (ACC0A/31)	D		
	P: TMethR2p3 (ACC0A/31)	D	−0.08	
	T: TMethR2p3TS (ACC1A/31)	D		+1.00
3F1	$H_2C{=}CH_2$ group detaches, leaving >CH$\bullet$ on Adam sidewall			
	R: TMethR2 (ACC0A/31)	D		
	P: AdamDot (ACC0A/25) + C2H4 (ACC0A/6)	D + S	+0.59	
4	**Hydrogenate $CH_2 \bullet$ radical site using HDon tool**			
	R: TMethR2 (ACC0A/31) + HDon (ACC0A/26)	D + S		
	P: TMethR1 (ACC0B/32) + GeRad (ACC0A/25)	S + D	−0.66	

RS20.   Add 2nd CH$_3$ in chain to Adam bridgehead.

	Step 1	Step 2	Step 3	Step 4	

Step	Description of Reaction	Mult.	Ener. (eV)	Barr. (eV)
1	**Abstract H from Adam bridgehead CH$_3$ using HAbst tool**			
	R: AdamCH3 (ACC0A/29) + HAbst (ACC0A/27)	S + D		
	P: Meth tool (ACC0A/28) + HAbstH (ACC0A/28)	D + S	−1.50	
2	**Join GM tool to apical radical site on chain**			
	R: Meth tool (ACC0A/28) + GM tool cluster (ACC0A/7)	D + D		
	P: Bridge3 (ACC0A/35) **[two-handled polyethylene chain]**	S	−3.12	
2A	H steal from GM tool to workpiece CH$_2$● radical site			
	R: Meth tool (ACC0A/28) + GM tool (ACC0A/28)	D + D		
	P: AdamCH3 (ACC0A/29) + GMA5HS (ABB0A/27)	S + S	+0.93	
	P: AdamCH3 (ACC0A/29) + GMA5HT (ACC0A/27)	S + T	+0.22	
	T: Bridge3p1TTS (ACC1A/35)	T		+0.64
2B1	H steal from workpiece to GM tool			
	R: Meth tool (ACC0A/28) + GM tool (ACC0A/28)	D + D		
	P: AdamCHS (ACC0A/27) + GMACH3 (ACC0A/29)	S + S	+0.50	
	P: AdamCHT (ACC0A/27) + GMACH3 (ACC0A/29)	T + S	+0.36	
	T: Bridge3p2TTS (ACC1A/35)	T		+0.69
3	**Detach GeRad handle from workpiece**			
	R: Bridge3 (ACC0A/35)	S		
	P: Bridge4 (ACC0A/31) + GeH3 (ACC0A/4)	D + D	+2.74	
3B1	H steal from workpiece by departing GeRad handle			
	R: Bridge3 (ACC0A/35)	S		
	T: Bridge4p1STS (ACC1A/30) + GeH4 (ACC0A/5)	S + S		+3.81
	P: Bridge4p1TTS (ACC0A/30) + GeH4 (ACC0A/5)	T + S	+3.71	
3D1	H migrates to radical from adjacent CH$_2$ in chain			
	R: Bridge4 (ACC0A/31)	D		
	P: Bridge4p2 (ACC0A/31)	D	−0.14	
	T: Bridge4p2TS (ACC1A/31)	D		+1.62
3D2	H migrates to radical from adjacent Adam sidewall CH$_2$			
	R: Bridge4 (ACC0A/31)	D		
	P: Bridge4p3 (ACC0A/31)	D	−0.07	
	T: Bridge4p3TS (ACC1A/31)	D		+1.10
3F1	H$_2$C=CH$_2$ group detaches, leaving C● on Adam bridgehead			
	R: Bridge4 (ACC0A/31)	D		
	P: AdamRad (ACC0A/25) + C2H4 (ACC0A/6)	D + S	+0.68	
	T: Bridge4p5TS (ACC1A/31)	D		+0.97
4	**Hydrogenate CH$_2$● radical site using HDon tool**			
	R: Bridge4 (ACC0A/31) + HDon (ACC0A/26)	D + S		
	P: Bridge5 (ACC0A/32) + GeRad (ACC0A/25)	S + D	−0.65	

RS21. Add CH_3 to Adam sidewall w/CH_3 on adjacent sidewall.

Step	Description of Reaction	Mult.	Ener. (eV)	Barr. (eV)
1	**Abstract H from Adam sidewall site using HAbst tool**			
	R: Cluster53run2 (ABB0A/29) + HAbst (ACC0A/27)	S + D		
	P: SHSM2A (ACC0A/28) + HAbstH (ACC0A/28)	D + S	−1.58	
1B2	H steal from CH_3 group on apposing sidewall			
	R: Cluster53run2 (ABB0A/29) + HAbst (ACC0A/27)	S + D		
	P: SHAM1 (ACC0A/28) + HAbstH (ACC0A/28)	D + S	**−1.58** [a]	
2	**Join GM tool to sidewall radical site**			
	R: SHSM2A (ACC0A/28) + GM5 cluster (ACC0A/16)	D + D		
	P: Side2MS3 (ACC0B/44)	S	−2.96	
2A	H steal from GM tool to workpiece radical site			
	R: SHSM2A (ACC0A/28) + GM tool (ACC0A/28)	D + D		
	P: Cluster53run2 (ABB0A/29) + GMA5HS (ABB0A/27)	S + S	+1.02	
	P: Cluster53run2 (ABB0A/29) + GMA5HT (ACC0A/27)	S + T	+0.31	
	R: SHSM2A (ACC0A/28) + GM5 cluster (ACC0A/16)	S + T		
	T: Adam2DotMTH-QST3run2 (ACC2A/44)	T		+0.74
2B1	H steal from workpiece to GM tool			
	R: SHSM2A (ACC0A/28) + GM tool (ACC0A/28)	D + D		
	P: Adam2DotMS (ACC0B/27) + GMACH3 (ACC0A/29)	S + S	+0.21	
	R: SHSM2A (ACC0A/28) + GM5 cluster (ACC0A/16)	D + D		
	T: Adam2DotMS-QST3 (ACC1A/44)	S		+0.54
	P: Adam2DotMT (ACC1A/30) + GMACH3 (ACC0A/29)	T + S	+0.33	
	R: SHSM2A (ACC0A/28) + GM5 cluster (ACC0A/16)	D + D		
	T: Adam2DotMTTS (ACC1A/44)	T		+0.64
3	**Detach GeRad handle from workpiece**			
	R: Side2MS3 (ACC0B/44)	S		
	P: Cluster52A (ACC0A/31) + CH33Ge (ACC0A/13)	D + D	+2.77	
3B1	H steal from workpiece by departing GeRad handle			
	R: Side2MS3 (ACC0B/44)	S		
	P: Side2MSHSTS (ACC1A/30) + CH33GeH (ACC0A/14)	S + S	+4.09	
	P: Side2MSHTTS (ACC1A/30) + CH33GeH (ACC0A/14)	T + S	+3.78	
4	**Hydrogenate $CH_2 \bullet$ radical site using HDon tool**			
	R: Cluster52A (ACC0A/31) + HDon (ACC0A/26)	D + S		
	P: Cluster53A (ACC0A/32) + GeRad (ACC0A/25)	S + D	−0.59	

[a] Pathology 1B2 (singlet) can occur barrierlessly [8], but requires a very large mispositioning of the HAbst tooltip by >2.08 Å, hence can be avoided by proper positional control.

To achieve this, the force required to break the one bond between the handle and the fulcrum atom on the workpiece must be less than the force required to break the bond(s) that bind the fulcrum atom to the workpiece.

For bonds under large tensile load a useful simple empirical relation for potential energy V as a function of internuclear distance r, based on standard experimental values for bond energy D_e (=potential well depth = bond dissociation energy + zero point vibrational energy), bond length r_0, and bond stretching stiffness k_s, is the Morse function,[102] or $V_{Morse} = D_e\{(1 - \exp[-\beta(r - r_0)])^2 - 1\}$ where $\beta = (k_s/2D_e)^{1/2}$, hence the exertable tensile force $F(r) = -(\partial/\partial r) V_{Morse} = 2\beta D_e\{\exp[-2\beta(r - r_0)] - \exp[-\beta(r - r_0)]\}$ which reaches a maximum (F_{max}) at the Morse function inflection point $r_i = r_0 + ((\ln 2)/\beta)$, that is, at $F_{max} = F(r_i)$. For the C-C bond, $D_e = 3.47$ eV,[103] $r_0 = 1.523$ Å,[104] $k_s = 440$ N/m,[104] giving $F_{max} = 5.53$ nN. For the C-Ge bond, $D_e = 2.44$ eV,[105] $r_0 = 1.950$ Å,[104]

RS22. Add CH_3 to Adam sidewall w/CH_3 on adjacent bridgehead.

Step 1	Step 2	Step 3	Step 4	

Step	Description of Reaction	Mult.	Ener. (eV)	Barr. (eV)
1	**Abstract H from Adam sidewall site using HAbst tool**			
	R: AdamCH3 (ACC0A/29) + HAbst (ACC0A/27)	S + D		
	P: BMHS1 (ACC0A/28) + HAbstH (ACC0A/28)	D + S	−1.60	
2	**Join GM tool to sidewall radical site**			
	R: BMHS1 (ACC0A/28) + GM5 cluster (ACC0A/16)	D + D		
	P: Side2MSB3 (ACC0A/44)	S	−3.00	
2A	H steal from GM tool to workpiece radical site			
	R: BMHS1 (ACC0A/28) + GM tool (ACC0A/28)	D + D		
	P: AdamCH3 (ACC0A/29) + GMA5HS (ABB0A/27)	S + S	+1.04	
	P: AdamCH3 (ACC0A/29) + GMA5HT (ACC0A/27)	S + T	+0.33	
	R: BMHS1 (ACC0A/28) + GM5 cluster (ACC0A/16)	S + T		
	T: CH3AdamHCH-QST3 (ACC1A/44)	T		+0.70
2B1	H steal from workpiece to GM tool			
	R: BMHS1 (ACC0A/28) + GM tool (ACC0A/28)	D + D		
	P: CH3Adam2RadS (ACC0A/27) + GMACH3 (ACC0A/29)	S + S	+0.21	
	R: BMHS1 (ACC0A/28) + GM5 cluster (ACC0A/16)	D + D		
	T: CH3Adam2RadS-QST2 (ACC1A/44)	S		+0.46
	P: CH3Adam2RadT (ACC0A/27) + GMACH3 (ACC0A/29)	T + S	+0.34	
	R: BMHS1 (ACC0A/28) + GM5 cluster (ACC0A/16)	D + D		
	T: CH3Adam2RadT-QST3 (ACC1A/44)	T		+0.66
3	**Detach GeRad handle from workpiece**			
	R: Side2MSB3 (ACC0A/44)	S		
	P: BMHSM1 (ACC0A/31) + CH33Ge (ACC0A/13)	D + D	+2.78	
3B1	H steal from workpiece by departing GeRad handle			
	R: Side2MSB3 (ACC0A/44)	S		
	P: BMHSM1HSTS (ACC1A/30) + CH33GeH (ACC0A/14)	S + S	+4.07	
	P: BMHSM1HTTS (ACC1A/30) + CH33GeH (ACC0A/14)	T + S	+3.74	
4	**Hydrogenate $CH_2 \bullet$ radical site using HDon tool**			
	R: BMHSM1 (ACC0A/31) + HDon (ACC0A/26)	D + S		
	P: CH3AdamCH3 (ACC0A/32) + GeRad (ACC0A/25)	S + D	−0.61	

$k_s = 270$ N/m,[104] giving $F_{max} = 3.64$ nN. For the Ge-Ge bond, $D_e = 1.95$ eV,[106] $r_0 = 2.41$ Å,[106] $k_s = 140$–180 N/m (est.),[104] giving $F_{max} \sim 2.40$ nN. For the C=C double bond, $D_e = 7.53$ eV,[107] $r_0 = 1.34$ Å,[104] $k_s = 960$ N/m,[104] giving $F_{max} = 12.03$ nN. Hence for the two-handle structure Adam-CH_2-GeRad, pulling the handles oppositely yields Adam-$CH_2 \bullet$ and $\bullet$GeRad because the stronger C-C bond between Adam handle and methyl group can apply a higher load (~ 5.53 nN) than the weaker C-Ge bond between methyl group and GeRad handle can tolerate (~ 3.64 nN), a force differential of $\Delta F \sim 1.89$ nN. The bond scission is reliable at 300 K because $\Delta F \geq \Delta F_{min} \sim 0.64$ nN, the minimum force differential required to ensure a minimum +0.40 eV energy differential at 300 K (Section 1) across a C-C bond rupture distance of ~ 1 Å,[3] or $\Delta F_{min} \sim 0.32$ nN for +0.20 eV for reliable operation at 80 K. If two bonds of tensile strength F_1 and F_2 join at an angle θ_{tools} to bind a fulcrum atom, say, to a workpiece, then the condition for reliably breaking a third bond of tensile strength F_3 between the fulcrum atom and a detachable handle is $\theta_{tools} \leq \theta_{max} = 2\cos^{-1}\{(F_3 + F_{min})/(F_1 + F_2)\}$. Due to steric constraints (Section 3.4), at minimum we also require $\theta_{tools} > 60°$ to avoid "handle crash."

Bond angle bending also may be used to fine-tune reaction energetics, selectively adding energy to a specific bond thus increasing its scission propensity. For

RS23.   Add CH_3 to Adam bridgehead w/CH_3 on adjacent sidewall.

Step	Description of Reaction	Mult.	Ener. (eV)	Barr. (eV)
1	**Abstract H from Adam bridgehead site using HAbst tool**			
	R: Cluster53run2 (ABB0A/29) + HAbst (ACC0A/27)	S + D		
	P: BMS2 (ACC0A/28) + HAbstH (ACC0A/28)	D + S	−1.53	
2	**Join GM tool to bridgehead radical site**			
	R: BMS2 (ACC0A/28) + GM5 cluster (ACC0A/16)	D + D		
	P: Side2MBS3 (ACC0A/44)	S	−3.07	
2A	H steal from GM tool to workpiece radical site			
	R: BMS2 (ACC0A/28) + GM tool (ACC0A/28)	D + D		
	P: Cluster53run2 (ABB0A/29) + GMA5HS (ABB0A/27)	S + S	+0.97	
	P: Cluster53run2 (ABB0A/29) + GMA5HT (ACC0A/27)	S + T	+0.26	
	R: BMS2 (ACC0A/28) + GM5 cluster (ACC0A/16)	S + T		
	T: Side2MBS3HTS (ACC1A/44)	T		+0.60
3	**Detach GeRad handle from workpiece**			
	R: Side2MBS3 (ACC0A/44)	S		
	P: BMHSM2 (ACC0A/31) + CH33Ge (ACC0A/13)	D + D	+2.75	
3B1	H steal from workpiece by departing GeRad handle			
	R: Side2MBS3 (ACC0A/44)	S		
	P: Side2MBSSTS (ACC1A/30) + CH33GeH (ACC0A/14)	S + S	+4.04	
	P: Side2MBSTTS (ACC1A/30) + CH33GeH (ACC0A/14)	T + S	+3.82	
4	**Hydrogenate $CH_2\bullet$ radical site using HDon tool**			
	R: BMHSM2 (ACC0A/31) + HDon (ACC0A/26)	D + S		
	P: Side2MBS5 (ACC0A/32) + GeRad (ACC0A/25)	S + D	−0.66	

example, the bond-angle bending spring constant is $k_{bend} \sim$ 1.3–3.7 eV/rad² for C/H molecules and 1.4–4.0 eV/rad² for C/Ge/H molecules,[104] hence the addition to potential energy approximates $\Delta V_{bend} \sim (1/2)\, k_{bend}(\Delta\theta_{bend})^2 \sim$ 0.08−0.24 eV for a $\Delta\theta_{bend} = 20°$ bond angle bend away from the equilibrium bond angle, or 0.50–1.50 eV for $\Delta\theta_{bend} = 50°$, consistent with the results in, e.g., Step 3 of RS5, Step 6 of RS41, or Figure 5.

4. TOOL RECHARGE

After the HAbst tool has been used to remove a hydrogen atom from a specific site on a workpiece, the tool must be refreshed by removing the hydrogen atom now bonded to the ethynyl radical. This is not easy because the ethynyl radical has a higher H affinity than almost any other structure[6]—e.g., 5.49–5.69 eV bond dissociation energy (experimental) for HCC-H,[108, 109] compared to 4.81 eV for C_6H_5-H,[103] 4.56 eV for CH_3-H,[103] and 4.44 eV for H-H.[110] Several possible methods have been proposed.

Musgrave et al.[6] calculated that the HCC-H bond strength is only 1.81 eV in the ${}^3B_u$ excited state, which suggests that a photoexcitation of the alkynyl tip from its ground state to the ${}^1B_u$ excited state, followed by relaxation to the ${}^3B_u$ triplet state, might facilitate the breaking of the tip-hydrogen bond, but no further details were provided. Merkle[4] proposed one method (his Reaction 15) to refresh a hydrogenated ethynyl tool by attacking it with one radical tool and a second ethynyl tool, leaving a 4-carbon polyyne chain similar to butadiyne (H-C≡C-C≡C-H) bound between two handles. However, if the handles are mechanically pulled apart, DFT predicts that the breaking of either single C-C bond between polyyne and handle (yielding a handle monoradical and a butadiyne radical pathology) is energetically preferred by −1.68 eV to the breaking of the polyyne central single C-C bond (yielding the desired two ethynyl radicals), hence this method would be unsatisfactory; the use of two additional Si radical handles to select which C-C bond to break was not explicitly called out but in hindsight might be inferred from a similar treatment, described in the paper, of a hexadiyne

RS24. Add CH_3 to C111 bridgehead w/CH_3 on adjacent bridgehead.

Step		Step 1	Step 2	Step 3	Step 4	

Step	Description of Reaction	Mult.	Ener. (eV)	Barr. (eV)
1	**Abstract H from C111 bridgehead site using HAbst tool**			
	R: DiamM1 (ACC0A/53) + HAbst (ACC0A/27)	S + D		
	P: DiamM2 (ACC0A/52) + HAbstH (ACC0A/28)	D + S	−1.62	
1D3	H migrates to radical from adjacent C111 bridgehead CH			
	R: DiamM2 (ACC0A/52)	D		
	T: DiamM2H26TS (ACC1A/52)	D		+2.21
1D4	H migrates to radical from adjacent C111 bridgehead CH_3 group			
	R: DiamM2 (ACC0A/52)	D		
	P: DiamM2H (ACC0A/52)	D	+0.05	
	T: DiamM2HTS	D		+1.25
2	**Join GM tool to C111 bridgehead radical site**			
	R: DiamM2 (ACC0A/52) + GM tool cluster (ACC0A/7)	D + D		
	P: DiamM3 (ACC0A/59)	S	−2.16	
2A	H steal from GM tool to workpiece radical site			
	R: DiamM2 (ACC0A/52) + GM tool (ACC0A/28)	D + D		
	P: DiamM1 (ACC0A/53) + GMA5HS (ABB0A/27)	S + S	+1.05	
	P: DiamM1 (ACC0A/53) + GMA5HT (ACC0A/27)	S + T	+0.35	
	R: DiamM2 (ACC0A/52) + GM tool cluster (ACC0A/7)	D + D		
	T: DiamM2p1T-QST3 (ACC1B/59)	T		+0.77
2B2	H steal from adjacent CH site on workpiece by GM tool			
	R: DiamM2 (ACC0A/52) + GM tool (ACC0A/28)	D + D		
	P: DiamM2p2S (ACC0A/51) + GMACH3 (ACC0A/29)	S + S	+0.80	
	P: DiamM2p2T (ACC0A/51) + GMACH3 (ACC0A/29)	T + S	−0.14	
	R: DiamM2 (ACC0A/52) + GM tool cluster (ACC0A/7)	D + D		
	T: DiamM2p2TTSrun1 (ACC2A/59)	T		+0.56
2B3	H steal from adjacent C-CH_3 site on workpiece by GM tool			
	R: DiamM2SS (ACC0A/60) + GM tool (ACC0A/28)	D + D		
	P: DiamM2p3SS (ACC0A/59) + GMACH3 (ACC0A/29)	S + S	−0.57	
	T: DiamM2p3SS-QST2 (ACC1A/59) + GMACH3 (ACC0A/29)	S + S		+0.78
	R: DiamM2 (ACC0A/52) + GM tool (ACC0A/28)	D + D		
	P: DiamM2p3Trun2 (ACC0A/51) + GMACH3 (ACC0A/29)	T + S	−0.07	
	R: DiamM2 (ACC0A/52) + GM tool cluster (ACC0A/7)	D + D		
	T: DiamM2p3TTS (ACC2A/59)	T		+0.68
2C1	CH_3 steal from adjacent C-CH_3 site on workpiece by GM tool			
	R: Diam4HH (ACC0A/52) + GM tool cluster (ACC0A/7)	D + D		
	P: Diam2RadS (ACC0A/48) + CH3CH2GeH3 (ACC0A/11)	S + S	+0.47	
	P: Diam2RadT (ACC0A/48) + CH3CH2GeH3 (ACC0A/11)	T + S	−0.47	
	T: Diam4HHGMTTS (ACC1C/59)	T		+1.91
3	**Detach GeRad handle from workpiece**			
	R: DiamM3 (ACC0A/59)	S		
	P: DiamM4 (ACC0A/55) + GeH3 (ACC0A/4)	D + D	+2.22	
3B1	H steal from worksite on workpiece by departing GeRad handle			
	R: DiamM3 (ACC0A/59)	S		
	T: DiamM4HSTS (ACC1A/54) + GeH4 (ACC0A/5)	S + S		+3.42
	P: DiamM4HT (ACC0B/54) + GeH4 (ACC0A/5)	T + S	+3.07	
3B3	H steal from adjacent CH_3 on workpiece by departing GeRad handle			
	R: DiamM3 (ACC0A/59)	S		
	T: C111CH2CH2STS (ACC1A/54) + GeH4 (ACC0A/5)	S + S		+4.38
	P: C111CH2CH2T (ACC0A/54) + GeH4 (ACC0A/5)	T + S	+2.80	

794

J. Comput. Theor. Nanosci. 5, 760–861, 2008

3D5	H migrates to $CH_2\bullet$ radical site from adjacent surface site			
	R: DiamM4 (ACC0A/55)	D		
	P: DiamM4p4 (ACC0A/55)	D	+0.06	
	T: DiamM4p4 (ACC1A/55)	D		+0.97
3D6	H migrates to $CH_2\bullet$ radical site from adjacent CH_3 surface site			
	R: DiamM4 (ACC0A/55)	D		
	T: DiamM4H4TS (ACC1A/55)	D		+0.56
4	**Hydrogenate $CH_2\bullet$ radical site using HDon or HTrans tool**			
	R: DiamM4 (ACC0A/55) + HDon (ACC0A/26)	D + S		
	P: DiamM5 (ACC0A/56) + GeRad (ACC0A/25)	S + D	−0.45	
	R: DiamM4 (ACC0A/55) + S15cis (ACCCA/11)	D + D		
	P: DiamM5 (ACC0A/56) + S16Run0 (ACCCA/10)	S + S	−1.28	

bound between two handles, though this increases steric congestion. An earlier general proposal by Drexler[3] (his Fig. 8.14) to recharge an ethynyl radical by attacking the spent tool with two similar (but unidentified, inferentially hydrocarbon-based from the text) radicals is the inspiration for the specific 3-tool method proposed here (RS5). However, it should also be noted that Drexler's original proposal included a "supporting structure provid[ing] nonbonded contacts" that is geometrically equivalent to employing four proximated tool handles in the vicinity of the apical carbon atom, producing unacceptable steric congestion that would violate one of the constraints on reaction pathway design imposed in this paper. Apparently no support structure is required because the low barrier in Step 1 of RS5 is readily overcome by mechanical force which produces minimal ethynyl flexure in free space during the reaction; for Step 2 of RS5, independent TS and QST3 searches using DFT found no intermediate singlet transition states, indicating the reaction barrier may be zero.

After the DimerP tool has been used to add a C_2 dimer to a specific site on a workpiece, the tool may be refreshed by bonding a new dimer across the two Ge radical adamantyl substituent sites of the discharged DimerP tool using RS6. Force constraints indicate $\theta_{max} = 64°$ at 300 K (73° at 80 K) in Step 2, workable for $\theta_{tools} > 60°$. In Step 5, $\theta_{max} = 108°$ at 300 K (114° at 80 K); the DFT-optimized geometry gives the range of accessible $\theta_{tools} = 74°$ (Ge-C-Ge) to 114° (Ge-C-C), and the nondetached GeRad handle may also assist. For Step 6, θ_{max} is the same as Step 5 and the range of accessible $\theta_{tools} = 74°$ (Ge-C-Ge) to 109° (C-C-Ge). DimerP refresh by simple exposure to C_2H_2 gas as proposed by Mann et al.[19] is problematic. Acetylene addition to the two $\bullet$Ge monoradical sites on a discharged DimerP tool in the desired horizontal configuration is exoergic by −3.10 eV using DFT/GGA with the VASP simulation package as reported by Mann et al.,[19] confirmed as −2.74 eV singlet, −3.84 triplet, using DFT in the present work. The DFT/GGA analysis predicts a +1.49 eV energy barrier which cannot be overcome by exposing the monoradical sites to room temperature pressurized bulk gas (cf. Section 6) because a C_2H_2 pressure of at least 5–10 K atm would be needed, but at 300 K pure

acetylene gas decomposes by deflagration above 2 atm and can detonate above 3.2 atm.[111] Mann et al.[19] proposed raising the temperature, not the pressure, of the bulk C_2H_2 gas to overcome the barrier, yielding a more reasonable $k_{react}^{-1} = 0.3$ sec at 600 K. DFT studies show that bonding between the $\bullet$Ge monoradicals and C_2H_2 may yield either: (1) a one-Ge-bonded "ethynyl" Ge-CHCH$\bullet$ carbon monoradical adjacent to an unused $\bullet$Ge monoradical, which transitions to singlet DimerP-C_2H_2 when the $\bullet$CH radical couples to the unused $\bullet$Ge monoradical through a +0.31 eV barrier, or (2) a two-Ge-bonded "carbenic" Ge-CH(-CH:)-Ge carbon diradical, which transitions to singlet DimerP-C_2H_2 when the diradical inserts into an existing acetylenic Ge-C single bond through a +0.15 eV barrier. Unfortunately, there is also a third competing reaction pathway, apparently barrierless and exoergic by −1.38 eV, in which newly arriving C_2H_2 gas molecules bond to the exposed acetylenic distal $\bullet$CH radical, with each addition creating a new distal $\bullet$CH radical to seed the next addition, triggering a spontaneously extending polyacetylene chain reaction (Section 8.3.2). Hence DimerP recharge directly from C_2H_2 gas appears feasible only (1) at high temperature, and (2) when exposure to just a single C_2H_2 gas molecule during the recharge cycle can be assured.

After the HDon tool has been used to add a hydrogen atom to a specific site on a workpiece, converting it to a GeRad handle, the GeRad may be refreshed back to HDon by adding a new H atom to the Ge atom at the substituent site on the germano-adamantyl radical by employing Step 2 of RS5. Exposing GeRad to bulk H_2 gas will not recharge an HDon tool because the reaction, also yielding a free H ion, is endoergic by +0.98 eV. The GeRad tool handle may be refreshed from an HDon tool by employing RS2 on a (possibly bulk-prepared) dehydrogenated diamond surface (the H dump).

The AdamRad tool handle is obtained from a handled adamantane cage using RS1; the energetics of the adamantyl radical are well-studied.[112] Simple heating of an adamantane stub of diamond C(111) to >1200 K might achieve complete depassivation[113] and yield a useful adamantyl radical, though graphitization,[114] multiradical formation, and reconstruction upon cooling are potential problems with this approach. Note that an AdamRad

RS25. Add CH$_3$ to C110 ridge site w/CH$_3$ on adjacent ridge site.

Step	Description of Reaction	Mult.	Ener. (eV)	Barr. (eV)
1	**Abstract H from C110 ridge site using HAbst tool**			
	R: C110E (ACC0A/45) + HAbst (ACC0A/27)	S + D		
	P: C110MB (ACC0A/44) + HAbstH (ACC0A/28)	D + S	−1.59	
1D5	H migrates to radical from adjacent ridge site			
	R: C110MB (ACC0A/44)	D		
	T: C110MBTS (ACC1A/44)	D		+2.58
1D6	H migrates to radical from adjacent ridge CH$_3$ group			
	R: C110MB (ACC0A/44)	D		
	P: C110MBH (ACC0A/44)	D	−0.03	
	T: C110MBHTS (ACC1A/44)	D		+2.01
2	**Join GM tool to C110 ridge radical site**			
	R: C110MB (ACC0A/44) + GM tool cluster (ACC0A/7)	D + D		
	P: C110MC (ACC0A/51)	S	−3.00	
2A	H steal from GM tool to workpiece radical site			
	R: C110MB (ACC0A/44) + GM tool (ACC0A/28)	D + D		
	P: C110E (ACC0A/45) + GMA5HS (ABB0A/27)	S + S	+1.09	
	P: C110E (ACC0A/45) + GMA5HT (ACC0A/27)	S + T	+0.32	
	R: C110MB (ACC0A/44) + GM tool cluster (ACC0A/7)	D + D		
	T: C110MCp1TTS (ACC1A/51)	T		+0.63
2B2	H steal from adjacent CH site on same ridge by GM tool			
	R: C110MB (ACC0A/44) + GM tool (ACC0A/28)	D + D		
	P: C110MBp2S (ACC0A/43) + GMACH3 (ACC0A/29)	S + S	−0.65 [a]	
	P: C110MBp2T (ACC0A/43) + GMACH3 (ACC0A/29)	T + S	−0.13	
	R: C110MB (ACC0A/44) + GM tool cluster (ACC0A/7)	D + D		
	T: C110MBp2TTS (ACC1B/51)	T		+0.69
2B3	H steal from adjacent C-CH$_3$ site on same ridge by GM tool			
	R: C110MB (ACC0A/44) + GM tool (ACC0A/28)	D + D		
	T: C110MBp3STS (ACC1A/43) + GMACH$_3$ (ACC0A/29)	S + S		+0.95
	P: C110MBp3Trun2 (ACC0A/43) + GMACH3 (ACC0A/29)	T + S	−0.15	
	R: C110MB (ACC0A/44) + GM tool cluster (ACC0A/7)	D + D		
	T: C110MBp3TTS2 (ACC1A/51)	T		+0.61
2B4	H steal from nearest CH site on adjacent ridge by GM tool [b]			
	R: C110E (ACC0A/45) + GM tool (ACC0A/28)	S + D		
	P: C110MB (ACC0A/44) + GMACH3 (ACC0A/29)	D + S	−0.12	
	R: C110A (ACC0A/42) + GM tool cluster (ACC0A/7)	S + D		
	T: C110MBp5TS (ACC1A/49)	D		+0.51
3	**Detach GeRad handle from workpiece**			
	R: C110MC (ACC0A/51)	S		
	P: C110MD (ACC0A/47) + GeH3 (ACC0A/4)	D + D	+2.75	
3B1	H steal from worksite on workpiece by departing GeRad handle			
	R: C110MC (ACC0A/51)	S		
	P: C110MDHS (ACC0B/46) + GeH4 (ACC0A/5)	S + S	+3.81	
	P: C110MDHT (ACC0A/46) + GeH4 (ACC0A/5)	T + S	+3.69	
3D5	H migrates to CH$_2$• radical site from adjacent surface site			
	R: C110MD (ACC0A/47)	D		
	P: C110MDp4 (ACC0A/47)	D	−0.09	
	T: C110MDp4TS (ACC1A/47)	D		+1.32

Continued

3D6	H migrates to CH$_2$• radical site from adjacent CH$_3$ surface site			
	R: C110MD (ACC0A/47)	D		
	T: C110MDp5TS (ACC1A/47)	D		+ 0.91
4	**Hydrogenate CH$_2$• radical site using HDon tool**			
	R: C110MD (ACC0A/47) + HDon (ACC0A/26)	D + S		
	P: C110ME (ACC0A/48) + GeRad (ACC0A/25)	S + D	−0.64	

[a] Pathology 2B2 (singlet) can occur (no barrier found), resulting in ethenylation (C=C) of single-bonded surface atoms; however, this requires a very large mispositioning of the tooltip by ~2.51 Å, hence can be avoided by proper positional control.

[b] Pathology 2B4 is prevented by a barrier, but is readily avoided by maintaining good positional control.

is recovered each time a Meth tool or Germ tool is discharged, thus may be recycled.

The HAbst (RS37–RS39), HTrans (RS5), Meth (RS40), GM (RS41), and Germ (RS42) tools can be recharged by refabrication on an AdamRad (RS33 + RS34) or GeRad (RS35 + RS36) handle base. The GM tool is obtained from the Meth tool via RS41, and the Meth tool is obtained from the GM tool via Steps 1–3 of RS9. The hydrogen dump, which can be a very large surface (clean diamond C(111) has > 10^7 sites/micron^2), is periodically refreshed after deposition of waste H atoms by baking at high temperature to desorb the H and restore clean surface.

5. BASIC METHYLATION REACTIONS

5.1. Stability of H/CH$_3$ Near Adamantane Radical Sites

The foundational reactions of DMS employ adamantane cages upon which radical sites are transiently created in the presence of neighboring H atoms or on (or near) cage-bonded methyl groups. Prior to designing reaction sequences it is necessary to ascertain whether the presence of these radical sites might allow unwanted: (1) surface migrations of H or CH$_3$ groups, or (2) structural rearrangements involving insertion of methylene radicals (•CH$_2$) into nearby C-C bonds comprising the adamantane cage.

Table I gives reaction energies and barriers for all plausible migrations of H atoms or methyl groups on adamantane, when either or both are present near a •C or •CH$_2$ monoradical site, along with some representative cases involving two methyl groups and one monoradical. (A "bridgehead" site is a C atom in the adamantane cage with 3 bonds to other C atoms in the cage; a "sidewall" C atom has only 2 bonds to other C atoms in the cage.) Substantial energy barriers normally prevent both the insertion of methyl radicals into the adamantane cage and the migration of an H atom or a methyl group to a nearby monoradical site. DFT searches for transition states for *cis-trans* flips of an H atom and a CH$_3$ group attached to the same sidewall C atom, both with and without the presence of a second CH$_3$ group on the adjacent sidewall C atom, consistently resulted in dissociation of the CH$_3$ group from the sidewall C atom which thus requires a *cis-trans* flip

barrier of at least +3.40 eV to accommodate a C-CH$_3$ bondbreaking, hence such isomeric rearrangements apparently are not thermally accessible at 300 K. In the case of two methyl groups placed on adjacent sidewall C atoms, where an H atom is then abstracted from one of the CH$_3$ groups to create a •CH$_2$ monoradical site on one side, the barrier to one H atom "hopping" back and forth between the two methyl groups is only +0.60 eV, very near our lowest acceptable barrier height of +0.40 eV (Section 1). Additionally, the migration of a sidewall methyl H atom to a sidewall •C monoradical site, and the migration of a sidewall H atom or a bridgehead methyl H atom to a sidewall •CH$_2$ monoradical site, are only blocked by barriers of about +1.0 eV. Closer scrutiny is warranted of any reaction sequence step involving an adamantane cage structure that results in the proximation of H atoms, methyl groups, and monoradical sites having these particular configurations.

5.2. Add First Methyl Group

The most common basic task in DMS is the site-specific addition of a single methyl group (-CH$_3$) to a diamondoid workpiece structure using a positionally controlled GM tool or Meth tool, the former usually being preferred because the latter requires an extra 4 steps to execute a "handle exchange" operation in which the original AdamRad handle is replaced by a GeRad handle to facilitate subsequent forced mechanical detachment. The available reaction pathways identified in the present work include CH$_3$ addition to:

(1) an adamantane sidewall site (2-adamantyl radical) using a GM tool (RS7) or Meth tool (RS8);

(2) an adamantane bridgehead site (1-adamantyl radical) using a GM tool (RS9) or Meth tool (RS10, or RS11 illustrating use of a carbene intermediate);

(3) a diamond C(111) bridgehead site using a GM tool (RS12);

(4) a diamond C(110) ridge site (RS13) and a diamond C(110) ledge site (RS12, tilted 30°), both using a GM tool;

(5) a diamond C(100) dimer site using a GM tool (RS14);

(6) a lonsdaleite C(111) gap bridgehead site using a GM tool (RS15) or Meth tool (RS16); note alternate Steps 2–4 and 2^1–4^1, with $\theta_{max} = 95°$ at 300 K (101° at 80 K) for the

RS26.   Add CH_3 to C100 dimer site w/CH_3 on same dimer.

	Step 1	Step 2	Step 3	Step 4	

Step	Description of Reaction	Mult.	Ener. (eV)	Barr. (eV)
1	**Abstract H from C100 dimer site using HAbst tool**			
	R: C100MA (ACC0A/38) + HAbst (ACC0A/27)	S + D		
	P: C100MB (ACC0A/37) + HAbstH (ACC0A/28)	D + S	−1.38	
1D5	H migrates to radical from nearest adjacent dimer site			
	R: C100MB (ACC0A/37)	D		
	P: C100MBp3 (ACC0A/37)	D	0.00	
	T: C100MBp3TS (ACC1A/37)	D		+2.76
1D6	H migrates to radical from same dimer CH_3 group			
	R: C100MB (ACC0A/37)	D		
	P: C100MBp2 (ACC0A/37)	D	−0.17	
	T: C100MBp2TSrun2 (ACC1A/37)	D		+1.74
1E	CH_3 migrates to radical on same dimer			
	R: C100MB (ACC0A/37)	D		
	T: C100MBp1TS (ACC1A/37)	D		+2.97
2	**Join GM tool to C100 dimer radical site**			
	R: C100MB (ACC0A/37) + GM tool cluster (ACC0A/7)	D + D		
	P: C100MC (ACC0B/44)	S	−3.38	
2A	H steal from GM tool to workpiece radical site			
	R: C100MB (ACC0A/37) + GM tool (ACC0A/28)	D + D		
	P: C100MA (ACC0A/38) + GMA5HS (ABB0A/27)	S + S	+0.82	
	P: C100MA (ACC0A/38) + GMA5HT (ACC0A/27)	S + T	+0.11	
	R: C100MB (ACC0A/37) + GM tool cluster (ACC0A/7)	D + D		
	T: C100MCp1TTS (ACC1B/51)	T		+0.45
2B3	H steal from adjacent C-CH_3 site on same dimer by GM tool			
	R: C100MB (ACC0A/37) + GM tool (ACC0A/28)	D + D		
	T: C110MCp2STS (ACC1A/36) + GMACH₃ (ACC0A/29)	S + S		+1.28
	P: C100MCp2T (ACC0A/36) + GMACH₃ (ACC0A/29)	T + S	−0.07	
	R: C100MB (ACC0A/37) + GM tool cluster (ACC0A/7)	D + D		
	T: C100MCp2TTS (ACC1A/44)	T		+0.60
2B4	H steal from nearest CH site on adjacent dimer by GM tool			
	R: C100MB (ACC0A/37) + GM tool (ACC0A/28)	D + D		
	P: C100MCp3S (ACC0A/36) + GMACH₃ (ACC0A/29)	S + S	+0.68	
	P: C100MCp3T (ACC0A/36) + GMACH₃ (ACC0A/29)	T + S	+0.10	
	R: C100MB (ACC0A/37) + GM tool cluster (ACC0A/7)	D + D		
	T: C100MCp3TTS (ACC1A/44)	T		+0.57
2C2	CH_3 steal from adjacent C-CH_3 site on same dimer by GM tool			
	R: C100MB (ACC0A/37) + GM tool cluster (ACC0A/7)	D + D		
	P: C100MCp4S (ACC0A/33) + CH3CH2GeH3 (ACC0A/11)	S + S	−0.89	
	T: C100MCp4STS (ACC1B/44)	S		+1.97
	P: C100MCp4T (ACC0A/33) + CH3CH2GeH3 (ACC0A/11)	T + S	+0.41	
	T: C100MCp4TTS (ACC1A/44)	T		+2.20
3	**Detach GeRad handle from workpiece**			
	R: C100MC (ACC0B/44)	S		
	P: C100MD (ACC0A/40) + GeH3 (ACC0A/4)	D + D	+2.79	
3B1	H steal from CH_2 on workpiece by departing GeRad handle			
	R: C100MC (ACC0B/44)	S		
	P: C100MDp1S (ACC0A/39) + GeH4 (ACC0A/5)	S + S	+3.82	
	P: C100MDp1T (ACC0A/39) + GeH4 (ACC0A/5)	T + S	+3.75	

3D5	H migrates to $CH_2\bullet$ radical from nearest CH site on adjacent dimer				
	R: C100MD (ACC0A/40)	D			
	P: C100MDp6 (ACC0A/40)	D	+0.15		
	T: C100MDp6TSrun2 (ACC1A/40)	D		+1.29	
3D6	H migrates to $CH_2\bullet$ radical site from CH_3 site on same dimer				
	R: C100MD (ACC0A/40)	D			
	T: C100MDp5TS (ACC1A/40)	D		+1.01	
3E	CH_3 migrates to $CH_2\bullet$ radical site on same dimer				
	R: C100MD (ACC0A/40)	D			
	P: C100MDp7 (ACC0B/40)	D	+0.35		
	T: C100MDp7TS (ACC1A/40)	D		+3.03	
4	**Hydrogenate $CH_2\bullet$ radical site using HDon tool**				
	R: C100MD (ACC0A/40) + HDon (ACC0A/26)	D + S			
	P: C100ME (AXCXA/41) + GeRad (ACC0A/25)	S + D	−0.80		

AdamRad detachment step of all handle exchanges using a Meth tool;

(7) the free tip of a single-handled polyyne chain whose tip has first been H-passivated via RS1, using a GM tool (RS17) (an unpassivated polyyne chain tip is an ethynyl radical that would pathologically abstract a methyl H from the incoming GM tool exoergically by −0.55 eV singlet, −1.25 eV triplet);

(8) any carbon atom along the length of a two-handled polyyne chain (RS18); and

(9) a free CH site of an Adam-mounted aromatic ring (Steps 1–3 of RS63). Regarding the methylidyne C**:** diradical tool intermediate that appears in Steps 4–7 of RS11, the methylene (**:**CH_2) divalent radical has a long and well-known history in organic chemistry,[115] with the singlet lying +0.4 eV above the ground state triplet with an intersystem crossing time from singlet to triplet of $\sim10^{-9}$ sec and a reaction time of **:**CH_2 with gas-phase ethylene extrapolated to 5 M concentration of $\sim10^{-12}$ sec for the singlet and $\sim10^{-6}$ sec for the triplet.[116]

5.3. Add Second Methyl Group

Reaction pathways have been identified for using a GM tool to add a second CH_3 to:

(1) an existing methyl on an adamantane sidewall site (RS19);

(2) an existing methyl on an adamantane bridgehead site (RS20);

(3) an adamantane sidewall site adjacent to an existing methyl on the nearest sidewall (RS21) or bridgehead (RS22) site;

(4) an adamantane bridgehead site adjacent to an existing methyl on the nearest sidewall (RS23) site;

(5) a diamond C(111) bridgehead site adjacent to an existing methyl on the nearest bridgehead (RS24) site;

(6) a diamond C(110) ridge site adjacent to an existing methyl on the nearest ridge site (RS25);

(7) a diamond C(100) dimer site adjacent to an existing methyl on the same dimer (RS26) or on the nearest site on the adjacent dimer (RS27); and

(8) a lonsdaleite C(111) gap bridgehead site adjacent to an existing methyl on the nearest apposing gap bridgehead site (RS28). An additional 4-step handle exchange operation is required if a Meth tool is used in place of a GM tool in these reactions.

5.4. Add Third and Fourth Methyl Groups

Explicit reaction pathways are reported for using a GM tool to add a third CH_3 to:

(1) an existing two-methyl chain on an adamantane sidewall site (RS29);

(2) an existing methyl on an adamantane sidewall site adjacent to an existing methyl on the nearest sidewall (RS30) site; and

(3) an adamantane sidewall site adjacent to an existing methyl on each of the two nearest sidewall sites (RS31). A reaction pathway is also reported for using a GM tool to add a fourth CH_3 to an existing three-methyl chain on an adamantane sidewall site (RS32). Additional permutations and extensions to longer chains are readily recognized but are omitted for brevity because the energetics should be essentially identical to those previously reported.

6. DIAMONDOID CAGE AND LATTICE FABRICATION

To add a new adamantane cage (Adam/AdamRad) to the distal end of an existing fully hydrogenated adamantane stub mounted on a positionally-controlled handle, we begin by fabricating a handled three-methyl chain on an Adam sidewall site (RS29), then attaching the handled distal end of that chain to an adjacent second sidewall site in the direction it is desired to extend the diamond lattice (RS33) (aka. "propylation"; Section 8.2). The energies required for forced chain rotations in Steps 1–2 are an order of magnitude smaller than the 2.44 eV Ge-C bond dissociation energy binding a GeRad handle to the workpiece. The new cage is completed by bonding a fourth methyl group between the second methyl group in the three-methyl

RS27. Add CH₃ to C100 dimer site nearest to CH₃ on adjacent dimer.

Step	Description of Reaction	Mult.	Ener. (eV)	Barr. (eV)
1	**Abstract H from nearest C100 adjacent dimer site w/HAbst tool**			
	R: C100MMA (ACC0A/38) + HAbst (ACC0A/27)	S + D		
	P: C100MMB (ACC0A/37) + HAbstH (ACC0A/28)	D + S	−1.42	
1D5	H migrates to radical from same dimer site			
	R: C100MMB (ACC0A/37)	D		
	P: C100MBp3 (ACC0A/37)	D	+0.04	
	T: C100MMBp3TS (ACC1A/37)	D		+2.20
1D6	H migrates to radical from adjacent dimer CH₃ group			
	R: C100MMB (ACC0A/37)	D		
	P: C100MMBp2 (ACC0A/37)	D	−0.13	
	T: C100MMBp2TS (ACC1A/37)	D		+1.13
1E	CH₃ migrates to radical on adjacent dimer			
	R: C100MMB (ACC0A/37)	D		
	T: C100MMBp1TS (ACC2A/37)	D		+3.45
2	**Join GM tool to C100 dimer radical site**			
	R: C100MMB (ACC0A/37) + GM tool cluster (ACC0A/7)	D + D		
	P: C100MMC (ACC0A/44)	S	−3.13	
2A	H steal from GM tool to workpiece radical site			
	R: C100MMB (ACC0A/37) + GM tool (ACC0A/28)	D + D		
	P: C100MMA (ACC0A/38) + GMA5HS (ABB0A/27)	S + S	+0.86	
	P: C100MMA (ACC0A/38) + GMA5HT (ACC0A/27)	S + T	+0.15	
	R: C100MMB (ACC0A/37) + GM tool cluster (ACC0A/7)	D + D		
	T: C100MMCp1T-QST3run5 (AXCXB/44)	T		+0.57
2B3	H steal from C-CH₃ site on adjacent dimer by GM tool			
	R: C100MMB (ACC0A/37) + GM tool (ACC0A/28)	D + D		
	T: C110MMCp2STSrun2 (ACC1A/36) + GMACH3 (ACC0A/29)	S + S		+1.03
	P: C100MMCp2T (ACC0A/36) + GMACH₃ (ACC0A/29)	T + S	−0.08	
	R: C100MMB (ACC0A/37) + GM tool cluster (ACC0A/7)	D + D		
	T: C100MMCp2TTS (ACC1A/44)	T		+0.65
2B4	H steal from CH site on same dimer by GM tool			
	R: C100MMB (ACC0A/37) + GM tool (ACC0A/28)	D + D		
	P: C100MCp3S (ACC0A/36) + GMACH₃ (ACC0A/29)	S + S	−0.99	
	R: C100MMB (ACC0A/37) + GM tool cluster (ACC0A/7)	D + D		
	T: C100MMCp3S-QST3 (ACC1C/44)	S		+1.20
	P: C100MMCp3T (ACC0A/36) + GMACH3 (ACC0A/29)	T + S	+0.30	
	R: C100MMB (ACC0A/37) + GM tool cluster (ACC0A/7)	D + D		
	T: C100MMCp3TTS (ACC1A/44)	T		+0.65
2C3	CH₃ steal from C-CH₃ site on adjacent dimer by GM tool			
	R: C100MMB (ACC0A/37) + GM tool cluster (ACC0A/7)	D + D		
	P: C100MMCp4S (ACC0A/33) + CH3CH2GeH₃ (ACC0A/11)	S + S	+0.86	
	P: C100MMCp4T (ACC0A/33) + CH3CH2GeH₃ (ACC0A/11)	T + S	+0.25	
	T: C100MMCp4TTS (ACC1A/44)	T		+2.15
3	**Detach GeRad handle from workpiece**			
	R: C100MMC (ACC0A/44)	S		
	P: C100MMD(ACC0A/40) + GeH3 (ACC0A/4)	D + D	+2.69	
3B1	H steal from worksite on workpiece by departing GeRad handle			
	R: C100MMC (ACC0A/44)	S		
	P: C100MMDp1S (ACC0A/39) + GeH4 (ACC0A/5)	S + S	+3.57	
	P: C110MMDp1T (ACC0A/39) + GeH4 (ACC0A/5)	T + S	+3.59	

3D5	H migrates to $CH_2\bullet$ radical from CH site on same dimer				
	R: C100MMD (ACC0A/40)		D		
	P: C100MMDp6 (ACC0A/40)		D	+0.26	
	T: C100MMDp6TS (ACC1A/40)		D		+1.99
3D6	H migrates to $CH_2\bullet$ radical site from CH_3 site on adjacent dimer				
	R: C100MMD (ACC0A/40)		D		
	T: C100MMDp5TS (ACC1A/40)		D		+0.51
3E	CH_3 on adjacent dimer migrates to $CH_2\bullet$ radical site				
	R: C100MMD (ACC0A/40)		D		
	P: C100MMDp7 (ACC0A/40)		D	+0.17	
	T: C100MMDp7TS (ACC1A/40)		D		+2.25
4	**Hydrogenate $CH_2\bullet$ radical site using HDon tool**				
	R: C100MMD (ACC0A/40) + HDon (ACC0A/26)		D + S		
	P: C100MME (AXCXA/41) + GeRad (ACC0A/25)		S + D	−0.72	

chain and an adjacent third sidewall site (RS34), yielding a larger Adam handle or a new AdamRad tool after application of RS1. Note that we used a ring-closing diradical/nonradical bonding operation in RS33 (here the C**:** singlet lies −0.17 eV below the triplet) and a cage-closing monoradical/monoradical bonding operation in RS34 to illustrate that either approach may be used, since both Reaction Sequences involve attaching a handled methyl group to an adamantane sidewall CH_2 site and thus have similar energetics and pathologies. The other three possible variants for RS33 + RS34, obtained by choosing the alternative reactant site to dehydrogenate in Step 4 of either or both of RS33 and RS34, should work equally well.

RS33 + RS34 can be applied iteratively to add to the Adam workpiece a second, third, or successive cages along any of the *X*, *Y* or *Z* directions, allowing fabrication of the diamond lattice to be extended in all three dimensions without process-imposed size limits (Fig. 4). Pandey reconstruction[117] of the growing C(111) surface is prevented by maintaining complete hydrogenation of the surface except at the one or two C atom sites where an addition reaction is in progress. Similarly, repeated application of RS4 using the DimerP tool quickly and efficiently extends the diamond crystal without limit in the C(110) direction (Section 3.3).[19–22] Since the C(110) surface does not reconstruct, it is unnecessary to maintain continuous hydrogen passivation while building large blocks of this surface, though rows terminating in other crystal faces must be H-terminated at the end of each row to control reconstruction on those other faces (e.g., C(111), C(100)), using RS2. RS2 is also used to passivate the final C(110) layer with hydrogen. Finally, the diamond C(100) crystal plane can be indefinitely extended using the same two reaction pathways, or via the third method of dehydrogenating methyls (RS50), but in all cases with dimers laid down in rows running North-South and East-West in alternating layers across the nonhydrogenated reconstructed C(100)-(2 × 1) surface.

C(110) might also be fabricated via a chain deposition process using a one-handled polyyne chain (RS52) that is applied in a zigzag pattern across a C(110) trough to build the next layer, inferentially using RS48 because the 3.04 Å C/C distance across a C(110) trough is similar to but larger than the 2.71 Å (triplet) C/C distance across the DCB6C gap in RS48, likely increasing the barrier to pathology 3H in RS48 as should be confirmed using larger models than those available for this study. Maintaining positional control of a longer polyyne chain will be more difficult due to chain flex. To avoid this problem, the relatively short polyyne chain that is being used as the deposition tool may be extended indefinitely in length during deposition of a long course on C(110) by the insertion of additional C_2 dimer (RS54) or methyl (RS55) units via handle exchange at the deposition tool handle. The course may be finished with a handle exchange from AdamRad to GeRad (e.g., Steps 1–5 of RS10) after placement of the last -C≡C- dimer if necessary to facilitate handle detachment without disrupting the new lattice structure. (Handle detachment or exchange during the aforementioned chain deposition process can be facilitated using a GeRad-handled variant of the HAbst tool (i.e., GeRad-C≡C•, rather than Adam-C≡C•, with a Ge-bridgehead-attached C_2 dimer) which may be fabricated using Step 1 of RS60, followed by Step 6 of RS41 (Fig. 5), Steps 2–4 of RS39, and then RS5.) This is similar to the cumulene "strand deposition process" previously proposed by Drexler[3] except that polyyne is the more stable chain structure (Section 8.3.1) and possesses C-C single bonds that may permit more convenient bending during deposition.

Fabrication of a new Ge-substituted 1,1-germanoadamantane cage (HDon/GeRad) proceeds similarly, with fabrication of a handled -CH_2-GeH_2-CH_2- chain followed by attachment of its handled distal end to an adjacent second sidewall site (RS35), and the cage then completed by bonding a methyl group between the central germyl group in the chain and an adjacent third sidewall site (RS36), yielding a new HDon tool readily convertible to GeRad upon application of RS1. The Ge**:** diradical formed in Step 5 of RS35 appears to be stable, and similar species such as **:**GeH_2,[118–120] and reactive intermediates such as diphenylgermylene (($C_6H_5)_2$-GeH_2),[121] dimethylgermylene divalent radical (($CH_3)_2$-Ge**:**),[122] and

RS28. Add CH_3 to DCB6C bridgehead w/CH_3 on opposing bridgehead.

	Step 1	Step 2	Step 3	Step 4

Step	Description of Reaction	Mult.	Ener. (eV)	Barr. (eV)
1	**Abstract H from DCB6C bridgehead using HAbst tool**			
	R: Cluster53B (ACC0A/49) [RS15 Step 4] + HAbst (ACC0A/27)	S + D		
	P: C52Bpath (ACC0A/48) + HAbstH (ACC0A/28)	D + S	−1.92	
1D2	H migrates to radical from adjacent shoulder sidewall CH_2			
	R: C52Bpath (ACC0A/48)	D		
	P: C52BpH39 (ACC0A/48)	D	+0.32	
	T: C52BpH39TS (ACC1A/48)	D		+2.65
1D3	H migrates to radical from adjacent bridgehead CH			
	R: C52Bpath (ACC0A/48)	D		
	P: C52BpH26 (ACC0A/48)	D	+0.30	
	T: C52BpH26TS (ACC1A/48)	D		+2.63
1D9	H migrates to radical from apposing DCB6C bridgehead CH_3			
	R: C52Bpath (ACC0A/48)	D		
	P: Cluster52B (ACC0A/48)	D	+0.17	
	T: C52Bpath-QST2 (ACC1A/48)	D		+0.58
1E	CH_3 migrates to radical from apposing DCB6C bridgehead			
	R: C52Bpath (ACC0A/48)	D		
	T: C52BpCH3TS (ACC1A/48)	D		+2.46
2	**Join GM tool to DCB6C bridgehead radical site**			
	R: C52Bpath (ACC0A/48) + CH33GeCH2 (ACC0A/16)	D + D		
	P: Cluster51BB (ACC0A/64)	S	−1.67	
2A	H steal from GM tool to DCB6C bridgehead radical site			
	R: C52Bpath (ACC0A/48) + GM tool (ACC0A/28)	D + D		
	P: Cluster53B (ACC0A/49) + GMA5HS (ABB0A/27)	S + S	+1.36	
	P: Cluster53B (ACC0A/49) + GMA5HT (ACC0A/27)	S + T	+0.65	
2B7	H steal from adjacent shoulder sidewall CH_2 by GM tool			
	R: C52Bpath (ACC0A/48) + GM tool cluster (ACC0A/7)	D + D		
	P: C52BH39S (ACC0A/47) + GeH3CH3 (ACC0A/8)	S + S	−0.65	
	T: C52BH39GMS-QST3 (ACC1A/55)	S		+0.84
	P: C52BH39T (ACC0A/47) + GeH3CH3 (ACC0A/8)	T + S	−0.11	
	T: C52BH39GMTTS (ACC1A/55)	T		+0.63
2B10	H steal from apposing DCB6C bridgehead CH_3 by GM tool			
	R: C52Bpath (ACC0A/48) + GM tool (ACC0A/28)	D + D		
	P: C52BHS (ACC0A/47) + GMACH3 (ACC0A/29)	S + S	−2.94	
	T: C52BHSTSStep28 (ACC1D/47) + GMACH3 (ACC0A/29)	S + S		+0.85
	P: C52BHTAF (ACC0A/47) + GMACH3 (ACC0A/29)	T + S	−0.05	
	R: C52Bpath (ACC0A/48) + GM tool cluster (ACC0A/7)	D + D		
	T: C52BHTp2ATTS (ACC1A/55)	T		+0.79
2C1	CH_3 steal from apposing DCB6C bridgehead by GM tool			
	R: C52Bpath (ACC0A/48) + GM tool cluster (ACC0A/7)	D + D		
	P: Cluster88S (ACC0A/44) + CH3CH2GeH3 (ACC0A/11)	S + S	+0.25	
	T: C88GMS-QST3 (ACC3D/55)	S		+3.30
	P: Cluster88T (ACC0A/44) + CH3CH2GeH3 (ACC0A/11)	T + S	−0.13	
	T: C88GMTTS (ACC1A/55)	T		+2.73
3	**Detach GeRad handle from workpiece**			
	R: Cluster51BB (ACC0A/64)	S		
	P: Cluster52BB (ACC0A/51) + CH33Ge (ACC0A/13)	D + D	+2.30	
3B1	H steal from CH_2 by departing GeRad handle			
	R: Cluster51BB (ACC0A/64)	S		
	P: C52BBCS-TS (ACC1A/47) + CH33GeH (ACC0A/14)	S + S	+2.83	
	P: C52BBCarbT (ACC0A/47) + CH33GeH (ACC0A/14)	T + S	+3.09	

Continued

REVIEW

3D2	H migrates to $CH_2\bullet$ radical from adjacent shoulder sidewall CH_2			
	R: Cluster52BB (ACC0A/51)	D		
	P: C52BBH39 (ACC0A/51)	D	+0.22	
	T: C52BBH39-QST3 (ACC1A/51)	D		+1.63
3D3	H migrates to $CH_2\bullet$ radical from adjacent bridgehead CH			
	R: Cluster52BB (ACC0A/51)	D		
	P: C52BBH26 (ACC0A/51)	D	+0.27	
	T: C52BBH26-QST2 (ACC0A/51)	D		+2.16
3D10	H migrates to $CH_2\bullet$ radical from apposing DCB6C bridgehead CH_3			
	R: Cluster52BB (ACC0A/51)	D		
	T: C52BB-QST2 (ACC1A/51)	D		**+0.08** [a]
3E	CH_3 migrates to $CH_2\bullet$ radical from apposing DCB6C bridgehead			
	R: Cluster52BB (ACC0A/51)	D		
	P: C52BBCH2CH3 (ACC0A/51)	D	−0.57	
	T: C52BBCH2CH3-QST3 (ACC1A/51)	D		+1.48
4	**Hydrogenate $CH_2\bullet$ radical site using HDon or HTrans tool**			
	R: Cluster52BB (ACC0A/51) + HDon (ACC0A/26)	D + S		
	P: LonsA5run2 (ACC0A/52) + GeRad (ACC0A/25)	S + D	−0.30	
	R: Cluster52BB (ACC0A/51) + S15cis (ACCCA/11)	D + D		
	P: LonsA5run2 (ACC0A/52) + S16Run0 (ACCCA/10)	S + S	−1.13	

[a] With such a low barrier to migration, the migrating H atom will transit repeatedly between methyl groups at a frequency of $\sim(k_B T/h)\, P_{react} \sim 3 \times 10^{11}$ sec^{-1} at $T = 300$ K. In the subsequent Step 4 of this Reaction Sequence, a hydrogen donation tool presented to either methyl group, possibly repeatedly, for a duration $\gg 3 \times 10^{-12}$ sec should discharge its H payload upon arrival of the radical site into its vicinity, thus completing the H donation reaction.

diphenylgermylene divalent radical $((C_6H_5)_2\text{-Ge:})$[123] are being investigated both theoretically and experimentally in conventional chemistry. In Step 4 of RS36, the Ge$\bullet$ radical is hydrogenated to avoid pathological Ge=C germene[124, 125] bond formation (as observed experimentally in other molecules[126–128]) after dehydrogenation of the CH_2 payload of the attached GM tool in a later Step. Finally, as with RS33 + RS34, the other three possible variants for RS35 + RS36 involving diradical/nonradical or monoradical/monoradical coupling, obtained by choosing the alternative reactant site for dehydrogenation in Step 10 of RS35 and/or Step 6 of RS36, should work equally well.

In Step 6 of RS35, hydrogenation of the Ge: diradical singlet (−1.27 eV below triplet) is endoergic by +1.31 eV using HDon and +0.48 eV using HTrans, thus requires hydrogenation via pressurized bulk H_2, a process which is exoergic by −1.37 eV. Becerra et al.[129] calculate a barrier of +0.60 eV for the singlet :GeH$_2$ + $H_2 \to GeH_4$ reaction which may be overcome by adding mechanical energy to the reactants by compressing them to a pressure $P_{reactants} \sim E_{barrier}/(V_{H_2} + V_{GeH_2}) \sim 6300$ atm at 300 K, where $E_{barrier} = 0.60$ eV, V_{H_2} is the molecular volume of H_2 as a function of pressure computed using van der Waals constants[130] $A_{H_2} = 2.444 \times 10^{-7}$ m^6-atm/mole^2 and $B_{H_2} = 2.661 \times 10^{-5}$ m^3/mole, and V_{GeH_2} is the similarly calculated molecular volume of :GeH$_2$ with van der Waals constants estimated as $A_{GeH_2} = 5 \times 10^{-6}$ m^6-atm/mole^2 and $B_{GeH_2} = 6 \times 10^{-5}$ m^3/mole, the precise value of which does not sensitively affect the conclusions. Using Arrhenius rate estimates by Newman[131] for the reverse

reaction (GeH$_4 \to$:GeH$_2$ + H_2), the population of decomposed GeH$_4$ molecules is only $\sim 10^{-10}$ at 300 K and $\sim 10^{-57}$ at 80 K. Nevertheless, this method of hydrogenation adds a rate-limiting bulk chemistry reaction step into an otherwise fully positionally-controlled DMS fabrication process for building the germano-adamantane cage. In other cases, feedstock hydrogen enters the DMS system under full positional control, either from an imported CH_2 or GeH$_2$ group installed using a Meth, GM or Germ tool, or directly from the H dump, which is then abstracted via HAbst (RS1) yielding HAbstH, followed by recharge of HAbstH to HAbst (RS5) which transfers the H to GeRad, yielding HDon.

7. FABRICATION OF TOOLS

7.1. Hydrogen Abstraction Tool Fabrication

The only previously published explicit proposals for HAbst tool fabrication are by Merkle.[4, 16] In Merkle's first paper,[4] his Reactions 3 and 4 are reported as exoergic by −2.56 eV using AM1, but employ Si rather than Ge atoms and require the sterically-challenging simultaneous presence of 4 positionally-precise tool handles in the close vicinity of a 4-carbon polyyne chain similar to butadiyne (H-C≡C-C≡C-H), with simultaneous multiple-tool motions and with one tooltip targeting each of the 4 adjacent carbon atoms. Merkle's second paper[16] proposes an anthracene handle and a nitrogen-substituted anthracene handle with an ethynyl group bonded between them that are pulled apart to yield an ethynyl radical tool and a lone

RS29.   Add 3rd CH$_3$ in chain to Adam sidewall.

Step	Description of Reaction	Mult.	Ener. (eV)	Barr. (eV)
1	**Abstract H from apical sidewall chain CH$_3$ w/HAbst tool**			
	R: TMethR1 (ACC0B/32) + HAbst (ACC0A/27)	S + D		
	P: TMethR2 (ACC0A/31) + HAbstH (ACC0A/28)	D + S	−1.53	
2	**Join GM tool to apical radical site on chain**			
	R: TMethR2 (ACC0A/31) + GM tool cluster (ACC0A/7)	D + D		
	P: TMethR3 (ACC0A/38)	S	−3.31	
2A	H steal from GM tool to workpiece CH$_2$● radical site			
	R: TMethR2 (ACC0A/31) + GM tool (ACC0A/28)	D + D		
	P: TMethR1 (ACC0B/32) + GMA5HS (ABB0A/27)	S + S	+0.97	
	P: TMethR1 (ACC0B/32) + GMA5HT (ACC0A/27)	S + T	+0.26	
	R: TMethR2 (ACC0A/31) + GM tool cluster (ACC0A/7)	D + D		
	T: TMethR3p1TTS (ACC1A/38)	T		+0.65
2B1	H steal from workpiece to GM tool			
	R: TMethR2 (ACC0A/31) + GM tool (ACC0A/28)	D + D		
	P: TTMeth4p1STS (ACC1A/30) + GMACH3 (ACC0A/29)	S + S	+0.62	
	P: TTMeth4p1TTS (ACC1A/30) + GMACH3 (ACC0A/29)	T + S	+0.42	
	R: TMethR2 (ACC0A/31) + GM tool cluster (ACC0A/7)	D + D		
	T: TTMethR3p2TTS (ACC1A/38)	T		+0.66
3	**Detach GeRad handle from workpiece**			
	R: TMethR3 (ACC0A/38)	S		
	P: GRAPZ4 (ACC0A/34) + GeH3 (ACC0A/4)	D + D	+2.91	
3B1	H steal from workpiece by departing GeRad handle			
	R: TMethR3 (ACC0A/38)	S		
	P: GRAPZ4p1S (ACC0A/33) + GeH4 (ACC0A/5)	S + S	+4.06	
	P: GRAPZ4p1T (ACC0A/33) + GeH4 (ACC0A/5)	T + S	+3.91	
3D1	H migrates to CH$_2$● radical from adjacent CH$_2$ in chain			
	R: GRAPZ4 (ACC0A/34)	D		
	P: GRAPZ4p2 (ACC0A/34)	D	−0.20	
	T: GRAPZ4p2TS (ACC1A/34)	D		+1.59
3D2	H migrates to CH$_2$● radical from adjacent Adam sidewall CH$_2$			
	R: GRAPZ4 (ACC0A/34)	D		
	P: GRAPZ4p3 (ACC0A/34)	D	−0.01	
	T: GRAPZ4p3TS (ACC1A/34)	D		+0.78
3D3	H migrates to CH$_2$● radical from adjacent Adam bridgehead CH			
	R: GRAPZ4 (ACC0A/34)	D		
	P: GRAPZ4p5 (ACC0A/34)	D	−0.10	
	T: GRAPZ4p5TS (ACC1A/34)	D		+0.63

3D7	H migrates to CH$_2\bullet$ radical from same Adam sidewall worksite			
	R: GRAPZ4 (ACC0A/34)	D		
	P: GRAPZ4p4 (ACC0A/34)	D	−0.27	
	T: GRAPZ4p4TS (ACC1A/34)	D		+0.81
3F1	H$_2$C=CH$_2$ group detaches, leaving >CH-CH$_2\bullet$ on Adam sidewall			
	R: GRAPZ4 (ACC0A/34)	D		
	P: Cluster52 (ACC0A/28) + C2H4 (ACC0A/6)	D + S	+0.63	
4	**Hydrogenate CH$_2\bullet$ radical site using HDon tool**			
	R: GRAPZ4 (ACC0A/34) + HDon (ACC0A/26)	D + S		
	P: GRAPZ5 (ACC0A/35) + GeRad (ACC0A/25)	S + D	−0.69	

handle radical; however: (1) the ethynyl radical is equally likely to be found on either handle (requiring testing, a conditional selection step rejected in the present paper, or handle tilting, which is not mentioned in the paper), (2) the synthesis of the dianthracene starting molecule is unspecified, and (3) the larger handle structures are undefined. The present work proposes three far simpler single-handle HAbst fabrication processes each employing only single-tool-at-a-time motions.

The first such process (RS37) incorporates a simple method for positionally-controlled importation of carbon atoms that begins with a Ge surface which is heated to ~600 K, causing all surface hydrogen to desorb.[132] Acetylene (C$_2$H$_2$) feedstock gas is then slowly flowed over the surface at room temperature which can achieve up to 100% monolayer coverage of C$_2$H$_2$ covalently bonded to the Ge surface, as has been demonstrated (and imaged) experimentally.[133] For example, acetylene may chemisorb on the clean Ge(100)-2 × 1 surface in two horizontal configurations: 38% on-top di-σ (thermal desorption energy 1.33 eV, thermal desorption temperature 520 K) and 62% p-bridge tetra-σ (1.43 eV, 560 K), at saturation coverage.[133] No interconversion between on-top and p-bridge configurations and no surface diffusion is observed at room temperature, and reacted and unreacted C$_2$H$_2$ molecules are clearly distinguishable in STM images.[133] (However, a subsequent *ab initio* DFT/GGA theoretical study[134] suggests that the on-top configuration should be more stable.) The thermal behavior of C$_2$H$_2$ on Ge(100) differs from that reported for C$_2$H$_2$ on Si(100) in which >95% of chemisorbed acetylene dissociates on the Si(100) surface, a difference attributed to the 0.6–0.7 eV weaker bond strength for Ge-C than for Si-C.[133] Starting with this (or another similar) positionally constrained source of carbon atoms (which may be mapped by SPM prior to use), the HAbst tool is then fabricated by using an AdamRad handle (RS33 + RS34 + RS1) to pull the CC dimer off the Ge surface. Note the convenient H transfer in Step 4 of RS37 when the intermediate tool structure resembles the H-donation-prone HTrans tool.

The remaining two processes employ carbon atoms already present in the system to build HAbst, one by using an AdamRad to remove a CC dimer from a charged DimerP tool, yielding an HAbst tool (RS38), the other by

sequentially abstracting 4 H atoms from a previously fabricated 2-methyl chain on an adamantane bridgehead site (Step 4 of RS20), yielding HAbstH (RS39) which is then recharged to an HAbst tool using RS5.

A practical method for preparing the first HAbst tool experimentally would begin with the direct chemisorption of C$_2$ dimers onto a depassivated Ge surface (a strongly exoergic (−8.37 eV, DFT) reaction analogous to Step 1 of RS37), as already demonstrated on diamond surface using C$_2$-producing C$_{60}$ precursors,[134A] followed by the application of Steps 1–3 of RS38 to yield a finished HAbst tool.

7.2. Methylene Tool Fabrication

The monoradical Methylene tool (Adam-CH$_2\bullet$) (Fig. 1(G)) is a novel tooltype reported here for the first time that consists of a methylene group bound to the bridgehead carbon atom of an adamantyl handle. Methylene additions to hydrocarbon radical sites are typically barrierless[25] and even direct additions into C=C bonds have relatively low barriers (e.g., +0.34 eV for methylene addition to ethylene[135]). To build the Methylene tool, a partially methylated germanium surface may provide a source of positionally controlled single-carbon feedstock molecules analogous to that previously employed for C$_2$ dimers in Section 7.1. Such a surface can be prepared by thermal adsorption and reaction of CH$_4$ gas on Ge(100)[149] or by ion bombardment of clean Ge(111) at low substrate temperature (<470 K) using low-energy $\bullet$CH$_3$ ions, a strongly exoergic radical coupling reaction. CVD of diamond and diamond-like carbon or DLC (C:H films) onto Ge substrates without carbide formation using CH$_4$ feedstock gas is well-known,[136, 137] and related techniques such as physical vapor deposition (PVD), laser CVD, direct ion beam deposition, dual ion beam sputtering, RF/DC glow discharge or microwave discharge might also be employed. After hydrocarbon CVD on Ge surfaces, absorption spectra indicate that bonding is mainly type sp^3 with CH, CH$_2$, and CH$_3$ bonds.[136] For comparison, one experiment on Si substrate found 19.4% sp^3 CH$_3$, 23.4% sp^3 CH$_2$, and 45.6% sp^3 CH species by observing C-H stretch absorption bands.[138] Another experiment used electron cyclotron resonance (ECR) plasma processing to deposit a layer of

RS30. Add 2nd CH₃ in chain to Adam sidewall with lone CH₃ on adjacent sidewall.

	Step 1	Step 2	Step 3	Step 4

Step	Description of Reaction	Mult.	Ener. (eV)	Barr. (eV)
1	**Abstract H from Adam sidewall CH₃ using HAbst tool**			
	R: TMeth1 (ACC0A/32) + HAbst (ACC0A/27)	S + D		
	P: TMeth2 (ACC0A/31) + HAbstH (ACC0A/28)	D + S	−1.60	
1D6	H migrates from adjacent sidewall CH₃ to CH₂● radical site			
	R: SMHSM1Arun2 (ACC0A/31)	D		
	P: SM HSM2Arun2 (ACC0A/31)	D	−0.01	
	T: SMHSMA-QST3 (ACC1A/31)	D		+0.60
2	**Join GM tool to apical radical site on chain**			
	R: TMeth2 (ACC0A/31) + GM tool cluster (ACC0A/7)	D + D		
	P: TMeth3 (ACC0A/38)	S	−3.21	
2A	H steal from GM tool to workpiece CH₂● radical site			
	R: TMeth2 (ACC0A/31) + GM tool (ACC0A/28)	D + D		
	P: TMeth1 (ACC0A/32) + GMA5HS (ABB0A/27)	S + S	+1.04	
	P: TMeth1 (ACC0A/32) + GMA5HT (ACC0A/27)	S + T	+0.33	
	T: TMeth3p1TTS (ACC1A/38)	T		+0.71
2B1	H steal from workpiece to GM tool			
	R: TMeth2 (ACC0A/31) + GM tool (ACC0A/28)	D + D		
	P: Side2MSHSTS (ACC1A/30) + GMACH3 (ACC0A/29)	S + S	+0.68	
	P: Side2MSHTTS (ACC1A/30) + GMACH3 (ACC0A/29)	T + S	+0.37	
	T: TMeth3p2TTS (ACC1A/38)	T		+0.66
3	**Detach GeRad handle from workpiece**			
	R: TMeth3 (ACC0A/38)	S		
	P: TMeth4 (ACC0A/34) + GeH3 (ACC0A/4)	D + D	+2.88	
3B1	H steal from workpiece by departing GeRad handle			
	R: TMeth3 (ACC0A/38)	S		
	T: TMeth4p1STS (ACC1A/33) + GeH4 (ACC0A/5)	S + S		+4.16
	T: TMeth4p1TTS (ACC1A/33) + GeH4 (ACC0A/5)	T + S		+3.99
3D1	H migrates to radical from adjacent CH₂ in chain			
	R: TMeth4 (ACC0A/34)	D		
	P: TMeth4p3 (ACC0A/34)	D	−0.01	
	T: TMeth4p3TSrun3 (ACC1A/34)	D		+1.59
3D2	H migrates to radical from adjacent Adam sidewall CH₂			
	R: TMeth4 (ACC0A/34)	D		
	P: TMeth4p2 (ACC0B/34)	D	+0.21	
	T: TMeth4p2TS (ACC1A/34)	D		+0.70
3D3	H migrates to radical from adjacent Adam bridgehead CH			
	R: TMeth4 (ACC0A/34)	D		
	P: TMeth4p5 (ACC0A/34)	D	−0.03	
	T: TMeth4p5TS (ACC1A/34)	D		+1.06
3F1	H₂C=CH₂ group detaches, leaving >CH● on Adam sidewall			
	R: TMeth4 (ACC0A/34)	D		
	P: SHSM2A (ACC0A/28) + C2H4 (ACC0A/6)	D + S	+0.46	
	T: TMeth4p4TSrun3 (ACC1A/34)			+1.01
4	**Hydrogenate CH₂● radical site using HDon tool**			
	R: TMeth4 (ACC0A/34) + HDon (ACC0A/26)	D + S		
	P: TMeth5 (ACC0B/35) + GeRad (ACC0A/25)	S + D	−0.65	

RS31. Add CH_3 to nearest Adam sidewall with lone CH_3 on each of two adjacent sidewalls.

Step	Description of Reaction	Mult.	Ener. (eV)	Barr. (eV)
1	**Abstract H from nearest Adam sidewall site using HAbst tool**			
	R: Cluster53A (ACC0A/32) + HAbst (ACC0A/27)	S + D		
	P: FMeth4 (ACC0B/31) + HAbstH (ACC0A/28)	D + S	−1.65	
1D6	H migrates to radical site from adjacent CH_3 sidewall site			
	R: FMeth4 (ACC0B/31)	D		
	P: FMeth4p2 (ACC0A/31)	D	+0.04	
	T: FMeth4p2TS (ACC0A/31)	D		+1.21
1E	CH_3 on adjacent sidewall migrates to radical site			
	R: FMeth4 (ACC0B/31)	D		
	T: FMeth4p3TS (ACC1A/31)	D		+3.13
2	**Join GM tool to sidewall radical site**			
	R: FMeth4 (ACC0B/31) + GM tool cluster (ACC0A/7)	D + D		
	P: FMeth5 (ACC0A/38)	S	−2.90	
2A	H steal from GM tool to workpiece radical site			
	R: FMeth4 (ACC0B/31) + GM tool (ACC0A/28)	D + D		
	P: Cluster53A (ACC0A/32) + GMA5HS (ABB0A/27)	S + S	+1.08	
	P: Cluster53A (ACC0A/32) + GMA5HT (ACC0A/27)	S + T	+0.37	
	R: FMeth4 (ACC0B/31) + GM tool cluster (ACC0A/7)	S + T		
	T: FMeth5p2TTS (ACC1A/38)	T		+0.79
2B1	H steal from workpiece to GM tool			
	R: FMeth4 (ACC0B/31) + GM tool (ACC0A/28)	D + D		
	P: FMeth5p1S (ACC0A/30) + GMACH3 (ACC0A/29)	S + S	+0.25	
	R: FMeth4 (ACC0B/31) + GM tool cluster (ACC0A/7)	D + D		
	T: FMeth5p1S-QST2 (ACC2B/38)	S		+0.49
	P: FMeth5p1T (ACC0A/30) + GMACH3 (ACC0A/29)	T + S	+0.31	
	R: FMeth4 (ACC0B/31) + GM tool cluster (ACC0A/7)	D + D		
	T: FMeth5p1TTS (ACC0A/38)	T		+0.59
3	**Detach GeRad handle from workpiece**			
	R: FMeth5 (ACC0A/38)	S		
	P: FMeth2 (ACC0A/34) + GeH3 (ACC0A/4)	D + D	+2.72	
3B1	H steal from workpiece by departing GeRad handle			
	R: FMeth5 (ACC0A/38)	S		
	T: FMeth2p2SasTS (ACC1A/33) + GeH4 (ACC0A/5)	S + S		+4.09
	P: FMeth2p2T (ACC0A/33) + GeH4 (ACC0A/5)	T + S	+3.67	
3D3	H migrates to $CH_2\bullet$ radical from adjacent Adam bridgehead CH			
	R: FMeth2 (ACC0A/34)	D		
	P: FMeth2p4 (ACC0A/34)	D	+0.09	
	T: FMeth2p4TS (ACC1A/34)	D		+2.14
3D6	H migrates to $CH_2\bullet$ radical from adjacent CH_3 sidewall site			
	R: FMeth2 (ACC0A/34)	D		
	T: FMeth2p1TS (ACC1A/34)	D		+0.63
3D7	H migrates to $CH_2\bullet$ radical from same Adam sidewall worksite			
	R: FMeth2 (ACC0A/34)	D		
	P: FMeth2p3run3 (ACC0A/34)	D	−0.40	
	T: FMeth2p3TS (ACC1A/34)	D		+1.43

4	**Hydrogenate CH$_2$• radical site using HDon tool**			
	R: FMeth2 (ACC0A/34) + HDon (ACC0A/26)	D + S		
	P: FMeth1 (ACC0A/35) + GeRad (ACC0A/25)	S + D	−0.54	

Ge on Si substrate, with the fractional C content of the Ge layer controlled by the mix ratio of germylmethane precursor gases which are converted predominantly to •GeH$_3$ and •CH$_3$ radicals in the plasma.[139] It may also be possible to prepare a CH$_3$-decorated Ge surface via conventional solution-phase chemical methylation,[140–142] since methylated germanium is found in the natural environment.[143, 144]

Finally, the chemisorption of related species such as CH$_3$SiH$_3$,[145, 149] SiH$_4$,[146, 149] and NH$_3$,[147–149] on the Ge(100) surface, of CH$_4$ on the Si(100) surface,[149–151] and of •CH$_3$ on the SiC(100) surface[152] is well-documented, and the CH$_3$-terminated Si(111)-(1 × 1) surface is also well-characterized experimentally.[153] Starting with a positionally constrained source of carbon atoms in the form of

RS32. Add 4th CH$_3$ in chain to Adam sidewall (polyethylene chain).

	Step 1	Step 2	Step 3	Step 4

Step	Description of Reaction	Mult.	Ener. (eV)	Barr. (eV)
1	**Abstract H from apical sidewall chain CH$_3$ w/HAbst tool**			
	R: GRAPZ5 (ACC0A/35) + HAbst (ACC0A/27)	S + D		
	P: GRAPZ4 (ACC0A/34) + HAbstH (ACC0A/28)	D + S	−1.50	
2	**Join GM tool to apical radical site on chain**			
	R: GRAPZ4 (ACC0A/34) + GM tool cluster (ACC0A/7)	D + D		
	P: GRAP1 (ACC0A/41)	S	−3.34	
3	**Detach GeRad handle from workpiece**			
	R: GRAP1 (ACC0A/41)	S		
	P: GRAPZ8 (ACC0A/37) + GeH3 (ACC0A/4)	D + D	+2.92	
3D2	H migrates to CH$_2$• radical from adjacent Adam sidewall CH$_2$			
	R: GRAPZ8 (ACC0A/37)	D		
	P: GRAPZ8p3 (ACC0A/37)	D	−0.12	
	T: GRAPZ8p3TS (ACC1A/37)	D		+0.94
3D3	H migrates to CH$_2$• radical from adjacent Adam bridgehead CH			
	R: GRAPZ8 (ACC0A/37)	D		
	P: GRAPZ8p5run2 (ACC0A/37)	D	−0.10	
	T: GRAPZ8p5TS (ACC1A/37)	D		+0.58
3D7	H migrates to CH$_2$• radical from same Adam sidewall worksite			
	R: GRAPZ8 (ACC0A/37)	D		
	P: GRAPZ8p4 (ACC0A/37)	D	−0.16	
	T: GRAPZ8p4TS (ACC1A/37)	D		+0.57
4	**Hydrogenate CH$_2$• radical site using HDon tool**			
	R: GRAPZ8 (ACC0A/37) + HDon (ACC0A/26)	D + S		
	P: GRAPZ9 (ACC0A/38) + GeRad (ACC0A/25)	S + D	−0.69	

RS33. Add -CH$_2$-CH$_2$-CH$_2$- between adjacent Adam sidewall atoms [tools omitted from illustrations; GeRad handle modeled as GeH$_3$].

Step 1	Step 2	Step 3 …

… Step 3	Step 4	Step 5	Step 6 …

… Step 6	Step 7	

Step	Description of Reaction	Mult.	Ener. (eV)	Barr. (eV)
1	**Rotate handled 3-methyl chain from Trans to Cis**			
	R: TMethR3 (ACC0A/38) [from Step 2 of RS29]	S		
	P: TMethRR6 (ACC0A/38)	S	+0.22	
	T: TMethRR6-QST2 (ACC1A/38)	S		+0.28
	Reverse Barrier, Cis to Trans:			
	R: TMethRR6 (ACC0A/38):	S		
	T: TMethRR6-QST2 (ACC1A/38)	S		+0.06
2	**Rotate handled 3-methyl chain from Cis to CisCis**			
	R: TMethRR6 (ACC0A/38)	S		
	P: TMethRR7 (ACC0A/38)	S	+0.21	
	T: TMethRR7-QST2 (ACC1A/38)	S		+0.16
	Reverse Barrier, CisCis to Cis:			
	R: TMethRR7 (ACC0A/38)	S		
	T: TMethRR7-QST2 (ACC1A/38)	S		−0.04
3	**Abstract H from adjacent Adam sidewall CH$_2$ using HAbst tool**			
	R: TMethRR7 (ACC0A/38) + HAbst (ACC0A/27)	S + D		
	P: TMethRR8 (ACC0A/37) + HAbstH (ACC0A/28)	D + S	−1.69	
3D1a	H migrates to CH• radical from proximal CH$_2$ group in chain			
	R: TMethRR8 (ACC0A/37)	D		
	P: TMethRR8p4 (ACC0A/37)	D	−0.43	
	T: TMethRR8p4-QST3run2 (ACC1A/37)	D		+0.74
3D1b	H migrates to CH• radical from middle CH$_2$ group in chain			
	R: TMethRR8 (ACC0A/37)	D		
	P: TMethRR8p3 (ACC0A/37)	D	−0.30	
	T: TMethRR8p3TS (ACC1A/37)	D		**+0.37** [a]
3D1c	H migrates to CH• radical from terminal CH$_2$ group in chain (near Ge)			
	R: TMethRR8 (ACC0A/37)	D		
	P: TMethRR8p1 (ACC0A/37)	D	0.00	
	T: TMethRR8p1-QST2 (ACC1A/37)	D		+0.43
4	**Abstract H from adjacent Adam sidewall CH• using HAbst tool**			
	R: TMethRR8 (ACC0A/37) + HAbst (ACC0A/27)	D + D		
	P: TMethRR9S (ACC0A/36) + HAbstH (ACC0A/28)	S + S	−1.32	

Continued

	P: TMethRR9T (ACC0A/36) + HAbstH (ACC0A/28)	T + S	−1.15	
4D1a	H migrates to C: radical from proximal CH$_2$ group in chain			
	R: TMethRR9S (ACC0A/36)	S		
	P: TMethRR9p3SasTS (ACC1A/36)	S	+0.29	
	T: TMethRR9p3STSrun2 (ACC1A/36)	S		+0.61
	R: TMethRR9T (ACC0A/36)	T		
	P: TMethRR9p3T (ACC0A/36)	T	−0.79	
	T: TMethRR9p3TTS (ACC1A/36)	T		+0.70
4D1b	H migrates to C: radical from middle CH$_2$ group in chain			
	R: TMethRR9S (ACC0A/36)	S		
	T: TMethRR9p4STS (ACC1A/36)	S		+0.83
	R: TMethRR9T (ACC0A/36)	T		
	P: TMethRR9p4T (ACC0A/36)	T	−0.80	
	T: TMethRR9p4T-QST3 (ACC1A/36)	T		**+0.26** [a]
4D1c	H migrates to C: radical from terminal CH$_2$ group in chain (near Ge)			
	R: TMethRR9S (ACC0A/36)	S		
	T: TMethRR9p5SasTS (ACC1A/36)	S		+0.73
	R: TMethRR9T (ACC0A/36)	T		
	P: TMethRR9p5T (ACC1A/36)	T	−0.54	
	T: TMethRR9p5TTS (ACC1A/36)	T		**+0.27** [b]
4G4	C: radical inserts between middle and terminal CH$_2$ groups in chain			
	R: TMethRR9S (ACC0A/36)	S		
	P: TMethRR9p6 (ACC0A/36)	S	−3.53	
	T: TMethRR9p6-QST2 (ACC1A/36)	S		+2.32
5	**Join terminal CH$_2$ group in chain to Adam sidewall C: diradical**			
	R: TMethRR9S (ACC0A/36)	S		
	P: TMethR6 (ACC0A/36) [no barrier found]	S	−3.57	
	R: TMethRR9T (ACC0A/36)	T		
	P: TMethR6 (ACC0A/36)	S	−3.73	
6	**Detach GeRad handle from workpiece, leaving CH• radical**			
	R: TMethR6 (ACC0A/36)	S		
	P: TMethR7 (ACC0A/32) + GeH3 (ACC0A/4)	D + D	+2.60	
6B1	H steal from workpiece by departing GeRad handle			
	R: TMethR6 (ACC0A/36)	S		
	P: TMethR7p1Srun2 (ACC0A/31) + GeH4 (ACC0A/5)	S + S	+3.42	
	P: TMethR7p1T (ACC0A/31) + GeH4 (ACC0A/5)	T + S	+3.51	
6D1	H migrates to CH• radical from adjacent CH$_2$ in chain			
	R: TMethR7 (ACC0A/32)	D		
	P: TMethR7p2 (ACC0A/32)	D	−0.11	
	T: TMethR7p2TS (ACC1A/32)	D		+1.63
6D2	H migrates to CH• radical from adjacent Adam sidewall CH$_2$			
	R: TMethR7 (ACC0A/32)	D		
	P: TMethR7p5 (ACC0A/32)	D	+0.01	
	T: TMethR7p5TS (ACC1A/32)	D		+1.07
6D3	H migrates to CH• radical from adjacent Adam bridgehead CH			
	R: TMethR7 (ACC0A/32)	D		
	P: TMethR7p6 (ACC0A/32)	D	+0.18	
	T: TMethR7p6TS (ACC1A/32)	D		+2.43
6D7	H migrates to CH• radical from same Adam sidewall worksite			
	R: TMethR7 (ACC0A/32)	D		
	P: TMethR7p3 (ACC0A/32)	D	+0.08	
	T: TMethR7p3TS (ACC1B/32)	D		+1.92
6I	Middle CH$_2$ group in chain flips from down (Chair) to up (Boat)			
	R: TMethR7 (ACC0A/32) [Chair]	D		
	P: TMethR7Up (ACC0A/32) [Boat]	D	+0.02	
	T: TMethR7-QST2 (ACC1A/32)	D		**+0.04** [c]
	Reverse Barrier, Boat to Chair:			
	R: TMethR7Up (ACC0A/32) [Boat]	D		
	T: TMethR7-QST2 (ACC1A/32)	D		**+0.02** [c]
7	**Hydrogenate CH• radical site using HDon or HTrans tool**			
	R: TMethR7 (ACC0A/32) + HDon (ACC0A/26)	D + S		

Continued

	P: TMeth8D (ACC0A/33) + GeRad (ACC0A/25)	S + D	−0.44	
	R: TMethR7 (ACC0A/32) + S15cis (ACCCA/11)	D + D		
	P: TMeth8D (ACC0A/33) + S16Run0 (ACCCA/10)	S + S	−1.27	
7I	Middle CH$_2$ group in chain flips from down (Chair) to up (Boat)			
	R: TMeth8D (ACC0A/33) [Chair]	S		
	P: TMeth8 (ACC0A/33) [Boat]	S	+0.07	
	T: TMeth8D-QST2 (ACC1A/33)	S		+0.19[c]
	Reverse Barrier, Boat to Chair:			
	R: TMeth8 (ACC0A/33) [Boat]	S		
	T: TMeth8D-QST2 (ACC1A/33)	S		+0.12[c]

[a] Despite the slightly low energy barriers blocking pathologies 3D1b/4D1b, these H migration pathologies are preventable because of the very large nominal initial distances (3.79 Å / 3.63 Å) between the closest migrating H and the recipient radical site on TMethRR8/TMethRR9T, which may be maintained by proper positional handle control following the creation of the radical site.

[b] For pathology 4D1c (triplet) to occur, first the C: carbene in TMethRR9S (singlet) must convert to the higher-energy TMethRR9T (triplet) which lies +0.17 eV uphill, then the migrating H must surmount an additional +0.27 eV transition barrier, giving an effective misreaction total barrier of +0.44 eV starting from the lowest-energy TMethRR9S (singlet) structure. (Also applies during Step 5.)

[c] With only small barriers blocking pathologies 6I and 7I, the apical CH$_2$ group will flip often between Chair and Boat configurations.

CH$_3$ (which may be mapped by SPM prior to use), the Meth tool is then fabricated (RS40) by using an Adam-Rad handle (RS33 + RS34 + RS1) to extract the once-dehydrogenated CH$_2$ group from the Ge surface.

A practical method for preparing the first Methylene tool experimentally would begin with the direct chemisorption of :CH$_2$ diradicals onto a depassivated Ge surface followed by the application of Steps 3–4 of RS40 to yield a finished Methylene tool, a reaction that is net exoergic by −0.99 eV using full cage models.

7.3. Germylmethylene Tool Fabrication

The monoradical Germylmethylene tool (GeRad-CH$_2$•) (Fig. 1(H)) is a novel tooltype reported here for the first time that consists of a methylene group bound to the bridgehead Ge atom of a germano-adamantyl (GeRad) handle. The GM tool is generally preferred for methylation operations because it releases its methylene payload −0.41 eV more exoergically than the Meth tool, demands fewer reaction steps and creates less steric congestion than the Meth tool during use. However, the GM tool is slightly more difficult to build than the Meth tool because the fabrication of GM (RS41) requires:

(1) a Meth tool as an input,

(2) a rate-limiting bulk chemistry step in RS35 to make the GeRad handle, and, for RS41,

(3) a relatively sterically challenging handle exchange operation and

(4) coordinated simultaneous rotation of two apposed tooltips (Fig. 5).

If the tool rotation maneuver described in Step 6 of RS41 (Fig. 5) proves untenable experimentally, the precursor two-handled structure can still be pulled apart but then either:

(1) a conditional testing step (e.g., resistive force monitoring as the tip from each of the two resulting handles, after hydrogenation, is brought to a known height above a nonreactive hydrogenated diamond C(111) surface; e.g., Fig. 6, similar to nanoindentation resistance curves) is required to determine upon which GeRad handle the methyl payload resides. Hydrogenation is necessary because H abstraction from Adam bridgehead (−0.12 eV) or sidewall (−0.11 eV) sites by GM tool radical is slightly exoergic. Hydrogenation of each handle is attempted using separate HTrans tools, in each case presenting the donable H atom to the Ge atom at a proper bonding distance via dead reckoning, then with the same tool presenting similarly to the methyl radical (assuming it was present), resulting in two definitely hydrogenated handles and two definitely discharged HTrans tools; or

(2) the two tools, one a GM tool and one a GeRad handle, may be applied identically to the workpiece in sequence ("two-stroke" operation) as if both possessed the payload, producing, in most instances of first or second methylations, a properly methylated workpiece and two known empty GeRad handles.

A practical method for preparing the first GM tool experimentally might begin with the direct chemisorption of :CH$_2$ diradicals onto a depassivated Ge surface followed by Step 4′ of RS40, analogous to Steps 3–4 of RS40 but substituting GeRad for the AdamRad handle, exoergically yielding a finished GM tool despite the presence of Ge-C bonds of nominally equal strength on both sides of the fulcrum of tensile bond scission.

RS34. Add 4th CH$_2$ to complete Adam cage [tools omitted from illustrations; GeRad handle modeled as GeH$_3$].

Step 1	Step 2	Step 3 …

… Step 3	Step 4	Step 5 …

… Step 5	Step 6	Step 7

Step	Description of Reaction	Mult.	Ener. (eV)	Barr. (eV)
1	**Abstract H from apical CH$_2$ on sidewall ring using HAbst tool**			
	R: TMeth8D (ACC0A/33) + HAbst (ACC0A/27)	S + D		
	P: TMethR7p2 (ACC0A/32) + HAbstH (ACC0A/28)	D + S	−1.86	
1D1	H migrates to CH● radical from adjacent CH$_2$ in ring			
	R: TMethR7p2 (ACC0A/32)	D		
	P: TMethR7 (ACC0A/32)	D	+0.11	
	T: TMethR7p2TS (ACC1A/32)	D		+1.74
1D2	H migrates to CH● radical from adjacent Adam sidewall CH$_2$			
	R: TMethR7p2 (ACC0A/32)	D		
	P: FourC2p2 (ACC0A/32)	D	+0.11	
	T: FourC2p2TS (ACC1A/32)	D		+0.67
1I	Middle CH● group in ring flips from down (Chair) to up (Boat)			
	R: TMethR7p2 (ACC0A/32) [Chair]	D		
	P: TMethR7p2UpTSrun2 (ABB0D/32) [Boat]	D	+0.47	
2	**Join GM tool to CH● radical on ring in Down position**			
	R: TMethR7p2 (ACC0A/32) + GM tool cluster (ACC0A/7)	D + D		
	P: FourC4run1 (ACC1A/39)	S	−2.66	
2A	H steal from GM tool to workpiece CH● radical site			
	R: TMethR7p2 (ACC0A/32) + GM tool (ACC0A/28)	D + D		
	P: TMeth8D (ACC0A/33) + GMA5HS (ABB0A/27)	S + S	+1.30	
	P: TMeth8D (ACC0A/33) + GMA5HT (ACC0A/27)	S + T	+0.59	
2B1	H steal from workpiece CH● radical site to GM tool			
	R: TMethR7p2 (ACC0A/32) + GM tool (ACC0A/28)	D + D		
	P: FourC3p2S (ACC0A/31) + GMACH3 (ACC0A/29)	S + S	+0.18	
	R: TMethR7p2 (ACC0A/32) + GM tool cluster (ACC0A/7)	D + D		
	T: FourC3p2S-QST3 (ACC1A/39)	S		+0.66
	P: FourC3p2T (ACC0A/31) + GMACH3 (ACC0A/29)	T + S	+0.27	
	R: TMethR7p2 (ACC0A/32) + GM tool cluster (ACC0A/7)	D + D		

Continued

	T: FourC3p2TTSrun2 (ACC1A/39)	T		+0.60
3	**Abstract H from adjacent Adam sidewall CH$_2$ using HAbst tool**			
	R: FourC4run1 (ACC1A/39) [Down] + HAbst (ACC0A/27)	S + D		
	P: FourC5 (ACC0A/38) [Down] + HAbstH (ACC0A/28)	D + S	−1.80	
3D2	H migrates to Adam CH● radical from adjacent CH$_2$ in ring			
	R: FourC5UD (ACC0A/38) [Up]	D		
	T: FourC5p4-QST2 (ACC1A/38) [Up]	D		+0.88
	R: FourC5 (ACC0A/38) [Down]	D		
	T: FourC5p4-QST2 (ACC1A/38) [Up]	D		+0.76
3D11	H migrates to Adam CH● radical from CH$_2$ being added by GM tool			
	R: FourC5 (ACC0A/38)	D		
	P: FourC5p2 (ACC0A/38)	D	0.00	
	T: FourC5p2TS (ACC1A/3)8	D		**+0.37** [a]
3I	Apical CH$_2$ on sidewall ring flips from Down position to Up position			
	R: FourC5 (ACC0A/38) [Down]	D		
	P: FourC5UD (ACC0A/38) [Up]	D	**−0.12** [b]	
4	**Abstract H from GM tool payload CH$_2$ group using HAbst tool**			
	R: FourC5 (ACC0A/38) + HAbst (ACC0A/27)	D + D		
	P: FourC7 (ACC0A/37) + HAbstH (ACC0A/28)	S + S	−5.20	
	R: FourC5 (CCC0A/38) + HAbst (CCC0A/27)			
	T: FourC6STSrun1 (CCC1A/37) + HAbstH (CCC0A/28)	S + S		−1.56
	P: FourC6T (ACC1A/37) + HAbstH (ACC0A/28)	T + S	−1.69	
4D12	H migrates to Adam sidewall CH● from CH● of attached GM tool			
	R: FourC6STSrun1 (CCC1A/37)	S		
	P: FourC6p2SasTS (CCC1A/37)	S	+0.62	
	R: FourC6T (ACC1A/37)	T		
	P: FourC6p2T (ACC0A/37)	T	+0.20	
	T: FourC6p2TTS (ACC1A/37)	T		**+0.38** [c]
	Reverse triplet pathology:			
	R: FourC6p2T (ACC0A/37)	T		
	P: FourC6T (ACC1A/37)	T	−0.20	
	T: FourC6p2TTS (ACC1A/37)	T		+0.18
4D13	H migrates to CH● of attached GM tool from Adam sidewall CH●			
	R: FourC6STSrun1 (CCC1A/37)	S		
	P: FourC6p1S (CCC1A/37)	S	+0.13	
	T: FourC6p2TTS (CCC1A/37)	S		**+0.16** [d]
	Reverse triplet pathology:			
	R: FourC6p1S (CCC1A/37)	S		
	P: FourC6STSrun1 (CCC1A/37)	S	−0.13	
	T: FourC6p2TTS (CCC1A/37)	S		+0.03
	R: FourC6T (ACC1A/37)	T		
	P: FourC6p2T (ACC0A/37)	T	+0.49	
	T: FourC6p1TTS (ACC1A/37)	T		+0.70
4D14	H migrates to radical site from apposing Adam bridgehead CH site			
	R: FourC6STSrun1 (CCC1A/37)	S		
	T: FourC6p6STS (ACC1A/37)	S		+1.96
	R: FourC6T (ACC1A/37)	T		
	P: FourC6p6T (ACC0A/37)	T	+0.20	
	T: FourC6p6TTS (ACC1A/37)	T		+0.55
4D15	H migrates to CH● radical site from nearest CH group in ring			
	R: FourC6STSrun1 (CCC1A/37)	S		
	P: FourC6p3SasTS (CCC1A/37)	S	+0.20	
	R: FourC6p3SasTS (ACC1A/37) − 0.20 eV	S		
	T: FourC6p3STSrun2 (ACC1A/37)	S		+1.82
	R: FourC6T (ACC1A/37)	T		
	P: FourC6p3T (ACC0A/37)	T	−0.52	
	T: FourC6p3TTS (ACC1A/37)	T		+1.30
4D16	H migrates to CH● radical site from nearest CH$_2$ group in ring			
	R: FourC6STSrun1 (CCC1A/37)	S		
	P: FourC6p3SasTS (CCC1A/37)	S	+1.10	
	R: FourC6T (ACC1A/37)	T		
	P: FourC6p4Trun2 (ACC0A/37)	T	−0.11	

Continued

REVIEW

	T: FourC6p4TTS (ACC1A/37)	T		+1.47
5	**Join payload CH• radical to Adam sidewall CH• radical**			
	R: FourC6STSrun1 (CCC1A/37)	S		
	P: FourC7 (CCC0A/37)	S	−3.92	
	R: FourC6T (ACC1A/37)	T		
	P: FourC7 (ACC0A/37)	S	−3.51	
6	**Detach GeRad handle from workpiece**			
	R: FourC7 (ACC0A/37)	S		
	P: FourC8 (ACC0A/33) + GeH3 (ACC0A/4)	D + D	+2.72	
6B1	H steal from workpiece by departing GeRad handle			
	R: FourC7 (ACC0A/37)	S		
	P: FourC8p2S (ACC0A/32) + GeH4 (ACC0A/5)	S + S	+3.57	
	P: FourC8p2T (ACC0A/32) + GeH4 (ACC0A/5)	T + S	+3.69	
6D3	H migrates to CH• radical from adjacent bridgehead CH			
	R: FourC8 (ACC0A/33)	D		
	P: FourC8p1 (ACC0B/33)	D	+0.04	
	T: FourC8p1TS (ACC1A/33)	D		+2.63
7	**Hydrogenate CH• radical site using HDon tool**			
	R: FourC8 (ACC0A/33) + HDon (ACC0A/26)	D + S		
	P: FourC9 (ACC0A/34) + GeRad (ACC0A/25)	S + D	−0.60	

[a] Despite the slightly low energy barrier blocking pathology 3D11, this H migration pathology is preventable by using positional control to ensure that the C atom in the Adam CH• radical and the C atom in the CH$_2$ group being added by the GM tool maintain a mutual separation exceeding at least >2.66 Å (the computed separation between these C atoms in the transition geometry (FourC5p2TS)) – e.g., the same separation (3.03 Å) as in the Product geometry (FourC5). The same result occurs regardless of dehydrogenation order of the CH$_2$ groups in this and the next step.

[b] Although there is a weak energetic preference for the Up position, positional control can maintain the system in the Down position; mechanical force can be applied through the GM tool handle to ensure the system returns to the Down position if it has flipped to the Up position during the reaction.

[c] Despite the slightly low energy barrier blocking triplet pathology 4D12, the spontaneous reversal of this pathology is moderately exoergic with a barrier height half as high as the forward reaction, so reactant is favored over product. H migration from the adjacent CH group in the ring to the C: carbene is blocked by a +1.36 eV barrier. Finally, since the singlet (FourC6STSrun1) and triplet (FourC6T) reactants are approximately equiergic ($\Delta_{S \to T}$ = −0.02 eV), intersystem crossings between singlet and triplet states should occur frequently, allowing mechanically-induced C-C bond formation in Step 5.

[d] The low energy barrier blocking singlet pathology 4D13 cannot reliably prevent the endoergic pathology even at 80 K; however, the reverse pathology is exoergic and has no barrier, so the H will transit rapidly between the two structures until the two CH• radicals combine to produce the desired C-C bond in Step 5, a barrierless reaction (Four C6p1S → Four C7) which is exoergic by −3.71 eV. H migration from the Adam CH bridgehead adjacent to the C: carbene of pathology 4D13 is blocked by a +2.38 eV barrier.
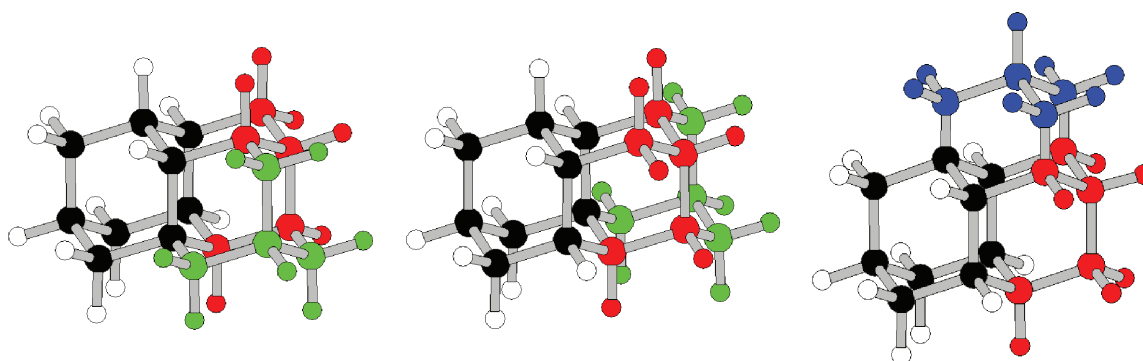
Fig. 4.   Building outward from the starting adamantane cage (black), successive cages may be added in the X (red), Y (green), or Z (blue) coordinate directions, placing the entire cubic diamond lattice within the manufacturing envelope.

RS35. Add -CH$_2$-GeH$_2$-CH$_2$- between adjacent Adam sidewall atoms [tools omitted from illustrations; Adam and GeRad handles modeled as CH$_3$ and GeH$_3$] (includes one rate-limiting bulk-processing step: Step 6).

Step 1	Step 2	Step 3 ...

... Step 3	Step 4	Step 5	Step 6 ...

... Step 6	Step 7	Step 8	Step 9 ...

... Step 9	Step 10	Step 11	Step 12 ...

... Step 12	Step 13	

Step	Description of Reaction	Mult.	Ener. (eV)	Barr. (eV)
1	**Abstract H from Adam sidewall CH$_3$ using HAbst tool**			
	R: Cluster53run2 (ABB0A/29) [RS7 Step4] + HAbst (ACC0A/27)	S + D		
	P: Cluster52 (ACC0A/28) + HAbstH (ACC0A/28)	D + S	−1.52	
2	**Join Germ tool to Adam sidewall CH$_2$● radical site**			
	R: Cluster52 (ACC0A/28) + Germ tool cluster (ACC0A/7)	D + D		
	P: TMethGe2 (ACC0B/35)	S	−2.80	
2A	H steal from Germ tool to workpiece CH$_2$● radical site			
	R: Cluster52 (ACC0A/28) + Germ tool (ACC0A/28)	D + D		
	P: Cluster53run2 (ABB0A/29) + AdamGeHS (ACC0A/27)	S + S	−1.71 [a]	
	P: Cluster53run2 (ABB0A/29) + AdamGeHTrun5 (ABB1A/27)	S + T	−0.68 [a]	

Continued

2B1	*Proximity Continuation Reaction:*
	  R: Cluster53run2 (ABB0A/29) + GeHCH3S (ACC0A/6)
	  P: TMethGe2 (ACC0B/35)
	    T: TMethGe2p2STS (ABB1A/35)
	H steal from workpiece CH$_2$• radical site to Germ tool
	  R: Cluster52 (ACC0A/28) + Germ tool (ACC0A/28)
	  P: AdamCHS (ACC0A/27) + AdamGeH3 (ACC0A/29)
	  P: AdamCHT (ACC0A/27) + AdamGeH3 (ACC0A/29)
		S + S
		S
		S
		
		D + D
		S + S
		T + S
			−1.02
			
			+1.11
			+0.97
				+1.84[b]

3
 	
3D1
	Abstract H from GeH$_2$ group using HAbst tool
	  R: TMethGe2 (ACC0B/35) + HAbst (ACC0A/27)
	  P: TMethGe3 (ABB0A/34) + HAbstH (ACC0A/28)
	H migrates to CH• radical from adjacent CH$_2$ group in chain
	  R: TMethGe3 (ABB0A/34)
	  P: TMethGe3p1 (ACC0A/34)
		S + D
		D + S
		
		D
		D
			−2.23
			
			+0.51	

4
 	
4A
 	
4B1
	Join GM tool to GeH• radical site
	  R: TMethGe3 (ABB0A/34) + GM tool cluster (ACC0A/7)
	  P: TMethGe4 (ACC0B/41)
	H steal from GM tool to workpiece GeH• radical site
	  R: TMethGe3 (ABB0A/34) + GM tool (ACC0A/28)
	  P: TMethGe4p1Srun2 (ABB0A/33) + GMACH3 (ACC0A/29)
	  P: TMethGe4p1Trun2 (ABB0A/33) + GMACH3 (ACC0A/29)
	  Proximity Continuation Reaction:
	    R: TMethGe4p1Srun2 (ABB0A/33) + GeH3CH3 (ACC0A/8)
	    P: TMethGe4 (ACC0B/41)
	      T: TMethGe3 (ABB0A/34) + GM tool cluster (ACC0A/7)
	H steal from workpiece GeH• radical site to GM tool
	  R: TMethGe3 (ABB0A/34) + GM tool (ACC0A/28)
	  P: TMethGe2 (ACC0B/35) + GMA5HS (ABB0A/27)
	  P: TMethGe2 (ACC0B/35) + GMA5HT (ACC0A/27)
		D + D
		S
		
		D + D
		S + S
		T + S
		
		S + S
		S
		D + D
		
		D + D
		S + S
		S + T
			−2.91
			
			−1.91[c]
			−0.57[c]
			
			−0.97
			
			+1.67
			+0.96
				+1.94[d]

5
 	
5A
 	
5D1
 	
5D7
	Detach H-Adam handle from workpiece, leaving Ge: diradical[e]
	  R: TMethGe4 (ACC0B/41)
	  P: TMethGe5p1Srun2 (ABB0A/36)[e] + CH4 (ACC0A/5)
	  P: TMethGe5p1Trun2 (ABB0A/36)[e] + CH4 (ACC0A/5)
	H steal from H-Adam handle back to workpiece Ge: diradical site
	  R: TMethGe4 (ACC0B/41)
	  P: TMethGe5 (ACC0A/37) + CH3 (ACC0A/4)
	H migrates to Ge: diradical from adjacent CH$_2$ group in chain
	  R: TMethGe5p1Srun2 (ABB0A/36)
	    T: TMethGe5pBSTSrun2 (ABB1A/36)
	  R: TMethGe5p1Trun2 (ABB0A/36)
	  P: TMethGe5pBT (ABB0A/36)
	    T: TMethGe5pBTTS (ABB1A/36)
	H migrates to Ge: diradical from same Adam sidewall worksite
	  R: TMethGe5p1Srun2 (ABB0A/36)
	    T: TMethGe5pDSTS (ABB1A/36)
		S
		S + S
		T + S
		
		S
		D + D
		
		S
		S
		T
		T
		T
		
		S
		S
			
			+0.94
			+2.21
			
			+3.12
			
			+0.47
			
				+1.70
				
				+2.11
				
				+0.50

6
 	
6A
	Hydrogenate Ge: diradical to GeH$_2$ using pressurized H$_2$ gas
	  R: TMethGe5p1Srun2 (ABB0A/36) + H2 (ACC0A/2)
	  P: TMethGeRR5 (ACC0A/38)
	    T: Becerra et al. [129]
	H steal from H$_2$ to workpiece Ge: diradical site, leaving free H•
	  R: TMethGe5p1Srun2 (ABB0A/36) + H$_2$ (ACC0A/2)
	  P: TMethGe5 (ACC0A/37) + H• (ACC0A/1)
		
		S + S
		S
		S
		
		S + S
		D + D
			
			−1.37
			
			+2.29
				+0.60[f]

7	**Rotate handled CH$_2$-GeH$_2$-CH$_2$ chain from Trans to Cis**
	  R: TMethGeRR5 (ACC0A/38)
	  P: TMethGeRR6run2 (ACC0B/38)
	    T: TMethGeRR6-QST2 (ACC1A/38)
	  Reverse Barrier, Cis to Trans:
	  R: TMethGeRR6run2 (ACC0B/38)
	    T: TMethGeRR6-QST2 (ACC1A/38)
		
		S
		S
		S
		
		S
		S
			
			+0.22
			
				+0.24
				
				+0.02

8	**Rotate handled CH$_2$-GeH$_2$-CH$_2$ chain from Cis to CisCis**
	  R: TMethGeRR6run2 (ACC0B/38)
	  P: TMethGeRR7 (ACC0A/38)
		
		S
		S
			
			+0.10	

Continued

	T: TMethGeRR7-QST2 (ACC1A/38)	S		+0.08
	Reverse Barrier, CisCis to Cis:			
	R: TMethGeRR7 (ACC0A/38)	S		
	T: TMethGeRR7-QST2 (ACC1A/38)	S		−0.02
9	**Abstract H from adjacent Adam sidewall CH$_2$ using HAbst tool**			
	R: TMethGeRR7 (ACC0A/38) + HAbst (ACC0A/27)	S + D		
	P: TMethGeRR8 (ACC0B/37) + HAbstH (ACC0A/28)	D + S	−1.68	
9D1a	H migrates to CH● radical from proximal CH$_2$ group in chain			
	R: TMethGeRR8 (ACC0B/37)	D		
	P: TMethGeRR8p4 (ACC0A/37)	D	−0.22	
	T: TMethGeRR8p4-QST2 (ABB1A/37)	D		+0.83
9D1b	H migrates to CH● radical from middle GeH$_2$ group in chain			
	R: TMethGeRR8 (ACC0B/37)	D		
	P: TMethGeRR8p3 (ACC0A/37)	D	−0.58 [g]	
9D1c	H migrates to CH● radical from terminal CH$_2$ group in chain			
	R: TMethGeRR8 (ACC0B/37)	D		
	P: TMethGeRR8p1 (ACC0A/37)	D	+0.06	
	T: TMethGeRR8p1-QST3 (ACC1A/37)	D		+0.51
10	**Abstract H from adjacent Adam sidewall CH● using HAbst tool**			
	R: TMethGeRR8 (ACC0B/37) + HAbst (ACC0A/27)	D + D		
	P: TMethGeRR9Srun2 (ABB0B/36) + HAbstH (ACC0A/28)	S + S	−1.43	
	P: TMethGeRR9T (ACC0A/36) + HAbstH (ACC0A/28)	T + S	−1.21	
10D1a	H migrates to C: radical from proximal CH$_2$ group in chain			
	R: TMethGeRR9Srun2 (ABB0B/36)	S		
	P: TMethGeRR9p3SasTS (ABB1A/36)	S	+0.24	
	T: TMethGeRR9p3STS (ABB1A/36)	S		+0.74
	R: TMethGeRR9T (ACC0A/36)	T		
	P: TMethGeRR9p3Trun2 (ABB0A/36)	T	−0.74	
	T: TMethGeRR9p3TTS (ABB1A/36)	T		+0.74
10D1b	H migrates to C: radical from middle GeH$_2$ group in chain			
	R: TMethGeRR9Srun2 (ABB0B/36)	S		
	T: TMethGeRR9p4SasTS (ABB1A/36)	S		**+0.39 [h]**
	R: TMethGeRR9T (ACC0A/36)	T		
	P: TMethGeRR9p4Trun2 (ACC0A/36)	T	−1.11	
	T: TMethGeRR9p4T-QST3 (ACC1A/36)	T		**+0.15 [hi]**
10D1c	H migrates to C: radical from terminal CH$_2$ group in chain			
	R: TMethGeRR9Srun2 (ABB0B/36)	S		
	T: TMethGeRR9p5SasTS (ABB1A/36)	S		+0.66
	R: TMethGeRR9T (ACC0A/36)	T		
	P: TMethGeRR9p5T (ABB0A/36)	T	−0.50	
	T: TMethGeRR9p5T-QST2 (ABB1A/36)	T		**+0.20 [i]**
10G4	C: radical inserts between middle GeH2 and terminal CH$_2$ in chain			
	R: TMethGeRR9Srun2 (ABB0B/36)	S		
	P: TMethGeRR9p6 (ACC0A/36)	S	−3.04	
	T: TMethGeRR9p6S-QST2 (ACC1A/36)	S		+1.32
11	**Join terminal CH$_2$ group in chain to Adam sidewall C: diradical**			
	R: TMethGeRR9Srun2 (ABB0B/36)	S		
	P: TMethGeRR10 (ABB0A/36)	S	−3.33	
	T: TMethGeRR10-QST2 (ABB1A/36)	S		+0.13
	R: TMethGeRR9T (ACC0A/36)	T		
	P: TMethGeRR10 (ABB0A/36)	S	−3.55	
12	**Detach GeRad handle from workpiece, leaving CH● radical**			
	R: TMethGeRR10 (ABB0A/36)	S		
	P: TMethGeRR11 (ABB0B/32) + GeH3 (ACC0A/4)	D + D	+2.69	
12B1	H steal from workpiece CH group by departing GeRad handle			
	R: TMethGeRR10 (ABB0A/36)	S		
	P: TMethGeRR11p1S (ABB0A/31) + GeH4 (ACC0A/5)	S + S	+3.93	
	P: TMethGeRR11p1T (ABB0A/31) + GeH4 (ACC0A/5)	T + S	+3.45	
12D1	H migrates to CH● radical from adjacent GeH$_2$ in chain			
	R: TMethGeRR11 (ABB0B/32)	D		
	P: TMethGeRR11p2 (ABB0A/32)	D	−0.48	
	T: TMethGeRR11p2-QST2 (ABB1A/32)	D		+1.61

Continued

12D2	H migrates to CH• radical from adjacent Adam sidewall CH$_2$			
	R: TMethGeRR11 (ABB0B/32)	D		
	P: TMethGeRR11p5 (ABB0A/32)	D	−0.03	
	T: TMethGeRR11p5-QST2 (ABB1A/32)	D		+1.15
12D3	H migrates to CH• radical from adjacent Adam bridgehead CH			
	R: TMethGeRR11 (ABB0B/32)	D		
	P: TMethGeRR11p6 (ABB0A/32)	D	+0.12	
	T: TMethGeRR11p6TS (ABB1A/32)	D		+2.15
12D7	H migrates to CH• radical from same Adam sidewall worksite			
	R: TMethGeRR11 (ABB0B/32) [Down]	D		
	P: TMethGeRR11p3 (ABB0A/32) [Down]	D	−0.21	
	R: TMethGeRR11p4asTS (ABB0D) [Up]	D		
	T: TMethGeRR11p3TS (ABB1A/32) [Up]	D		+0.98
12I	Middle GeH$_2$ group in chain flips from Down to Up			
	R: TMethGeRR11 (ABB0B/32) [Down]	D		
	P: TMethGeRR11p4asTS (ABB0D) [Up]	D	+0.69	
13	**Hydrogenate CH• radical site using HDon or HTrans tool**			
	R: TMethGeRR11 (ABB0B/32) + HDon (ACC0A/26)	D + S		
	P: TMethGeRR12 (ABB0A/33) + GeRad (ACC0A/25)	S + D	−0.49	
	R: TMethGeRR11 (ABB0B/32) + S15cis (ACCCA/11)	D + D		
	P: TMethGeRR12 (ABB0A/33) + S16Run0 (ACCCA/10)	S + S	−1.32	
13I	Middle GeH$_2$ group in chain flips from Down to Up			
	R: TMethGeRR12 (ABB0A/33) [Down]	S		
	P: TMethGeRR12p1-QST2 (ABB0C/33) [Up]	S	+0.17	
	T: TMethGeRR12p1asTS (ABB0D/33)	S		**+0.35** [j]
	Reverse Barrier, Up to Down:			
	R: TMethGeRR12p1-QST2 (ABB0C/33) [Up]	S		
	T: TMethGeRR12p1asTS (ABB0D/33)	S		**+0.18** [j]

[a] Pathology 2A is highly exoergic and will occur. However, the singlet Germylidyne (AdamGeHS) is strongly preferred energetically (−1.03 eV) over the triplet (AdamGeHT), hence after a brief wait to allow an intersystem crossing if necessary, the Germylidyne should reliably reside in the singlet state.

[b] After Pathology 2A (singlet) has occurred, continuing to hold the singlet Products in close proximity for a sufficient time while applying adequate mechanical force to overcome the substantial reverse reaction barrier (+1.83 eV) allows them to undergo an exoergic reverse reaction downhill (−1.02 eV) to yield the desired end Product of this reaction step (TMethGe2).

[c] Pathology 4A is highly exoergic and will occur. However, the singlet Ge: radical in TMethGe4p1S is strongly preferred energetically (−1.33 eV) over the triplet Ge: radical in TMethGe4p1T, hence after a brief wait to allow an intersystem crossing if necessary, the Ge: radical should reliably reside in the singlet state.

[d] After Pathology 4A (singlet) has occurred, continuing to hold the singlet Products in close proximity for a sufficient time while applying adequate mechanical force to overcome the substantial reverse reaction endoergicity (+1.94 eV) allows them to undergo an exoergic reverse reaction downhill (−0.97 eV) to yield the desired end Product of this reaction step (TMethGe4).

[e] The singlet Ge: radical in TMethGe5p1S is strongly preferred energetically (−1.27 eV) over the triplet Ge: radical in TMethGe5p1T, hence after a brief wait to allow an intersystem crossing if necessary, the Ge: radical should reliably reside in the singlet state.

[f] The +0.60 eV barrier is overcome by exposing the Ge: diradical to H$_2$ gas pressurized to 6300 atm at 300 K, or to 6100 atm at 400 K; see text, Section 6.

[g] Although no barrier was found to block pathology 9D1b (which is an H donation reaction from a Ge-based group), this H migration pathway is preventable because of the very large nominal initial distance (4.47 Å) between the migrating H and the recipient radical site on TMethGeRR8, which may be maintained by proper positional control following the creation of the radical site.

[h] Despite the low energy barriers blocking pathologies 10D1b singlet (+0.39 eV) and triplet (+0.15 eV), these H migration pathologies are preventable because of the very large nominal initial distances (3.68 Å/2.92 Å) between the closest migrating H and the recipient radical site on TMethGeRR9S/TMethGeRR9S, which may be maintained by proper positional control following the creation of the radical site.

[i] For pathologies 10D1b (triplet) and 10D1c (triplet) to occur, first the C: carbene in TMethGeRR9S (singlet) must convert to the higher-energy TMethGeRR9S (triplet) which lies +0.22 eV uphill, then the migrating H must surmount an additional +0.15 eV (TMethGeRR9p4T-QST3)/+0.20 eV (TMethGeRR9p5T-QST2) transition barrier, giving an effective misreaction total barrier of +0.37 eV (10D1b triplet)/+0.42 eV (10D1c triplet) starting from the lowest-energy TMethGeRR9S (singlet) structure.

[j] With a slightly low barrier (+0.35 eV) to block pathology 13I, the GeH$_2$ group will occasionally flip from Down to Up, but the smaller reverse barrier (+0.18 eV) allows the structure to quickly flip back to Down, ensuring predominant population of the Down configuration.

RS36. Add 4th CH₂ to complete GeRad cage [tools omitted from illustrations; GeRad handles modeled as GeH₃].

Step 1	Step 2	Step 3 …

… Step 3	Step 4	Step 5 …

… Step 5	Step 6	Step 7 …

… Step 7	Step 8	Step 9

Step	Description of Reaction	Mult.	Ener. (eV)	Barr. (eV)
1	**Abstract H from GeH₂ on sidewall ring using HAbst tool**			
	R: TMethGeRR12 (ABB0A/33) + HAbst (ACC0A/27)	S + D		
	P: TMethGeRR11p2 (ABB0A/32) + HAbstH (ACC0A/28)	D + S	−2.17	
1D1	H migrates to GeH● radical from adjacent CH₂ in ring			
	R: TMethGeRR11p2HD (ABB0A/32)	D		
	P: TMethGeRR11 (ABB0B/32)	D	+0.46	
	T: TMethGeRR11p2-QST2 (ABB1A/32)	D		+2.07
1D2	H migrates to GeH● radical from adjacent Adam sidewall CH₂			
	R: TMethGeRR11p2 (ABB0A/32)	D		
	P: FourCGe2p2 (ABB0A/32)	D	+0.44	
	T: FourCGe2p2TS (ABB1A/32)	D		+0.97
1I	Middle GeH● group in ring flips from Down to Up			
	R: TMethGeRR11p2 (ABB0A/32) [Down]	D		
	P: FourCGe2p3asTS (ABB0D/32) [Up]	D	**+0.15**[a]	
2	**Abstract H from GeH● on sidewall ring using HAbst tool**			
	R: TMethGeRR11p2 (ABB0A/32) + HAbst (ACC0A/27)	D + D		

<div align="right">Continued</div>

	P: FourCGe4p2S (ABB0A/31) + HAbstH (ACC0A/28)	S + S	−3.60	
	P: FourCGe4p2T (ABB0A/31) + HAbstH (ACC0A/28)	T + S	−2.00	
2D1	H migrates to Ge: radical from adjacent CH$_2$ in ring			
	R: FourCGe4p2S (ABB0A/31)	S		
	P: FourCGe3p1S (ABB0A/31) [includes a Ge=C bond]	S	+0.81	
	T: FourCGe3p1STS (ABB1A/31)	S		+1.74
	R: FourCGe4p2T (ABB0A/31)	T		
	P: FourCGe3p1T (ABB0A/31)	T	+0.42[b]	
2D2	H migrates to Ge: radical from adjacent Adam sidewall CH$_2$			
	R: FourCGe4p2S (ABB0A/31)	S		
	P: FourCGe3p2S (ABB0A/31)	S	−0.46	
	T: FourCGe3p2STS (ABB0A/31)	S		+0.55
	R: FourCGe4p2T (ABB0A/31)	T		
	P: FourCGe3p2T (ABB0A/31)	T	+0.41[b]	
2I	Middle Ge: radical in ring flips from Down to Up			
	R: FourCGe4p2S (ABB0A/31) [Down]	S		
	P: FourCGe3p3SasTS (ABB0C/31) [Up]	S	+0.28[a]	
	T: FourCGe3p3S-QST3 (ABB0B/31)	S		+0.26
	Reverse Barrier, Up to Down:			
	R: FourCGe3p3SasTS (ABB0C/31) [Up]	S		
	T: FourCGe3p3S-QST3 (ABB0B/31)	S		−0.01[a]
3	**Join GM tool to Ge: radical on ring into Down position**			
	R: FourCGe4p2S (ABB0A/31) + GM tool cluster (ACC0A/7)	S + D		
	P: FourCGe5 (ABB0A/38)	D	−1.50	
	R: FourCGe4p2T (ABB0A/31) + GM tool cluster (ACC0A/7)	T + D		
	P: FourCGe5 (ABB0A/38)	D	−3.09	
3A	H steal from GM tool to workpiece Ge: radical site			
	R: FourCGe4p2S (ABB0A/31) + GM tool (ACC0A/28)	S + D		
	P: TMethGeRR11p2 (ABB0A/32) + GMA5HS (ABB0A/27)	D + S	+3.03	
	R: FourCGe4p2T (ABB0A/31) + GM tool (ACC0A/28)	T + D		
	P: TMethGeRR11p2 (ABB0A/32) + GMA5HT (ACC0A/27)	D + T	+0.73	
3D1	H migrates to Ge: radical from adjacent CH$_2$ in ring			
	R: FourCGe5 (ABB0A/38)	D		
	P: FourCGe5p3 (ABB0A/38)	D	+0.41	
	T: FourCGe5p3TS (ABB1A/38)	D		+2.01
3D2	H migrates to Ge: radical from adjacent Adam sidewall CH$_2$			
	R: FourCGe5 (ABB0A/38)	D		
	P: FourCGe5p4 (ABB1B/38)	D	+0.45	
4	**Hydrogenate Ge● radical site using HTrans tool**			
	R: FourCGe5 (ABB0A/38) + S15cis (ACCCA/11)	D + D		
	P: FourCGe6A (ABB1A/39) + S16Run0 (ACCCA/10)	S + S	−0.86	
5	**Abstract H from adjacent Adam sidewall CH$_2$ using HAbst tool**			
	R: FourCGe6A (ABB1A/39) + HAbst (ACC0A/27)	S + D		
	P: FourCGe7A (ABB1A/38) + HAbstH (ACC0A/28)	D + S	−1.71	
5D11	H migrates to Adam CH● radical from CH$_2$ being added by GM tool			
	R: FourCGe7A (ABB1A/38)	D		
	P: FourCGe7Ap2 (ABB0A/38)	D	+0.11	
	T: FourCGe7Ap2TS (ABB1A/38)	D		+0.65
5D15	H migrates to CH● radical site from GeH group in ring			
	R: FourCGe7A (ABB1A/38)	D		
	P: FourCGe5 (ABB0A/38)	D	−0.45	
	R: FourCGe7A (DXB1A/38)	D		
	P: FourCGe5 (DXB0A/38)	D	−1.03	
	T: FourCGe7Ap4AM1SP (DXDXM/38)	D		+3.38
5D16	H migrates to CH● radical site from nearest CH$_2$ group in ring			
	R: FourCGe7A (ABB1A/38)	D		
	P: FourCGe7Ap1 (ABB0A/38)	D	−0.04	
	T: FourCGe7Ap1-QST3 (ABB1A/38)	D		+1.09
5I	Apical GeH● on sidewall ring flips from Down to Up position			
	R: FourCGe7A (AXB1A/38) [Down]	D		
	P: FourCGe7Ap5 (AXBXA/38) [Up]	D	+0.17[a]	
6	**Abstract H from GM tool payload CH$_2$ group using HAbst tool**			
	R: FourCGe7A (ABB1A/38) + HAbst (ACC0A/27)	D + D		

Continued

820

J. Comput. Theor. Nanosci. 5, 760–861, 2008

	P: FourCGe9A (ABB0A/37) + HAbstH (ACC0A/28)	S + S	−4.56	
	T: FourCGe8ASsingpt (AXBXS/37) + HAbstH (ACC0A/28)	S + S		−0.43
	P: FourCGe8AT (ABB0A/37) + HAbstH (ACC0A/28)	T + S	−1.62	
6D12	H migrates to Adam sidewall CH● from CH● of attached GM tool			
	R: FourCGe8ASsingpt (AXBXS/37)	S		
	P: FourCGe8Ap2S (AXB0A/37)	S	−0.23[c]	
	T: FourCGe8Ap2STS (AXB2C/37)	S		−0.37
	Reverse singlet pathology:			
	R: FourCGe8Ap2S (AXB0A/37)	S		
	P: FourCGe8ASsingpt (AXBXS/37)	S	+0.23	
	T: FourCGe8Ap2STS (AXB2C/37)	S		−0.14
	Proximity Continuation Reaction:			
	R: FourCGe8Ap2S (ABB0B/37)	S		
	P: FourCGe9A (ABB0A/37)	S	−3.95[c]	
	T: FourCGe8Ap2STS (ABB2C/37)	S		−0.21
	R: FourCGe8AT (ABB0A/37)	T		
	P: FourCGe8Ap2T (ABB0A/37)	T	+0.21	
	T: FourCGe8Ap2TTS (ABB1A/37)	T		+0.68
6D13	H migrates to CH● of attached GM tool from Adam sidewall CH●			
	R: FourCGe8ASsingpt (AXBXS/37)	S		
	P: FourCGe8Ap1S (AXB0A/37)	S	−0.81[d]	
	T: FourCGe8Ap1S-QST2 (AXB1A/37)	S		−0.66
	Reverse singlet pathology:			
	R: FourCGe8Ap1S (AXB0A/37)	S		
	P: FourCGe8ASsingpt (AXBXS/37)	S	+0.81	
	T: FourCGe8Ap1S-QST2 (AXB1A/37)	S		+0.15
	Proximity Continuation Reaction:			
	R: FourCGe8Ap1S (ABB0A/37)	S		
	P: FourCGe9A (ABB0A/37)	S	−3.32[d]	
	T: FourCGe8Ap1S-QST2 (ABB1A/37)	S		+0.09
	R: FourCGe8AT (ABB0A/37)	T		
	P: FourCGe8Ap1T (ABB1A/37)	T	+0.43	
	T: FourCGe8Ap1TTS (ABB1A/37)	T		+0.79
6D14	H migrates to tool CH● radical from apposing Adam CH bridgehead			
	R: FourCGe8ASsingpt (AXBXS/37)	S		
	T: FourCGe8Ap6STSrun2 (AXB1A/37)	S		+1.13
	R: FourCGe8AT (ABB0A/37)	T		
	P: FourCGe8Ap6T (ABB0A/37)	T	+0.12	
	T: FourCGe8Ap6TTS (ABB1A/37)	T		+1.84
6D15a	H migrates to tool CH● radical site from GeH group in ring			
	R: FourCGe8ASsingpt (AXBXS/37)	S		
	T: FourCGe8Ap3STSrun3 (AXB3F/37)	S		+1.66
	R: FourCGe8AT (ABB0A/37)	T		
	P: FourCGe8Ap3T (ABB0A/37)	T	−0.51	
	T: FourCGe8Ap3TTS (ABB1A/37)	T		+1.44
6D15b	H migrates to workpiece CH● radical site from GeH group in ring			
	R: FourCGe8AT (ABB0A/37) [H exohedral]	T		
	P: FourCGe8Ap5T (ABB0A/37) [H endohedral]	T	−0.01	
	T: FourCGe8Ap5T-QST3 (ABB4D/37)	T		+2.52
6D16	H migrates to tool CH● radical site from nearest CH_2 group in ring			
	R: FourCGe8ASsingpt (AXBXS/37)	S		
	T: FourCGe8Ap4STS (AXB1A/37)	S		+1.05
	R: FourCGe8AT (ABB0A/37)	T		
	P: FourCGe8Ap4T (ABB0A/37)	T	−0.08	
	T: FourCGe8Ap4TTS (ABB1A/37)	T		+1.71
7	**Join payload CH● radical to Adam sidewall CH● radical**			
	R: FourCGe8ASsingpt (AXBXS/37)	S		
	P: FourCGe9A (AXB0A/37)	S	−4.30	
	R: FourCGe8AT (ABB0A/37)	T		
	P: FourCGe9A (ABB0A/37)	S	−2.94	
8	**Detach GeRad handle from workpiece**			
	R: FourCGe9A (ABB0A/37)	S		
	P: FourCGe10A (ABB0A/33) + GeH3 (ACC0A/4)	D + D	+2.81	

Continued

8B1	H steal from workpiece by departing GeRad handle			
	R: FourCGe9A (ABB0A/37)	S		
	P: FourCGe10Ap1S (ABB0A/32) + GeH4 (ACC0A/5)	S + S	+3.99	
	P: FourCGe10Ap1T (ABB0A/32) + GeH4 (ACC0A/5)	T + S	+3.65	
8D2	H migrates to CH● radical from adjacent sidewall CH₂			
	R: FourCGe10A (ABB0A/33)	D		
	P: FourCGe10Ap4 (ABB0A/33)	D	0.00	
	T: FourCGe10Ap4TS (ABB1A/33)	D		+2.03
8D3a	H migrates to CH● radical from adjacent bridgehead GeH			
	R: FourCGe10A (ABB0A/33)	D		
	P: FourCGe10Ap2 (ABB0A/33)	D	−0.59	
	T: FourCGe10Ap2TS (ABB1A/33)	D		+2.37
8D3b	H migrates to CH● radical from adjacent bridgehead CH			
	R: FourCGe10A (ABB0A/33)	D		
	P: FourCGe10Ap3 (ABB0A/33)	D	−0.27	
	T: FourCGe10Ap3TS (ABB1A/33)	D		+2.19
9	**Hydrogenate CH● radical site using HDon tool**			
	R: FourCGe10A (ABB0A/33) + HDon (ACC0A/26)	D + S		
	P: FourCGe11A (ABB0A/33) + GeRad (ACC0A/25)	S + D	−0.59	

[a] The small energy preferences for the Down configuration with apparently negligible transition barriers should ensure predominant population of the Down configurations.

[b] The Ge**:** diradical triplet state is not kinetically accessible from the singlet state because the Ge**:** diradical singlet has a large energy preference (−1.59 eV) compared to the triplet.

[c] For pathology 6D12 singlet, the small energy preference (−0.23 eV) for the singlet C**:** diradical with zero transitional barriers should ensure predominant population of the singlet diradical configuration; however, continuing to hold the singlet Product in close proximity barrierlessly induces a strongly exoergic reverse reaction downhill (−3.95 eV) to yield the desired end Product (FourCGe9A) of the following reaction step.

[d] For pathology 6D13 singlet, the large energy preference (−0.81 eV) for the singlet C**:** diradical with zero transitional barriers should ensure predominant population of the singlet diradical configuration; however, continuing to hold the singlet Product in close proximity barrierlessly induces a strongly exoergic reverse reaction downhill (−3.32 eV) to yield the desired end Product (FourCGe9A) of the following reaction step.

7.4. Germylene Tool Fabrication

The monoradical Germylene tool (Adam-GeH₂●) (Fig. 1(I)) is a novel tooltype reported here for the first time that consists of a germylene group bound to the bridgehead carbon atom of an adamantyl handle. (A germylgermylene tool, GeRad-GeH₂●, might have better energetics but is not required for the minimal toolset.) Isolated germyl monoradicals such as the ●GeH₃ monoradical[119, 120] and the 1,6,7-trigermabicyclo[4.1.0]hept-3-en-7-yl mono-radical[154] are being investigated theoretically[119] and experimentally,[120, 154] and radical addition/combination organic reactions involving germyl monoradicals have been studied.[155, 156]

In order to build molecular structures containing germanium using the Germ tool, an appropriate means for positionally-controlled importation of Ge atoms is first required. A simple method to achieve this begins with a Ge(111) surface which is heated to ~600 K, causing all surface hydrogens to desorb.[132] Alternatively, upon crystal lattice cleavage a clean Ge(111) surface reconstructs to Ge(111)-2 × 1 similar to the Pandey reconstruction for C(111), with buckled pi-bonded chain configurations (tilted dimers) favored energetically and negative buckling of the chain confirmed experimentally.[157] Upon annealing at 373 K the clean surface further reconstructs to

the Ge(111)-c(2 × 8) structure,[158] resulting in decreased surface free energy and reactivity. Digermane (Ge₂H₆) feedstock gas is then flowed over the depassivated (clean) Ge(111) surface with the following experimentally-observed results: Digermane (H₃Ge-GeH₃; m.p. 164 K, b.p. 302 K), a gas with a pungent odor and a propensity to ignite on exposure to air that is often used in atomic layer epitaxy,[159] predominantly physisorbs to bare Ge(111) when flowed below 120 K.[132] Digermane on Ge(111) dissociates via Ge-Ge bond scission to form chemisorbed GeH₃ between 120–150 K; yields chemisorbed surface germyl (GeH₃), germylene (GeH₂), and germylidyne (GeH) species when flowed at 200 K; and produces only chemisorbed GeH₂ and GeH when flowed at 300 K and 400 K, with a much lower concentration of GeH₂ at 400 K; surface GeH₂ and GeH species are also generated by the successive decomposition of GeH₃ upon heating.[132] (Digermane on clean Ge(100) has also been studied experimentally.[160]) The activation energy for diffusion in bulk Ge is ~2.5 eV,[161] which is fairly high under mechanosynthesis conditions. Thus feedstock gas flowed over clean Ge(111) between 120–150 K reliably yields nonmigrating GeH₃ on Ge(111) at high surface coverage. Starting with this positionally constrained source of Ge atoms in the form of GeH₃ (which may be mapped by SPM prior to use), the Germylene tool is then fabricated

822

J. Comput. Theor. Nanosci. 5, 760–861, 2008

RS37. Build HAbst tool by pulling bound C_2H_2 off of a Ge surface [isobutane model for Adam handle].

Step	Description of Reaction	Mult.	Ener. (eV)	Barr. (eV)
1	**Chemisorb C_2H_2 onto dehydrogenated Ge(111) surface**			
	R: Cluster41GeA (ACX5S/21) + C2H2 (ACC0A/4)	S + S		
	P: Cluster38 (ACC0A/25)	S	3.39	
2	**Abstract H from C_2H_2 bonded to Ge surface using HAbst tool**			
	R: Cluster38 (ACC0A/25) + HAbst (ACC0A/27)	S + D		
	P: C1751 (ACC0A/24) + HAbstH (ACC0A/28)	D + S	−1.57	
2D8	H migrates to C• radical from CH on same dimer			
	R: C1751 (ACC0A/24)	D		
	T: C1751p1TS (ACC1A/24)	D		+1.78
3	**Join AdamRad handle to C• radical site**			
	R: C1751 (ACC0A/24) + CH33C (ACC0A/13)	D + D		
	P: C1752 (ACC0A/37)	S	−2.54	
3B6	H steal from CH on same dimer by incoming AdamRad handle			
	R: C1751 (ACC0A/24) + AdamRad (ACC0A/25)	D + D		
	P: C1752p1S (ACC0A/23) + Adam (ACC0A/26)	S + S	−1.56[a]	
	P: C1752p1T (ACC0A/23) + Adam (ACC0A/26)	T + S	+0.86	
4	**Detach dimer from workpiece attachment site with H transfer to Ge•**			
	R: Cluster40a (ACC0A/37)	S		
	P: Cluster41a3 (ACC0A/37)	S	+0.55	
4D8	H migrates to C• radical site from CH group on same dimer			
	R: Cluster40a (ACC0A/37)	S		
	T: Out2Step33-QST2 (ACC3D/37)	S		+3.04
4J	H does not transfer to Ge• as dimer detaches from that atom			
	R: Cluster40a (ACC0A/37)	S		
	T: Out3R2Step3 (ACC2F/37)	S		+1.87
5	**Detach dimer from other attachment site on Ge(111) surface**			
	R: Cluster41a3 (ACC0A/37)	S		
	P: Cluster42b (ACC0A/22) + CH33CCC (ACC0A/15)	D + D	+4.47	
5D2	H migrates to C≡C• radical site from adjacent sidewall CH_2			
	R: HAbst (ACC0A/27)	D		
	T: HAbst defect structure (from Temelso et al. [8])	D		+2.47
5F5	C_2 dissociates from Adam tool handle on HAbst tool			
	R: HAbst (ACC0A/27)	D		
	P: AdamRad (ACC0A/25) + C2S (ACC0A/2)	D + S	+5.40	
	P: AdamRad (ACC0A/25) + C2T (ACC0A/2)	D + T	+5.61	

[a] Pathology 3B6 (singlet) can occur but requires a large mispositioning of the tooltip by ~2.14 Å because the H atom cannot migrate away from its distal position on the dimer due to a +1.78 eV barrier, hence this pathology can be avoided by proper positional control.

RS38. Build HAbst tool by pulling C_2 dimer off DimerP tooltip [full cage models illustrated].

Step	Description of Reaction	Mult.	Ener. (eV)	Barr. (eV)
1	**Join AdamRad handle to C_2 dimer held by DimerP tool**			
	R: DimerP (ACC0A/46) + CH33C (ACC0A/13)	S + D		
	P: Cluster35 (ACC0A/59)	D	−1.37	
2	**Detach dimer from attachment side of DimerP tool**			
	R: Cluster35 (ACC0A/59)	D		
	P: Cluster36 (ACC0A/59)	D	+0.21	
3	**Detach dimer from other side of DimerP tool**			
	R: Cluster36 (ACC0A/59)	D		
	P: DCB6GeOffS (ACC0A/44) + CH33CCC (ACC0A/15)	S + D	+3.89	
	P: DCB6GeOffT (ACC0A/44) + CH33CCC (ACC0A/15)	T + D	+4.99	

(RS42) by using an AdamRad handle (RS33 + RS34 + RS1) to extract the once-dehydrogenated GeH_2 group from the Ge surface, with the first 3 of these positionally controlled reaction steps performed at ≤150 K to avoid unscheduled GeH_3 decomposition, and with the conversion of GeH: to GeH_3 by exposure to bulk H_2 pressurized to ~6300 atm (Section 6) performed in Step 5. Note that chiral germanes incorporating a substituted adamantyl group, roughly analogous to the Germylene tooltip structure, have already been prepared using conventional methods of chemical synthesis.[162]

7.5. Dimer Placement Tool Fabrication

The DimerP tool is built upon a Ge-substituted hexagonal diamond (lonsdaleite) handle base that is equivalent to two side-fused GeRad cages. Hence the *de novo* fabrication of this tool (RS43) starts with the fabrication of a second mirror-image germano-adamantyl cage on the unsubstituted C(111) face of a GeRad handle, followed by tool recharge (RS6), requiring the sequential application of 8 previously-defined Reaction Sequences. A practical method for preparing the first DimerP (DCB6Ge) tool experimentally is described by Freitas.[23]

8. FABRICATION OF OTHER STRUCTURES

8.1. Hexagonal Diamond (Lonsdaleite) Fabrication

The minimal toolset can be used to build diamond polytype structures, including the most common cubic

diamond form (Section 4) and the rarer hexagonal diamond or lonsdaleite polytype.[163] The *de novo* fabrication of this latter structure (RS44) starts with the fabrication of a second mirror-image adamantane cage on the C(111) face of an Adam stub, requiring the sequential application of 4 previously-defined Reaction Sequences. Hexagonal diamond structures and related diamond polytypes[164] are readily extended to indefinitely large crystal arrays using various combinations of RS33 + RS34 and RS44, including structures incorporating bridgehead Ge substituent atoms by substituting RS35 + RS36 in place of RS33 + RS34.

8.2. Ethylation, Propylation, and Related Reactions

A common task in DMS will be the site-specific addition of hydrogenated dimers or ethyl tabs (-CH_2-CH_2-) to a growing diamondoid workpiece structure. The available ethylation reaction pathways identified in the present work include ethyl addition:
(1) across adjacent adamantane sidewall sites via methyl dehydrogenation (RS45);
(2) across a lonsdaleite C(111) gap bridgehead site by using (a) methyl dehydrogenation (RS46), (b) DimerP-deposited dimer hydrogenation (RS47), or (c) HAbst-deposited dimer hydrogenation (RS48);
(3) across adjacent diamond C(111) bridgehead sites using methyl dehydrogenation (RS49), roughly equivalent to ethylation between two adamantane sidewall sites as in RS45, or inferentially by dimer hydrogenation as already demonstrated in the more difficult lonsdaleite case (RS47);

RS39. Build HAbstH tool by dehydrogenating two-methyl chain on Adam.

	Step 1	Step 2	Step 3	Step 4

Step	Description of Reaction	Mult.	Ener. (eV)	Barr. (eV)
1	**Abstract H from distal CH$_3$ of 2-methyl chain using HAbst tool**			
	R: Bridge5 (ACC0A/32) [RS20 Step 4] + HAbst (ACC0A/27)	S + D		
	P: Bridge4 (ACC0A/31) + HAbstH (ACC0A/28)	D + S	−1.55	
2	**Abstract H from proximal CH$_2$ of 2-methyl chain using HAbst tool**			
	R: Bridge4 (ACC0A/31) + HAbst (ACC0A/27)	D + D		
	P: HAb3S (ACC0A/30) + HAbstH (ACC0A/28)	S + S	−4.27	
	P: HAb3T (ACC0A/30) + HAbstH (ACC0A/28)	T + S	−1.64	
2F3	●HC=CH$_2$ group detaches from Adam handle			
	R: HAb3S (ACC0A/30)	S		
	P: AdamRad (ACC0A/25) + HCCH2 (ACC0A/5)	D + D	+3.88	
	R: HAb3T (ACC0A/30)	T		
	P: AdamRad (ACC0A/25) + HCCH2 (ACC0A/5)	D + D	+1.24	
3	**Abstract H from distal CH$_2$ of 2-methyl chain using HAbst tool**			
	R: HAb3S (ACC0A/30) + HAbst (ACC0A/27)	S + D		
	P: AdamC2H2 (ACC0A/29) + HAbstH (ACC0A/28)	D + S	−1.09	
3D1	H migrates to apical CH● radical site from adjacent CH in chain			
	R: AdamC2H2 (ACC0A/29)	D		
	P: HAb4p1run2 (ACC0B/29)	D	−0.19	
	T: HAb4p1TS (ACC1A/29)	D		+1.93
3D2	H migrates to apical CH● radical site from adjacent sidewall CH$_2$			
	R: AdamC2H2 (ACC0A/29)	D		
	P: HAb4p2 (ACC0B/29)	D	−0.48	
	T: HAb4p2TS (ACC1A/29)	D		+1.02
3F2	HC≡CH group detaches from Adam handle			
	R: AdamC2H2 (ACC0A/29)	D		
	P: AdamRad (ACC0A/25) + C2H2 (ACC0A/4)	D + S	+0.89	
4	**Abstract H from proximal CH of 2-methyl chain using HAbst tool**			
	R: AdamC2H2 (ACC0A/29) + HAbst (ACC0A/27)	D + D		
	P: HAbstH (ACC0A/28) + HAbstH (ACC0A/28)	S + S	−4.24	
	P: HAb5T (ACC0A/28) + HAbstH (ACC0A/28)	T + S	−0.33 [a]	
4F3	●C≡CH group detaches from Adam handle			
	R: HAbstH (ACC0A/28)	S		
	P: AdamRad (ACC0A/25) + CCH (ACC0A/3)	D + D	+5.17	
	R: HAb5T (ACC0A/28)	T		
	P: AdamRad (ACC0A/25) + CCH (ACC0A/3)	D + D	+1.26	

[a] Triplet Product lies +3.91 eV above singlet Product in energy, hence is unlikely to occur; if the triplet does occur, it should rapidly transition downhill to the singlet via intersystem crossing.

(4) across a diamond C(110) trough via dimer placement using the DimerP tool (Section 3.3) followed by dimer hydrogenation as in RS47;

(5) across nearest sites on adjacent diamond C(100) dimers using methyl dehydrogenation (RS50) or inferentially by dimer hydrogenation as already demonstrated in the more difficult lonsdaleite case (RS47); and

(6) across adjacent sites on the same diamond C(100) dimer using methyl dehydrogenation (RS51), with the dimer hydrogenation method apparently ruled out because

dimer deposition via DimerP in this case is too endoergic (+2.66 eV singlet, +2.47 eV triplet). Ethyl addition along a diamond C(110) ridge site using methyl dehydrogenation following placement of two adjacent methyls on a ridge site using RS25 (roughly equivalent to ethylation between adamantane sidewall and bridgehead sites, requiring formation of a relatively unstable high-energy 4-carbon ring structure) is not reliable because a competing pathology (in which the two CH$_2$● radical sites ethenylize to two vertical C=CH$_2$ groups by dissociating the C-C ridge bond

RS40. Build Methylene tool by pulling bound CH_3 off of a Ge surface [full cage models illustrated].

<table>
<tr><th colspan="2">Step 1</th><th colspan="2">Step 2</th><th></th></tr>
<tr><td colspan="5"></td></tr>
<tr><th colspan="2">Step 3</th><th colspan="2">Step 4</th><th></th></tr>
<tr><td colspan="5"></td></tr>
</table>

Step	Description of Reaction	Mult.	Ener. (eV)	Barr. (eV)
1	**Chemisorb $CH_3\bullet$ onto dehydrogenated Ge(111) surface**			
	R: GermantaneRad (ACC2A/25) + CH_3 (ACC0A/4)	D + D		
	P: GermantaneCH₃ (ACC3A/29)	S	−2.63	
2	**Abstract H from CH_3 bonded to Ge surface using HAbst tool**			
	R: ClusterGCH3 (ACC1A/17) + HAbst (ACC0A/27)	S + D		
	P: ClusterGCH2 (ACC0A/16) + HAbstH (ACC0A/28)	D + S	−1.48	
3	**Join AdamRad handle to $CH_2\bullet$ radical site**			
	R: ClusterGCH2 (ACC0A/16) + Adam Rad (ACC0A/25)	D + D		
	P: ClusterGCH2Adam (ACC0A/41)	S	−3.14	
3B1	H steal from $CH_2\bullet$ radical site by incoming AdamRad handle			
	R: GermantaneCH2 (ACC0A/28) + AdamRad (ACC0A/25)	D + D		
	P: GermantaneCH-TS (ACC1A/27) + Adam (ACC0A/26)	S + S	+0.87	
	P: GermantaneCHT (ACC3A/27) + Adam (ACC0A/26)	T + S	+0.12	
	R: GermantaneCH2 (ACC0A/28) + CH3 (ACC0A/4)	D + D		
	T: GermCHTCH4-TS (ACC1A/32)	T		+0.54
4	**Detach Meth tool from Ge(111) surface**			
	R: ClusterGCH2Adam (ACC0A/41)	S		
	P: ClusterGRad (ACC1A/13) + Meth tool (ACC0A/28)	D + D	+2.43	
4A	H steal from departing Meth tool to surface Ge$\bullet$ radical site			
	R: ClusterGCH2Adam (ACC0A/41)	S		
	P: ClusterG (ACC1A/14) + AdamCHS (ACC0A/27)	S + S	+3.87	
	P: ClusterG (ACC1A/14) + AdamCHT (ACC0A/27)	S + T	+3.73	
4D2	H migrates to radical site from adjacent sidewall CH_2 in handle cage			
	R: Meth tool (ACC0A/28)	D		
	P: AdamCH3H (ACC0A/28)	D	−0.12	
	T: AdamCH3HStealTransrun2 (ACC1A/28)	D		+3.46
4F4	$CH_2\bullet$ dissociates from tool handle on Meth tool			
	R: Meth tool (ACC0A/28)	D		
	P: AdamRad (ACC0A/25) + CH2S (ACC0A/3)	D + S	+4.47	

	P: AdamRad (ACC0A/25) + CH2T (ACC0A/3)	D + T	+4.00	
4G7	Tool CH$_2\bullet$ radical inserts into adjacent sidewall CH$_2$ in handle cage			
	R: Meth tool (ACC0A/28)	D		
	P: AdamCH2Insrt (ACC0A/28)	D	+0.12	
	T: AdamCH2InsrtTrans (ACC1A/28)	D		+2.45
4′	**Join GeRad handle to CH$_2\bullet$, detach GM tool from Ge(111) surface**			
	R: GermantaneCH2 (ACC0A/28) + GeRad (ACC0A/25)	D + D		
	P: GermantaneRad (ACC2A/25) + GM tool (ACC0A/28)	D + D	−0.58	
4′B1	H steal from CH$_2\bullet$ radical site by incoming GeRad handle			
	R: GermantaneCH2 (ACC0A/28) + GeRad (ACC0A/25)	D + D		
	P: GermantaneCH-TS (ACC1A/27) + HDon (ACC0A/26)	S + S	+1.47	
	P: GermantaneCHT (ACC3A/27) + HDon (ACC0A/26)	T + S	+0.73	

to which they are attached) is exoergic by −3.13 eV, compared to −3.70 eV (singlet) and −1.64 eV (triplet) for the main reaction.

In both Step 6 of RS47 and Step 5 of RS48 the attachment of a GeRad (−0.13 eV) or AdamRad (+0.15 eV) handle to one end of the C=C bond to create a hydrogen-donable C-C radical site at the other end is insufficiently exoergic, and direct hydrogenation using HDon (+1.95 eV) or HTrans (+1.12 eV) is endoergic, hence both reactions must employ bulk pressurization hydrogenation (Section 6) to convert the C=C bond to a C-C bond. Experimentally, ethylene (H$_2$C=CH$_2$) is noncatalytically hydrogenated to ethane (H$_3$C-CH$_3$) by H$_2$ gas at 550 °C,[165] and C$_{60}$ fullerene is noncatalytically hydrogenated by H$_2$ gas at 500 atm and 300–350 °C.[166] Noncatalytic ethylene hydrogenation is strongly exoergic by $\Delta H_{298} = -1.42$ eV but with a high barrier of $E_{barrier} = +1.87$ eV.[165] This barrier may be overcome using H$_2$ gas pressurized to $P_{reactants} \sim E_{barrier}/(V_{H_2} + V_{H_2C=CH_2}) \sim 20{,}800$ atm at 300 K, where $V_{H_2C=CH_2}$ is the molecular volume of ethylene as a function of pressure computed using van der Waals constants[130] $A_{H_2C=CH_2} = 4.471 \times 10^{-6}$ m^6-atm/mole^2 and $B_{H_2C=CH_2} = 5.714 \times 10^{-5}$ m^3/mole, and V_{H_2} is as before (Section 6).

RS33 shows addition of a 3-methyl chain between two adjacent adamantane sidewall sites (i.e., propylation), and RS62 shows addition of a 4-methyl chain between adjacent adamantane sidewall and bridgehead sites (i.e., butylation). The opposite combination of chains and sites is readily inferred because the chemistry is almost identical. Combinations involving longer chains (e.g., 5-methyl chain addition or amylation) are also readily inferred because it is easy to extend methyl chains from sidewall (RS19) or bridgehead (RS20) sites during chain fabrication (Section 8.3.2). An ethenylation (-HC=CH-) addition is shown in Steps 1–5 of RS47, C$_2$ dimer placement (RS4) is an example of an ethynylation (-C≡C-) addition, and related variants are readily envisioned.

Many nonviable pathways also exist. For instance, if a radical site is created by dehydrogenation of the terminal methyl of a two-methyl chain attached to one adamantane sidewall and dehydrogenation of a single methyl on an adjacent sidewall in an attempt to allow self-assembly of a closed-ring propylation tab (-CH$_2$-CH$_2$-CH$_2$-; Section 8.2) via radical coupling, instead the single-methyl radical site barrierlessly abstracts an H atom from the proximal methyl on the long chain, leaving two adjacent radical sites on the two-methyl chain whose subsequent spontaneous ethenylation to -CH=CH$_2$ is strongly exoergic (−4.28 eV). Following this reaction, an attempt to close the ring by abstracting an H atom from the lone methyl creates a radical which will bond to either C atom of the -CH=CH$_2$ chain exoergically (−0.48 eV to the left carbon, a pathology, and −0.71 eV to the right carbon, the desired structure), hence both paths may be taken and so the reaction is unreliable for producing only the desired structure. Similarly, if to create a closed-ring propylation tab a CH: diradical site is created by two dehydrogenations of the terminal methyl of a two-methyl chain attached to one adamantane sidewall leaving a single methyl on an adjacent sidewall intact, the diradical will bond to the lone methyl exoergically (−3.83 eV) but can also steal an H atom from the adjacent methyl exoergically (−3.30 eV) again yielding the -CH=CH$_2$ pathology, hence both paths may be taken and again the reaction is unreliable for producing only the desired structure. As another example, if a "Germylmethylidyne" (i.e., carbene; GeRad-CH:) tool is brought up to an ethyl tab across adjacent adamantane sidewall sites fabricated via RS45 with the intent to insert the CH: into the saturated hydrocarbon ring[167] to create a closed-ring propylation tab, the reaction is exoergic (−4.25 eV singlet, −3.55 eV triplet) but so is pathological abstraction of a single H atom from either the left or right C atom in the existing ethyl tab (−1.18 eV and barrierless for singlet, −0.48 eV with an insufficient +0.16 eV barrier for triplet), hence the reaction appears unreliable because three different paths may be taken.

8.3. Hydrocarbon Chain Fabrication

8.3.1. Polyyne Chain

The linear chain of fully unsaturated carbon atoms known as carbyne—particularly the polyyne (-C≡C-C≡C-) form, a Peierls-distorted structure[168] energetically preferred to the cumulene (=C=C=C=C=) form

RS41. Build Germylmethylene (GM) tool.

| | | | Step 1 | | Step 2 | | Step 3 | | Step 4 … | |
| | | | … Step 4 | | Step 5 | | Step 6 | | | |

Step	Description of Reaction	Mult.	Ener. (eV)	Barr. (eV)
1	**Join GeRad tool to Meth tool CH$_2$● radical site**			
	R: Meth tool (ACC0A/28) + GeRad (ACC0A/25)	D + D		
	P: GMA7 (ACC0A/53)	S	−2.76	
1A	H steal from Meth tool to GeRad radical site			
	R: Meth tool (ACC0A/28) + GeRad (ACC0A/25)	D + D		
	P: AdamCHS (ACC0A/27) + HDon (ACC0A/26)	S + S	+1.22	
	P: AdamCHT (ACC0A/27) + HDon (ACC0A/26)	T + S	+1.08	
2	**Abstract H from CH$_2$ between tool handles using HAbst tool**			
	R: GMA7 (ACC0A/53) + HAbst (ACC0A/27)	S + D		
	P: GMA8 (ACC0A/52) + HAbstH (ACC0A/28)	D + S	−1.70	
3	**Join second GeRad tool to CH● radical site**			
	R: GM8 (ACC0A/28) + CH33Ge (ACC0A/13)	D + D		
	P: GM1 (ACC0A/41)	S	−2.29	
3B1	H steal from CH● radical to second GeRad tool, yielding C**:**			
	R: GM8 (ACC0A/28) + GeRad (ACC0A/25)	D + D		
	P: GM9S (ACC0A/27) + HDon tool (ACC0A/26)	S + S	+1.49	
	P: GM9T (ACC0A/27) + HDon tool (ACC0A/26)	T + S	+0.69	
4	**Detach Adam handle from workpiece (handle exchange)**			
	R: GM1 (ACC0A/41)	S		
	P: GM2 (ACC0A/28) + CH33C (ACC0A/13)	D + D	+2.28	
4B1	H steal from workpiece by departing Adam handle			
	R: GM1 (ACC0A/41)	S		
	P: GM3S (ACC0A/27) + CH33CH (ACC0A/14)	S + S	+3.47	
	P: GM3T (ACC0B/27) + CH33CH (ACC0A/14)	T + S	+2.52	
	T: GM2p1TTS (ACC1A/41)	T		+3.02
5	**Hydrogenate CH● radical site using HDon tool**			
	R: GMA2 (ACC0A/52) + HDon (ACC0A/26)	D + S		
	P: GMA4 (ACC0A/53) + GeRad (ACC0A/25)	S + D	−0.55	

Continued

828

J. Comput. Theor. Nanosci. 5, 760–861, 2008

6	**Detach GeRad handle from workpiece [a]**			
	R: GMA4 (ACC0A/53)	S		
	P: GM tool (ACC0A/28) + GeRad (ACC0A/25)	D + D	+2.89	
6B1	H steal from CH_2 on workpiece by departing GeRad handle			
	R: Diam3 (ACC0A/56)	S		
	P: GMA5HS (ABB0A/27) + HDon tool (ACC0A/26)	S + S	+4.52	
	P: GMA5HT (ACC0A/27) + HDon tool (ACC0A/26)	T + S	+3.81	
4D2	H migrates to radical site from adjacent sidewall CH_2 in handle cage			
	R: GM tool (ACC0A/28)	D		
	P: GMA5H14 (ACC0A/28)	D	−0.12	
	T: GMA5H14-QST3 (ACC1A/28)	D		+2.47
4F4	$CH_2\bullet$ dissociates from tool handle on GM tool			
	R: GM tool (ACC0A/28)	D		
	P: GeRad (ACC0A/25) + CH2S (ACC0A/3)	D + S	+4.06	
	P: GeRad (ACC0A/25) + CH2T (ACC0A/3)	D + T	+3.59	
4G7	Tool $CH_2\bullet$ radical inserts into adjacent sidewall CH_2 in handle cage			
	R: GM tool (ACC0A/28)	D		
	P: GMA5Ins7 (ACC1A/28)	D	−0.12	
	T: GMA5Ins7-QST3 (ACC1A/28)	D		+2.62

[a] Asymmetrically tilting the departing GeRad handle by 25° prior to detachment increases bond strain energy and biases bond-breaking in favor of that handle by +0.50 eV, ensuring that the CH_2 group remains attached to the other GeRad handle and creating a GM tool on a known handle; see text. Increasing bond strain by +0.50 eV may also decrease the triplet pathology 6B1 surplus endoergicity from +0.92 eV to +0.42 eV, still sufficient to prevent the triplet pathology 6B1 at 300 K.

by 1.2 eV per CC unit[169–171]—has been studied since the late 1960s[172] and is readily bulk-synthesized in the laboratory today.[173] For instance, diacetylenic molecules containing a C_4 (-C≡C-C≡C-) group are commonly used as precursors to synthesize carbon-rich π-conjugated networks.[174, 175] While both polyyne and cumulene species have been observed experimentally with long-term stability in carbyne-rich films,[176] there is experimental evidence that polyyne is the preferred form for chains having even numbers of C atoms, though for odd-numbered chains the polyyne structure is impossible thus mandating the cumulene structure.[177] Merkle[4] proposed a method
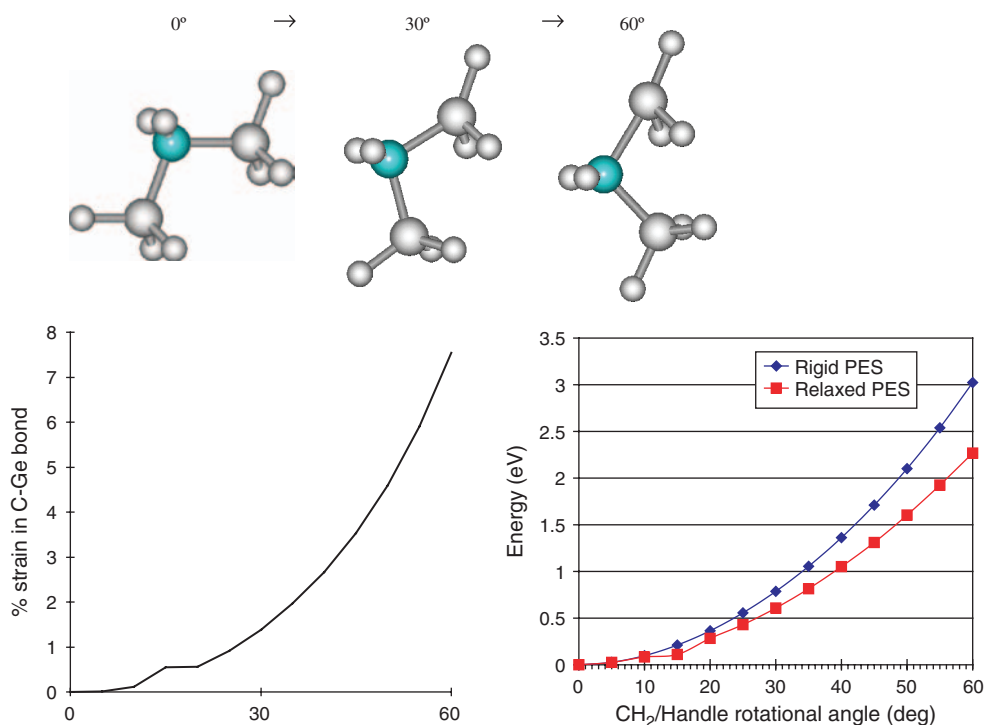
Fig. 5. Controlled asymmetrical bond scission of Germylmethylene tool precursor, modeled as a positionally restrained H_3Ge-CH_2-GeH_3 cluster and simulated with DFT; % strain computed from stressed/unstressed H_2C-GeH_3 bondlength ratio.

REVIEW

RS42. Build Germylene tool by pulling bound GeH_3 off of a Ge surface (includes one rate-limiting bulk-processing step: Step 5).

Step	Description of Reaction	Mult.	Ener. (eV)	Barr. (eV)
1	**Chemisorb GeH_3 ● onto dehydrogenated Ge(111) surface**			
	R: ClusterGRad (ACC1A/13) + GeH3 (ACC0A/4)	D + D		
	P: ClusterGGeH3 (ACC0A/17)	S	−2.59	
2	**Abstract H from GeH_3 bonded to Ge surface using HAbst tool**			
	R: ClusterGGeH3 (ACC0A/17) + HAbst (ACC0A/27)	S + D		
	P: ClusterGGeH2 (ACC0A/16) + HAbstH (ACC0A/28)	D + S	−2.26	
3	**Join AdamRad handle to GeH_2 ● radical site**			
	R: ClusterGGeH2 (ACC0A/16) + AdamRad (ACC0A/25)	D + D		
	P: Cluster70a (ACC1B/41)	S	−2.55	
3B1	H steal from GeH_2 ● radical site by incoming AdamRad handle			
	R: ClusterGCH2 (ACC0A/16) + AdamRad (ACC0A/25)	D + D		
	P: C69ApathS (ACC1A/15) + Adam (ACC0A/26)	S + S	−1.67 [a]	
	Proximity Continuation Reaction:			
	R: C69ApathS (ACC1A/15) + Adam (ACC0A/26)	S + S		
	P: Cluster70a (ACC1B/41)	S	−0.88 [a]	
	T: C70a-QST2 (ABB1A/41)	S		+1.55 [a]
	P: C69ApathT (ACC0A/15) + Adam (ACC0A/26)	T + S	−0.77 [b]	
4	**Detach handled germylidyne (GeH:) from Ge(111) surface**			
	R: Cluster70a (ACC1B/41)	S		
	P: AdamGeHS (ACC0A/27) + ClusterG (ACC1A/14)	S + S	+1.64	
	P: AdamGeHTrun5 (ABB1A/27) + ClusterG (ACC1A/14)	T + S	+2.68	
4B1	H steal from Ge surface by departing Germ tool			
	R: Cluster70a (ACC1B/41)	S		
	P: ClusterGRad (ACC1A/13) + Germ tool (ACC0A/28)	D + D	+2.46	
4D2	H migrates to GeH: radical site from adjacent handle sidewall CH_2			
	R: AdamGeHS (ACC0A/27)	S		
	P: AdamGeHStealS (ACC1A/27)	S	+3.09	
	R: AdamGeHTrun5 (ABB1A/27)	T		
	P: AdamGeHStealT (ACC0B/27)	T	+0.61	
4G2	GeH: radical inserts into adjacent sidewall CH_2 in handle cage			
	R: AdamGeHS (ACC0A/27)	S		
	P: AdamGeHInsertS (ACC0A/27)	S	+1.45	
	R: AdamGeHTrun5 (ABB1A/27)	T		
	P: AdamGeHInsertT (ACC0A/27)	T	+0.65	

Continued

5	**Hydrogenate GeH: diradical to GeH$_3$ using pressurized H$_2$ gas**			
	R: AdamGeHS (ACC0A/27) + H2 (ACC0A/2)	S + S		
	P: AdamGeH3 (ACC0A/29)	S	−1.53	
	T: Becerra et al. [129]	S		**+0.60** [c]
	R: AdamGeHTrun5 (ABB1A/27) + H2 (ACC0A/2)	T + S		
	P: AdamGeH3 (ACC0A/29)	S	−2.57	
6	**Abstract H from GeH$_3$ group using HAbst tool**			
	R: AdamGeH$_3$ (ACC0A/29) + HAbst (ACC0A/27)	S + D		
	P: Germ tool (ACC0A/28) + HAbstH (ACC0A/28)	D + S	−2.15	
4D2	H migrates to radical site from adjacent sidewall CH$_2$ in handle cage			
	R: Germ tool (ACC0A/28)	D		
	P: AdamGeH3HSteal (ACC0A/28)	D	+0.54	
	T: AdamGeH3HStealTrans-QST3run2 (ACC1A/28)	D		+1.93
4F4	GeH$_2$• dissociates from tool handle on Germ tool			
	R: Germ tool (ACC0A/28)	D		
	P: AdamRad (ACC0A/25) + GeH2S (ACC0A/3)	D + S	+1.69	
	P: AdamRad (ACC0A/25) + GeH2T (ACC0A/3)	D + T	+2.85	
4G7	Tool GeH$_2$• radical inserts into adjacent sidewall CH$_2$ in handle cage			
	R: Germ tool (ACC0A/28)	D		
	P: AdamGeH2Insrt (ACC0A/28)	D	+0.58	
	T: AdamGeH2InsrtTrans (ACC1A/28)	D		+2.57

[a] Pathology 3B1 (singlet) can occur because it is exoergic (−1.67 eV), albeit less so than the main reaction (−2.55 eV). However, after Pathology 3B1 (singlet) has occurred, continuing to hold the singlet Products in close proximity for a sufficient time while applying adequate mechanical force to overcome the substantial reverse reaction barrier (+1.55 eV) allows them to undergo an exoergic reverse reaction downhill (−0.88 eV) to yield the desired end Product of this reaction step (Cluster70a).

[b] Pathology 3B1 triplet lies +0.90 eV above the singlet in energy, hence is unlikely to occur; if the triplet does occur, it should rapidly transition downhill to the singlet via intersystem crossing.

[c] The +0.60 eV barrier is overcome by exposing the Ge: diradical to H$_2$ gas pressurized to 6300 atm at 300 K, or to 6100 atm at 400 K; see text, Section 6.

for extending a polyyne chain indefinitely from positionally controlled handles by attacking a butadiyne feedstock molecule bound between two silicon radicals (SiRad-C≡C-C≡C-SiRad) with two HAbst tools (Adam-C≡C•) on either side of the central C-C bond (4 proximated tools), yielding two copies of Adam-C≡C-C≡C-SiRad which are then pulled apart, preferentially breaking at the slightly weaker C-Si bond, yielding •SiRad and Adam-C≡C-C≡C•, a polyyne chain extended by one carbyne unit (a process that may be iterated indefinitely). While workable, this sequence requires the maximum limit of 4 proximated tools, the use of chemically unstable butadiyne feedstock, and the exploitation of a C-Si/C-C bond force differential of only 0.72 nN which provides less reliable bond dissociation than the much larger C-Ge/C-C bilateral force differential of 1.89 nN (Section 3.5). Merkle[4] also proposed a similar method for transferring a single C atom from one single-handled cumulene chain to another, on the assumption that such a chain would be stable throughout the mechanosynthetic process and would not convert to polyyne.

Several reaction pathways are identified in the present work for fabricating polyyne chains of any length. First, a one-handled polyyne chain is built on an Adam bridgehead by applying an HAbst tool to a DimerP tool, then pulling off the C$_2$ dimer in 2 subsequent steps to yield an Adam-C≡C-C≡C• (bearing the extended polyyne chain)

and a discharged DimerP tool requiring refresh (RS52); this may be iterated as necessary to make longer chains. RS52 could alternatively be performed by two GeRad tools loaded with C$_2$ dimer (as in Step 4 of RS6) and operated in tandem in place of the one dimer-charged DimerP tool. One-handled chains also may be extended in single-atom
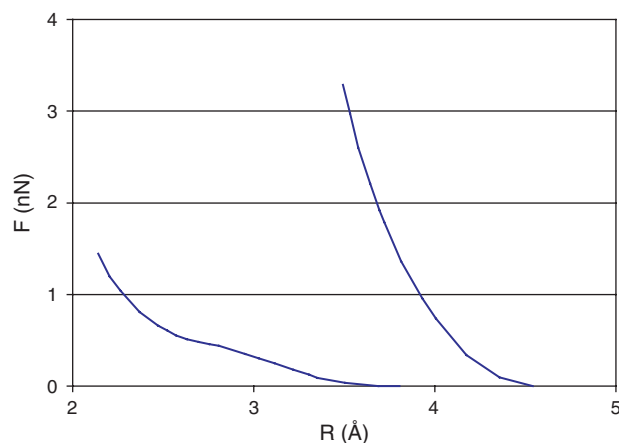
Fig. 6. Repulsive force in nanonewtons as a function of distance in Angstroms for hydrogenated GeRad (left) and hydrogenated GM (right) tooltips perpendicularly approaching a bridgehead hydrogen atom on a hydrogenated diamond C(111) surface, using semiempirical AM1; the force differential exceeds 3 nN at 3.5 Å which should be detectable experimentally.

RS43. Build DimerP tool using a series of previous reaction sequences.

	Step 1	Step 2	Step 3	Step 4 …

… Step 4	Step 5	Step 6	

Step	Description of Reaction	Mult.	Ener. (eV)	Barr. (eV)
1	Add –CH$_2$-GeH$_2$-CH$_2$- bridge across HDon tool sidewalls (RS35)			
2	Build Adam cage below –CH$_2$-GeH$_2$-CH$_2$- bridge (RS33 + RS34)			
3	Add –CH$_2$-CH$_2$-CH$_2$- bridge across lower right sidewalls (RS33)			
4	Add CH$_2$ group to complete GeRad cage on right side (RS36)			
5	Abstract H from each of two Ge atoms (RS1 + RS1)			
6	**Recharge DimerP tool (RS6)**			
6F5	C$_2$ dissociates from Adam tool handle			
	R: DimerP (ACC0A/46)	S		
	P: DCB6GeOffS (ACC0A/44) + C2S (ACC0A/2)	S + S	+7.81	
	P: DCB6GeOffS (ACC0A/44) + C2T (ACC0A/2)	S + T	+8.01	

RS44. Build lonsdaleite using a series of previous reaction sequences.

	Step 1	Step 2	Step 3 …

… Step 3	Step 4	

Step	Description of Reaction	Mult.	Ener. (eV)	Barr. (eV)
1	Add –CH$_2$-CH$_2$-CH$_2$- bridge across Adam sidewalls (RS33)			
2	Build Adam cage below –CH$_2$-CH$_2$-CH$_2$- bridge (RS33 + RS34)			
3	Add –CH$_2$-CH$_2$-CH$_2$- bridge across lower right sidewalls (RS33)			
4	Add CH$_2$ group to complete Adam cage on right side (RS34)			

832

J. Comput. Theor. Nanosci. 5, 760–861, **2008**

RS45. Add -CH_2-CH_2- across adjacent adamantane sidewall sites using CH_3 dehydrogenation.

Step	Description of Reaction	Mult.	Ener. (eV)	Barr. (eV)
1	**Add 1st CH_3 to Adam sidewall site using GM tool (RS7)**			
2	**Add 2nd CH_3 to Adam sidewall site, with CH_3 on adjacent sidewall, using GM tool (RS21)**			
3	**Abstract H from first CH_3 on Adam sidewall using HAbst tool**			
	R: Cluster53A (ACC0A/32) + HAbst (ACC0A/27)	S + D		
	P: Cluster52A (ACC0A/31) + HAbstH (ACC0A/28)	D + S	−1.60	
4	**Abstract H from second CH_3 on Adam sidewall using HAbst tool**			
	R: Cluster52A (ACC0A/31) + HAbst (ACC0A/27)	D + D		
	P: C56pathS (ACC0A/30) + HAbstH (ACC0A/28)	S + S	−4.69	
	P: C56T (ACC1A/30) + HAbstH (ACC0A/28)	T + S	−1.51[a]	
4D19	**H migrates to $CH_2\bullet$ radical site from adjacent $CH_2\bullet$ leaving CH_3 & CH:**			
	R: Cluster52A (ACC0A/31) + HAbst (ACC0A/27)	D + D		
	P: C56pathSTS (ACC1A/30) + HAbstH (ACC0A/28)	S + S	−0.98	
	Proximity Continuation Reaction:			
	R: C56pathSTS (ACC1A/30)	S		
	P: C56pathS (ACC0A/30)	S	−3.71	
	P: C56pathT (ACC0A/30) + HAbstH (ACC0A/28)	T + S	−1.14	
	Proximity Continuation Reaction:			
	R: C56pathT (ACC0A/30)	T		
	P: C56T (ACC1A/30)	T	−0.38[a]	

[a] Triplet Product lies +3.17 eV above singlet Product in energy, hence is unlikely to occur; if the triplet does occur, it should rapidly transition downhill to the singlet via intersystem crossing.

increments by terminal methylation as shown in RS17. Second, a two-handled polyyne chain is built between Adam bridgeheads by dehydrogenating a polyacetylene chain (RS53) that had been previously fabricated from two Meth tools using RS58, or more directly by joining two HAbst tools coaxially; this chain is extended indefinitely in two-carbon (C_2) increments by bonding a third HAbst tool to the apical C atom in the chain, then detaching the surplus AdamRad handle (RS54), or in single-carbon (CH_2) increments by applying a Meth tool followed by AdamRad handle detachment (RS55). Third, a three- or four-handled polyyne chain is built between Adam bridgeheads by attaching successive HAbst tools at radical
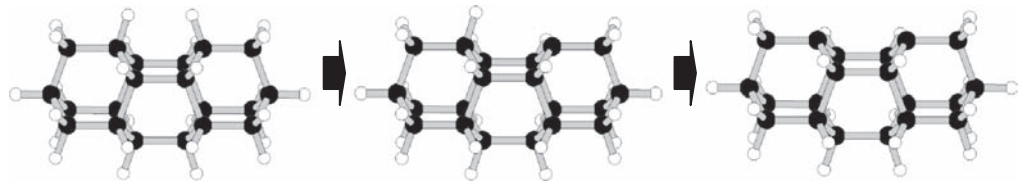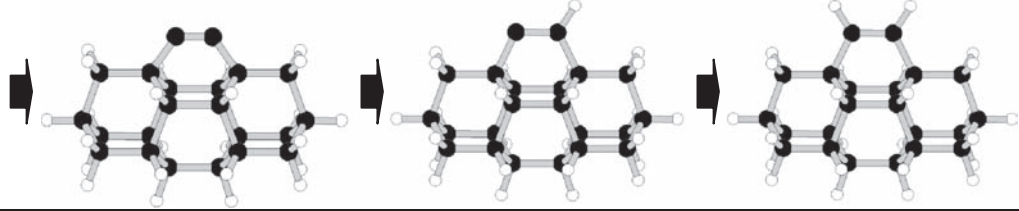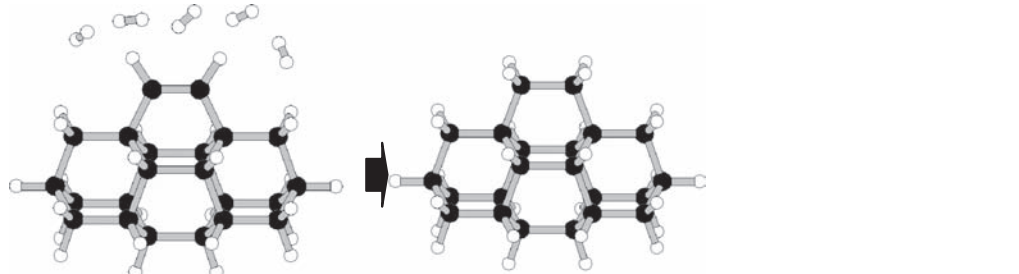
sites opened by GeRad attack of an adjacent chain carbon atom (RS56), with any branch indefinitely extendable using RS54 or RS55. GeRad attack on an adjacent chain atom can open up any desired polyyne chain atom for selective hydrogenation by an HTrans tool (Steps 1–2 of RS57) or for selective methylation by a GM tool (RS18), or may allow two polyyne chains to be joined across any two C atoms along their respective lengths via simple radical coupling except in cases of excessive steric congestion. Application of RS54 or RS55 to a C atom more distant from the second AdamRad handle allows longer chains to be broken into smaller chains via "subtractive handle exchange."

RS46.   Add -CH_2-CH_2- across DCB6C gap using CH_3 dehydrogenation.

Step 1		Step 2 ...

... Step 2	

Step	Description of Reaction	Mult.	Ener. (eV)	Barr. (eV)
1	**Abstract H from right CH$_3$ on LonsA5 w/HAbst tool**			
	R: LonsA5run2 (ACC0A/52) [RS28 Step 4] + HAbst (ACC0A/27)	S + D		
	P: Cluster52BB (ACC0A/51) + HAbstH (ACC0A/28)	D + S	−1.89	
1D10	H migrates to CH$_2$• radical from apposing DCB6C bridgehead CH$_3$			
	R: Cluster52BB (ACC0A/51)	D		
	P: Cluster52BBL (ACC0A/51)	D	0.00	
	T: C52BB-QST2 (ACC1A/51)	D		**+0.08** [a]
2	**Abstract H from left CH$_3$ w/HAbst tool, CH$_2$• radical on right**			
	R: Cluster52BB (ACC0A/51) + HAbst (ACC0A/27)	D + D		
	P: Cluster98 (ACC0A/50) + HAbstH (ACC0A/28)	S + S	−5.99	
	T: C52BBCarbsTS (ACC1A/50) + HAbstH (ACC0A/28)	S + S		−0.15
2a	R: C52BBCarbsTS (ACC1A/50)	S		
	P: Cluster98 (ACC0A/50)	S	−5.84	−2.93
	T: C52BBC-QST2 (ACC1A/50)	S		
	R: C52BBC-QST2 (ACC1A/50)	S		
	P: C52BBCS-TS (ACC1A/50)	S	+1.49	
	P: C52BBCarbT (ACC0A/50) [after ISC]	T	+1.75	
	P: C52BBCarbtTS (ACC1A/50) + HAbstH (ACC0A/28)	T + S	**−1.61** [b]	
2b	R: C52BBCarbtTS (ACC1A/50)	T		
	P: C52BBCarbsTS (ACC1A/50)	S	+1.46	
	P: Cluster98 (ACC0A/50)	S	−4.38	
	T: C52BBC-QST2 (ACC1A/50) [after ISC]	S		−1.46
	P: Cluster98 (ACC0A/50) [after ISC]	S	−4.38	
	T: C52BBCT-QST2 (ACC1A/50)	T		+0.23
	R: C52BBCT-QST2 (ACC1A/50)	T		
	P: C52BBCarbT (ACC0A/50)	T	+0.05	
	R: C52BBCarbT (ACC0A/50)	T		
	P: Cluster98 (ACC0A/50)	S	−4.66	
	T: C52BBCS-TS (ACC1A/50) [after ISC]	S		−0.26
	P: [go to 2d]	T	(see 2d)	
	Abstract H from left CH$_2$• radical w/HAbst tool, CH3 on right			
	R: Cluster52BBL (ACC0A/51) + HAbst (ACC0A/27)	D + D		
	P: Cluster98 (ACC0A/50) + HAbstH (ACC0A/28)	S + S	−5.99	
	T: C52BBCS-TS (ACC1A/50) + HAbstH (ACC0A/28)	S + S		−1.59
2c	R: C52BBCS-TS (ACC1A/50)	S		
	P: Cluster98 (ACC0A/50)	S	−4.40	
	T: C52BBC-QST2 (ACC1A/50)	S		−1.49

		S		
	R: C52BBC-QST2 (ACC1A/50)	S		
	P: C52BBCarbsTS-QST2 (ACC1A/50)	S	+2.93	
	P: C52BBCarbtTS-QST2 (ACC1A/50)	T	+1.46	
	P: Cluster98 (ACC0A/50) [after ISC]	S	−4.40	
	T: C52BBCT-QST2 (ACC1A/50) [after ISC]	T		+0.21
	R: C52BBCT-QST2 (ACC1A/50)	T		
	P: Cluster98 (ACC0A/50)	S	−4.61	
	T: C52BBC-QST2 (ACC1A/50) [after ISC]	S		−1.69
	P: C52BBCarbtTS (ACC1A/50) **[go to 2b]**	T	−0.23	
2G1a	CH: radical inserts into adjacent bridgehead CH in handle cage			
	R: C52BBCS-TS (ACC1A/50)	S		
	P: C52BBIns22 (ACC0A/50)	S	−1.89	
	T: C52BBIns22-QST3 (ACC1A/50)	S		+1.27
	P: C52BBIns22T (ACC0A/50)	T	−0.25	
	T: C52BBIns22T-QST3 (ACC1A/50) [after ISC]	T		+2.44
2G2	CH: radical inserts into adjacent sidewall CH$_2$ in handle cage			
	R: C52BBCS-TS (ACC1A/50)	S		
	P: C52BBIns8 (ACC0A/50)	S	−2.20	
	T: C52BBIns8-QST3 (ACC1A/50)	S		**+0.14**[c]
	P: C52BBCarbT (ACC0A/50) [after ISC]	T	+0.26	
	R: C52BBCarbT (ACC0A/50)	T		
	P: C52BBIns8T (ACC0A/50)	T	−1.17	
	T: C52BBIns8T-QST3 (ACC1A/50)	T		+1.87
2D2	H migrates from adjacent sidewall CH$_2$ to CH: radical			
	R: C52BBCS-TS (ACC1A/50)	S		
	P: C52BBH-TS (ACC1A/50)	S	+1.56	
	T: C52BBH-QST3 (ACC1A/50)	S		+1.49
	R: C52BBCarbT (ACC0A/50) [after ISC]	T		
	P: C52BBHT-TS (ACC1A/50)	T	+0.02	
	T: C52BBHT2-QST3 (ACC1A/50)	T		+1.67
2G3	CH: radical cross-bonds to apposing C-CH$_3$, abstracting the CH$_3$			
	R: C52BBCS-TS (ACC1A/50)	S		
	P: C52BBIns45 (ACC0A/50)	S	−3.78	
	T: C52BBIns45-QST3 (ACC1A/50)	S		+2.45
	P: C52BBCarbT (ACC0A/50) [after ISC]	T	+0.26	
	R: C52BBCarbT (ACC0A/50)	T		
	T: C52BBIns45T-QST3 (ACC1A/50)	T		+1.94
2d	R: C52BBCarbT (ACC0A/50)	T		
	P: Cluster98 (ACC0A/50) [after ISC]	S	−4.66	
	T: C52BBCT-QST2 (ACC1A/50)	T		−0.05
	R: C52BBCT-QST2 (ACC1A/50)	T		
	T: C52BBCarbtTS (ACC1A/50) **[go to 2b]**	T		−0.23
	P: Cluster98 (ACC0A/50)	S	−4.66	
	T: C52BBC-QST2 (ACC1A/50) [after ISC]	S		−1.75
	R: C52BBC-QST2 (ACC1A/50)	S		
	T: C52BBCarbtTS (ACC1A/50) [after ISC]	T		+1.46
	P: C52BBCS-TS (ACC1A/50) [after ISC] **[go to 2c]**	S	−0.26	
2G1b	CH: radical inserts into adjacent bridgehead CH in handle cage			
	R: C52BBCarbT (ACC0A/50)	T		
	P: C52BBIns22 (ACC0A/50)	S	−2.16	
	T: C52BBIns22-QST3 (ACC1A/50) [after ISC]	S		+1.01
	P: C52BBIns22T (ACC0A/50)	T	−0.51	
	T: C52BBIns22T-QST3 (ACC1A/50)	T		+2.44

[a] With such a low barrier to migration, the migrating H atom will transit repeatedly between methyl groups at a frequency of ~3 x 10^{11} sec^{-1}.

[b] Triplet Product lies +4.38 eV above singlet Product in energy, hence is unlikely to occur; if the triplet does occur, it should rapidly transition downhill to the singlet via intersystem crossing.

[c] The continuing physical presence of the HAbstH tool positioned between the CH: radical and the adjacent sidewall CH$_2$ acts as a major supplemental barrier to block this pathology, thus allowing the extremely exoergic (−5.99 eV) main reaction to be rapidly consummated.

RS47. Add -CH$_2$-CH$_2$- across DCB6C gap using DimerP tool (includes one rate-limiting bulk-processing step: Step 6).

	Step 1	Step 2	Step 3 …

… Step 3	Step 4	Step 5	

	Step 6		

Step	Description of Reaction	Mult.	Ener. (eV)	Barr. (eV)
1	**Abstract H from DCB6C bridgehead using HAbst tool**			
	R: Cluster86 (ACC0B/46) + HAbst (ACC0A/27)	S + D		
	P: Cluster87 (ACC0A/45) + HAbstH (ACC0A/28)	D + S	−1.69	
2	**Abstract H from DCB6C bridgehead using HAbst tool**			
	R: Cluster87 (ACC0A/45) + HAbst (ACC0A/27)	D + D		
	P: Cluster88S (ACC0A/44) + HAbstH (ACC0A/28)	S + S	−1.19	
	P: Cluster88T (ACC0A/44) + HAbstH (ACC0A/28)	T + S	−1.57	
3	**Donate C$_2$ across DCB6C bridgehead radicals using DimerP tool**			
	R: Cluster88S (ACC0A/44) + DimerP (ACC0A/46)	S + S		
	P: Cluster92 (ACC0A/46) + DCB6GeOffS (ACC0A/44)	S + S	−0.78	
	R: Cluster88T (ACC0A/44) + DimerP (ACC0A/46)	T + S		
	P: Cluster92 (ACC0A/46) + DCB6GeOffS (ACC0A/44) [after ISC][a]	S + S	−0.40	
4	**Hydrogenate C≡C group using HTrans tool**			
	R: Cluster92 (ACC0A/46) + S15cis (ACCCA/11)	D + D		
	P: Cluster93 (ACC0A/47) + S16Run0 (ACCCA/10)	S + S	−0.93	
5	**Hydrogenate •C=CH radical site using HDon or HTrans tool**			
	R: Cluster93 (ACC0A/47) + HDon (ACC0A/26)	D + S		
	P: Cluster94 (ACC0A/48) + GeRad (ACC0A/25)	S + D	−1.12	
	R: Cluster93 (ACC0A/47) + S15cis (ACCCA/11)	D + D		
	P: Cluster94 (ACC0A/48) + S16Run0 (ACCCA/10)	S + S	−1.95	
6	**Hydrogenate HC=CH group to H$_2$C–CH$_2$ using pressurized H$_2$ gas**			
	R: Cluster94 (ACC0A/48) + H2 (ACC0A/2)	S + S		
	P: Cluster98 (ACC0A/50)	S	−1.04	
	T: Steacie (1938); see text	S		+1.87[b]
6^{1}1	**Hydrogenate HC=CH group to H$_2$C–CH• using H• bombardment**			
	R: Cluster94 (ACC0A/48) + H (ACC0A/1)	S + D		
	P: Cluster97 (ACC0A/49)	D	−1.56	
6^{1}2	**Hydrogenate H$_2$C–CH• group to H$_2$C–CH$_2$ using H• bombardment**			
	R: Cluster97 (ACC0A/49) + H (ACC0A/1)	D + D		
	P: Cluster98 (ACC0A/50)	S	−3.97	

Continued

836

J. Comput. Theor. Nanosci. 5, 760–861, 2008

[a] An ISC will rapidly occur because the discharged DimerP tool singlet (DCB6GeOffS) lies –1.10 eV below the discharged DimerP tool triplet (DCB6GeOffS).

[b] The approximately +1.87 eV barrier (Steacie, 1938) may be overcome by exposing the ethylene group to H_2 gas pressurized to 20,800 atm at 300 K; see text.

RS48. Add -CH_2-CH_2- across DCB6C gap using HAbst tool (p. 1254) (full cage models illustrated; includes one rate-limiting bulk-processing step: Step 5).

Step	Description of Reaction	Mult.	Ener. (eV)	Barr. (eV)
1	**Abstract two H's from DCB6C bridgehead C atoms (Steps 1–2, RS47)**			
2	**Attach terminal C of HAbst tool to left DCB6C bridgehead C**			
	R: Cluster88S (ACC0A/44) + CH3CC (ACC0A/6)	S + D		
	P: HACC1 (ACC1A/50)	D	–5.42	
	R: Cluster88T (ACC0A/44) + CH3CC (ACC0A/6)	T + D		
	P: HACC1 (ACC1A/50)	D	–5.05	
3	**Attach proximal C of HAbst tool to right DCB6C bridgehead C**			
	R: HACC1 (ACC1A/50)	D		
	P: HACC2 (ACC0A/50)	D	–0.64	
	T: HACC2-QST2 (ACC0B/50)	D		+0.01
3B8	H steal from adjacent bridgehead CH on DCB6C			
	R: HACC1 (ACC1A/50)	D		
	T: HACC2p1TS (ACC1S/50)	D		+3.21
3H	Terminal C in HAbst tool crossbonds to right DCB6C bridgehead C atom			
	R: HACC1 (ACC1A/50)	D		
	P: HACC2p2 (ACC0B/50)	D	–0.20[a]	
	T: HACC2p2-QST2 (ACC1A/50)	D		+0.33[a]
4	**Detach AdamRad handle from dimer on DCB6C bridgehead**			
	R: HACC2 (ACC0A/50)	D		
	P: Cluster92 (ACC0A/46) + CH3 (ACC0A/4)	S + D	–0.78	
5	**Hydrogenate C≡C group using Steps 4–6 of RS47**			

[a] Main reaction and crossbonding pathology 3H are exoergic, hence both can occur. The +0.33 eV barrier to 3H is high enough, with the apparently barrierless main reaction, to ensure reliable 80 K operation; at 300 K, the reaction may not be sufficiently reliable unless positional control can be used to steer the proximal C of the HAbst tool to its intended target.

RS49. Add -CH$_2$-CH$_2$-across adjacent C111 bridgeheads using CH$_3$ dehydrogenation.

Step	Description of Reaction	Mult.	Ener. (eV)	Barr. (eV)
1	**Add 1st CH$_3$ to C111 bridgehead using GM tool (RS12)**			
2	**Add CH$_3$ to C111 bridgehead w/CH$_3$ on adjacent bridgehead (RS24)**			
3	**Abstract H from first CH$_3$ on C111 bridgehead using HAbst tool**			
	R: DiamM5 (ACC0A/56) + HAbst (ACC0A/27)	S + D		
	P: DiamM4 (ACC0A/55) + HAbstH (ACC0A/28)	D + S	−1.74	
4	**Abstract H from second CH$_3$ on C111 bridgehead using HAbst tool**			
	R: DiamM4 (ACC0A/55) + HAbst (ACC0A/27)	D + D		
	P: DiamM6S (ACC0A/54) + HAbstH (ACC0A/28)	S + S	−4.77	
	P: DiamM6T (ACC0A/54) + HAbstH (ACC0A/28)	T + S	**−1.53** [a]	

[a] Triplet Product lies +3.23 eV above singlet Product in energy, hence is unlikely to occur; if the triplet does occur, it should rapidly transition downhill to the singlet via intersystem crossing.

Once a desired polyyne chain structure has been fabricated the structure can be site-selectively dehandled using a handle exchange operation for polyyne chain (Steps 1–2 of RS6). In this chain dehandling operation, the attachment atom of an unwanted AdamRad handle is attacked by a GeRad handle and the AdamRad handle is detached, whereupon the chain may be (1) passivated by H donation and the GeRad handle detached, yielding a free chain end, or (2) attached to a radical site on another structure at the detachment-created radical site via radical coupling. By this latter means, simple polyyne chain networks can also be attached to other simple chain networks to build up more complex polyyne nets of larger size.

8.3.2. Polyacetylene and Polyethylene Chains

Polyacetylene (-CH═CH-CH═CH-)—another well-known "linear" carbon polymer[178, 179] whose structure was reported as early as 1958[180]—is monohydrogenated polyyne that may be synthesized via positionally controlled mechanosynthesis by: (1) additive conversion (hydrogenation) of a two-handled polyyne chain to a polyacetylene chain (RS57); or (2) subtractive conversion (dehydrogenation) of a two-handled polyethylene chain (made from two Meth tools) to a polyacetylene chain (RS58). A continuous chain of polyacetylene also may be drawn on a single handle by first bringing an AdamRad or GeRad tooltip into contact with bulk acetylene feedstock gas of high purity, whereupon an impinging C$_2$H$_2$ molecule bonds to the exposed monoradical site in a vertical configuration, creating a complementary monoradical site on the distal end of the newly-added acetylene. The chain is perpetuated indefinitely as successive C$_2$H$_2$ molecules impinge on the distal monoradical growth site, adding CH pairs to the growing polyacetylene chain (RS59) in an apparently barrierless reaction. Methods for manipulating or spooling the self-assembling chain would need to be devised for a practical manufacturing system. An experiment using site-specific H abstraction to create a dangling bond that subsequently seeds atomically registered styrene chain formation oriented along an underlying dimer row on the Si(100)-2 × 1:H surface has been reported by Basu et al.[37]

RS50.   Add -CH$_2$-CH$_2$-across adjacent C100 dimers using CH$_3$ dehydrogenation.

Step	Description of Reaction	Mult.	Ener. (eV)	Barr. (eV)
1	**Add 1st CH$_3$ to C100 dimer site using GM tool (RS14)**			
2	**Add CH$_3$ to C100 dimer site nearest to CH$_3$ on adjacent dimer (RS27)**			
3	**Abstract H from left CH$_3$ on C100 dimer using HAbst tool**			
	R: C100MME (AXCXA/41) + HAbst (AXC0A/27)	S + D		
	P: C100MMD (AXC0A/40) + HAbstH (AXC0A/28)	D + S	−1.55	
4	**Abstract H from right CH$_3$ on C100 dimer using HAbst tool**			
	R: C100MMD (ACC0A/40) + HAbst (ACC0A/27)	D + D		
	P: C100MMFS (ACC0A/39) + HAbstH (ACC0A/28)	S + S	−4.68	
	P: C100MMFT (ACC0A/39) + HAbstH (ACC0A/28)	T + S	**−1.55** [a]	

[a] Triplet Product lies +3.13 eV above singlet Product in energy, hence is unlikely to occur; if the triplet does occur, it should rapidly transition downhill to the singlet via intersystem crossing.

Fully saturated "linear" polyethylene (-CH$_2$-CH$_2$-) chains, or "linear" hydrocarbons of any length and branching structure, are most easily produced via positional mechanosynthesis by repeated methylation starting from an Adam sidewall (RS7, RS19, RS29, RS32) or bridgehead (RS9, RS20) site using a GM tool, yielding a single-handled polyethylene chain. A two-handled polyethylene chain may be fabricated using Step 1 of RS58, which chain may be extended indefinitely in length or connectivity by substituting a GM tool (with GeRad handle detached after each methylation as in RS60) for the Meth tool in each reaction iteration, except for the last methylation which would use a Meth tool (to terminate the chain with an AdamRad handle). A two-handled polyethylene chain between two GeRad handles (initially, from combining two GM tools), indefinitely extensible via handle exchange of GM tool for GeRad handle (RS60), may be convenient for chain deposition operations because both handles are readily detached as the chain is bonded to another carbon workpiece structure, and because such a chain is readily converted to polyacetylene or polyyne chain via dehydrogenation.

8.4. Graphene Fabrication

Graphene sheets consisting of sp^2 carbon bonding include six-carbon aromatic rings and related structures, graphite, and most importantly the class of carbon allotropes known as fullerenes (cages) and carbon nanotubes (cylinders),[181] along with hybrid nanotube-diamond structures.[182, 183]

Aromatic rings may be fabricated on an adamantane stub by building a handled four-carbon polyethylene chain extending from an adamantane sidewall site, then attaching the handled end of the chain to the adjacent bridgehead site to form a closed ring; four excess H atoms are then removed from the ring, either in a sequence of alternating sites (RS61) that forces aromatic bonds to form as slowly as possible (the least stable and undesired reaction order), or in a sequence of adjacent sites (RS62) continuously moving counterclockwise (CCW) around the ring to form aromatic bonds as quickly as possible (the most stable and desired reaction order), with similar pathologies as previously analyzed in RS61. A second aromatic ring is added to the first ring by building a handled four-carbon

RS51. Add -CH$_2$-CH$_2$-across same C100 dimer using CH$_3$ dehydrogenation.

Step	Description of Reaction	Mult.	Ener. (eV)	Barr. (eV)
1	**Add 1st CH$_3$ to C100 dimer site using GM tool (RS14)**			
2	**Add CH$_3$ to C100 dimer site with CH$_3$ on same dimer (RS26)**			
3	**Abstract H from upper CH$_3$ on C100 dimer using HAbst tool**			
	R: C100ME (AXCXA/41) + HAbst (AXC0A/27)	S + D		
	P: C100MD (AXC0A/40) + HAbstH (AXC0A/28)	D + S	−1.48	
4	**Abstract H from lower CH$_3$ on C100 dimer using HAbst tool**			
	R: C100MD (ACC0A/40) + HAbst (ACC0A/27)	D + D		
	P: C100MFSrun3 (ACC0A/39) + HAbstH (ACC0A/28)	S + S	−3.73	
	P: C100MFT (ACC0A/39) + HAbstH (ACC0A/28)	T + S	**−1.54** [a]	

[a] Triplet Product lies +2.18 eV above singlet Product in energy, hence is unlikely to occur; if the triplet does occur, it should rapidly transition downhill to the singlet via intersystem crossing.

polyethylene chain extending from one of the two distal carbon atoms on the first ring (RS63), then attaching the handled end of the chain to the adjacent distal carbon atom site on the first ring to form a closed second ring which is subsequently partially dehydrogenated in a continuous CCW sequence (RS64). Further rings can be added in any direction within the same plane to form a complete 2D graphene sheet via successive applications of RS63 + RS64, with the handled polyethylene additive chain consisting of either three or four methyl units (depending on direction of sheet extension) which have similar positional chemistries. Single-layer graphene sheet has been prepared and imaged experimentally by mechanical exfoliation of highly oriented pyrolytic graphite,[184] and the atomic growth process of carbon nanotubes synthesized using 500 °C methane and nanoscale nickel catalyst with step edges having spatiotemporally dynamic active sites has been imaged.[185]

Comprehensive specification of positional reaction pathways for all major families of 3D graphene structures is beyond the scope of this paper, so we illustrate the ability of our minimal toolset to synthesize 3D graphene using the example of the 4.7 Å diameter conductive zigzag (6, 0) nanotube,[186] a representative structure in the graphene nanotube class. The (6, 0) carbon nanotube has long been regarded as having the smallest experimentally realizable diameter, since tubes with a smaller diameter are thermodynamically unstable.[187, 188] Although (3, 0) and (2, 2) carbon nanotubes have been proposed theoretically by employing mixed sp^2/sp^3 bonding patterns to make stable nanowires,[189, 190] early theoretical considerations[187] and more recent simulations[191, 192] suggest that the 3.3 Å diameter (4, 0) carbon nanotube is the thinnest possible pure sp^2 nanotube structure, though only metastable because it is energetically less favorable than a graphene sheet.[191] It is claimed that the (4, 0) nanotube has been fabricated by mass-selected carbon ion beam deposition inside multiwall nanotubes[193, 194] and also synthesized inside a zeolite channel template[195] which surrounds the (4, 0) nanotube and stabilizes its delicate structure. Experimentally, (n, 0) nanotubes appear far less abundant than the (n, n) nanotubes that are routinely synthesized catalytically by laser vaporization of graphite or by decomposition of hydrocarbons,[186] but there have been theoretical

RS52. Build one-handled polyyne chain on Adam bridgehead [full cage models illustrated].

	Step 1	Step 2	Step 3

Step	Description of Reaction	Mult.	Ener. (eV)	Barr. (eV)
1	**Join HAbst tool to C₂ dimer held by DimerP tool**			
	R: CH3CC (AXC0A/6) + DimerP (AXC0A/46)	D + S		
	P: DimerPCCCH3 (AXCXA/52)	D	−3.73	
2	**Detach dimer from attachment side of DimerP tool**			
	R: DimerPCCCH3 (AXCXA/52)	D		
	P: DimerPC4CH3 (AXCXA/52)	D	+0.15	
3	**Detach dimer from other side of DimerP tool**			
	R: DimerPC4CH3 (AXCXA/52)	D		
	P: CH3CCCC (AXB0A/8) + DCB6GeOffS (AXC0A/44)	D + S	+4.16	
	P: CH3CCCC (AXB0A/8) + DCB6GeOffT (AXC0A/44)	D + T	+5.36	

RS53. Subtractive conversion of two-handled polyacetylene chain to polyyne chain [full cage models illustrated].

	Step 1	Step 2	

Step	Description of Reaction	Mult.	Ener. (eV)	Barr. (eV)
1	**Abstract H from first carbon in chain using HAbst tool**			
	R: ChainP3S (ABB0A/12) + HAbst (ACC0A/27)	S + D		
	P: ChainP4 (ACC0A/11) + HAbstH (ACC0A/28)	D + S	−1.22	
1D1	H migrates to radical site from adjacent CH in chain			
	R: ChainP4 (ACC0A/11)	D		
	T: ChainP4p1TS (ACC1A/11)	D		+2.09
2	**Abstract H from second carbon in chain using HAbst tool**			
	R: ChainP4 (ACC0A/11) + HAbst (ACC0A/27)	D + D		
	P: ChainH4 (ACC0A/10) + HAbstH (ACC0A/28)	S + S	−4.18	

RS54. Build two-handled polyyne chain between Adam bridgeheads [full cage models illustrated].

Step	Description of Reaction	Mult.	Ener. (eV)	Barr. (eV)
1	**Join apical radical sites of two HAbst tools coaxially**			
	R: CH33CCC (ACC0A/15) + CH33CCC (ACC0A/15)	D + D		
	P: Cluster20 (ACC0A/30)	S	−7.09	
2	**Join 3rd HAbst tool to 4th carbon atom in chain**			
	R: Cluster20 (ACC0A/30) + CH33CCC (ACC0A/15)	S + D		
	P: Cluster140 (ACC0A/45)	D	−2.94	
3	**Detach Adam handle from 4th carbon atom in chain**			
	R: Cluster140 (ACC0A/45)	D		
	P: Cluster141 (ACC0A/32) + CH33C (ACC0A/13)	S + D	+0.71	

RS55. Increment 2-handled polyyne chain between Adam bridgeheads by 1 methyl group [full cage models illustrated].

Step	Description of Reaction	Mult.	Ener. (eV)	Barr. (eV)
1	**Join Meth tool to 4th carbon atom in polyyne chain**			
	R: ChainOne1 (ACC0A/12) **[RS54]** + CH3CH2 (ACC0A/7)	S + D		
	P: ChainOne2 (ACC1B/19)	D	−1.07	
1A	H steal from Meth tool to DCB6C bridgehead radical site			
	R: ChainOne1 (ACC0A/12) + CH3CH2 (ACC0A/7)	S + D		
	P: ChainOne2p1 (ACC0A/13) + CH3CHS (ACC0A/6)	D + S	+2.93	
	P: ChainOne2p1 (ACC0A/13) + CH3CHT (ACC0A/6)	D + T	+2.73	
2	**Detach Adam handle from 4th carbon atom in polyyne chain**			
	R: ChainOne2 (ACC1B/19)	D		
	P: ChainOne3 (ACC0A/15) + CH3 (ACC0A/4)	S + D	+1.21	

842

*J. Comput. Theor. Nanosci. 5, 760–861, **2008***

RS56. Build four-handled branched polyyne chain with Adam handles [full cage models illustrated].

Step	Description of Reaction	Mult.	Ener. (eV)	Barr. (eV)
1	**Join GeRad handle to third carbon atom in handled C$_6$ polyyne chain** R: BCR1 (ABB0A/14) + GeH3 (ACC0A/4) P: BCR2 (ABB0B/18)	S + D D	−0.65	
2	**Join C● of handled C$_2$ chain (an HAbst tool) to C● on C$_6$ chain** R: CH3CC (ACC0A/6) + BCR2 (ABB0B/18) P: BCR3 (ABB2B/24)	D + D S	−5.00	
3	**Detach GeRad handle from third carbon atom in C$_6$ chain** R: BCR3 (ABB2B/24) P: BCR4 (ABB0A/20) + GeH3 (ACC0A/4)	S D + D	+2.90	
4	**Join C● of handled C$_2$ chain (an HAbst tool) to C● on C$_6$ chain** R: CH3CC (ACC0A/6) + BCR4 (ABB0A/20) P: BCR5 (ABB2B/26)	D + D S	−5.26	

RS57. Additive conversion of two-handled polyyne chain to polyacetylene chain [full cage models illustrated].

Step	Description of Reaction	Mult.	Ener. (eV)	Barr. (eV)
1	**Join GeRad handle to 3rd carbon atom in handled C6 polyyne chain** R: BCR1 (ABB0A/14) + GeH3 (ACC0A/4) P: BCR2 (ABB0B/18)	S + D D	−0.65	
2	**Hydrogenate C● on 4th C atom of C$_6$ chain w/HDon or HTrans tool** R: BCR2 (ABB0B/18) + HDon (ACC0A/26) P: Chain3run2 (ABB2A/19) + GeRad (ACC0A/25) R: BCR2 (ABB0B/18) + S15cis (ACCCA/11) P: Chain3run2 (ABB2A/19) + S16Run0 (ACCCA/10)	D + S S + D D + D S + S	−0.46 −1.28	
3	**Detach GeRad handle from third carbon atom in C$_6$ chain** R: Chain3run2 (ABB2A/19) P: Chain4 (ABB0C/15) + GeH3 (ACC0A/4)	S D + D	+2.91	
3B2	H steal from CH group adjacent to detachment site by departing GeRad R: Chain3run2 (ABB2A/19) P: BCR1 (ABB0A/14) + GeH4 (ACC0A/5)	S S + S	**+1.03** [a]	
4	**Hydrogenate C● on third carbon atom of C$_6$ chain using HDon tool** R: Chain4 (ABB0C/15) + HDon (ACC0A/26) P: Chain5 (ABB2A/16) + GeRad (ACC0A/25)	D + S S + D	−0.62	

[a] Given the geometric similarity to the HTrans tool, abstraction of the previously attached H atom is net exoergic by −1.88 eV; however, the pathology appears avoidable by positional control because the Ge atom of the departing GeRad handle lies 3.93 Å away from the target H atom, which is ≫1.56 Å, the equilibrium Ge-H bond distance.

REVIEW

RS58. Subtractive conversion of two-AdamRad-handled polyethylene chain to polyacetylene chain [full cage models illustrated].

Step	Description of Reaction	Mult.	Ener. (eV)	Barr. (eV)
1	**Join CH$_2$ • of 2 Meth tools to get handled (CH$_2$)$_2$ polyethylene chain**			
	R: CH3CH2 (ABB0A/7) + CH3CH2 (ABB0A/7)	D + D		
	P: ChainP1 (ABB0A/14)	S	−3.31	
1A	One Meth tool steals H from the other Meth tool			
	R: CH3CH2 (ACC0A/7) + CH3CH2 (ACC0A/7)	D + D		
	P: CH3CH3 (ACC0A/8) + CH3CHS (ACC0A/6)	S + S	+0.62	
	P: CH3CH3 (ACC0A/8) + CH3CHT (ACC0A/6)	S + T	+0.42	
2	**Abstract H from first carbon in chain using HAbst tool**			
	R: ChainP1 (ABB0A/14) + HAbst (ACC0A/27)	S + D		
	P: ChainP2 (ABB0A/13) + HAbstH (ACC0A/28)	D + S	−1.67	
3	**Abstract H from second carbon in chain using HAbst tool**			
	R: ChainP2 (ABB0A/13) + HAbst (ACC0A/27)	D + D		
	P: ChainP3S (ABB0A/12) + HAbstH (ACC0A/28)	S + S	−4.25	
	P: ChainP3T (ABB0A/12) + HAbstH (ACC0A/28)	T + S	**−1.62** [a]	
3D1	H migrates to radical site from adjacent CH• in chain leaving a -CH$_2$-C:-			
	R: ChainP3S (ABB0A/12)	S		
	P: ChainP3p1S (ABB2B/12)	S	+3.01	
	R: ChainP3T (ABB0A/12)	T		
	P: ChainP3p1T (ABB0A/12)	T	**+0.39** [a]	

[a] Reaction 3 triplet Product lies +2.63 eV above singlet Product in energy, hence is unlikely to occur; if the triplet does occur, it should rapidly transition downhill to the singlet via intersystem crossing, creating a two-handled -CH=CH- bonded polyacetylene chain.

studies of (6, 0) nanotube formation inside zeolites[196] and the (6, 0) nanotube is a popular structure for analytical studies.[197, 198] Sinnott et al.[199] have used atomistic simulations to model bonded interfaces between diamond C(111) surface planes and (6, 0) carbon nanotubes, and generalized rules for bonding nanotubes to C(111) and C(100) are described by Shenderova et al.[200, 201]—e.g., (n, 0) nanotubes with n = 6, 8, 10, 12, and 18 are readily mated to the C(111) surface, but nanotubes with n = 7, 9, 11, 13, and 15 are geometrically incompatible.[182]

The first course of a (6, 0) carbon nanotube (12 carbon atoms) is constructed perpendicular to a 3 × 3 cage array of an unreconstructed H-passivated diamond C(111)-H(1 × 1) surface, using the GM tool as a carbon source (RS65). The nanotube central axis geometrically intersects with, but is unbonded to, a central bridgehead C atom that may or may not be dehydrogenated prior to nanotube fabrication.

The new nanotube bonds to the diamond surface through 6 bridgehead carbon atoms in the C(111) surface lying closest to the unbonded central bridgehead C atom. These 6 carbon attachment atom sites, residing at the vertices of a hexagon, are individually dehydrogenated only immediately prior to mechanosynthesis to avoid Pandey reconstruction of the C(111) surface during the fabrication process.

After the first course of 12 carbon atom additions (and 12 hydrogen atom abstractions) has been completed, the nanotube is extended without process limit in the direction normal to the diamond surface in successive 12-carbon-atom courses by iterating reactions analogous to RS65. Subsequent courses after the first should have somewhat more favorable energetics, since bond strains are slightly lower due to greater distance from the small lattice mismatches between nanotube and diamond surface. Larger

RS59. Pull continuous polyacetylene chain from C_2H_2 gas precursor.

Step	Description of Reaction	Mult.	Ener. (eV)	Barr. (eV)
1	**Expose bridgehead Adam● monoradical to C_2H_2 gas, add CHCH●**			
	R: AdamRad (ACC0A/25) + C2H2 (ACC0A/4)	D + S		
	P: AdamC2H2 (ACC0A/29)	D	−0.89	
1D1	H migrates to radical site from adjacent CH in C=C chain			
	R: AdamC2H2 (ACC0A/29)	D		
	P: Poly2D (ACC0A/29)	D	−0.15	
	T: Poly2DTS (ACC1A/29)	D		+1.86
1D18	H migrates from radical site to adjacent CH in C=C chain			
	R: AdamC2H2 (ACC0A/29)	D		
	P: Poly1D (ACC0A/29)	D	+2.34	
	P: Poly1Q (ACC0A/29)	Q	+3.70	
1^1	**Expose bridgehead GeRad● monoradical to C_2H_2 gas, add CHCH●**			
	R: GeRad (ACC0A/25) + C2H2 (ACC0A/4)	D + S		
	P: GeRadC2H2run1 (ACC1A/29)	D	−0.55	
2	**Expose Adam CHCH● monoradical to C_2H_2 gas, add 2nd CHCH●**			
	R: AdamC2H2 (ACC0A/29) + C2H2 (ACC0A/4)	S + D		
	P: AdamCHCHCHCH (ACC0A/33)	D	−1.38	

diameter nanotubes have still smaller mismatch, thus even lower bond strains and still more favorable energetics for fabrication. On the other hand, nanotube structures are increasingly susceptible to mechanical and thermally-driven flexure and buckling as they are constructed at more extended lengths or at wider diameters. Adequate positional registration for mechanosynthesis may be maintained either by attaching temporary GeRad handles near the distal terminus to restrain flexure and vibrational freedom close to the nanotube growth site, or by lowering the operating temperature.

Note that (1) the ethylation of adjacent Adam sidewall sites, the propylation of adjacent Adam bridgehead and sidewall sites, or the substitution of 3-member chains in RS64, thus making 5-membered rings, plus (2) the butylation of adjacent Adam sidewall sites, amylation of adjacent Adam bridgehead and sidewall sites, or the substitution of 5-member chains in RS64, thus making 7-member rings, may allow the fabrication of graphene sheets containing any desired pattern of embedded convex or concave curvatures, including closed spheroids analogous to fullerenes.

An attempt to build $(6, 0)$ carbon nanotube via simple polyyne/cumulene chain deposition was unsuccessful because:

(1) the desired bonding of -C≡C- at a trimer position along the chain to a dehydrogenated nanotube "crown" radical site appears endoergic by +0.95 eV,

(2) the competing unwanted bonding of -C≡C- at a dimer position along the chain is exoergic by −0.43 eV (allowing the possibility that subsequent C insertion via carbene tool (GeRad-CH:) might work), and

(3) the second -C≡C- in the chain is not readily hydrogenated to -●C=CH- (which would create a positionally-controlled radical site more convenient for bonding to the nanotube radical site), a product structure virtually identical to HTrans, an H-donation tool.

9. FREQUENCY ANALYSIS OF TOOLS AND STRUCTURES

With one minor exception, all primary tools and handles have lowest-mode vibrational frequencies at the B3LYP/ 3-21G* level of theory exceeding 100 cm^{-1}: GM tool

RS60. Build two-handled polyethylene chain using GeRad handles [full cage models illustrated].

Step	Description of Reaction	Mult.	Ener. (eV)	Barr. (eV)
1	**Join CH$_2$• of two GM tools to get handled (CH$_2$)$_2$ polyethylene chain**			
	R: GeH3CH2 (ACC0A/7) + GeH3CH2 (ACC0A/7)	D + D		
	P: ChainPP1 (ACC0A/14)	S	−3.31	
1A	One GM tool steals H from the other GM tool, creating CH$_3$ and CH:			
	R: GeH3CH2 (ACC0A/7) + GeH3CH2 (ACC0A/7)	D + D		
	P: GeH3CH3 (ACC0A/8) + GeH3CHS (ACC0A/6)	S + S	+0.92	
	P: GeH3CH3 (ACC0A/8) + GeH3CHT (ACC0A/6)	S + T	+0.22	
	Proximity Continuation Reaction:			
	R: GeH3CH3 (ACC0A/8) + GeH3CHT (ACC0A/6)	S + T		
	P: ChainPP1 (ACC0A/14)	S	−3.53	
2	**Abstract H from distal carbon in chain using HAbst tool**			
	R: ChainPP1 (ACC0A/14) + HAbst (ACC0A/27)	S + D		
	P: ChainPP2 (ACC0A/13) + HAbstH (ACC0A/28)	D + S	−1.74	
3	**Join third GeRad tool to distal CH• radical site**			
	R: ChainPP2 (ACC0A/13) + GeH3CH2 (ACC0A/7)	D + D		
	P: ChainPP3 (ACC0A/20)	S	−2.92	
3A	H steal from third GeRad tool to workpiece CH• radical, yielding CH$_2$			
	R: ChainPP2 (ACC0A/13) + GeH3CH2 (ACC0A/7)	D + D		
	P: ChainPP1 (ACC0A/14) + GeH3CHS (ACC0A/6)	S + S	+1.22	
	P: ChainPP1 (ACC0A/14) + GeH3CHT (ACC0A/6)	S + T	+0.53	
3B1	H steal from workpiece CH• radical to third GeRad tool, yielding C:			
	R: ChainPP2 (ACC0A/13) + GeH3CH2 (ACC0A/7)	D + D		
	P: ChainPP3p1S (ACC0D/12) + GeH3CH3 (ACC0A/8)	S + S	+0.73	
	P: ChainPP3p1T (ACC1A/12) + GeH3CH3 (ACC0A/8)	T + S	**0.00**[a]	
	Proximity Continuation Reaction:			
	R: ChainPP3p1T (ACC1A/12) + GeH3CH3 (ACC0A/8)	T + S		
	P: ChainPP3 (ACC0A/20)	S	−2.92	
4	**Detach GeRad handle from second carbon (CH) in chain**			
	R: ChainPP3 (ACC0A/20)	S		
	P: ChainPP4 (ACC0A/16) + GeH3 (ACC0A/4)	D + D	+2.35	
5	**Hydrogenate CH• on second carbon in chain using HTrans tool**			
	R: ChainPP4 (ACC0A/16) + HDon (ACC0A/26)	D + S		
	P: ChainPP5 (ACC0A/17) + GeRad (ACC0A/25)	S + D	−0.32	
	R: ChainPP4 (ACC0A/16) + S15cis (ACC0A/11)	D + S		
	P: ChainPP5 (ACC0A/17) + S16Run0 (ACCCA/10)	S + D	−1.15	

[a] Although workpiece Product triplet lies −0.74 eV below workpiece Product singlet and thus is favored energetically, reaction Product and reaction Reactant are equiergic and should rapidly interconvert while workpiece and tool are held in proximity, allowing the desired and highly exoergic desired pathway eventually to be taken.

(20.0 cm^{-1}, methyl rotation; 142.6 cm^{-1}, methyl wag), HAbst (100.5 cm^{-1}, tip C wag), Meth tool (105.5 cm^{-1}, methyl rotation; 245.0 cm^{-1}, methyl wag), Germ tool (107.4 cm^{-1}, methyl rotation), HAbstH (141.4 cm^{-1}, tip H wag), DimerP (143.2 cm^{-1}, body), GeRad (184.1 cm^{-1}, body), HDon (186.5 cm^{-1}, body), AdamRad (305.1 cm^{-1}, body), and Adam (312.0 cm^{-1}, body). The relatively low resistance of the GM tool to methyl rotation should not affect placement accuracy or reaction reliability in DMS because the GM tool is used for carbon atom, not hydrogen atom, placement. However, some intermediate reaction structures and pathological structures have lowest

846

RS61. Build 1st ring to Adam sidewall and adjacent bridgehead using alternating dehydrogenations (least stable reaction order: forms aromatic bonds as slowly as possible).

Step 1	Step 2	Step 3	Step 4 …	

… Step 4	Step 5	Step 6	Step 7	Step 8	

Step	Description of Reaction	Mult.	Ener. (eV)	Barr. (eV)
1	**Abstract H from distal CH$_2$ in handled (CH$_2$)$_4$ chain w/HAbst**			
	R: GRAP1 (ACC0A/41) [RS32 Step2] + HAbst (ACC0A/27)	S + D		
	P: GRAP2 (ACC0A/40) + HAbstH (ACC0A/28)	D + S	−1.64	
1D1	H migrates to CH• radical from adjacent CH$_2$ group in chain			
	R: GRAP2 (ACC0A/40)	D		
	P: GRAP2p1 (ACC0A/40)	D	−0.13	
	T: GRAP2p1TS (ACC1A/40)	D		+1.56
2	**Abstract H from adjacent Adam bridgehead CH w/HAbst tool**			
	R: GRAP2 (CCC0A/40) + HAbst (CCC0A/27)	D + D		
	P: GRAP3S (CCC1A/39) + HAbstH (CCC0A/28)	S + S	−1.52	
	R: GRAP2 (ACC0A/40) + HAbst (ACC0A/27)	D + D		
	P: GRAP3T (ACC0A/39) + HAbstH (ACC0A/28)	T + S	−1.58	
2D1a	H migrates to bridgehead C• from proximal CH$_2$ group in chain			
	R: GRAP3S (CCC1A/39)	S		
	P: GRAP3p3SasTS (CCC1A/39)	S	+1.05	
	T: GRAP3p3STSrun2 (CCC2C/39)	S		+2.92
	R: GRAP3T (ACC0A/39)	T		
	P: GRAP3p3T (ACC2A/39)	T	−0.11	
	T: GRAP3p3TTS (ACC2A/39)	T		+1.97
2D1b	H migrates to bridgehead C• from second CH$_2$ group in chain			
	R: GRAP3S (CCC1A/39)	S		
	P: GRAP3p1SasTS (CCC1A/39)	S	+0.01	
	T: GRAP3p1STS (CCC1A/39)	S		+1.59
	R: GRAP3T (ACC0A/39)	T		
	P: GRAP3p1T (ACC1A/39)	T	−0.08	
	T: GRAP3p1TTS (ACC1A/39)	T		+1.02
2D1c	H migrates to bridgehead C• from third CH$_2$ group in chain			
	R: GRAP3S (CCC1A/39)	S		
	P: GRAP3p2S (CCC1B/39)	S	−2.46	
	T: GRAP3p2S-QST3run1 (CCC2C/39)	S		+1.48
	R: GRAP3T (ACC0A/39)	T		
	P: GRAP3p2T (ACC0A/39)	T	−0.13	
	T: GRAP3p2TTS (ACC1A/39)	T		+0.63

Continued

2D7	H migrates to bridgehead C● from chain attachment sidewall site			
	R: GRAP3S (CCC1A/39)	S		
	P: GRAP3p4S (CCC1A/39)	S	−0.15	
	T: GRAP3p4STS (CCC1A/39)	S		+3.73
	R: GRAP3T (ACC0A/39)	T		
	P: GRAP3p4T (ACC1A/39)	T	−0.16	
	T: GRAP3p4TTS (ACC2A/39)	T		+2.60
3	**Join terminal CH● group in chain to Adam bridgehead C●**			
	R: GRAP3S (CCC1A/39)	S		
	P: GRAP4 (CCC0A/39)	S	−3.16	
	R: GRAP3T (ACC0A/39)	T		
	P: GRAP4 (ACC0A/39)	S	−2.77	
3A	H steal from attached methylation tool to Adam bridgehead C●			
	R: GRAP3S (CCC1A/39)	S		
	P: GRAP4p1S (CCC0B/39)	S	+0.75	
	T: GRAP4p1STS (CCC2C/39)	S		+0.53
	R: GRAP3T (ACC0A/39)	T		
	P: GRAP4p1T (ACC1B/39)	T	+0.19	
	T: GRAP4p1TTS (ACC1A/39)	T		+0.55
4	**Abstract H from 2nd CH_2 in original chain using HAbst tool**			
	R: GRAP4 (ACC0A/39) + HAbst (ACC0A/27)	S + D		
	P: GRAP5 (ACC0B/38) + HAbstH (ACC0A/28)	D + S	−1.76	
4D15a	H migrates to CH● radical site from Adam sidewall CH in ring			
	R: GRAP5 (ACC0B/38)	D		
	P: GRAP5p2 (ACC0A/38)	D	−0.26	
	T: GRAP5p2-QST2 (ACC1A/38)	D		+1.74
4D15b	H migrates to CH● radical site from GeRad-joined CH group in ring			
	R: GRAP5 (ACC0B/38)	D		
	P: GRAP5p3run2 (ACC0A/38)	D	−0.25	
	T: GRAP5p3TSrun2 (ACC1A/38)	D		+1.52
4D16	H migrates to CH ● radical site from nearest CH_2 group in ring			
	R: GRAP5 (ACC0B/38)	D		
	P: GRAP5p1 (ACC0A/38)	D	−0.22	
	T: GRAP5p1TS (ACC1A/38)	D		+1.55
5	**Detach GeRad handle from workpiece, leaving CH● radical**			
	R: GRAP5 (ACC0B/38)	D		
	P: GRAP6SasTS (ACC1A/34) + GeH3 (ACC0A/4)	S + D	**+3.92**[a]	
	P: GRAP6T (ACC0A/34) + GeH3 (ACC0A/4)	T + D	+2.39	
5B1	H steal from workpiece by departing GeRad handle			
	R: GRAP5 (ACC0B/38)	D		
	P: GRAP6p1D (ACC0A/33) + GeH4 (ACC0A/5)	D + S	+3.16	
	P: GRAP6p1Q (ACC0A/33) + GeH4 (ACC0A/5)	Q + S	+3.30	
5D15	H migrates to CH● radical site from Adam sidewall CH in ring			
	R: GRAP6T (ACC0A/34)	T		
	P: GRAP6p3T (ACC0A/34)	T	+0.65	
	T: GRAP6p3TTS (ACC1A/34)	T		+2.63
5D16	H migrates to CH● radical site from nearest CH_2 group in ring			
	R: GRAP6T (ACC0A/34)	T		
	P: GRAP6p2T (ACC0A/34)	T	+0.29	
	T: GRAP6p2TTS (ACC1A/34)	T		+1.87
5H	Bridgehead-attached CH● group crossbonds with distal CH● group			
	R: GRAP5 (ACC0B/38)	D		
	P: GRAP6S (ACC0A/34) + GeH3 (ACC0A/4)	S + D	+0.41	
	T: GRAP6SasTS (ACC1A/34) + GeH3 (ACC0A/4)	S + D		+3.92
6	**Abstract H from ring-attached Adam sidewall CH w/HAbst tool**			
	R: GRAP6T (ACC0A/34) + HAbst (ACC0A/27)	T + D		
	P: GRAP7D (ACC0A/33) + HAbstH (ACC0A/28)	D + S	−1.81	
	P: GRAP7Q (ACC0A/33) + HAbstH (ACC0A/28)	Q + S	−1.81	
6D16a	H migrates to bridgehead-attached CH● from nearest ring CH_2			
	R: GRAP7D (ACC0A/33)	D		
	P: GRAP7p1DasTS (ACC1A/33)	D	−2.50	
	T: GRAP7p1DTS (ACC1A/33)	D		+0.45
	R: GRAP7Q (ACC0A/33)	Q		
	P: GRAP7p1Q (ACC0A/33)	Q	+0.19	

Continued

848

J. Comput. Theor. Nanosci. 5, 760–861, **2008**

	T: GRAP7p1QTS (ACC1A/33)	Q		+1.85
6D16b	H migrates to bridgehead-attached CH● from farthest ring CH$_2$			
	R: GRAP7D (ACC0A/33)	D		
	P: GRAP7p3D (ACC0A/33)	D	−3.24	
	T: GRAP7p3D-QST3 (ACC1A/33)	D		+0.55
	R: GRAP7Q (ACC0A/33)	Q		
	P: GRAP7p3Q (ACC0A/33)	Q	+0.45	
	T: GRAP7p3QTS (ACC1A/33)	Q		+2.29
6D16c	H migrates to distal CH● from distal ring CH$_2$			
	R: GRAP7D (ACC0A/33)	D		
	P: GRAP7p4D (ACC0A/33)	D	−2.61	
	T: GRAP7p4DTSrun3 (ABB1A/33)	D		+0.41
	R: GRAP7Q (ACC0A/33)	Q		
	P: GRAP7p4Q (ACC0A/33)	Q	+0.24	
	T: GRAP7p4QTS (ACC1A/33)	Q		+1.94
6D16d	H migrates to distal CH● from sidewall-attached CH$_2$			
	R: GRAP7D (ACC0A/33)	D		
	P: GRAP7p5D (ACC0A/33)	D	−2.63	
	T: GRAP7p5DTS (ACC2C/33)	D		+0.50
	R: GRAP7Q (ACC0A/33)	Q		
	P: GRAP7p5Q (ACC0A/33)	Q	+0.35	
	T: GRAP7p5QTS (ACC1A/33)	Q		+1.98
6D16e	H migrates to sidewall C● from sidewall-attached CH$_2$			
	R: GRAP7D (ACC0A/33)	D		
	P: GRAP7p7D (ACC0A/33)	D	−2.48	
	T: GRAP7p7DTS (ACC1A/33)	D		+0.52
	R: GRAP7Q (ACC0A/33)	Q		
	P: GRAP7p7Q (ACC0A/33)	Q	+0.29	
	T: GRAP7p7QTS (ACC1A/33)	Q		+1.81
6D17a	H migrates to bridgehead-attached CH● from distal ring CH●			
	R: GRAP7D (ACC0A/33)	D		
	P: GRAP7p2D (ACC0A/33)	D	+0.28	
	T: GRAP7p2DTSrun2 (ACC1A/33)	D		+0.72
	R: GRAP7Q (ACC0A/33)	Q		
	P: GRAP7p2Q (ACC0A/33)	Q	+0.52	
	T: GRAP7p2QTS (ACC1A/33)	Q		+2.45
6D17b	H migrates to sidewall C● from bridgehead-attached ring CH●			
	R: GRAP7D (ACC0A/33)	D		
	P: GRAP7p6DasTS (ACC1A/33)	D	+0.51	
	T: GRAP7p6DTS (ACC1A/33)	D		+1.78
	R: GRAP7Q (ACC0A/33)	Q		
	P: GRAP7p6Q (ACC0A/33)	Q	+0.60	
	T: GRAP7p6QTS (ACC1A/33)	Q		+2.74
6Ha	Bridgehead-attached CH● group crossbonds with distal CH●			
	R: GRAP7D (ACC0A/33)	D		
	P: GRAP7p8D (ACC0A/33)	D	−2.07	
	T: GRAP7p8D-QST3run2 (ABB1D/33)	D		+0.55
	R: GRAP7Q (ACC0A/33)	Q		
	P: GRAP7p8D (ACC0A/33)	D	−2.06	
	T: GRAP7p8D-QST3run2 (ABB1D/33) [after ISC]	D		+0.55
6Hb	Bridgehead-attached CH● group crossbonds with sidewall C●			
	R: GRAP7D (ACC0A/33)	D		
	P: GRAP7p9Drun2 (ACC0A/33)	D	−0.43	
	T: GRAP7p9D-QST2 (ACC1A/33)	D		**+0.36** [b]
	T: GRAP7p9D-QST3 (ABB1A/33)	D		**+0.29** [b]
6Hc	Distal CH● group crossbonds with sidewall C●			
	R: GRAP7D (ACC0A/33)	D		
	P: GRAP7p10D (ACC0A/33)	D	−1.96	
	T: GRAP7p10D-QST3run3 (ABB1D/33)	D		+0.41
7	**Abstract H from 3rd CH$_2$ in original chain using HAbst tool**			
	R: GRAP7D (ACC0A/33) + HAbst (ACC0A/27)	D + D		
	P: GRAP8SasTS (ACC1A/32) + HAbstH (ACC0A/28)	S + S	**−3.89** [c]	
	P: GRAP8T (ACC0A/32) + HAbstH (ACC0A/28)	T + S	−4.96	

Continued

7D16	H migrates to CH● group from nearest ring CH$_2$			
	R: GRAP8T (ACC0A/32)	T		
	P: GRAP8p2T (ACC0A/32)	T	+0.96	
	T: GRAP8p2TTS (ACC1A/32)	T		+2.23
7D17	H migrates to CH● radical site from nearest ring CH●			
	R: GRAP8T (ACC0A/32)	T		
	P: GRAP8p1T (ACC0A/32)	T	+3.50	
	T: GRAP8p1TTS (ACC1A/32)	T		+3.51
8	**Abstract H from distal ring CH$_2$ using HAbst tool**			
	R: GRAP8T (ACC0A/32) + HAbst (ACC0A/27)	T + D		
	P: GRAP9D (ACC0A/31) + HAbstH (ACC0A/28)	D + S	−4.69	
	P: GRAP9Q (ACC2A/31) + HAbstH (ACC0A/28)	Q + S	**−1.10**[d]	
8D16	H migrates to sidewall C● from sidewall-attached ring CH●			
	R: GRAP9D (ACC0A/31)	D		
	P: GRAP9p2D (ACC0A/31)	D	+1.76	
	T: GRAP9p2DTS (ACC1A/31)	D		+3.29
8D17	H migrates to one distal CH● radical from other distal ring CH●			
	R: GRAP9D (ACC0A/31)	D		
	P: GRAP9p1D (ACC0A/31)	D	+1.57	
	T: GRAP9p1DTS (ACC1A/31)	D		+3.65

[a] The transition structure leading to an unwanted singlet state with two crossbonded CH● groups (see pathology 5H) lies +1.53 eV above the triplet structure, constituting an effective barrier to the singlet path, hence only the noncrossbonded triplet path will be taken.

[b] The barrier preventing this crossbonding pathology appears sufficient at 80 K but only marginal at 300 K; however, the crossbonding atoms are initially 2.51 Å apart (~1.6 C-C bondlengths) and this large distance combined with the large stiffness of the molecular ring structure should prevent these groups from coming into reactive range.

[c] The transition structure leading to an unwanted singlet state with two crossbonded CH● groups lies +1.07 eV above the triplet structure, constituting an effective barrier to the singlet path, hence only the noncrossbonded triplet path will be taken.

[d] Quartet Product lies +3.59 eV above doublet Product in energy, hence is unlikely to occur; if the quartet does occur, it should rapidly transition downhill to the doublet via intersystem crossing.

normal modes <100 cm^{-1}, so further analysis is required to assess (1) the possible loss of reaction reliability due to slightly increased positional uncertainty in these cases, and (2) the ability to regain reliability in these cases by lowering operating temperature, which reduces positional uncertainty.

10. CONCLUSIONS

We have proposed a minimal toolset for positionally controlled diamond mechanosynthesis consisting of nine primary, auxiliary, and compound tooltypes that together can achieve 100% process closure in building the three principal low-index diamond surfaces. A complete set of reaction steps is explicitly specified for the first time. The toolset employs only three element types (C, Ge, and H) and only four feedstock molecules—CH$_4$ and C$_2$H$_2$ as carbon sources, Ge$_2$H$_6$ as the germanium source, and H$_2$ as a hydrogen source. With these simple bulk-produced chemical inputs, the present work shows that the 9-tooltype toolset can use 65 reaction sequences to:
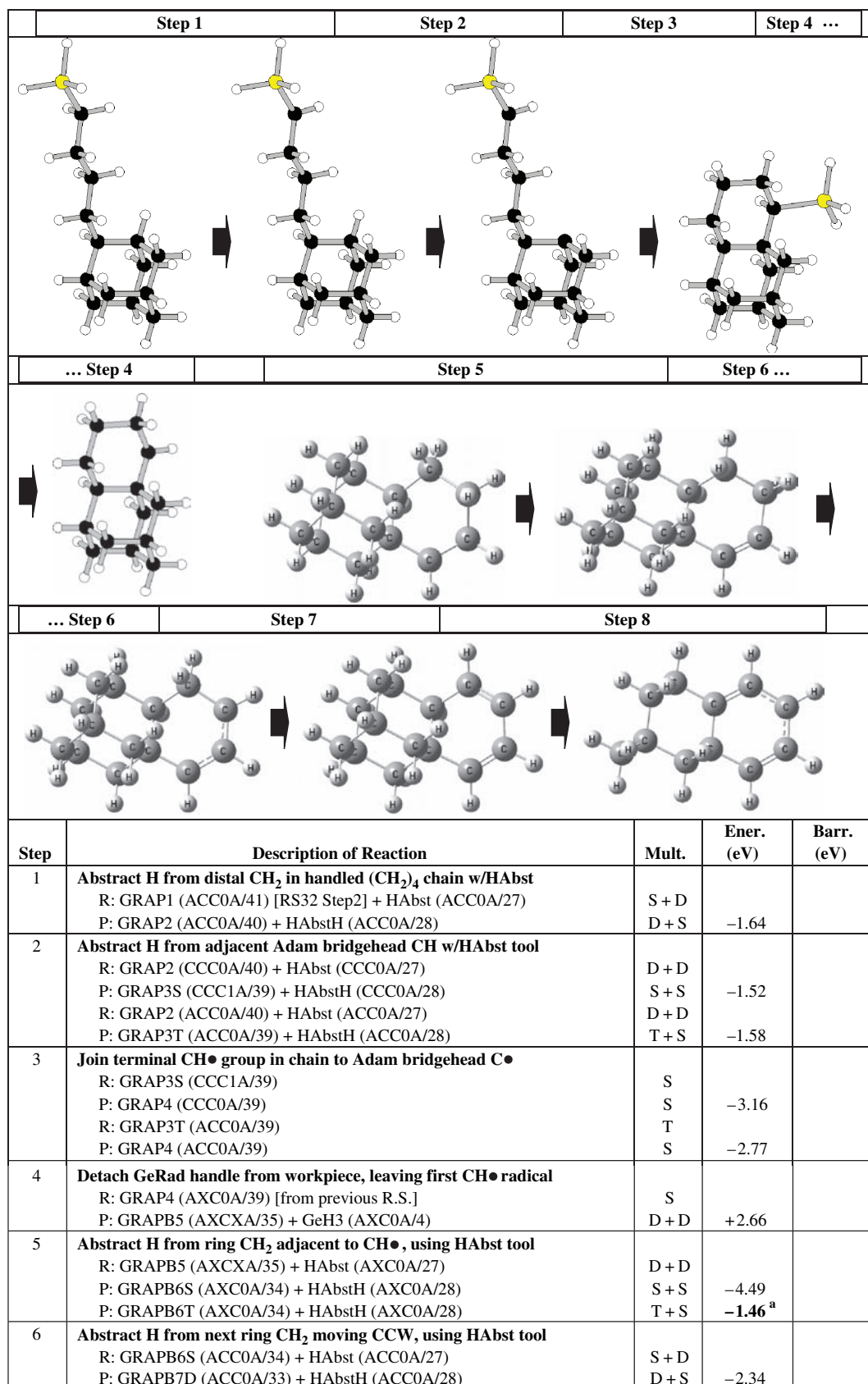(1) fabricate all nine tooltypes, including their adamantane handle structures, starting from flat diamond surface;
(2) recharge all nine tooltypes; and

(3) build molecularly-precise cubic diamond C(111)/C(110)/C(100) and hexagonal diamond surfaces, both clean and hydrogenated and including some Ge-substituted variants, methylated and ethylated surface structures, polyyne, polyacetylene and polyethylene chains of process-unlimited length, and both flat graphene sheet and curved graphene nanotubes.

Useful mechanosynthetic operations and insights identified in the present work include:
(1) the use of a radical tool as a reversible mechanical bonding tool or handle to permit kinematic manipulation of intermediate workpieces (e.g., RS6, RS33–RS36);
(2) the ability to perform a "handle exchange" operation for a tool handle bonded to a particular atom (e.g., RS6, RS8, RS10, RS11, RS16, RS41), including chain shortening operations as in "subtractive handle exchange" (Section 8.3.1);
(3) the use of chain dehandling operations (e.g., Section 8.3.1);
(4) the use of bond angle bending during a reaction to influence reaction energetics (e.g., Fig. 2, Section 3.5, RS5, RS41);
(5) the use of geometry-isomeric tool configurations (e.g., cis/trans: Table I, RS33, RS35; chair/boat: RS33, RS34) to influence reaction energetics;

RS62. Build 1st ring to Adam sidewall and adjacent bridgehead using sequential dehydrogenations (most stable reaction order: forms aromatic bonds as quickly as possible).

Step	Description of Reaction	Mult.	Ener. (eV)	Barr. (eV)
1	**Abstract H from distal CH₂ in handled (CH₂)₄ chain w/HAbst**			
	R: GRAP1 (ACC0A/41) [RS32 Step2] + HAbst (ACC0A/27)	S + D		
	P: GRAP2 (ACC0A/40) + HAbstH (ACC0A/28)	D + S	−1.64	
2	**Abstract H from adjacent Adam bridgehead CH w/HAbst tool**			
	R: GRAP2 (CCC0A/40) + HAbst (CCC0A/27)	D + D		
	P: GRAP3S (CCC1A/39) + HAbstH (CCC0A/28)	S + S	−1.52	
	R: GRAP2 (ACC0A/40) + HAbst (ACC0A/27)	D + D		
	P: GRAP3T (ACC0A/39) + HAbstH (ACC0A/28)	T + S	−1.58	
3	**Join terminal CH● group in chain to Adam bridgehead C●**			
	R: GRAP3S (CCC1A/39)	S		
	P: GRAP4 (CCC0A/39)	S	−3.16	
	R: GRAP3T (ACC0A/39)	T		
	P: GRAP4 (ACC0A/39)	S	−2.77	
4	**Detach GeRad handle from workpiece, leaving first CH● radical**			
	R: GRAP4 (AXC0A/39) [from previous R.S.]	S		
	P: GRAPB5 (AXCXA/35) + GeH3 (AXC0A/4)	D + D	+2.66	
5	**Abstract H from ring CH₂ adjacent to CH●, using HAbst tool**			
	R: GRAPB5 (AXCXA/35) + HAbst (AXC0A/27)	D + D		
	P: GRAPB6S (AXC0A/34) + HAbstH (AXC0A/28)	S + S	−4.49	
	P: GRAPB6T (AXC0A/34) + HAbstH (AXC0A/28)	T + S	**−1.46** [a]	
6	**Abstract H from next ring CH₂ moving CCW, using HAbst tool**			
	R: GRAPB6S (ACC0A/34) + HAbst (ACC0A/27)	S + D		
	P: GRAPB7D (ACC0A/33) + HAbstH (ACC0A/28)	D + S	−2.34	

	P: GRAPB7Q (ACC0A/33) + HAbstH (ACC0A/28)	Q + S	+1.35	
6H	Bridgehead-attached CH● group crossbonds with distal CH●			
	R: GRAPB7D (ACC0A/33)	D		
	P: GRAPB7p1D (ACC0A/33)	D	+1.90	
7	**Abstract H from next ring CH$_2$ moving CCW, using HAbst tool**			
	R: GRAPB7D (ACC0A/33) + HAbst (ACC0A/27)	D + D		
	P: GRAPB8S (ACC0A/32) + HAbstH (ACC0A/28)	S + S	−3.66	
	R: GRAPB7Q (ACC0A/33) + HAbst (ACC0A/27)	Q + D		
	P: GRAPB8T (ACC0A/32) + HAbstH (ACC0A/28)	T + S	**−5.29**[b]	
7Ha	Bridgehead-attached CH● in ring crossbonds with distal CH● in ring			
	R: GRAPB8S (ACC0A/32)	S		
	T: GRAPB8p1SasTS (ACC1D/32)	S		+4.57
	R: GRAPB8T (ACC0A/32)	T		
	P: GRAPB8p1T (ACC0A/32)	T	+1.59	
7Hb	Bridgehead-attached CH● crossbonds with sidewall-attached CH●			
	R: GRAPB8S (ACC0A/32)	S		
	T: GRAPB8p2SasTS (ACC1A/32)	S		+5.34
	R: GRAPB8T (ACC0A/32)	T		
	T: GRAPB8p2TasTS (ACC2D/32)	T		+5.87
7Hc	Distal CH● crossbonds in ring with sidewall-attached CH● in ring			
	R: GRAPB8S (ACC0A/32)	S		
	T: GRAPB8p3SasTS (ACC1D/32)	S		+4.51
	R: GRAPB8T (ACC0A/32)	T		
	P: GRAPB8p3T (ACC0B/32)	T	+1.69	
8	**Abstract H from sidewall CH, moving CCW, using HAbst tool**			
	R: GRAPB8S (ACC0A/32) + HAbst (ACC0A/27)	S + D		
	P: GRAP9D (ACC0A/31) + HAbstH (ACC0A/28)	D + S	−2.85	
	P: GRAP9Q (ACC2A/31) + HAbstH (ACC0A/28)	Q + S	**−1.31**[c]	

[a] Triplet Product lies +3.03 eV above singlet Product in energy, hence is unlikely to occur; if the triplet does occur, it should rapidly transition downhill to the singlet via intersystem crossing.

[b] Quartet Reactant and triplet Product lie +3.68 eV/+2.05 eV above doublet Reactant and singlet Product in energy, respectively, hence the Q/T reaction is unlikely to occur; if either does occur, it should rapidly transition downhill to the lower (D/S) spin multiplicity via intersystem crossing.

[c] Quartet Product lies +3.59 eV above doublet Product in energy, hence is unlikely to occur; if the quartet does occur, it should rapidly transition downhill to the doublet via intersystem crossing.

(6) the use of one or two handles on one or both sides of a bond to precisely control the site of bond breakage (e.g., RS6, RS54, Section 3.5);

(7) the overcoming of reaction barriers temporarily created by the formation of low-energy reaction intermediates or pathologies, using positional control to maintain tooltip proximity and to apply additional mechanical force to effectuate a desired exoergic reaction (e.g., RS16, RS35, RS36, RS42, RS44, RS60, RS63);

(8) the use of a radical tool as a bond strength modulator (e.g., RS5);

(9) the use of positionally controlled divalent radicals as relatively stable reaction intermediates (e.g., RS11, RS33, RS35, RS36, RS42);

(10) employing dehydrogenated radical-rich surfaces (e.g., germanium) for positionally constrained feedstock molecule acquisition, obviating the need for engineered binding sites (e.g., RS37, RS40, RS42);

(11) a "transfer of uncertainty" operation, in which a donation tool is presented in turn to two possible radical sites, one of which arises from a pathological H migration, definitely ensuring hydrogenation at both sites; any

uncertainty in the subsequent state of the donation tool is eliminated by contacting the donation tool to a known radical site on the H dump (e.g., RS16, RS28);

(12) a "two-stroke" operation, in which two tools in unknown states are applied to a workpiece in sequence, yielding the desired result while placing the two tools in known states (e.g., Section 7.3);

(13) the passivation of positionally controlled divalent radicals without a positionally controlled hydrogen donation tool, using positionally unconstrained high-purity bulk hydrogen gas (e.g., RS35, RS42, RS47, RS48), or more broadly, the combination of positionally constrained and unconstrained techniques in a single process to achieve molecularly precise nanofabrication;

(14) the performance of methylation operations (RS7–RS32) using either the Meth tool or the GM tool, the former requiring more reaction steps to use the tool, the latter requiring more reaction steps to fabricate the tool;

(15) adding C atoms two at a time (e.g., via DimerP tool; RS4) rather than one at a time (e.g., via Meth tool; RS15 + RS28), roughly halving the number of required reaction steps per added C atom; and

852

J. Comput. Theor. Nanosci. 5, 760–861, 2008

RS63.   Build GeRad-handled $(CH_2)_4$ chain on Adambenzene.

Step 1	Step 2	Step 3	Step 4	Step 5	Step 6	Step 7	Step 8	

Step	Description of Reaction	Mult.	Ener. (eV)	Barr. (eV)
1	**Abstract H from distal CH on first ring using HAbst tool**			
	R: GRAP9D (ACC0A/31) + HAbst (ACC0A/27)	D + D		
	P: GRAPA2S (ACC1A/30) + HAbstH (ACC0A/28)	S + S	−0.89	
	P: GRAPA2T (ACC0A/30) + HAbstH (ACC0A/28)	T + S	−1.03	
2	**Join GM tool to distal C• site on first ring; 1st methyl added**			
	R: GRAPA2S (ACC1A/30) + GM tool cluster (ACC0A/7)	S + D		
	P: GRAPA2A (ACC0A/37)	D	−4.16	
	R: GRAPA2T (ACC1A/30) + GM tool cluster (ACC0A/7)	T + S		
	P: GRAPA2A (ACC0A/37)	D	−4.02	
2A	H steal from GM tool to C• radical site on first ring			
	R: GRAPA2S (ACC1A/30) + GM tool (ACC0A/28)	S + D		
	P: GRAP9D (ACC0A/31) + GMA5HS (ABB0A/27)	D + S	**+0.32**[a]	
	R: GRAPA2S (ACC1A/30) + GM tool cluster (ACC0A/7)	S + D		
	T: GRAPA2Ap2DTS (ACC3C/37)	D		**+0.17**[a]
	Proximity Continuation Reaction:			
	R: GRAP9D (ACC0A/31) + GeH3CHS (ACC0A/6)	D + S		
	P: GRAPA2A (ACC0A/37)	D	−4.53	
	T: GRAPA2Ap2DTS (ACC3C/37)	D		−0.20
	R: GRAPA2T (ACC1A/30) + GM tool (ACC0A/28)	T + D		
	P: GRAP9D (ACC0A/31) + GMA5HT (ACC0A/27)	D + T	−0.24	
	R: GRAPA2T (ACC1A/30) + GM tool cluster (ACC0A/7)	S + D		
	T: GRAPA2Ap2QTS (ACC1A/37)	Q		**+0.22**[b]
	Proximity Continuation Reaction:			
	R: GRAP9D (ACC0A/31) + GeH3CHT (ACC0A/6)	D + T		
	P: GRAPA2A (ACC0A/37)	D	−3.83	
	T: GRAPA2Ap2QTS (ACC1A/37)	Q		+0.40
2B2	H steal to GM tool from first-ring CH adjacent to C•			
	R: GRAPA2S (ACC1A/30) + GM tool (ACC0A/28)	S + D		
	P: GRAPA2Ap1D (ACC0A/29) + GMACH3 (ACC0A/29)	D + S	−0.19	
	R: GRAPA2S (ACC1A/30) + GM tool cluster (ACC0A/7)	S + D		
	T: GRAPA2Ap1TS (ACC2C/37)	D		+0.46
	R: GRAPA2T (ACC1A/30) + GM tool (ACC0A/28)	T + D		
	P: GRAPA2Ap1Q (ACC0A/29) + GMACH3 (ACC0A/29)	Q + S	+0.70	
3	**Detach GeRad handle from workpiece**			
	R: GRAPA2A (ACC0A/37)	D		
	P: GRAPA2BS (ACC0A/33) + GeH3 (ACC0A/4)	S + D	+1.01	
	P: GRAPA2BT (ACC0A/33) + GeH3 (ACC0A/4)	T + D	**+3.05**[c]	
3B1	H steal from CH_2 group on workpiece by departing GeRad handle			
	R: GRAPA2A (ACC0A/37)	D		
	P: GRAPA2Bp1D (ACC0A/32) + GeH4 (ACC0A/5)	D + S	+2.19	
	P: GRAPA2Bp1Q (ACC0A/32) + GeH4 (ACC0A/5)	Q + S	+4.29	
3D15	H migrates to CH_2• radical site from nearest CH group in ring			
	R: GRAPA2BS (ACC0A/33)	S		
	P: GRAPA2Bp3S (ACC0A/33)	S	+2.12	
	T: GRAPA2Bp3STS (ACC1A/33)	S		+3.73
3H	CH_2• radical site crossbonds to adjacent CH site on first ring			
	R: GRAPA2BS (ACC0A/33)	S		
	T: GRAPA2Bp2SasTS (ACC1A/33)	S		+4.65
4	**Join GM tool to apical CH_2• site on chain; 2nd methyl added**			
	R: GRAPA2BS (ACC0A/33) + GM tool cluster (ACC0A/7)	S + D		
	P: GRAPA2C (ACC0A/40)	D	−1.35	

Continued

	R: GRAPA2BT (ACC0A/33) + GM tool cluster (ACC0A/7)	T + D		
	P: GRAPA2C (ACC0A/40)	D	−3.39	
5	**Detach GeRad handle from workpiece**			
	R: GRAPA2C (ACC0A/40)	D		
	P: GRAPA2DSasTS (ACC1A/36) + GeH3 (ACC0A/4)	S + D	+3.66	
	P: GRAPA2DT (ACC2A/36) + GeH3 (ACC0A/4)	T + D	+2.95	
6	**Join GM tool to apical CH₂• site on chain; 3rd methyl added**			
	R: GRAPA2DSasTS (ACC1A/36) + GM tool cluster (ACC0A/7)	S + D		
	P: GRAPA2E (ACC0A/43)	D	−4.09	
	R: GRAPA2DT (ACC2A/36) + GM tool cluster (ACC0A/7)	T + D		
	P: GRAPA2E (ACC0A/43)	D	−3.38	
7	**Detach GeRad handle from workpiece**			
	R: GRAPA2E (ACC0A/43)	D		
	P: GRAPA2FSasTS (ACC1A/39) + GeH3 (ACC0A/4)	S + D	+4.10	
	P: GRAPA2FT (ACC0A/39) + GeH3 (ACC0A/4)	T + D	+2.93	
8	**Join GM tool to apical CH₂• site on chain; 4th methyl added**			
	R: GRAPA2FSasTS (ACC1A/39) + GM tool cluster (ACC0A/7)	S + D		
	P: GRAPA3D (ACC0A/46)	D	−4.44	
	R: GRAPA2FT (ACC0A/39) + GM tool cluster (ACC0A/7)	T + D		
	P: GRAPA3D (ACC0A/46)	D	−3.27	

[a] Pathology 2A singlet has insufficient endoergicity and barrier height to guarantee blockage, but continuing to hold the Products in proximity allows barrierless consummation of the original reaction.

[b] Pathology 2A triplet has insufficient barrier height to guarantee blockage, but continuing to hold the Products in proximity allows consummation of the original reaction by application of mechanical force sufficient to overcome the +0.40 eV barrier.

[c] Triplet Product lies +2.04 eV above singlet Product in energy, hence is unlikely to occur; if the triplet does occur, it should rapidly transition downhill to the singlet via intersystem crossing.

(16) avoiding reaction intermediates that can lead to an "ethenylation pathology," in which an H migration to an adjacent radical site moves two radical sites into juxtaposition, allowing an energy-favored C=C bond to form. An ethenylation pathology may occur due to tooltip-mediated chain dehydrogenations near or adjacent to in-chain radical sites (Section 5.4), or due to gross mispositioning of reactive tooltips (e.g., RS7–RS10, RS13–RS15, RS25). In some cases a potentially ethenyl (C=C) structure may remain diradical (•C-C•) as suggested by Fort[202] in the case of adamantene.

Future work should:
(1) replicate the results of the present work to confirm all reaction details;
(2) examine details of specific tool trajectories;
(3) establish that all changes in tool-workpiece angles, shifts between two or more multitool isomeric configurations, rotations and translations of existing deployed tools to accommodate an arriving or departing tool, and other exogenous sources of bond strain occurring during each mechanosynthetic step will allow reaction exoergicities and barrier heights to remain near energy minima or at least within acceptable ranges;
(4) examine the possible role of surface-layer reconstructions of intermediate nanoscale structures and the resulting restrictions on fabrication sequences, if any; and
(5) map the working envelope of reliable tool placement during each mechanosynthetic operation as constrained by tool-workpiece vibrational modes, tool-workpiece positional uncertainties, and the presence of reactive radical sites on neighboring or intermediate structures.

While the minimal toolset described here should be able to fabricate regular diamondoid crystalline nanostructures, several specialized diamondoid structures are more challenging and will require further study to successfully construct, including:

(1) *Concave structures*. Highly concave structures, such as inside corners or cavities inside blocks, might be difficult for tools in the existing minimal toolset to reach due to steric constraints. However, it may be possible to build most such structures by judicious design of the assembly sequence, with fabrication proceeding in successive planar layers to incorporate concavities and other necessary inclusions while avoiding the premature creation of sterically inaccessible locations. Also, the proposed minimal toolset is sufficiently versatile to fabricate additional tools, including specialized asymmetrical tool structures that could afford access to otherwise inaccessible geometries or processes, and in principle also a wider toolset capable of manipulating atoms other than C/Ge/H.

(2) *Thin-walled structures*. In the limit of highly cribriform, foamy, or fenestrated zeolite-like diamondoid structures, it may be difficult to apply the necessary forces without disrupting the thin walls (perhaps 1–2 atomic layers thick) of neighboring cells. Such thin-walled structures
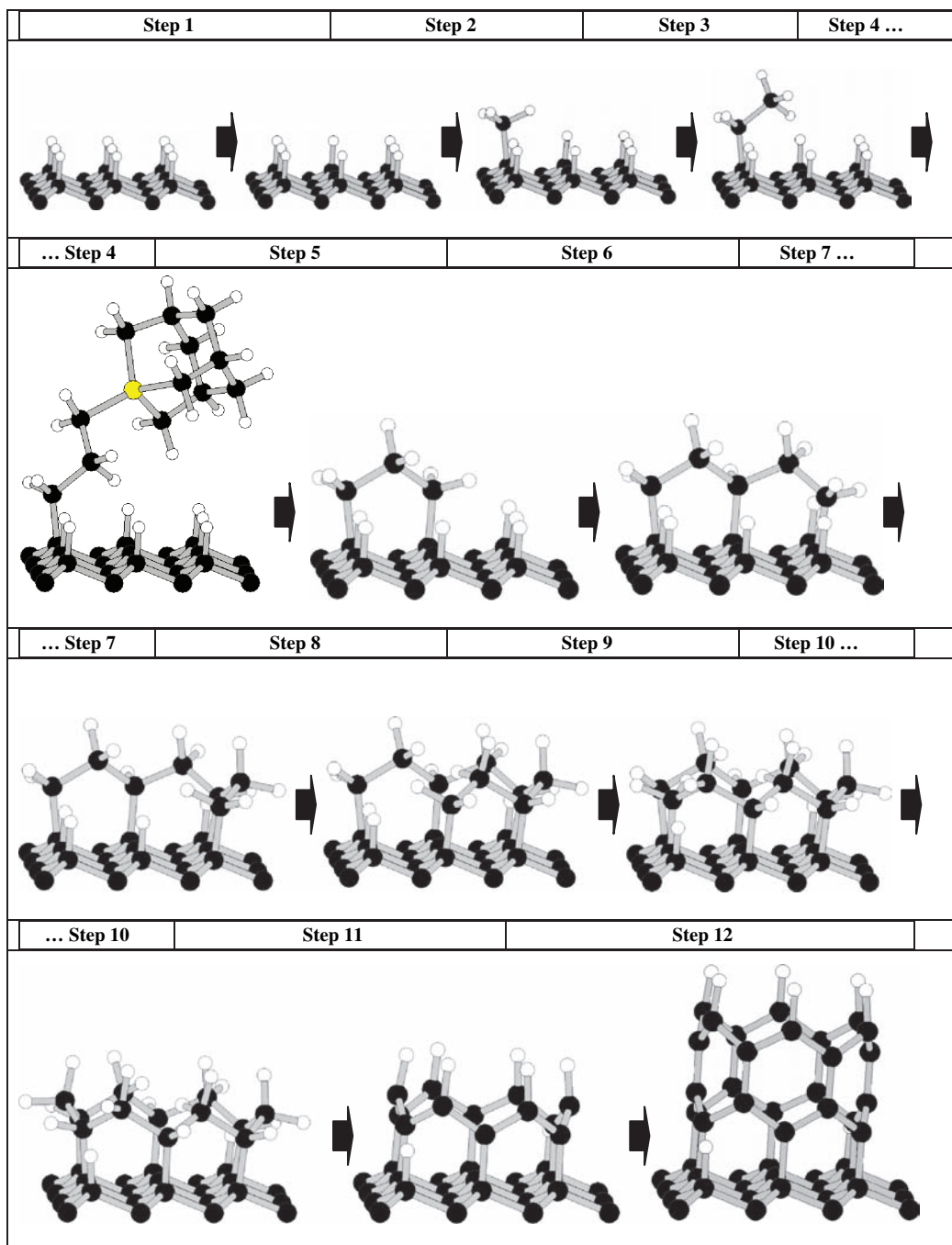
RS64.   Build 2nd ring attached to the Adambenzene 1st ring.

Step	Description of Reaction	Mult.	Ener. (eV)	Barr. (eV)
1	**Abstract H from distal CH$_2$ in handled (CH$_2$)$_4$ chain w/HAbst**			
	R: GRAPA3D (CCC0A/46) + HAbst (CCC0A/27)	D + D		
	P: GRAPA4SasTS (CCC1A/45) + HAbstH (CCC0A/28)	S + S	−1.54	
	R: GRAPA3D (ACC0A/46) + HAbst (ACC0A/27)	D + D		
	P: GRAPA4T (ACC0A/45) + HAbstH (ACC0A/28)	T + S	−1.66	
2	**Abstract H from adjacent distal first-ring CH w/HAbst tool**			
	R: GRAPA4SasTS (CCC1A/45) + HAbst (CCC0A/27)	S + D		
	P: GRAPA5Drun3 (CBB1A/44) + HAbstH (CCC0A/28)	D + S	−1.29	
	R: GRAPA4T (ACC0A/45) + HAbst (ACC0A/27)	T + D		
	P: GRAPA5Q (ACC0A/44) + HAbstH (ACC0A/28)	Q + S	−1.07	
3	**Join terminal CH● group in chain to distal first-ring C● group**			
	R: GRAPA5Drun2 (ABB1A/44)	D		
	P: GRAPA6D (ACC0A/44)	D	−3.37	
	R: GRAPA5Q (ACC0A/44)	Q		
	P: GRAPA6D (ACC0A/44)	D	−3.75	
4	**Detach GeRad handle from workpiece, leaving first CH● radical**			
	R: GRAPA6D (ACC0A/44)	D		
	P: GRAPA7S (ACC0A/40) + GeH3 (ACC0A/4)	S + D	+3.05	
	P: GRAPA7T (ACC0B/40) + GeH3 (ACC0A/4)	T + D	+2.05	
5	**Abstract H from CCW neighbor ring CH$_2$ using HAbst tool**			
	R: GRAPA7S (ACC0A/40) + HAbst (ACC0A/27)	S + D		
	P: GRAPA7AD (ACC0A/39) + HAbstH (ACC0A/28)	D + S	−4.78	
	R: GRAPA7T (ACC0B/40) + HAbst (ACC0A/27)	T + D		

	P: GRAPA7AD (ACC0A/39) + HAbstH (ACC0A/28)	D + S	−3.78
	P: GRAPA7AQ (ACC0A/39) + HAbstH (ACC0A/28)	Q + S	−1.39
6	**Abstract H from next CCW neighbor ring CH$_2$ using HAbst tool**		
	R: GRAPA7AD (ACC0A/39) + HAbst (ACC0A/27)	D + D	
	P: GRAPA9S (ACC0A/38) + HAbstH (ACC0A/28)	S + S	−1.80
	P: GRAPA9T (ACC0A/38) + HAbstH (ACC0A/28)	T + S	−2.59
7	**Abstract H from last CCW neighbor ring CH$_2$ using HAbst tool**		
	R: GRAPA9S (ACC0A/38) + HAbst (ACC0A/27)	S + D	
	P: GRAPA10Drun2 (ABB0A/37) + HAbstH (ACC0A/28)	D + S	−5.32
	R: GRAPA9T (ACC0A/38) + HAbst (ACC0A/27)	T + D	
	P: GRAPA10Drun2 (ABB0A/37) + HAbstH (ACC0A/28)	D + S	−4.53

RS65. Add first course of a $(6, 0)$ carbon nanotube to a 3×3 cage section of flat unreconstructed H-passivated diamond C(111) surface.

Continued

856

J. Comput. Theor. Nanosci. 5, 760–861, **2008**

Step	Description of Reaction	Mult.	Ener. (eV)	Barr. (eV)
1	Abstract H from C111 surface at center of ringbuilding site (RS1)			
2	Add 1st CH_3 to C111 bridgehead at 1st ringbuilding site using GM tool (RS12)			
3	Add 2nd CH_3 in methyl chain (RS20)			
4	Add 3rd CH_3 in methyl chain, leaving GeRad handle attached (Steps 1–2 of RS20)			
5	Attach $-CH_2-CH_2-CH_2-$ chain to adjacent C(111) bridgehead at 2nd ringbuilding site (Steps 1–4 of RS62); detachment of GeRad handle creates radical site needed for next reaction step			
6A	Methylate sidewall site of ring using GM tool (Steps 2–4 of RS7)			
6B	Methylate next adjacent C(111) bridgehead at 3rd ringbuilding site (RS23)			
6C	Ethylate two methyls via CH_3 dehydrogenation (Steps 3–4 of RS45 or RS49)			
7	Add $-CH_2-CH_2-$ between bridgehead-attached methyl and adjacent bridgehead C atom on 4th ringbuilding site on diamond C(111) surface (repeat Steps 6A+6B+6C)			
8	Add $-CH_2-CH_2-$ between bridgehead-attached methyl and adjacent bridgehead C atom on 5th ringbuilding site on diamond C(111) surface (repeat Steps 6A+6B+6C)			
9	Add $-CH_2-CH_2-$ between bridgehead-attached methyl and adjacent bridgehead C atom on 6th ringbuilding site on diamond C(111) surface (repeat Steps 6A+6B+6C)			
10	Add $-CH_2-$ to close the nanotube course (RS34)			
11	Abstract 12 H atoms alternating between CH and CH_2 groups moving CCW around the nanotube course, yielding 6 terminating CH groups atop 6 linked aromatic rings, requiring six applications of: RS1 (to de-H a bridgehead CH) + Step 1 of RS34 (to de-H a ring CH_2)			
12	Fabricate second course of carbon nanotube analogously to Steps 2–11			

may also be subject to rearrangements as normally occur on the clean or hydrogenated C(100) or the clean C(111) diamond surfaces. In many cases, these changes might be only transitional if adding additional bonds to build a successive layer can restore the original desired underlying crystal structure. Weak-force Ge-based handles might also be employed as temporary jigs to enhance stiffness during fabrication, then later be removed with minimal disruption.

(3) *Curved shell structures.* Curved shell diamond structures incorporating carefully targeted crystal dislocations to relieve internal strain will be challenging to build because of competing lattice rearrangements at almost every step, and the addition of Ge atoms to diamond structures will enable even more complex potentially pathological rearrangements. The extent of all rearrangements that may occur during a given construction sequence must be taken into account during sequence planning; a full analysis is beyond the scope of this paper.

(4) *Strained-shell structures.* Strained-shell structures, including rotationally symmetric structures useful for bearings and gears, may require specialized restraints, jigs, and other tools, whether to maintain constant strain during fabrication or to apply temporary strain to a partially completed structure. Such operations may create complex strain gradients throughout the workpiece that may alter the effectiveness of the forces applied by

mechanosynthetic tools, and may require the creation of new tools that can apply greater or lesser forces during specified operations in particular geometries. Detailed simulations will be required for each reaction step.

(5) *Detachable and embedded nonbonded structures.* Structures such as isolated nanoparts that are intended to be fabricated on a surface, then detached from that surface and transported elsewhere for further mechanosynthetic processing or for assembly into larger multipart mechanical systems, must be fabricated on jigs or surfaces that allow for convenient release of the finished nanopart without disturbing its molecular structure. Provision must also be made for additional tools that are capable of securely grasping the finished nanopart, transporting the nanopart to its remote destination, maintaining the nanopart in the preferred orientation at all times during transport, and releasing the transported nanopart once it has reached its destination. Unitary fabrication of nonbonded embedded components (e.g., a freely rotating bearing inside a race) will also require further study.

(6) *Structures requiring disassembly.* Specialized tools and tool operations will be needed to partially or completely disassemble a covalently bonded structure. For example, multitool operations using the minimal toolset can readily abstract C atoms from the diamond C(110) ridgeline, but avoiding destruction of adjacent bonding

patterns and unwanted reconstructions will be challenging and should be studied further.

References

1. D. M. Eigler and E. K. Schweizer, *Nature* 344, 524 (**1990**).
2. N. Oyabu, O. Custance, I. Yi, Y. Sugawara, and S. Morita, *Phys. Rev. Lett.* 90, 176102 (**2003**).
3. K. E. Drexler, Nanosystems: Molecular Machinery, Manufacturing, and Computation, John Wiley and Sons, New York (**1992**).
4. R. C. Merkle, *Nanotechnology* 8, 149 (**1997**).
5. M. Page and D. W. Brenner, *J. Am. Chem. Soc.* 113, 3270 (**1991**).
6. C. B. Musgrave, J. K. Perry, R. C. Merkle, and W. A. Goddard, III, *Nanotechnology* 2, 187 (**1991**).
7. X. Y. Chang, M. Perry, J. Peploski, D. L. Thompson, and L. M. Raff, *J. Chem. Phys.* 99, 4748 (**1993**).
8. B. Temelso, C. D. Sherrill, R. C. Merkle, and R. A. Freitas, Jr., *J. Phys. Chem. A* 110, 11160 (**2006**).
9. S. P. Walch and R. C. Merkle, *Nanotechnology* 9, 285 (**1998**).
10. F. N. Dzegilenko, D. Srivastava, and S. Saini, *Nanotechnology* 9, 325 (**1998**).
11. D. G. Allis and K. E. Drexler, *J. Comput. Theor. Nanosci.* 2, 45 (**2005**).
12. A. A. Evtukh, V. G. Litovchenko, Y. M. Litvin, D. V. Fedin, O. S. Dzyan, Y. N. Pedchenko, A. G. Chakhovskoi, and T. E. Felter, *J. Vac. Sci. Technol. B* 21, 627 (**2003**).
13. A. K. Singh, V. Kumar, and Y. Kawazoe, *Phys. Rev. B.* 71, 075312 (**2005**).
14. A. V. Hamza, G. D. Kubiak, and R. H. Stulen, *Surface Sci.* 206, L833 (**1988**).
15. V. I. Davydov, Germanium, Gordon and Breach, New York (**1966**).
16. R. C. Merkle, *Nanotechnology* 8, 23 (**1997**).
17. J. Asmussin and D. K. Reinhard (eds.), Diamond Films Handbook, Marcel Dekker, New York (**2002**).
18. K. S. Huang, T. S. Ku, and D. S. Lin, *Phys. Rev. B* 56, 4878 (**1997**).
19. D. J. Mann, J. Peng, R. A. Freitas, Jr., and R. C. Merkle, *J. Comput. Theor. Nanosci.* 1, 71 (**2004**).
20. J. Peng, R. A. Freitas, Jr., R. C. Merkle, J. R. Von Ehr, J. N. Randall, and G. D. Skidmore, *J. Comput. Theor. Nanosci.* 3, 28 (**2006**).
21. R. C. Merkle and R. A. Freitas, Jr., *J. Nanosci. Nanotechnol.* 3, 319 (**2003**).
22. J. Peng, R. A. Freitas, Jr., and R. C. Merkle, *J. Comput. Theor. Nanosci.* 1, 62 (**2004**).
23. Robert A. Freitas, Jr., U.S. Provisional Patent Application No. 60/543,802, February (**2005**).
24. R. A. Freitas, Jr., D. G. Allis, and R. C. Merkle, *J. Comput. Theor. Nanosci.* 4, 433 (**2007**).
25. I. G. Pitt, R. G. Gilbert, and K. R. Ryan, *J. Phys. Chem.* 99, 239 (**1995**).
26. L. Salem and C. Rowland, *Angew. Chem. Int. Ed. Engl.* 11, 92 (**1972**).
27. D. O. Cowan and R. L. Drisko, Elements of Organic Photochemistry, Plenum Press, New York (**1976**).
28. W. Adam, P. Hossel, W. Hummer, and H. Platsch, *J. Am. Chem. Soc.* 109, 7570 (**1987**).
29. S. M. King, C. Rothe, D. Dai, and A. P. Monkman, *J. Chem. Phys.* 124, 234903 (**2006**).
30. B. A. Baldwin and H. W. Offen, *J. Chem. Phys.* 48, 5358 (**1968**).
31. G. A. Zalesskaya, D. L. Yakovlev, and E. G. Sambor, *Third Internet Photochemistry and Photobiology Conference*, November–December (**2000**).
32. W. Ho and H. Lee, *Science* 286, 1719 (**1999**).
33. S.-W. Hla, L. Bartels, G. Meyer, and K.-H. Rieder, *Phys. Rev. Lett.* 85, 2777 (**2000**).
34. J. W. Lyding, K. Hess, G. C. Abeln, D. S. Thompson, J. S. Moore, M. C. Hersam, E. T. Foley, J. Lee, Z. Chen, S. T. Hwang, H. Choi, P. H. Avouris, and I. C. Kizilyalli, *Appl. Surf. Sci.* 130, 221 (**1998**).
35. E. T. Foley, A. F. Kam, J. W. Lyding, and P. H. Avouris, *Phys. Rev. Lett.* 80, 1336 (**1998**).
36. M. C. Hersam, G. C. Abeln, and J. W. Lyding, *Microelectron. Eng.* 47, 235 (**1999**).
37. R. Basu, N. P. Guisinger, M. E. Greene, and M. C. Hersam, *Appl. Phys. Lett.* 85, 2619 (**2004**).
38. M. J. S. Dewar, E. G. Zoebisch, E. F. Healy, and J. J. P. Stewart, *J. Am. Chem. Soc.* 107, 3902 (**1985**).
39. M. J. Frisch, G. W. Trucks, H. B. Schlegel, G. E. Scuseria, M. A. Robb, J. R. Cheeseman, V. G. Zakrzewski, J. A. Montgomery, Jr., R. E. Stratmann, J. C. Burant, S. Dapprich, J. M. Millam, A. D. Daniels, K. N. Kudin, M. C. Strain, O. Farkas, J. Tomasi, V. Barone, M. Cossi, R. Cammi, B. Mennucci, C. Pomelli, C. Adamo, S. Clifford, J. Ochterski, G. A. Petersson, P. Y. Ayala, Q. Cui, K. Morokuma, P. Salvador, J. J. Dannenberg, D. K. Malick, A. D. Rabuck, K. Raghavachari, J. B. Foresman, J. Cioslowski, J. V. Ortiz, A. G. Baboul, B. B. Stefanov, G. Liu, A. Liashenko, P. Piskorz, I. Komaromi, R. Gomperts, R. L. Martin, D. J. Fox, T. Keith, M. A. Al-Laham, C. Y. Peng, A. Nanayakkara, M. Challacombe, P. M. W. Gill, B. Johnson, W. Chen, M. W. Wong, J. L. Andres, C. Gonzalez, M. Head-Gordon, E. S. Replogle, and J. A. Pople, Gaussian 98, Revision A.11, Gaussian Inc., Pittsburgh, PA (**2001**).
40. A. D. Becke, *J. Chem. Phys.* 98, 5648 (**1993**); (A) A. C. Lee, W. Yang, and R. G. Parr, *Phys. Rev. B.* 37, 785 (**1988**).
41. J. B. Foresman and A. Frisch, Exploring Chemistry with Electronic Structure Methods: A Guide to Using Gaussian, 2nd edn., Gaussian Inc., Pittsburgh, PA (**1996**).
42. B. G. Johnson, C. A. Gonzales, P. M. W. Gill, and J. A. Pople, *Chem. Phys. Lett.* 221, 100 (**1994**).
43. Y. K. Zhang and W. T. Yang, *J. Chem. Phys.* 109, 2604 (**1999**).
44. S. Patchkovskii and T. Ziegler, *J. Chem. Phys.* 116, 7806 (**2002**).
45. P. G. Szalay, L. S. Thogersen, J. Olsen, M. Kallay, and J. Gauss, *J. Phys. Chem. A* 108, 3030 (**2004**).
46. S. M. Valone, M. Trkula, and J. R. Laia, *J. Mater. Res.* 5, 2296 (**1990**).
47. S. B. Sinnott, R. J. Colton, C. T. White, and D. W. Brenner, *Surf. Sci.* 316, L1055 (**1994**).
48. D. W. Brenner, S. B. Sinnott, J. A. Harrison, and O. A. Shenderova, *Nanotechnology* 7, 161 (**1996**).
49. A. Ricca, C. W. Bauschlicher, Jr., J. K. Kang, and C. B. Musgrave, *Surf. Sci.* 429, 199 (**1999**).
50. D. W. Brenner, *Phys. Rev. B* 42, 9458 (**1990**).
51. PubChem Substance (NCBI): DiscoveryGate (594781), SID 8691748, CID 594781; NIST (3104251768), SID 10425679, CID 594781; Thomson Pharma (01667625), SID 16300110, CID 594781.
52. PubChem Substance (NCBI): NIST (1182601031), SID 10433157, CID 599346.
53. L. J. Lauhon and W. Ho, *J. Phys. Chem.* 105, 3987 (**2000**).
54. D. R. Lander, K. G. Unfried, G. P. Glass, and R. F. Curl, *J. Phys. Chem.* 94, 7759 (**1990**).
55. B. Ceursters, H. M. T. Nguyen, J. Peeters, and M. T. Nguyen, *Chem. Phys. Lett.* 329, 412 (**2000**).
56. A. M. Renlund, F. Shokoohi, H. Reisler, and C. Wittig, *Chem. Phys. Lett.* 84, 293 (**1981**).

858

J. Comput. Theor. Nanosci. 5, 760–861, 2008

57. A. H. Laufer and A. M. Bass, *J. Phys. Chem.* 83, 310 (**1979**).
58. S. K. Farhat, C. L. Morter, and G. P. Glass, *J. Phys. Chem.* 97, 12789 (**1993**).
59. J. Peeters, H. Van Look, and B. Ceursters, *J. Phys. Chem.* 100, 15124 (**1996**).
60. J. W. Stephens, J. L. Hall, H. Solka, W.-B. Yan, R. F. Curl, and G. P. Glass, *J. Phys. Chem.* 91, 5740 (**1987**).
61. M. Koshi, N. Nishida, and H. Matsui, *J. Phys. Chem.* 96, 5875 (**1992**).
62. B. J. Opansky and S. R. Leone, *J. Phys. Chem.* 100, 19904 (**1996**).
63. B. Ceursters, H. M. T. Nguyen, J. Peeters, and M. T. Nguyen, *Chem. Phys.* 262, 243 (**2000**).
64. S. A. Carl, H. M. T. Nguyen, R. I. M. Elsamra, M. T. Nguyen, and J. Peeters, *J. Chem. Phys.* 122, 114307 (**2005**).
65. H. M. T. Nguyen, S. A. Carl, J. Peeters, and M. T. Nguyen, *Phys. Chem. Chem. Phys.* 6, 4111 (**2004**).
66. F. Goulay, B. Nizamov, and S. R. Leone, *Proceedings IAU Symposium No. 231* (**2005**).
67. S. A. Carl, R. M. Elsamra, R. M. Kulkarni, H. M. T. Nguyen, and J. Peeters, *J. Phys. Chem. A* 108, 3695 (**2004**).
68. B. Nizamov and S. R. Leone, *J. Chem. Phys. A* 108, 3766 (**2004**).
69. B. Ceursters, H. M. T. Nguyen, M. T. Nguyen, J. Peeters, and L. Vereecken, *Phys. Chem. Chem. Phys.* 3, 3070 (**2001**).
70. B. Nizamov and S. R. Leone, *J. Phys. Chem. A* 108, 1746 (**2004**).
71. E. Srinivasan, H. Yang, and G. N. Parsons, *J. Chem. Phys.* 105, 5467 (**1996**).
72. S. Sugahara, K. Hosaka, and M. Matsumura, *App. Surf. Sci.* 130, 327 (**1998**).
73. C. Chatgilialoglu, M. Ballestri, J. Escudie, and I. Pailhous, *Organometallics* 18, 2395 (**1999**).
74. L. Song, W. Wu, K. Dong, P. C. Hiberty, and S. Shaik, *J. Phys. Chem. A* 106, 11361 (**2002**).
75. T. I. Drozdova and E. T. Denisov, *Kinet. and Catal.* 43, 10 (**2002**).
76. J. Olander and K. M. E. Larsson, *Thin Solid Films* 458, 191 (**2004**).
77. B. Temelso, C. D. Sherrill, R. C. Merkle, and R. A. Freitas, Jr., *J. Phys. Chem. A* 111, 8677 (**2007**).
78. B. J. McIntyre, M. Salmeron, and G. A. Somorjai, *Science* 265, 1415 (**1994**).
79. W. T. Muller, D. L. Klein, T. Lee, J. Clarke, P. L. McEuen, and P. G. Schultz, *Science* 268, 272 (**1995**).
80. D. H. Huang and Y. Yamamoto, *Appl. Phys. A* 64, R419 (**1997**).
81. C. Thirstrup, M. Sakurai, T. Nakayama, and M. Aono, *Surf. Sci.* 411, 203 (**1998**).
82. S. Shimokawa, A. Namiki, M. N. Gamo, and T. Ando, *J. Chem. Phys.* 113, 6916 (**2000**).
83. R. S. Becker, J. A. Golovchenko, and B. S. Swartzentruber, *Nature* 325, 419 (**1987**).
84. C. J. Chen, Introduction to Scanning Tunneling Microscopy, Oxford University Press, Cambridge (**1993**).
85. D. Huang, H. Uchida, and M. Aono, *J. Vac. Sci. Technol. B* 12, 2429 (**1994**).
86. C. T. Salling and M. G. Lagally, *Science* 265, 502 (**1994**).
87. I.-W. Lyo and P. Avouris, *Science* 253, 173 (**1991**).
88. M. Aono, A. Kobayashi, F. Grey, H. Uchida, and D. H. Huang, *J. Appl. Phys.* 32, 1470 (**1993**).
89. P. Avouris, *Acc. Chem. Res.* 28, 95 (**1995**).
90. G. Meyer and K. H. Rieder, *Surf. Sci.* 377, 1087 (**1997**).
91. J. N. Israelachvili, Intermolecular and Surface Forces, 2nd edn., Academic Press, NY (**1992**).
92. J. J. Yao, S. C. Arney, and N. C. MacDonald, *J. Microelectromech. Syst.* 1, 14 (**1992**).
93. H. Morishita and Y. Hatamura, *Proc. 1993 IEEE/RSJ Intl. Conf. on Intelligent Robots and Systems*, Yokohama, Japan, July (**1993**), Vol. 3, pp. 1717.
94. V. Mancevski and P. F. McClure, *Proc. of the SPIE. Metrology, Inspection and Process Control for Microlithography XVI*, March (**2003**), Vol. 4689, p. 83.
95. P. F. McClure and V. Mancevski, *SPIE Microlithography 2005 Conference*, San Jose California, February–March (**2005**).
96. The MultiView 3000, Nanonics Imaging Ltd. (**2005**).
97. H. Grube, B. C. Harrison, J. F. Jia, and J. J. Boland, *Rev. Sci. Instr.* 72, 4388 (**2001**).
98. H. Okamoto and D. M. Chen, *Rev. Sci. Instr.* 72, 4398 (**2001**).
99. K. Takami, J. Mizuno, M. Akai-kasaya, A. Saito, M. Aono, and Y. Kuwahara, *J. Phys. Chem. B* 108, 16353 (**2004**).
100. M. Yu, M. J. Dyer, G. D. Skidmore, H. W. Rohrs, X. K. Lu, K. D. Ausman, J. von Ehr, and R. S. Ruoff, *6th Foresight Nanotechnology Conference*, November (**1998**).
101. R. F. Service, *Science* 282, 1620 (**1998**).
102. P. M. Morse, *Phys. Rev.* 34, 57 (**1929**).
103. D. F. McMillen and D. M. Golden, *Annu. Rev. Phys. Chem.* 33, 493 (**1982**).
104. HyperCube, Inc., HyperChem Computational Chemistry, Publication HC70-00-04-00, (**2002**); MM2 (1991) parameter set (/runfiles/mmpstr.txt and /runfiles/mmpben.txt) contributed by Norman Allinger.
105. M. Lesbre, P. Mazerolles, and J. Stage, The Organic Compounds of Germanium, John Wiley and Sons, New York (**1971**).
106. C. D. Schaeffer, Jr., C. A. Strausser, M. W. Thomsen, and C. H. Yoder, The wired chemist, a collection of chemistry resources, Data for General, Inorganic, Organic, and Physical Chemistry (**1989**);
107. J. A. Kerr, CRC Handbook of Chemistry and Physics, edited by D. R. Lide, 71st edn., CRC Press, Boca Raton, FL (**1990**).
108. P. G. Green, J. L. Kinsey, and R. W. Field, *J. Chem. Phys.* 91, 5160 (**1989**).
109. K. M. Ervin, S. Gronert, S. E. Barlow, M. K. Gilles, A. G. Harrison, V. M. Bierbaum, C. H. Depuy, W. C. Lineberger, and G. B. Ellison, *J. Am. Chem. Soc.* 112, 5750 (**1990**).
110. K. P. Huber and G. Herzberg, Molecular Structure IV: Constants of Diatomic Molecules, Van Nostrand Reinhold, New York (**1979**).
111. T. F. Rutledge, Acetylenic Compounds: Preparation and Substitution Reactions, Reinhold Book Corp., New York (**1968**).
112. G. Yan, N. R. Brinkmann, and H. F. Schaefer, III, *J. Phys. Chem. A* 107, 9479 (**2003**).
113. G. D. Kubiak, A. V. Hamza, E. Stulen, E. C. Sowa, and K. W. Kolasinski, New Diamond Science and Technology, edited by R. Messier, J. T. Glass, J. E. Butler, and R. Roy, Materials Research Society, Pittsburgh (**1991**).
114. J. Chen, S. Z. Deng, J. Chen, Z. X. Yu, and N. S. Xu, *Appl. Phys. Lett.* 74, 3651 (**1999**).
115. G. H. Duffey, *J. Chem. Phys.* 17, 840 (**1949**).
116. N. J. Turro, Y. Cha, and I. R. Gould, *J. Am. Chem. Soc.* 109, 2101 (**1987**).
117. K. C. Pandey, *Phys. Rev. B* 25, 4338 (**1982**).
118. A. Campargue and R. Escribano, *Chem. Phys. Lett.* 315, 397 (**1999**).
119. P. Antoniotti, P. Benzi, M. Castiglioni, and P. Volpe, *Eur. J. Inorg. Chem.* 1999, 323 (**1999**).
120. X. Wang, L. Andrews, and G. P. Kushto, *J. Phys. Chem.* 106, 5809 (**2002**).
121. W. J. Leigh and C. R. Harrington, *J. Am. Chem. Soc.* 127, 5084 (**2005**).
122. J. J. BelBruno, *Heteroatom Chem.* 9, 195 (**1998**).
123. C. R. Harrington, W. J. Leigh, B. K. Chan, P. P. Gaspar, and D. Zhou, *Can. J. Chem.* 83, 1324 (**2005**).
124. N. P. Toltl and W. J. Leigh, *J. Am. Chem. Soc.* 120, 1172 (**1998**).
125. T. L. Morkin and W. J. Leigh, *Organometallics* 20, 4537 (**2001**).
126. T. Tsumuraya, S. A. Batcheller, and S. Masamune, *Angew. Chem. Int. Ed. Engl.* 30, 902 (**1991**).
127. W. J. Leigh, *Pure Appl. Chem.* 71, 453 (**1999**).
128. F. Meiners, W. Saak, and M. Weidenbruch, *Zeitschrift für Anorg. Allgemeine Chem.* 628, 2821 (**2002**).
129. R. Becerra, S. E. Boganov, M. P. Egorov, V. I. Faustov, O. M. Nefedov, and R. Walsh, *Can. J. Chem.* 78, 1428 (**2000**).

130. R. C. Weast, Handbook of Chemistry and Physics, 49th edn., CRC, Cleveland, OH (**1968**).

131. C. G. Newman, J. Dzarnoski, M. A. Ring, and H. E. O'Neal, *Int. J. Chem. Kinetics* 12, 661 (**1980**).

132. G. Lu and J. E. Crowell, *J. Chem. Phys.* 98, 3415 (**1993**).

133. A. Kim, J. Y. Maeng, J. Y. Lee, and S. Kim, *J. Chem. Phys.* 117, 10215 (**2002**).

134. J.-H. Cho and L. Kleinman, *J. Chem. Phys.* 119, 2820 (**2003**); (A) D. M. Gruen, S. Liu, A. R. Krauss, and X. Pan, *J. Appl. Phys.* 75, 1758 (**1994**).

135. C. Gonzalez, C. Sosa, and H. B. Schlegel, *J. Phys. Chem.* 93, 2435 (**1989**).

136. J. Franks, *J. Vac. Sci. and Technol. A* 7, 2307 (**1989**).

137. C. A. Rego, P. W. May, E. C. Williamson, M. N. R. Ashfold, Q. S. Chia, K. N. Rosser, and N. M. Everitt, *Diam. Rel. Mater.* 3, 939 (**1994**).

138. D. S. Patil, K. Ramachandran, N. Venkatramani, M. Pandey, and R. d'Cunha, *Pramana J. Phys.* 55, 933 (**2000**).

139. J. T. Herrold and V. L. Dalal, *J. Non-Cryst. Solids* 270, 255 (**2000**).

140. W. Sundermeyer and W. Verbeek, *Angew. Chemie Intl. Ed. Engl.* 5, 1 (**1966**).

141. H. P. Mayer and S. Rapsomanikis, *Appl. Organomet. Chem.* 6, 173 (**1992**).

142. J. M. Buriak, *Chem. Rev.* 102, 1271 (**2002**).

143. B. L. Lewis, P. N. Froelich, and M. O. Andreae, *Nature* 313, 303 (**1985**).

144. P. J. Craig and J. T. Van Elteren, The Chemistry of Organic Germanium, Tin and Lead Compounds, edited by Saul Patai, John Wiley & Sons, Ltd. (**1995**), p. 843.

145. M. Fujiu, M. Sakuraba, T. Matsuura, and J. Murota, *First International Workshop on New Group IV (Si-Ge-C) Semiconductors: Control of Properties and Applications to Ultrahigh Speed and Opto-Electronic Devices*, Sendai, Japan, Abs. No. PVI-19 (**2001**).

146. T. Watanabe, M. Sakuraba, T. Matsuura, and J. Murota, *Jpn. J. Appl. Phys.* 36, 4042 (**1997**).

147. X. Lu, Z. Su, X. Xu, N. Q. Wang, and Q. E. Zhang, *Chem. Phys. Lett.* 371, 172 (**2003**).

148. R. Miotto, A. C. Ferraz, and R. H. Miwa, *Phys. Rev. B* 68, 115436 (**2003**).

149. J. Murota and M. Sakuraba, *International Workshop on Nano-Technology, Nano-Materials, Nano-Devices, and Nano-Systems*, Tohoku-Cambridge Forum—University of Cambridge, June (**2004**).

150. A. Izena, M. Sakuraba, T. Matsuura, and J. Murota, *J. Cryst. Growth* 188, 131 (**1998**).

151. Y. Noji, M. Sakuraba, and J. Murota, *4th Int. Conf. Silicon Epitaxy and Heterostructures (ICSI-4)*, Awaji-Island, Hyogo, Japan, May (**2005**).

152. A. J. Dyson and P. V. Smith, *Surf. Sci.* 396, 24 (**1998**).

153. T. Yamada, M. Kawai, A. Wawro, S. Suto, and A. Kasuya, *J. Chem. Phys.* 121, 10660 (**2004**).

154. Y. Ishida, A. Sekiguchi, K. Kobayashi, and S. Nagase, *Organometallics* 23, 4891 (**2004**).

155. J. C. Guillemin, L. Lassalle, and T. Janati, *Planet. Space Sci.* 43, 75 (**1995**).

156. S. Bernardoni, M. Lucarini, G. F. Pedulli, L. Valgimigli, V. Gevorgyan, and C. Chatgilialoglu, *J. Org. Chem.* 62, 8009 (**1997**).

157. S. Nie, R. M. Feenstra, J. Y. Lee, and M.-H. Kang, *J. Vac. Sci. Technol. A* 22, 1671 (**2004**).

158. R. S. Becker, B. S. Swartzentruber, J. S. Vickers, and T. Klitsner, *Phys. Rev. B* 39, 1633 (**1989**).

159. K.-H. Huang, T.-S. Ku, and D.-S. Lin, *Phys. Rev. B* 56, 4878 (**1997**).

160. S. Ateca, C. Bater, M. Sanders, and J. H. Craig, Jr., *Surf. Interface Anal.* 29, 194 (**2000**).

161. W. C. Dunlap, Jr., *Phys. Rev.* 94, 1531 (**1954**).

162. F. Reidmiller, G. L. Wegner, A. Jockisch, and H. Schmidbaur, *Organometallics* 18, 4317 (**1999**).

163. C. Frondel and U. B. Marvin, *Nature* 214, 587 (**1967**).

164. K. E. Spear, A. W. Phelps, and W. B. White, *J. Mater. Res.* 5, 2277 (**1990**).

165. R. N. Pease, *J. Am. Chem. Soc.* 52, 1158 (**1930**).

166. N. F. Goldshleger and A. P. Moravsky, *Russ. Chem. Rev.* 66, 323 (**1997**).

167. R. D. Bach, M.-D. Su, E. Aldabbagh, J. L. Andrds, and H. B. Schlegel, *J. Am. Chem. Soc.* 115, 10237 (**1993**).

168. M. Springborg, *J. Phys. C: Solid State Phys.* 19, 4473 (**1986**).

169. A. Karpfen, *J. Phys. C: Solid State Phys.* 12, 3227 (**1979**).

170. A. Abdurahman, A. Shukla, and M. Dolg, *Phys. Rev. B* 65, 115106 (**2002**).

171. I. Alkorta and J. Elguero, *Struct. Chem.* 16, 77 (**2005**).

172. A. G. Whittaker, *Science* 200, 763 (**1978**).

173. S. Eisler, N. Cahal, R. McDonald, and R. R. Tykwinski, *Chem. Eur. J.* 9, 2542 (**2003**).

174. R. Boese, B. J. Green, J. Mittendorf, D. L. Mohler, and K. P. C. Vollhardt, *Angew. Chem. Int. Ed. Engl.* 31, 1643 (**1992**).

175. J. J. Pak, T. J. R. Weakley, and M. M. Haley, *J. Am. Chem. Soc.* 121, 8182 (**1999**).

176. L. Ravagnan, F. Siviero, C. Lenardi, P. Piseri, E. Barborini, P. Milani, C. Casari, A. Li Bassi, and C. E. Bottani, *Phys. Rev. Lett.* 89, 285506 (**2002**).

177. T. Schlatholter, M. W. Newman, T. R. Niedermayr, G. A. Machicoane, J. W. McDonald, T. Schenkel, R. Hoekstra, and A. V. Hamza, *Eur. Phys. J. D* 12, 323 (**2000**).

178. A. J. Heeger, S. Kivelson, J. R. Schrieffer, and W.-P. Su, *Rev. Mod. Phys.* 60, 781 (**1988**).

179. J. Tsukamoto, *Adv. Phys.* 41, 509 (**1992**).

180. P. Corradini, *Atti Accad. Nazl. Lincei, Rend., Classe Sci. Fis., Mat. Nat.* 25, 517 (**1958**).

181. M. S. Dresselhaus, G. Dresselhaus, and P. C. Eklund, Science of Fullerenes and Carbon Nanotubules, Academic Press, San Diego (**1996**).

182. O. A. Shenderova, D. Areshkin, and D. W. Brenner, *Mater. Res.* 6, 11 (**2003**).

183. X. Xiao, J. W. Elam, S. Trasobares, O. Auciello, and J. A. Carlisle, *Adv. Mater.* 17, 1496 (**2005**).

184. K. S. Novoselov, A. K. Geim, S. V. Morozov, D. Jiang, Y. Zhang, S. V. Dubonos, I. V. Grigorieva, and A. A. Firsov, *Science* 306, 666 (**2004**).

185. S. Helveg, C. Lopez-Cartes, J. Sehested, P. L. Hansen, B. S. Clausen, J. R. Rostrup-Nielsen, F. Abild-Pedersen, and J. K. Norskov, *Nature* 427, 426 (**2004**).

186. L. G. Bulusheva, A. V. Okotrub, D. A. Romanov, and D. Tomanek, *J. Phys. Chem. A* 102, 975 (**1998**).

187. S. Sawada and N. Hamada, *Solid State Commun.* 83, 917 (**1992**).

188. A. A. Lucas, P. H. Lambin and R. E. Smalley, *J. Phys. Chem. Solids* 54, 586 (**1993**).

189. D. Stojkovic, P. Zhang, and V. H. Crespi, *Phys. Rev. Lett.* 87, 125502 (**2001**).

190. Y. Liu, R. O. Jones, X. Zhao, and Y. Ando, *Phys. Rev. B* 68, 125413 (**2003**).

191. L.-M. Peng, Z. L. Zhang, Z. Q. Xue, Q. D. Wu, Z. N. Gu, and D. G. Pettifor, *Phys. Rev. Lett.* 85, 3249 (**2000**).

192. N. Sano, M. Chhowalla, D. Roy, and G. A. J. Amaratunga, *Phys. Rev. B* 66, 113403 (**2002**).

193. H. Y. Peng, N. Wang, Y. F. Zheng, Y. Lifshitz, J. Kulik, R. Q. Zhang, C. S. Lee, and S. T. Lee, *Appl. Phys. Lett.* 77, 2831 (**2000**).

194. L.-C. Qin, X. Zhao, K. Hirahara, Y. Miyamoto, Y. Ando, and S. Iijima, *Nature* 408, 50 (**2000**).

195. N. Wang, Z. K. Tang, G. D. Li, and J. S. Chen, *Nature* 408, 50 (**2000**).

860

J. Comput. Theor. Nanosci. 5, 760–861, 2008

REVIEW

196. M. Hulman, H. Kuzmany, O. Dubay, G. Kresse, L. Li, and Z. K. Tang, *J. Chem. Phys.* 119, 3384 **(2003)**.

197. D. J. Mann and M. D. Halls, *J. Chem. Phys.* 116, 9014 **(2002)**.

198. X. Yang and J. Ni, *Phys. Rev. B* 69, 125419 **(2004)**.

199. S. B. Sinnott, O. A. Shenderova, C. T. White, and D. W. Brenner, *Carbon* 36, 1 **(1997)**.

200. D. W. Brenner, O. A. Shenderova, D. A. Areshkin, and J. D. Schall, *Comput. Modeling Eng. and Sci.* 3, 643 **(2002)**.

201. O. A. Shenderova, D. A. Areshkin, and D. W. Brenner, *Molec. Simul.* 29, 259 **(2003)**.

202. R. C. Fort, Jr., Adamantane: The Chemistry of Diamond Molecules, Marcel Dekker, New York **(1976)**.

REVIEW

*J. Comput. Theor. Nanosci. 5, 760–861, **2008***

861